



HAL
open science

Histone H3 Serine 28 is essential for efficient Polycomb-mediated gene repression in *Drosophila*

Yuk Kwong Yung

► **To cite this version:**

Yuk Kwong Yung. Histone H3 Serine 28 is essential for efficient Polycomb-mediated gene repression in *Drosophila*. Biochemistry, Molecular Biology. Université Montpellier, 2015. English. NNT : 2015MONTT001 . tel-01199169

HAL Id: tel-01199169

<https://theses.hal.science/tel-01199169>

Submitted on 15 Sep 2015

HAL is a multi-disciplinary open access archive for the deposit and dissemination of scientific research documents, whether they are published or not. The documents may come from teaching and research institutions in France or abroad, or from public or private research centers.

L'archive ouverte pluridisciplinaire **HAL**, est destinée au dépôt et à la diffusion de documents scientifiques de niveau recherche, publiés ou non, émanant des établissements d'enseignement et de recherche français ou étrangers, des laboratoires publics ou privés.

THÈSE

Pour obtenir le grade de
Docteur

Délivré par **Université Montpellier I**

Préparée au sein de l'école doctorale : Sciences
Chimiques et Biologiques pour la Santé
Et de l'unité de recherche : Institut de Génétique Humaine

Spécialité : **Biochimie et Biologie Moléculaire**

Présentée par **Philip Yuk Kwong YUNG**

**Histone H3 Serine 28 is essential for
efficient Polycomb-mediated gene
repression in *Drosophila*.**

Soutenue le 09 février 2015 devant le jury composé de

Mr Giacomo Cavalli, DR2
IGH - CNRS - UPR1142

Directeur de thèse

Mr Dominique Helmlinger, CR1
CRBM - CNRS - UMR5237

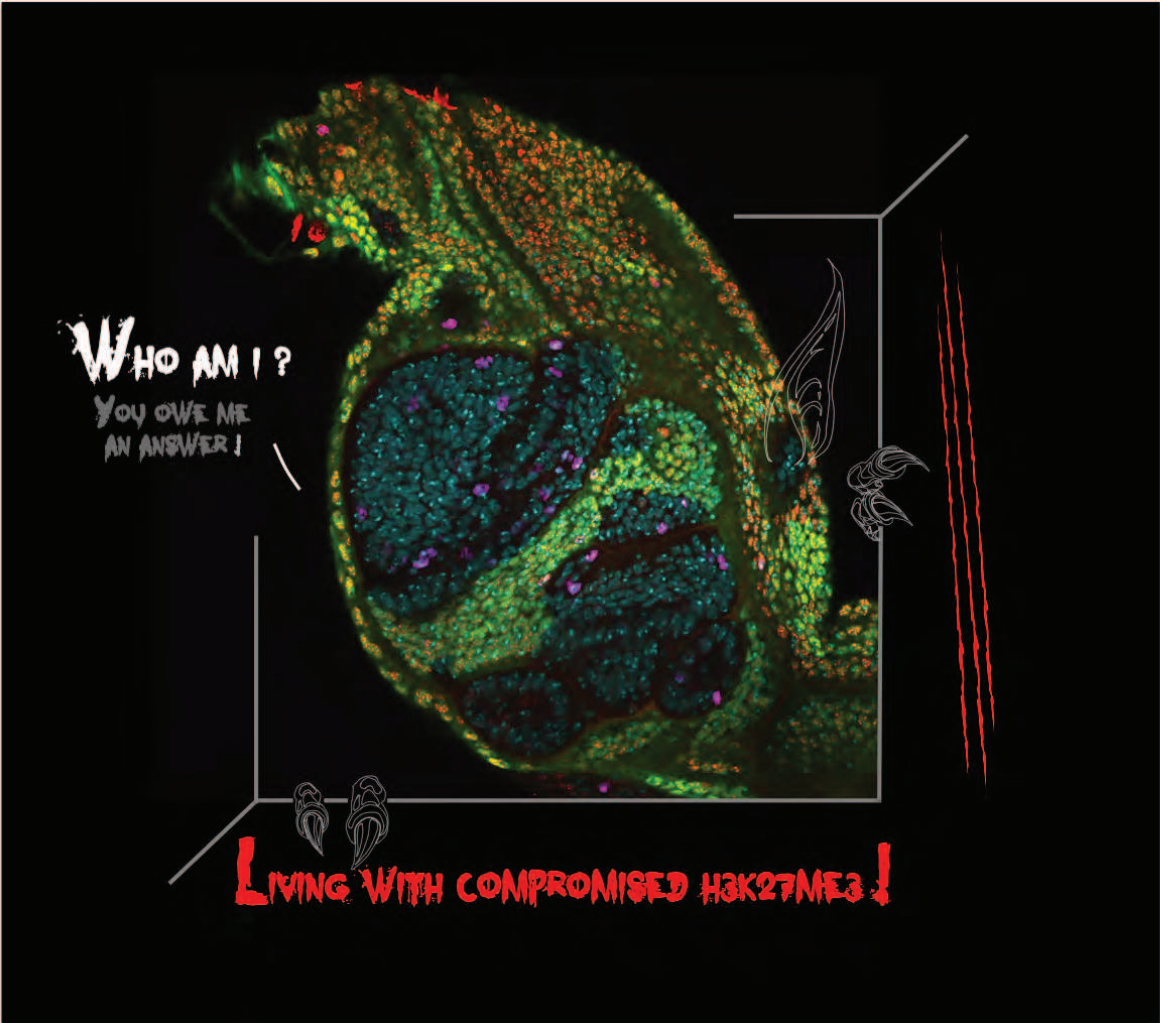
Examineur

Mme Frédérique Peronnet, DR
Université Pierre et Marie Curie-Paris 6 - CNRS - UMR7622

Rapporteur

Mme Nathalie Dostatni, DR2
UMR3664 - CNRS & Institut Curie

Rapporteur



WHO AM I?
YOU OWE ME
AN ANSWER!

LIVING WITH COMPROMISED H3K27ME3!

Acknowledgement

I can still remember the countless conversations I had with Giacomo Cavalli and his lab members over a Skype interview for a potential offer of a Ph.D. position. After more than four years gone then, I feel fortunate to have made the decision to come to the South of France for which I am utterly thankful to join the lab of Giacomo Cavalli for my Ph.D. training. With this invaluable opportunity, it opens the door to *Drosophila* epigenetics through which I was swarmed with talented minds for chromatin Biology.

I would consider Giacomo's lab as a hub of scholars, with each of the lab members working on a slightly different research direction and yet all under the same hood of Polycomb biology and chromatin Dynamics. The team members also act as a cohort of diverse technical expertise from which I can always get caring advices for experimental setups. In such an international and multi-cultural environment, I can picture an ideal research environment that encourages creativity and exchange of ideas. I would like to express my sincere thanks to previous and present lab members for making my lab life a constructive, enjoyable and ever-memorable experience. They include particularly Frederic Bantignies, Boyan Bonev, Tra-Ming Chang, Thierry Cheutin, Filippo Crabelli, Justa Cruz-Sanchez, Anna Delest, Inma Gonzalez, Nicola Iovino,

Caroline Jaquier-Labroche, Julio Mateo Zangerck, Benjamin Zebane, Manuela Portogo, Sammy Sakr, Satish Sati, Bernd Schüttengraber, Tom Sexton, Bernd Stadelmayer and Aubin Thomas.

As a germinating young scientist, I am exploring my way through the unknown and yet exciting future. In this regard, I am indebted to my thesis director Dr. Giacomo Cavalli and my jury committee members, which include Dr. Nathalie Dostadni, Dr. Dominique Heleninger and Dr. Frédérique Peromet for their invaluable advice and conceptual inputs for my thesis project. I am also blessed to have a fruitful collaboration with Dr. Wolfgang Fischele and Dr. Alexandra Stützer for their expertise in chromatin biochemistry. In addition, I would like to thank my M.Phil supervisor Dr. Chun Jiang and my undergraduate mentor Dr. Zhen Jiang for their endless support throughout my career development.

I always feel grateful about my adventure in the South of France where I find myself very fortunate to meet countless people, who are not only enthusiastic and passionate about research but also well aware of work-life balance. All these experience reinforce

my commitment in pursuing a sustainable research career. For this, I am much obliged to all my friends, including but not limited to Bridlin Buckenmann, Anne-Pascale Bottonnet, Yukiko Imai, Ola Zawera, Mikael Le Clech, Paulina Marzec, Natalia Pinzon Restrepo, Jerome Poli, Marta Rodriguez Martinez and Maria Joao Silva, with special thanks to the Spearfishing team: Fabien Celilla, Robert Rauer and Georges Soligmann.

Besides, I am particularly thankful for the technical assistance from Chantal Cayeville, Christophe Dupuy, the Montpellier PZO Imaging facility and the IGH Drosophila husbandry facility that are always eager to offer professional solutions to technical difficulties. Also, I would like to take this opportunity to thank the funding agencies which kindly support my thesis work. They include the Montpellier CBS2 graduate school, the Croucher Foundation and La Ligue contre le Cancer.

Finally, I owe my deepest gratitude to my parents and particularly my brother, Michael Yuk Ming Yung, for their unconditioned love and endless care. It would

Have never been possible for me to get through all the hurdles to pursue my dream of a scientist without them.

Science is beautiful, and I deeply believe that it deals with absolute novelty and sometimes dreadful depression that worth a lifetime commitment to experience.

Philip Yuk Kwong Yung
9th May, 2015.

Table of Content

Acknowledgement	I
Table of Content	V
List of Figures	VIII
Abbreviations	IX
Thesis Summary	XII
Thesis Summary (French)	XIV

Chapter I – Introduction

1. Overview of Chromatin Biology & Epigenetics	2
2. Histone Modifications	
2.1 H3K4me	4
2.2 H3K9me	6
2.3 H3K36me	7
2.4 H3K79me	8
2.5 H3K27me	9
2.6 H3K27ac	16
2.7 H2AK119ub	18
2.8 H3T3ph & H2AT120ph	22
2.9 H3S10ph	23
2.10 H3S28ph	26
2.11 H3T80ph	28
3. <i>Drosophila</i> Polycomb Group Proteins – Compositions & Functions	
3.1 PRC1	31
3.1.1 Pc	32
3.1.2 Ph	33
3.1.3 Psc	34
3.1.4 dRing	35
3.1.5 Scm	36
3.2 dRAF	37
3.3 Pho-RC	38
3.4 PRC2	40
3.4.1 Esc	41
3.4.2 E(z)	42
3.4.3 Su(z)12 & Nurf55	45
3.5 PRC2 auxiliary factors	46
3.5.1 Pcl	46
3.5.2 Jarid2	47
3.5.3 Jing/AEBP2	49
3.6 PR-DUB	51
4. Mechanisms of PcG-mediated Gene Repression	
4.1 Counteracting chromatin remodeling	53
4.2 Interference with the transcription machinery	53
4.3 Chromatin cross talks – Inhibition of active chromatin marks	55
4.4 Chromatin Compaction	57

4.4 3D genome organization – Formation of repressive topologically associating domain (TAD)	58
5. Mechanisms for Derepression of PcG Target Genes	
5.1 ZRF1	62
5.2 Interphasic H3S28ph	62
5.3 Aurora B inhibition of Ring1b-dependent H2Aub	63
5.4 H3K27 demethylation	64
5.5 DUB	65
6. Modulation of PcG Repression Activity	
6.1 H3K27me3	68
6.2 H2Aub	69
6.3 Polycomb-like	69
6.4 Nucleosome density	70
6.5 Active chromatin marks inhibit PRC2 activity	70
6.6 H3K27Ac	70
6.7 H3S28ph	71
6.8 H3.3	71
6.9 CpG methylation	71
6.10 RNA inhibition of PRC2 activity	72
7. Epigenetic Inheritance of PcG-mediated Repressive Chromatin States	
7.1 DNA replication	75
7.2 Mitosis	80
Chapter II – Results	
1. Cell cycle Dynamics of H3S28ph, H3K27me3 and Pc in <i>Drosophila</i> S2 Cells	87
2. <i>In vivo</i> RNAi against Aurora B kinase in <i>Drosophila</i>	90
3. Principle of the histone replacement system in <i>Drosophila</i>	94
4. Principle of mosaic analysis of histone mutants in <i>Drosophila</i> larval tissues	95
5. H3S28 is required for efficient polycomb-mediated Gene Repression in <i>Drosophila</i> (Submitted Manuscript)	97
6. Extended Results: Phenotyping <i>H3S28A</i> mutant in <i>dUtxΔ</i> background	123
Chapter III – Extended Discussions	
1. Future plans	
1.1 Cell cycle profile of isolated histone mutant cells	128
1.2 Detection of potential mitotic defects in <i>H3S28A</i> mutant cells	128
1.3 FACS-sorting mitotic cells for ChIP-seq analysis	131
2. Potential role of H3S28ph in the epigenetic inheritance of PcG repression through mitosis	134
3. Transcription-independent role of PcG proteins in mitotic progression	135
4. Phospho-methyl switches and mitotic progression	137
5. Alternative method to address the function of mitotic H3S28ph	138

Chapter IV – Materials & Methods

1. Plasmid constructions.....	140
2. <i>Drosophila</i> transgenesis	142
3. Generation of histone locus deficiency line	142
4. <i>Drosophila</i> genetics	143
5. Mosaic analysis and immunostaining	143
6. Scanning electron microscope	144
7. <i>In vitro</i> PRC2 histone methyltransferase assay	145
8. FACS-sorting of mitotic population from <i>Drosophila</i> S2 cell culture	146
9. Primer list	147
10. E.coli stocks	148
11. Fly stocks	149

References	150
-------------------------	-----

Appendix I

Accepted Manuscript in <i>Cell Reports</i> – Histone H3 Serine 28 is essential for efficient Polycomb-mediated gene repression in <i>Drosophila</i>	175
---	-----

List of Figures

I. Overview of a selection of histone modifications	30
II. A proposed possible model for the binding of the PRC2-AEBP2 complex to a di-nucleosome	44
III. <i>Drosophila</i> polycomb group proteins and related components	52
IV. Mechanisms of PcG-mediated gene repression	61
V. Mechanisms for derepression of PcG target genes	67
VI. Modulating the repressive activity of PcG components	74
VII. Epigenetic inheritance of PcG repression through DNA replication	78
VIII. Buffer model of H3K27me3 level for effective gene repression despite cell cycle fluctuation	79
IX. Epigenetic inheritance of PcG repression through mitosis	85
Fig 1. Cell cycle dynamics of H3S10ph, H3S28ph and H3K27me3.....	88
Fig 2. Cell cycle dynamics of H3S10ph, H3S28ph and Pc.....	89
Fig 3. <i>In vivo</i> RNAi against <i>Drosophila</i> Aurora B.....	91
Fig 4. H3K27me3, H3K27Ac, Pc and Ubx immunostaining patterns were unaffected upon RNAi against Aurora B	92
Fig 5. Antenna duplication defects in flies upon Aurora B knockdown	93
Fig 6 Principle of the <i>Drosophila</i> histone replacement systems	96
Manuscript Figures	
Fig M1 Validation of the mosaic histone replacement system	105
Fig M2 Strong reduction of H3K27 methylations in <i>H3S28A</i> mutant.....	107
Fig M3 Dereglulation of Hox and antenna selector genes in <i>H3K27R</i> and <i>H3S28A</i> mutants and their associating transformation phenotypes	109
Fig M4 H3S28A nucleosome is a suboptimal substrate for PRC2 activity.....	111
Fig S1. Homozygous $\Delta HisC$ clones are not viable in larval tissues	112
Fig S2. Validation of the mosaic histone replacement system	113
Fig S3. Hox genes derepression profiles in <i>H3S28A</i> and <i>H3K27R</i> clones.....	114
Fig S4. En and Antp were not derepressed in <i>WT</i> , <i>H3S28A</i> and <i>H3K27R</i> clones	116
Fig S5. Ectopic silencing of endogenous expression of PcG target genes in <i>H3K27R</i> clones	117
Fig S6. Heterogeneous Ubx derepression in <i>H3S28A</i> clones.....	118
Fig S7. Ectopic expression of Antp repressed of Hth in <i>Antp^{Ns}</i> antenna disc	119
Fig S8. Nuclear staining pattern of Pc and Ph remained unchanged in <i>H3S28A</i> and <i>H3K27R</i> mutant	120
Fig 7 Combining <i>dUtxA</i> with <i>H3S28A</i> mutant did not rescue reduction of H3K27 methylations	124
Fig 8 Mitotic abnormality in <i>H3S28A</i> mutant clones	130
Fig 9 FACS-sorting of mitotic populations from asynchronous <i>Drosophila</i> S2 cell culture	132
Fig 10 Using secondary antibodies to prevent H3S10ph contamination of ChIP-seq samples	133
Fig 11 Potential role of H3S28ph in the epigenetic inheritance of PcG repression through mitosis	136

Abbreviations

53BP1	p53-binding protein 1
Abd-B	Abdominal-B
AEBP2	AE-1 Binding Protein 2
ANT-C	Antennapedia Gene Complex
Antp	Antennapedia
AntpNs	Antennapedia Nasobemia
APC	Anaphase Promoting Complex
Ash1	Absent Small or Homeotic 1
Asx	Additional Sexcomb
Asxl	Additional Sexcomb like
ATXR5/6	ARABIDOPSIS TRITHORAX-RELATED PROTEINS5 5/6
BEAF	Boundary Element-associated Factor
BMI1	B cell-specific Moloney murine leukemia virus integration site 1
Bre1	Brefeldin A sensitivity
BSA	Bovine Serum Albumin
Bub1	Budding Uninhibited by Benzimidazole 1
BX-C	Bithorax complex
bxd	bithoraxoid
CAF1	Chromatin Assembly Factor 1
CBP	CREB-Binding Protein
CBX2	Chromobox homolog 2
CDK	Cyclin Dependent Kinase
CHD1	Chromodomain-helicase-DNA-binding protein 1
ChIP	Chromatin Immunoprecipitation
COMPASS	Complex of Proteins Associated with a Trithorax-related SET domain protein
CP190	Centrosomal protein 190kD
CPC	Chromosome Passenger Complex
CTCF	CCCTC- binding factor
CycB	Cyclin B
dac	dachshund
DAM-ID	DNA adenine methyltransferase identification
Dap	2, 3-diaminopropanoic acid
DNMT	DNA methyltransferase
Dot1	Disruptor of Telomeric Silencing
dRAF	dRing Associated Factors
dSfmbt	Drosophila Scm-related gene containing Four Mbt domains
DUB	Deubiquitinase
E(z)	Enhancer of zeste
Eaf3	Esa1p-Associated Factor 3
EDTA	Ethylenediaminetetraacetic acid
EED	Embryonic Ectoderm Development
EMF2	EMBRYONIC FLOWER 2
En	Engrailed
ES cells	Embryonic Stem Cells
Esc	Extra Sexcomb
Escl	Esc Like

Ezh2	Enhancer of Zeste Homolog 2
FACS	Fluorescence-activated Cell Sorting
FACT	Facilitates Chromatin Transcription
FIS2 2	FERTILIZATION INDEPENDENT SEED 2
FISH	Fluorescent In Situ Hybridization
FLP	Flippase
FRAP	Fluorescence Recovery After Photobleaching
FRT	FLP Recognition Targets
Glc7	Glycogen 7
GRO-seq	Genomewide Nuclear Run On Sequencing
HAT	Histone Acetyltransferase
HDAC	Histone Deacetylase
HERS	Histone gene-specific Epigenetic Repressor in late S phase
His-GU	Histone Gene Unit
HisC	Histone Complex
HMT	Histone Methyltransferase
Hox	Homeotic Cluster
HP1	Heterochromatin Protein 1
Hth	Homothorax
INCENP	Inner Centromere Protein
ING2	Inhibitor of Growth Family, Member 2
INO80	INositol requiring
ITC	Isothermal titration calorimetry
Jarid2	Jumonji, AT Rich Interactive Domain 2
JmjC	Jumonji C terminal domain
KDM	Lysine demethylase
Klf4	Kruppel-like Factor 4
Lid	Little Imaginal Disc
LMG	Lemming
lncRNA	Long non-coding RNA
LSD	Lysine-specific demethylase
MBT	Malignant Brain Tumor
Mes4	Mesoderm-expressed 4
MLL	Mixed-lineage Leukemia:
MPM2	Mitotic Protein Monoclonal 2
MS	Mass Spectrometry
MSK1	Mitogen- and Stress-activated Protein Kinase-1
MSL	Male Specific Lethal
Mute	Muscle Wasted
NHK-1	Nucleosomal Histone Kinase 1
NuRD	Nucleosome Remodeling and Deacetylase complex
NuRF	Nucleosome Remodeling Factor
p-TEFb	Positive Transcription Elongation Factor
PAGE	Polyacrylamide Gel Electrophoresis
PBS	Phosphate Buffer Saline
Pc	Polycomb
PcG	Polycomb Group
PCGF	Polycomb Ring Finger
PEV	Position Effect Variegated
Ph	Polyhomeotic

PHF19	PHD Finger Protein 19
Pho	Pleiohomeotic
Pho-RC	Pho Repressive Complex
PMSF	phenylmethanesulfonylfluoride
PP1	Protein Phosphatase 1
PP2A	Protein Phosphatase 2A
PR-DUB	Polycomb Repressive Deubiquitinase
PRC	Polycomb group Repressive Complex
PRE	Polycomb Responsive Element
Psc	Posterior Sexcomb
PWWP	Pro-Trp-Trp-Pro motif
RA	Retinoic Acid
RNAi	RNA interference
RNAPII	RNA Polymerase II
RNF2	Ring Finger Protein 2
Rpd3	Reduced Potassium Dependency
RYBP	RING1 and YY1 binding protein
SAM domain	domain Sterile Alpha Motif domain
SAM	S-adenosyl Methionine
Scx	Sexcomb Extra
Scm	Sexcomb on Midleg
Scr	Sexcomb Reduced
SDS	Sodium Dodecyl Sulfate
SET	Su(var)3-9 E(z) Trithorax
SILAC	Stable isotope labeling by amino acids in cell culture
Su(var)3-9	Suppressor of variegation 3-9
Su(z)12	Suppressor of zeste 12
SUMO	Small Ubiquitin-like Modifier
SWI/SNF	SWItch/Sucrose Non-Fermentable
TAD	Topologically Associating Domain
TAP	Tandem Affinity Purification
TBP	TATA-box binding protein
TFIID	Transcription Factor II D
TRR	Trithorax-related
TRX	Trithorax
TrxG	Trithorax Group
TSS	Transcription Start Site
Ubx	Ultrabithorax
USP16	Ubiquitin Specific Peptidase 16
UTX	Ubiquitously transcribed tetratricopeptide repeat, X chromosome
VEFS	VRN2- EMF2-FIS2-SUZ12 domain
VRN2	VERNALIZATION2
ZRF1	Zuotin-related Factor 1

Histone H3 Serine 28 is essential for efficient PcG-mediated gene repression in *Drosophila*.

Thesis Summary

Philip Yuk Kwong YUNG / CAVALLI Lab

Polycomb group (PcG) proteins are chromatin modifiers that preserve cellular identities by maintaining the repressive states of key developmental genes. Canonical PcG targets includes Homeotic (Hox) gene complexes, which are clusters of genes encoding transcription factors specifying cell fates along the anterior-posterior axis of segmented animals. Mutations in PcG genes result in derepression of Hox genes, leading to homeosis characterized by the transformation of one body segment into another. Central to the PcG function is the deposition of the repressive histone mark H3K27me₃, which can be regulated by a juxtaposed phosphorylation on H3S28. H3S28ph on one hand counteracts chromatin binding of PcG proteins, while on the other hand it shields H3K27me₃ from demethylation. Besides, H3S28ph is deposited by the mitotic Aurora B kinase and, like H3S10ph, it is highly enriched during mitosis. As such, H3S28ph might represent a cell-cycle link between PcG repression and epigenetic inheritance. To assess the importance of H3S28ph, we have generated a *Drosophila* mutant model in which the endogenous source of histone H3 is replaced with a non-phosphorylatable form of H3 (H3S28A) where the serine residue is substituted with an alanine.

Mosaic analysis of *H3S28A* clones in larval imaginal discs revealed a near-complete depletion of H3S28ph on mitotic chromosomes while bulk H3 and H3S10ph levels remained unchanged, as compared to the surrounding tissues or clones supplied with wild type H3 transgenes. Strikingly, all methylation states at H3K27 dropped drastically in *H3S28A* clones, while active chromatin marks such as H3K4me₃ are unaffected. Although nuclear staining patterns of polycomb (Pc) and polyhomeotic (Ph) proteins were not affected, *H3S28A* clones derepressed Hox genes and adult tissues developed homeotic transformations.

In vitro histone methyltransferase assay suggested that, while H3K27me₃S28A retained normal stimulatory effect on PRC2 activity assayed on nucleosomes reconstituted using

wild type recombinant histones, recombinant H3S28A nucleosomes appeared to be a suboptimal substrate for PRC2. Hence the observed phenotypes in *H3S28A* mutant *in vivo* could be in part caused by intrinsic structural defects introduced by the alanine substitution, in addition to the lack of H3S28ph.

Collectively, our data indicate an essential role of H3S28 in the catalysis of H3K27 methylation and its potential modes of action are discussed.

La sérine 28 de l'histone H3 joue un rôle essentiel dans la répression des gènes dépendante des protéines PcG chez la drosophile.

Résumé de la thèse

Philip Yuk Kwong YUNG / CAVALLI Lab

Les protéines du groupe Polycomb (PcG) sont des modificateurs chromatinien qui préservent l'identité cellulaire en maintenant la répression de gènes développementaux clés. Les cibles canoniques des protéines PcG incluent les complexes Homéotiques (Hox), des clusters de gènes codant pour des facteurs de transcription établissant l'identité des cellules le long de l'axe antéro-postérieur des animaux segmentés. Des mutations des gènes PcG conduisent à la dérégulation des gènes Hox, entraînant un changement d'identité de segments corporels. Le dépôt de la marque répressive H3K27me3 est le mécanisme fondamental de la répression PcG-dépendante. Cette modification d'histone peut être régulée par la juxtaposition d'une phosphorylation sur le résidu voisin, H3S28. Cette dernière modification, H3S28ph, empêche d'une part la fixation des protéines PcG et, d'autre part, protège la marque H3K27me3 de la déméthylation. H3S28ph est déposée par la kinase Aurora B et, de même que H3S10ph, elle est fortement enrichie au cours de la mitose. H3S28ph pourrait donc établir le lien entre répression dépendante de PcG et mémoire épigénétique à travers la division cellulaire. Afin d'étudier l'importance de H3S28ph, nous avons mis au point un modèle mutant de drosophile dans lequel nous avons remplacé la source endogène d'histone H3 par une forme non-phosphorylable (H3S28A), en substituant le résidu sérine 28 par une alanine.

L'analyse des clones mutants *H3S28A* dans des disques imaginaux d'yeux mosaïques révèle une disparition presque complète de H3S28ph tandis que le niveau global de H3S10ph reste inchangé. De manière frappante, tous les niveaux de méthylation de H3K27 diminuent drastiquement dans les clones mutants *H3S28A*, tandis que les niveaux des marques de chromatine active telle que H3K4me3 ne sont pas affectés. En conséquence, les gènes Hox sont dérégulés dans les clones mutants *H3S28A* et les tissus adultes développent des transformations homéotiques, sans que les profils d'immunomarquage

nucléaire de polycomb (Pc) et polyhomeotic (Ph) soient affectés.

Les tests *in vitro* de l'activité histone-méthyltransférase montrent, d'une part, qu'un peptide mutant H3K27me3S28A conserve sa capacité à stimuler l'activité de PRC2 sur des nucléosomes reconstitués et, d'autre part, que des nucléosomes reconstitués comportant la mutation H3S28A sont un substrat que PRC2 méthyle moins efficacement que les nucléosomes non mutés. Ainsi, les phénotypes observés dans des mutants *H3S28A in vivo* pourraient s'expliquer en partie par des défauts intrinsèques de structure des histones introduits par la substitution de la sérine 28 en alanine, en plus de l'absence de la phosphorylation H3S28ph.

Dans leur ensemble, ces résultats révèlent un rôle essentiel de H3S28 dans la catalyse des méthylation de H3K27 et les potentiels mécanismes d'action sont discutés.

Chapter I

Introduction

1. **Overview of chromatin biology & epigenetics**
2. **Histone Modifications**
3. ***Drosophila* Polycomb Group (PcG) Proteins - Components & Functions**
4. **Mechanisms of PcG-mediated Gene Repression**
5. **Mechanisms for Derepression of PcG Target Genes**
6. **Modulation of PcG Repression Activity**
7. **Epigenetic Inheritance of PcG-mediated Gene Repression**

1. Overview of chromatin biology and epigenetics

The genetic materials presented as long threads of DNA are organized as chromatin within the confined space of eukaryote nuclei. Specifically, small basic proteins known as histones constitute the fundamental packaging materials of our genome. There are five canonical histones namely the linker histone H1, and the core histones H2A, H2B, H3 and H4¹. Two H2A-H2B dimers assembled with a H3-H4 tetramer to form a histone octamer. A nucleosome core particle is formed with a DNA thread spanning 147 bp wrapping around the histone octamer for 1.67 turns. DNA fragments connecting adjacent nucleosomes are referred as linker DNA on which linker histone H1 can bind and regulate chromatin compaction. As such nucleosome represents the basic packaging unit of eukaryotic genome, and together with other chromatin-bound factors, successive nucleosomal arrays can be folded into higher order structures. Nucleosome occupancy of the underlying DNA sequence represents a general accessibility barrier to trans-acting factors. And since the first characterization of reversible acetylation on histone tails, we now recognize that histone proteins can capacitate a great variety of chemical modifications to elicit specific functions². This constitutes the histone code hypothesis³ in which specific histone modifications acting either individually or in a combinatorial manner to recruit specific trans-acting factors to trigger proper downstream responses. For less than two decades, a number of histone code writers (enzymes catalyze specific histone modifications), readers (proteins with specialized motif recognizing particular histone modification) and erasers (enzymes that remove specific histone modifications) are identified and are implicated in virtually any DNA-templated processes ranging from DNA replication, transcription, DNA repair and more. In Chapter I (p.2-30), a selection of histone modifications implicated in transcriptional control and mitosis are discussed. Apart from histone modifications, nucleosome occupancy, DNA methylation, histone variants, non-coding RNAs and nuclear organizations all together constitute extra layers of chromatin information to regulate various DNA metabolism¹. Such information plays pivotal roles to instruct cellular differentiation. In metazoans, all cells share the same genomic blueprint and yet specialized cell types are epigenetically defined by the underlying unique transcription programs during differentiation. The polycomb group (PcG) and trithorax group (trxG) proteins, first discovered in *Drosophila*, represent one of the best-documented examples of epigenetic inheritance⁴⁻⁸. Specifically, the Hox genes

expression patterns are established during early embryogenesis by specific interactions of transcription regulators. These expression guidelines disappeared at the later stages of development. Since then, PcG proteins maintain repressive chromatin states and trxG sustain active chromatin features of Hox genes through adulthood. Mutations in either PcG or trxG components distort epigenetic memory and lead to homeosis, as characterized by transformation of one body segment identity into another. Introduction of individual PcG components and how their repressive activities are elicited and regulated will be covered in Chapter I (p.31-74). How PcG proteins preserve repressive chromatin states along the cell cycle presents a challenging question that, only until recently, we begin to have molecular description of epigenetic inheritance, please refer to Chapter I (p.75-85) for details. Given the broad implications of epigenetic regulators in differentiation and diseases, lessons learnt from the PcG system will be transferable to chromatin events and benefits both basic and clinical research.

2. Histone Modifications

Post-translational modifications of histones represent one of the most central epigenetic regulations of DNA-templated processes. In this chapter, the function of a selection of histone marks (Fig. I) will be discussed in a *Drosophila*-centric view. Examples from other model organisms will also be included when necessary.

2.1 H3K4me

H3K4me is one of the hallmarks of active genes^{9,10}. In *Drosophila*, H3K4me1 is enriched at enhancer regions disregarded of their activity, it also appears at the middle of active genes¹¹. H3K4me2/3 marks are enriched at active gene promoters and TSS^{10,12-14}

Drosophila Trithorax (Trx) and Trithorax-related (Trr) are the principle enzymes that deposit H3K4me1. Both of their SET domains display H3K4me1-specific HMT activity in vitro. And their respective SET domain specific mutants (*trx^{z11}* and *trr³*) individually lead to a partial drop of H3K4me1 level. Combination of both mutants lead to a complete lost of H3K4me1 while render H3K4me3 level normal in *Drosophila* embryo¹⁵. Both Trx and Trr interact with CBP (CREB-binding protein), and in vitro HAT assay suggests that specifically H3K4me1, but not H3K4me2 and H3K4me3, enhances CBP-mediated H3K27ac¹⁵.

H3K4me1 is enriched at enhancers and PREs and since *trx^{z11}* mutant alleviated the transformation phenotype of *Pc³*, it is thought that H3K4me1 counteracts PcG silencing via CBP recruitment and H3K27ac¹⁵. CBP also interacts directly with dUtx, whose H3K27me3 demethylase activity would counteract PcG silencing¹⁶.

Drosophila Set1 protein was identified base on the search for sequence homology to yeast Set1 protein. Affinity purification of FLAG-HA-dSet1 interacting candidates identifies components similar to human and yeast COMPASS complex. And in vitro HMT assay confirmed dSet1 complex catalyzed all methylation states of at H3K4¹⁷. RNAi approach and genetic mutants confirmed that dSet1 was responsible to catalyze H3K4me2 and H3K4me3 *in vivo*^{18,19}. Also RNAi knock down of or mutation in COMPASS components including the TrxG protein Ash2 resulted in reduction of bulk H3K4 methylation states, most notably for H3K4me3¹⁹. Similar to yeast and mammalian models^{20,21}, the putative *Drosophila* H2B ubiquitin ligase dBre1, is required for efficient catalysis of H3K4me3^{18,20,22}.

H3K4me3 interacts with chromatin remodelers Isw1/NURF^{23,24}, Yng1-NuA3 HAT complex²⁵ as well as the basal transcription machinery TFIID²⁶. It also binds Chd1^{27,28}, through which spliceosome components are recruited²⁹. And in response to DNA damage, H3K4me3 of cell proliferation genes recruits ING2 and its associated HDAC complex for gene repression³⁰.

H3K4me1 and H3K4me2 are demethylation substrates of the amine oxidase dLsd1 / Su(var)3-3^{31,32}. Besides, another demethylase known as Lid, specifically removes H3K4me3^{33,34}. Intriguingly, Lid is genetically classified as a TRX group protein which might appear contradictory to the accumulation of H3K4me3 upon loss of function of Lid³⁵. One explanation is that the reader of H3K4me3 Chd1 is diluted upon over-accumulation of this histone mark and hence some of the Chd1 target genes cannot be appropriately activated³⁵. Another explanation lies in the fact that Lid inhibits Rpd3 HDAC, and loss of Lid might liberate Rpd3 and cause excessive deacetylation at H3K27 and favor ectopic PcG gene repressions³⁴.

Since H3K4me decorates active genes across the genome, it is expected to play a vital role in active transcription. However, a recent histone replacement study of combined non-methylatable *H3K4R* mutations on both H3.2 and H3.3 showed no deregulation of Hox genes and developmental regulators expression. This observation challenges the essential necessity of H3K4 methylation or it hints functional redundancy from other histone modifications³⁶.

2. 2 H3K9me

H3K9me decorates condensed heterochromatin in the fly genome, notably in the pericentromeric regions, the telomeres and the arms of chromosome 4. In a classical *Drosophila* model of position effect variegation³⁷⁻³⁹, the white gene required for red eye pigment synthesis is placed in proximity to the pericentromeric region as a result of chromosome rearrangement. The spreading of pericentromeric heterochromatin leads to varied degree of silencing of the white gene and hence a variegated eye color³⁷⁻³⁹. Enhancer and suppressor genetic screens based on this PEV model identify many players regulating heterochromatin biogenesis. Among them are the Suppressor of variegation 3-9, Su(var)3-9, the first characterized H3K9-specific histone methyltransferase⁴⁰ and Su(var)2-5/HP1, the chromodomain-containing reader of H3K9me2/3^{41,42}.

In addition to Su(var)3-9, dG9a is another H3K9 HMT⁴³⁻⁴⁵. In *Drosophila* germlinum, H3K9me3 is catalyzed by both Su(var)3-9 and dSETDB1/Eggless, with the latter HMT specifically required for germ cell pericentromeric H3K9me3 deposition⁴⁶. Notably, loss of germ cells H3K9me3 in eggless mutant resulted in sterility while double mutant of Su(var)3-9 and dG9a was fertile, despite a drastic reduction of all H3K9 methylation states⁴³. While in somatic tissue, dSETDB1 is primarily responsible for H3K9me3 on the arm of chromosome 4.

H3K9me3 level also depends on the RNAi machinery⁴⁷. In *Drosophila*, mutant of RNAi machinery showed a reduction of H3K9me3 and a diffused localization of HP1⁴⁸. It is demonstrated that pericentromeric H3K9me3 recruits HP1 via its chromodomain to establish heterochromatin^{41,42}, which is essential for kinetochore assembly and sister chromatids cohesion^{49,50}. Consistent with this idea, compromised pericentromeric heterochromatin leads to chromosome segregation defects^{51,52}. HP1 also helps to recruit and activate dKDM4A activity to regulate H3K36me3 level on heterochromatic genes^{53,54}. Recently, it is reported that Su(var)3-9 interacts with linker histone H1 to induce heterochromatin silencing on *Drosophila* transposable elements⁵⁵.

Finally, H3K9me3 can be removed by the dual-specific demethylases dKDM4A and dKDM4B, both of them also target H3K36me3^{56,57}.

2.3 H3K36me

Drosophila H3K36me is associated with active transcription and decorates along the gene body⁵⁸, with H3K36me2 peaks located in proximity to the promoter and higher level of H3K36me3 concentrated at 3' end of the gene. Both methylation marks are enriched on the histone variant H3.3^{11,59}.

Ash1, dSet2 and dMes4 are the primary enzymes for H3K36 methylations in *Drosophila*⁵⁹⁻⁶¹. dSet2 interacts with elongating RNA polymerase II (RNAPII)⁶⁰ and deposits H3K36me3 co-transcriptionally⁵⁸. RNAi against dSet2 in cultured cells and larva suggested that dSet2 primarily acted on premethylated histone to catalyze H3K36me3. It is believed that methylation of H3K36 by dMes4 provides a substrate for dSet2^{58,62}.

As a TrxG protein, Ash1 was once considered to deposit H3K4me3 in counteracting PcG silencing^{63,64}. However, in vitro HMT assay with the use of histone lysine scanning mutations and a larger purified SET domain clarified Ash1 catalytic activity as an H3K36-specific HMT⁶¹.

Lessons from yeast show that H3K36me inhibits ectopic transcription initiation from cryptic promoters within the gene body via various mechanisms. H3K36me recruits Rpd3S HDAC via the chromo-domain of Eaf3 to deacetylate H3 and H4 along the 3' end of the transcribing ORF to avoid cryptic transcription initiation the gene body^{65,66}. H3K36me also blocks the association of Asf1, to avoid exchange of preacetylated histones into the 3' end of the transcribing gene body⁶⁷. Besides, H3K36me recruits chromatin remodelers Isw1b, which acts together with Chd1 to prevent trans-histone exchange and inhibits incorporation of acetylated histones into the gene body^{68,69}.

H3K36me3 might also have a repressive function. In mammalian cells, the PWWP domain of DNMTA3 is recruited to H3K36me3 for DNA methylation⁷⁰. Besides, Tudor domain of mammalian Pcl homologs specifically recognizes H3K36me3 and is implicated in chromatin targeting of PRC2 repressive complex⁷¹⁻⁷⁴.

H3K36me is a substrate of the demethylases Kdm2A/B⁷⁵⁻⁷⁷ and Kdm4A/B^{53,54,56}. Intriguingly both *Drosophila*⁷⁷ and mammalian Kdm2B is a component of a non-canonical PRC1 complex. Mammalian Kdm2 harbors a CXXC domain, which binds unmethylated CpG islands and is implicated in targeting PRC1/2 complex⁷⁸⁻⁸¹ (See Chapter I, p.37). In addition, H3K36me3 was shown to inhibit PRC2 activity, as discussed in Chapter I, p.70.

2. 4 H3K79me

Drosophila Grappa is the yeast Dot1 homolog that is responsible for H3K79 methylations⁸². Grappa was recovered in a genetic screen as a suppressor of PcG silencing. A mini-white transgene is normally repressed under the control of the PRE-Mcp element. However, derepression of the white gene was observed in *gpp*^{1A} mutant background. Also, some of the heteroallelic combinations of grappa mutants showed arista-to-leg transformation. These phenotypes placed Grappa as a PcG gene⁸². However, some transheterozygote of grappa mutations also displayed TrxG phenotype, such as decoloration of posterior male tergites, an indication of abdominal transformation into anterior identity⁸². H3K79me level was developmentally regulated. It is undetectable in stage 4 *Drosophila* embryos by immunostaining and gradually accumulates in the later stage of embryogenesis⁸².

Genomic distribution of H3K79me3 correlates well with active transcription⁸³. In line with its genomic profile, mammalian DOT1L homolog was isolated in a complex with P-TEFb⁸⁴. A recent ChIP-seq study using FACS-sorted *Drosophila* mesodermal cells suggested that H3K79me3 cover the gene body of active genes as a broad peak. In addition, enrichment of H3K79me3, along with high level of H3K27Ac and Pol II occupancy appeared to be the signature of active enhancers in *Drosophila*¹¹.

In yeast, H2B mono-ubiquitination is required for trimethylation of H3K79⁸⁵. This mechanism seems to be conserved in *Drosophila*. In homozygous mutant embryo of dBre1, the *Drosophila* E3 ligase for H2B, H3K79me3 was reduced while mono- and dimethylation at H3K79 were not affected⁸⁶.

Studies from yeast and mammals suggest that H379me is cell cycle regulated⁸⁷. Finally, the identity of H3K79-specific demethylase remains unknown.

2.5 H3K27me

Catalysis

Four independent research effort identified PRC2 as the H3K27-specific HMT⁸⁸⁻⁹¹. In *Drosophila*, immunoprecipitate of ESC was detected with H3-specific HMT activity⁸⁹. Chromatography and affinity purification from embryos of either wild-type⁸⁹ or FLAG-ESC harboring transgenic flies⁸⁸ unequivocally identified Su(z)12, E(z), Nurf55 and Esc as the core components of PRC2. Importantly, E(z) alone is inactive⁴⁰ while complete reconstitution of the 4-component dPRC2 from insect cells exhibits robust HMT activity on nucleosomal substrate⁸⁸. The enzyme was not active on H3K27A mutant histone and Edman degradation on PRC2-treated polynucleosomes revealed H3K27 as the radiolabeled residue. These strongly argue H3K27 as the methylation target of dPRC2. Parallel studies in mammalian models using extensive chromatographic fractionation⁹⁰ and affinity purification⁹¹ also identified PRC2 as the H3K27 HMT. All studies established that Su(z)12, E(z), Nurf55 and Esc as the conserved core PRC2 components in *Drosophila* and mammals. Importantly, some accessory factors such as the histone deacetylase Rpd3^{89,92} and AEBP2⁹⁰ were also co-purified with PRC2.

The highly conserved SET domain of E(z) is essential for H3K27 methylation, mutation of which abolished HMT activity in vitro and failed to restore HOX gene silencing in E(z)-null mutant fly⁸⁸. Similarly, heat-inactivation of a temperature-sensitive E(z)⁶¹ mutant results in lost of H3K27me2 (⁹⁰) and derepression of HOX genes⁹³.

Consistent with the in vitro data, lost of function of individual PRC2 component such as E(z), Esc and Su(z)12 lead to reduction of H3K27me and derepression of HOX genes as tabulated below:

Loss of H3K27me associated with PRC2 mutants in <i>Drosophila</i>			
PRC2 components	Reference	Mutant examined	Phenotypes
E(z)	90	<i>E(z)⁶¹</i>	Western blot. Heat inactivation at 29°C leads to a complete loss of H3K27me2
	94	<i>E(z)⁶¹</i>	Western blot on embryo extracts. Heat inactivation at 29°C leads to a complete loss of H3K27me2 and H3K27me3
	95	<i>E(z)⁷³¹</i>	IF homozygous mutant clones in wing disc. Drop of H3K27me1 and H3K27me3.
Su(z)12	95	<i>Su(z)12⁴</i>	IF homozygous mutant clones in wing disc. Drop of H3K27me1 and H3K27me3.
	96	<i>Su(z)12¹</i>	IF homozygous mutant clones in wing disc. Drop of H3K27me3.
Esc	94	<i>esc²/esc¹⁰</i>	Western blot on embryo extracts detected a complete loss of H3K27me2 and H3K27me3.
Nurf55/Caf1	97	<i>Caf1^{long}</i> (missense) <i>Caf1^{short}</i> (null)	IF of mosaic Caf1 clones (missense or null) showing reduction of H3K27me3 in eye-antenna discs and wing discs.
Pcl	95	<i>Pcl^{21M22}</i>	IF homozygous mutant clones in wing disc. Small reduction of H3K27me3 but normal staining for H3K27me1.

Substrate preference of PRC2 - H3.2 vs. H3.3

A recent study in plants revealed enzymes (ATXR5, ATXR6) dedicated to monomethylation of H3K27⁹⁸. It was shown that replication-coupled deposition of H3.1 (analogous to the canonical H3.2 in *Drosophila*) is the preferred substrate for H3K27me1,

since the Thr31 residue of the transcription-coupled H3.3 inhibited both ATXR5/6 activities⁹⁹. Similarly, *Drosophila* and human H3.3 embodied a conserved hydrophilic Serine residue at position 31. However, dPRC2 seems to show less stringent substrate preference between H3.2 and H3.3. A *Drosophila* genetic system replacing endogenous H3.2 with H3.3 was shown to support normal embryogenesis. And clonal replacement of all H3.2 with H3.3 in wing imaginal disc displayed normal Ubx repression, it suggested that dPRC2 can act on H3.3, although H3K27me3 level was not determined in such experiment³⁶. However, introducing H3K27R (H3.2) mutation with the same genetic system was sufficient to almost deplete bulk H3K27me3 level¹⁰⁰. This suggests that the endogenous H3.3 is not the physiological substrate for dPRC2. It could be explained by the genomic distribution pattern of H3.3, which mainly covers active genes enriched with H3K4me2 and Pol II occupancy¹⁰¹ and hence H3.3 nucleosomes are not a natively available substrate for dPRC2.

Mammalian PRC2 also did not discriminate H3.1 and H3.3 histone isoforms. In-vitro MHT assay showed that PRC2 could methylate both histones presented as a heterotypic H3.1/H3.3 nucleosomal substrate¹⁰².

H3K27me is essential for gene repression.

Since mutations of all PRC2-specific components lead to Hox gene derepressions and homeotic transformations^{94-97,103}, it is suspected that H3K27me3 is the key substrate for PRC2 to elicit gene repression. This idea cannot be vigorously tested until the introduction of *Drosophila* histone replacement system¹⁰⁴ (See Chapter II, p.94) in which transgenes carrying various histone mutants are introduced at ectopic sites to replace the endogenous source of histones. As expected, *Drosophila* H3K27R mutant phenocopied E(z) mutant and shared the same Hox derepression profiles. This study consolidated the role of H3K27me3 as a key repressive mark¹⁰⁰. It is believed that H3K27me3 recruit PRC1 to assemble higher order chromatin and inhibit transcription^{88-91,105,106}. Recent advancement of chemical mimics on histone methylations¹⁰⁷ and full reconstitution of chromatin-templated in vitro transcription assay could further specify the mechanistic role of H3K27me3 in gene repression.

H3K27me has been implicated in other functions. The H3K27me1-specific reduction in plant *atxr5/6* double mutant is associated with chromatin decondensation, derepression of heterochromatic transposable elements⁹⁸ and rereplication of heterochromatin¹⁰⁸.

H3K27me3 readers

The chromodomain of Pc specifically recognizes H3K27me3^{90,91,105,106} and mutation on such chromodomain reduced polycomb association on polytene^{109,110} and lead to a lost of polycomb accumulation as nuclear bodies¹¹¹. Consistent with its role of reading repressive histone methylations, these mutants displayed homeotic transformation¹¹¹. Based on Pc recognition of PRC2-deposited H3K27me3, the field has been dominated by the dogma of one direction PRC2-PRC1 chromatin recruitment model, which is recently challenged. Using reconstituted oligonucleosomes decorated with PRC1 cognate histone mark H2AK119ub as bait, the entire PRC2 complex can be affinity purified. This suggests the opposite recruitment hierarchy¹¹².

The beta-propeller domain of ESC can also recognize H3K27me3, and such interaction robustly stimulates PRC2 HMT activity. This constitutes an enzymatic positive-feedback loop that is believed to be important to preserve PcG repressive chromatin during DNA replication¹¹³ (See Chapter I, p.75).

Genomic distribution profile of H3K27me

Array-based and deep-sequencing ChIP experiments revealed H3K27me3 covered the *Drosophila* genome as broad domains encompassing PRE, transcriptional units and regulatory regions of repressed genes^{13,14,114-116}. In contrast, genomic profiles of PRC1 and PRC2 components appeared as sharp peaks at PREs within H3K27me3 domains. Pc and H3K27me3 occupy over 200 domains across the *Drosophila* genome, their distribution negatively correlates well with gene activity.

Extensive epigenome studies in *Drosophila* suggest that repressive H3K27me3 is almost mutually exclusive from active mark such as H3K4me3^{13,14,114-116}. One strong exception is exemplified in mammalian embryonic stem cells where both functionally antagonistic modifications coexist as “bivalent” domains covering promoter regions of key developmental genes¹¹⁷. It is proposed that such bivalent signature on one hand represses lineage commitment genes to sustain pluripotency, and at the same time potentiates them at a poised state competent for robust activation¹¹⁸. Recent biochemical effort clarifies the molecular nature of bivalency where repressive H3K27me3 and active marks reside on separate H3 tails as asymmetrically modified nucleosomes¹¹⁹⁻¹²¹.

Importantly, comparative ChIP assay using wing vs. haltere disc samples showed that all PRC1 components and Su(z)12 binds to PREs at the Ubx locus in both transcriptionally repressed (wing discs) and active states (haltere discs) of Ubx¹²². Similarly, recent ChIP-seq experiment using FACS-sorted parasegment PS7-specific nuclei showed that Pc, Ph and Su(z)12 are recruited to actively transcribed Hox genes devoided of H3K27me3¹¹⁴. This indicates that genomic bindings of Pc and Ph are not the absolute determinant of gene repression and they can be recruited to PRE independent of H3K27me3. Since Su(z)12 is recruited to PRE without H3K27me3, it might suggest PRC2 associates with chromatin as a poised state¹²³, and its HMT activity depends on local chromatin environment¹¹⁴ (See Chapter I, p.73).

H3K27me demethylases

Guided with sequence homology with the JmjC domain⁷⁵, the proteins UTX, JMJD3 and UTY are suspected to be the H3K27 demethylases. Based on in-vitro demethylation assay, UTX and JMJD3 were shown to possess H3K27me3 and H3K27me2 demethylation activity¹²⁴⁻¹²⁸ while UTY was proved to be inactive^{126,127}. Depending on protein purification method and the type of histone substrates, UTX is show in some case to demethylase H3K27me1 on peptide or calf bulk histones^{126,127}.

ChIP profile reveals UTX enrichment in human HOX loci as sharp peaks downstream of TSS of both active and silent HOX genes. Consistent with its role as a demethylase, UTX binding profile matches a sharp drop of H3K27me3 level, even within the broad coverage of H3K27me3 domain¹²⁶.

Overexpression of UTX led to the drop of both H3K27me2 and H3K27me3 levels¹²⁵⁻¹²⁷. In ES cells, RA-induced differentiation is accompanied with activation of some Hox genes. The promoter regions of these genes recruit UTX and lose H3K27me3 and E(z) occupancy, and at the same time H3K4me3 level accumulates. However, upon RNAi against UTX, H3K27me3 and H2AK119Ub levels increase at their promoter region, resulting in a drop of HOX gene expression^{125,128}.

Notably, morpholinos knockdown of UTX in zebrafish embryo resulted in developmental defects in posterior somite regions where the responsible HOX genes expression levels are diminished¹²⁶. Also, mutation in one of the worm JMJD3 homologues displayed gonad disorganization¹²⁵. These highlight the important role of H3K27me demethylase in metazoan development.

dUtx

The *Drosophila* genome encodes a conserved UTX gene with the characteristic TRP and JmjC domain. Purified dUtx from insect cells only demethylates H3K27me3 and H3K27me2 but not H3K27me1 and other repressive or active histone marks. Consistent with studies in mammalian models, such in-vitro demethylase activity requires intact JmjC domain¹²⁹. However, there are discrepancies between publications concerning the characterization of dUtx in *Drosophila*.

Discrepancy on the effect of dUtx on H3K27me3 level: Loss of function study

RNAi against dUtx in S2 cells¹⁶ or in flies¹²⁹ with the use of ubiquitous Act5C-Gal4 drivers, both showed a mild increment of H3K27me3 level in cells and adult protein extracts, respectively. Importantly, lethality rates and adult phenotypes of such RNAi experiment were not mentioned! Since one would expect ectopic repression of PcG targets or Trx-like transformation phenotypes as a result of a global increase of H3K27me3 level. Subsequent mosaic analysis *dUtx*¹ mutant (with a premature STOP codon within the JmjC domain) clones also find increased H3K27me3 level in eye disc¹³⁰ and testis¹³¹.

However, re-evaluation of the mosaic analysis of *dUtx*¹ mutant and a newly generated molecular null mutant *dUtxΔ*, suggested that global levels of H3K27me3, H3K27Ac and H3K4me1 were indistinguishable from neighboring WT cells in wing discs¹³². Besides, western blot analysis using serially diluted samples from larval imaginal discs and brain extracts of *dUtx*¹/*Df(2L)BSC143* and *dUtxΔ*/*Df(2L)BSC143* transheterozygotes, failed to detect any noticeable differences in global levels of H3K27me3, H3K27Ac and H3K4me1, when compared to control wild-type extracts¹³².

Discrepancy on the effect of dUtx on H3K27me3 level: Gain of function study

Western blot analysis detected a drop of H3K27me3 level in adult extracts upon ubiquitous overexpression of dUtx with strong tub-Gal4 driver¹⁶. However, en-Gal4 driven overexpression of dUtx in the posterior compartment of wing disc fails to cause any noticeable changes in H3K27me3 level¹³⁰.

Discrepancy on the role of dUtx as a tumor suppressor

Using the MARCM system (Mosaic analysis with a repressible cell marker)¹³³, clones of homozygous *dUtx*¹ mutant showed over-proliferation in the eye-antenna disc and the corresponding adult eyes show rough and disorganized ommatidia development. Based on these data, the authors claimed that dUtx as a potential tumor suppressor¹³⁰. However, MARCM study of the same *dUtx*¹ allele or another molecular null allele *dUtxΔ* failed to

show over-proliferation¹³²! Importantly, only homozygous *dUtx^l* exhibits very low adult survival rate (<10%), this is in total contrast to other transheterozygous allelic combination, including homozygous *dUtxΔ*, all of which have a adult survival rate over 60%! In light of these discrepancies, it is worth suspecting a 2nd site mutation in the *dUtx^l* background; likely reside on the same chromosome arm as *dUtx*¹³². It is also possible that *dUtx^l* is a recessive gain-of-function allele where the premature STOP codon in the JmjC domain encodes a truncated protein that interferes with normal cellular functions.

The latest study suggests that the dUtx demethylation activity on H3K27me3 is specifically required during early embryogenesis¹³². Over 60% of homozygous zygotic mutants of *dUtxΔ* develop into adulthood without recognizable structural or cuticle defects, despite having a short life span. Intriguingly, maternal and zygotic *dUtxΔ* homozygotes mostly died at the end of embryogenesis with ectopic repression of Abd-B, those survived to L3 larval stage displayed patchy repression of Ubx in haltere discs. Unfortunately for both conditions of ectopic repression of Hox genes in embryos and imaginal discs, the level of H3K27me3 is not determined¹³². It is then difficult to reconcile these phenotypes with the suspected demethylase activity of dUtx.

Notably, *dUtxΔ* oocyte fertilized by WT dUtx sperm completely rescued lethality with a significant fraction (~30%) of the adult males displayed lost of A5 abdominal tergites pigmentation, indicating an A5 to A4 transformation reminiscent of *trx*-like phenotype¹³². Based on these data, the authors propose that dUtx is specifically required during early embryogenesis to oppose PcG silencing and it's role in H3K27me demethylation diminishes in later stage of development¹³². This early time window requirement of dUtx might explain the fact that no mutation on dUtx has even been identified as modifier of PcG silencing in classical genetic screens. Alternatively, the lack of *trx*-phenotypes in zygotic *dUtxΔ* mutant might suggest the existence of another H3K27me demethylase operates in later stage of development.

2. 6 H3K27Ac

Drosophila CBP is responsible for H3K27Ac. Recombinant CBP acetylates both H3K27 and H3K18 in vitro. In agreement with the in-vitro data, RNAi against CBP in S2 cells leads to reduction of both H3K27Ac and H3K18Ac¹³⁴.

HDAC activity is found to be associated with the immunoprecipitates of EED and Ezh2¹³⁵, and *Drosophila* HDAC1 Rpd3 was co-purified with PRC2 components^{89,92,136}. Subsequent experiment using RNAi against Rpd3 in S2 cells showed an increase in H3K27Ac. These suggest Rpd3 involvement in H3K27Ac deacetylation¹³⁴.

Genetics evidences also suggest a role of Rpd3 in PcG silencing. Ubx PRE-mediated repression of mini-white reporter gene was alleviated in Rpd3 mutant background, the resulting flies showed variegated eye color, as opposed to the strong PcG silencing and white-eye phenotype in wild-type background¹³⁶. Besides transheterozygotes of several Rpd3 alleles and particularly *Pc⁴/Hdac1*³²⁶ double heterozygotes showed extensive Ubx derepression in larval wing discs¹³⁷. Besides, both Rpd3 and dMi-2 associate as components of the NuRD complex. Importantly, dMi-2 also shows extensive genetic interactions with PcG proteins. Combined dMi-2 and PcG mutants synergize Hox derepression in both embryos and imaginal discs¹³⁸.

It is suspected that NuRD/Rpd3-mediated deacetylation of H3K27Ac facilitates PRC2-mediated H3K27 methylation and gene repressions. This idea is elaborated by a study in mammalian model. In ES cells, a subset of PcG targets with bivalent domains overlap with NuRD, and loss of a NuRD structural component in ES cells reduced PRC2 occupancy at these bivalent promoter¹³⁹, accompanied with a reduction of H3K27me3 level.

Genomic distribution of H3K27Ac appeared as broad domains well separated from H3K27me3. In *Drosophila* cultured Sg4 cells clonally derived from late embryos, Abd-B is active while all others Hox genes within the BX-C cluster are silenced. H3K27Ac covers only Abd-B and neatly separated from the broad repressive domain of H3K27me3 over the more anterior Hox genes¹⁴⁰. The counteracting nature between H3K27Ac and H3K27me3 is also exemplified in a reverse situation. In parasegment PS7 where only the anterior Hox genes Ubx and abd-A are expressed, they gain H3K27Ac, while the posterior Abd-B is covered with H3K27me3 and remained silenced¹¹⁴. In general, binding of TrxG proteins ASH1/TRX-NT are highly enriched with H3K27ac that spreads across both upstream and downstream of target genes. H3K27Ac domains without ASH1/TRX-NT tend to be more

confined as narrow peak slightly downstream of TSS. Importantly, active enhancers are particularly enriched with H3K27ac, H3K79me3 and Pol II¹¹.

Loss of individual PRC2 component (Ezh2, SUZ12 or EED) in ES cells¹⁴¹ or RNAi against E(z) in *Drosophila* S2 cells¹³⁴ depletes H3K27me3 with a concomitant global increase of H3K27Ac. This might suggest H3K27Ac involvement in transcriptional activation. Despite strong association of H3K27Ac with gene activity, its essential role in transcription activation has been challenged with the study of *H3K27R* histone mutant in *Drosophila*, where H3K27 can neither be methylated nor acetylated. Given the *H3K27R* mutant phenocopies the loss of E(z) with the same depression profiles of Hox genes, it suggests that ectopic Hox activation can occur without H3K27Ac. Hence H3K27Ac might function primarily in counteracting PcG silencing, potentially by blocking the lysine residue for methylation. In addition, there is evidence suggesting that H3K27Ac can directly inhibit PRC2 HMT activity¹⁰².

2. 7 H2AK119Ub

In mammalian cells, H2A is ubiquitinated at K119 while *Drosophila* H2A is modified at K118. To avoid confusion, I omit the specification of the amino acid residue and use H2Aub for both systems.

In an effort to identify H2A-specific E3 ligase, an in vitro ubiquitination assay was set up, with the use of E1, E2, ATP, FLAG-Ubiquitin, nucleosomal substrates and HeLa cells nuclear extracts. Exhaustive chromatographic purification isolated potential H2A E3 ligases, which were found by mass-spectrometry to be Ring1 (herein Ring1a) and Ring2 (herein Ring1b), the homolog of *Drosophila* dRing/SCE¹⁴². Subsequent IP-MS approach using anti-Ring1a antibody identified Ring1a, Ring1b, Bmi1 (homolog of *Drosophila* PSC) and HPH2 (homolog of *Drosophila* Ph). Notably PC is not isolated in such complex. Recombinant Ring1b, not Ring1a, and dRing showed RING-finger dependent E3 ligase activity on H2A¹⁴². Also, siRNA knockdown of Ring1b led to a drop of H2Aub level in HeLa cells. Similarly, conditional deletion of Ring1b in mouse ES cells also resulted in drastic reduction in H2Aub¹⁴³. Consistent with the E3 ligase activity, ChIP assay showed co-occupancy of dRing and H2Aub at the bxd PRE and immediate downstream of the TSS of Ubx in *Drosophila* wing discs and SL2 cells. Upon RNAi against dRing, Ubx was derepressed in SL2 cells and both H2Aub and Pc were lost from bxd PRE. Notably, ChIP signal of H3K27me3 was not affected in such condition¹⁴²!

The role of dRing as the main H2A E3 ligase is also supported by in vivo studies. RNAi against dRing in *Drosophila* larva abolished global level of H2Aub¹³². Importantly, dRing is found to associated in an alternative complex known as dRAF (dRING-associated factors), which is composed of three core components: dRing, Psc and dKDM2, a H3K36me2 demethylase⁷⁷. Systematic biochemical reconstitution of PRC1 and dRAF demonstrated that dRing alone showed limited ubiquitination activity, which was moderately enhanced by complexed with Psc, probably via heterodimerization of their RING domains^{144,145}, and maximal E3 ligase activity is achieved when dKDM2 is added to the PSC-dRing core. Importantly, adding Pc/Ph to the Psc-dRing complex did not show such stimulatory effect⁷⁷. This strongly argues that dRAF, but not PRC1, as the relevant complex catalyzing H2Aub. Consistent with this idea, RNAi against individual dRAF component, but not Pc or PH, abolished H2A ubiquitination⁷⁷. More recently, it is also demonstrated that ectopic tethering of mammalian PRC2 complex at a defined genomic locus results in establishment of H3K27me3 domain and recruitment of canonical PRC1

complex without catalyzing H2A ubiquitination. This argues against the role of canonical PRC1 in H2Aub deposition⁸¹.

Loss of dRing derepresses key PcG targets such as Hox genes in *Drosophila* embryo and larval wing discs^{16,146}, and mutation in dKdm2 enhances transformation phenotypes of Pc mutant while alleviates that of *trx* mutant⁷⁷. This supports the idea that H2Aub as an important repressive histone mark in the PcG system. However, the exact necessity of H2Aub is yet to be testified by the corresponding histone mutant. Particularly, it was shown that the Hox derepression phenotypes of dRing-null mutant could be rescued even by reintroducing a supposedly E3 ligase-dead allele. Further experiments with reliable anti-H2Aub antibody would be needed to assess to what extent H2Aub is disrupted under such conditions¹⁴⁷. Very recently, TRIM37 was found to be a new H2A E3 ligase which was amplified in some breast cancer cell lines¹⁴⁸. In these cell lines where TRIM37 is overexpressed, canonical PRC1 component Ring1b expression is lowered. Intriguingly, sucrose gradient sedimentation shows comigration of TRIM37 with PRC2 but not PRC1 components. Co-immunoprecipitation and mass-spectrometry methods confirm TRIM37 interactions with core PRC2 components. It was proposed that overexpression of TRIM37 delocalized PRC2 and caused ectopic silencing of tumor suppressor genes.

Genomic distribution of H2Aub

In mammalian models, the Bmi1-Ring1B (analogous to Psc-dRing in *Drosophila*) represents the basal catalytic core for H2A ubiquitination^{144,145}. Using Bmi1-null and wild-type MEF cells, ChIP-seq analysis was performed to define the genomic distribution of Bmi1-dependent H2Aub. H2Aub level peaks over TSS of target genes and is enriched in those promoters covered with H3K27me3. Notably, there is still a substantial fraction of H2Aub regions that do not overlap with H3K27me3. H2Aub target genes exhibit low levels of transcription and are derepressed upon the loss of Bmi1¹⁴⁹. In mouse ES cells, ChIP analysis defines a set of H2Aub target genes that are significantly occupied by Ring1B and H3K27me3. These include the Hox genes and many key developmental regulators¹⁵⁰. At present, there is no data available regarding the genomic distribution profile of H2Aub in *Drosophila*.

Effect on H2Aub in transcription

In mouse ES cells of Ring1A and Ring1B double knockout background, reintroducing catalytically dead Ring1b transgene restored PRC1 occupancy on its target genes and restored chromatin compaction of the Hoxb cluster, despite the lack of H2Aub. However these genes nevertheless gained H3K4me3 and Pol II binding, and derepressed. This suggests that the H2Aub modification is crucial for gene repression¹⁵⁰. Supporting the reciprocal relationship between H2Aub and active chromatin marks, isolated mononucleosomes from *Drosophila* did not show coexistence of H2Aub and H3K36me2⁷⁷. Besides, it was shown that chromatin template reconstituted with H2Aub was inactive substrates for MLL3-mediated H3K4 di- and trimethylation and was refractory to transcription initiation in vitro¹⁵¹. More recently, H2Aub was show to inhibit a broad panel of H3K36 methyltransferases¹⁵² (See Chapter I, p.55).

Effect of H2Aub on chromatin structure

It is postulated that the ubiquitin moiety attached on H2AK119 is positioned in close proximity to the linker histone H1 and hence it might impact chromatin folding¹⁵³. Reconstitution of homogenous 12-mer nucleosomal array using purified H2Aub displayed normal nucleosome assembly and compaction properties as those reconstituted with unmodified H2A. However, H2Aub nucleosomal array requires a lower salt concentration for magnesium-induced oligomerization than the unmodified counterparts. This property indicates that H2Aub chromatin might be more prone for establishing chromosomal contacts¹⁵⁴.

H2Aub-mediated establishment of H3K27me3 domain

It is commonly believed that PRC2-mediated H3K27me3 recruits PRC1 via the chromodomain of PC. This one directional recruitment hierarchy is challenged by recent studies in mammals, which show the seeding of H2AK119ub can establish H3K27me3 domain. Mammalian cells consist of dRAF-like PRC1 variant complex, which is composed of KDM2B, PCGF1 (Psc homolog), Ring1B and some other components. The CXXC zinc finger of KDM2B specifically recognizes non-methylated CpG Island in a genome-wide scale, and serves to target PCGF1-Ring1B core catalytic unit to deposit H2Aub at PcG target sites⁷⁸. Intriguingly, targeted deposition of H2Aub at a defined locus is sufficient to establish a *de novo* PcG domain comprising PRC2 complex, H3K27me3 and canonical

PRC1^{81,155}. Strikingly, loss of Ring1B in ES cells and hence depletion of the accompanied H2Aub, lead to a global reduction of PRC2 occupancy and H3K27me3 level at PcG target sites⁷³. All these data stress the importance of H2Aub in establishing of PcG repressive domains. Supporting this idea, PRC2 complex can be affinity-purified by oligonucleosomes assembled with H2Aub. Importantly, PRC2 HMT activity is higher on H2Aub nucleosomes in the presence of accessory factors Jarid2 and AEBP2¹¹².

Studies from *Drosophila* genetics suggest that both active ubiquitination (by dRAF) and deubiquitination (by PR-DUB, see Chapter I, p.55) is required for efficient PcG silencing. Whether H2Aub deubiquitination is needed for productive H3K27me3 catalysis is not rigorously tested yet. But there are scattered evidence to support this idea. The *Drosophila* PR-DUB complex is conserved in human and the cofactor exists as ASXL1 and ASXL2¹⁵⁶. Loss of ASXL2 in mice hearts led to a global over-accumulation of H2Aub and high level of H3K27me2, accompanied with a reciprocal decrease in H3K27me3. Some of the PcG target genes lost Ezh2 and H3K27me3. These mice displayed skeletal transformation phenotypes with their lumbar vertebra resembled posterior segment features^{157,158}. Likewise, reduction of H3K27me3 level was observed both in histone extracts and on the HoxA locus of human leukemia cell line lacking ASXL1¹⁵⁹. In *Drosophila*, however, it seems global H3K27me3 level, determined by either western blot or immunostaining, is unaffected in dRing¹⁶ and PR-DUB mutants¹⁵⁶. More sensitive assay such as ChIP is needed to better assess the locus-specific impact of H2AUB in regulating H3K27me3 level.

2. 8 H3T3ph & H2AT120ph

Histone H2A can be phosphorylated at T119 and T120 respectively in *Drosophila* and mammals. To avoid confusion, they are all referred to H2Aph unless otherwise specified.

Aurora B is a kinase essential for mitotic progression. Together with Survivin, INCENP and Borealin, Aurora B is assembled into the highly conserved Chromosome Passenger Complex (CPC) that displays distinct subcellular localization during mitosis progression¹⁶⁰. Full kinase activity of AuroraB requires binding to the C-terminus of INCENP and auto-phosphorylation of its activation loop. In addition, it is recently found out that mitotic phosphorylation of H3T3ph and H2AT120ph acts concertedly to activate the AuroraB kinase¹⁶¹.

The BIR domain of Survivin specifically recognizes phosphorylation of H3T3 deposited by the Haspin kinase. The Survivin-H3T3ph binding module thus serves as a targeting mechanism to nucleate CPC accumulation on chromatin for its autoactivation¹⁶²⁻¹⁶⁴. There are controversy concerning whether H3T3ph is centromere-specific¹⁶² or also distributed along chromosome arms^{163,164}. Specific antibody would be needed to clarify this issue. The kinetochore-localized kinase Bub1 phosphorylates H2AT120 to provide a binding site for Shugoshin in centromere¹⁶³. Shugoshin in turn recruits PP2A to protect centromeric cohesion by counteracting Polo-like kinase 1 mediated release of cohesion rings along chromosome arms during prophase¹⁶⁵. Importantly, Shugoshin also serves as a centromere adaptor for CPC¹⁶³. Hence it is proposed that both H3T3ph and H2AT120ph act to target and activate Aurora B kinase at centromere^{161,163}.

Putative Haspin homolog in *Drosophila* is less well characterized and to what extent the H3T3ph-H2AT120ph axis contributes to Aurora B activation and mitotic progressions awaits further investigations. Nonetheless, a recent study of the physical binding properties of MLL5, showed that the *Drosophila* homolog UpSET binding to H3K4me3 is repulsed by juxtapositioned phosphorylation on H3T3¹⁶⁶. This indicated a potential existence of H3T3phK4me3 phosphor-methyl switch. In *Drosophila*, it was initially thought that the Nucleosomal Histone Kinase 1 (NHK-1) was responsible for catalyzing H2AT119ph¹⁶⁷. Later on it is clarified that AuroraB is the H2AT119 kinase. Interestingly, H2AT119ph is distributed rather homogenously in interphase nuclei, other than being excluded from DAPI-dense chromocenter region. Importantly, H2AT119ph signal is restricted to centromere during mitosis¹⁶⁸.

Intriguingly, both juxtaposed lysine residues of H3T3 and H2AT120 can be modified by important epigenetic regulators as active mark H3K4me3 and repressive H2AK119ub respectively. The potential implication of these “double mark” would be discussed in Chapter III, p.137.

2. 9 H3S10ph

Mitotic progression

H3S10ph level is cell cycle regulated. Its strong enrichment during mitosis makes it a reliable mitotic marker from budding yeast to Human¹⁶⁹. From prophase to metaphase, Aurora B kinase deposits huge level of H3S10ph on mitotic chromosomes which are then gradually dephosphorylated upon mitotic exit from late anaphase by G1C7/PP1 in budding yeast and worms¹⁷⁰; and by Repo-Man/PP1 γ in chicken and mammalian cells¹⁷¹. Owing to its temporal profile with mitosis, it is generally thought that H3S10ph is necessary for mitotic condensation. Genetic evidence seems to support this idea. A non-phosphorylatable form of histone mutant, H3S10A, in *Tetrahymena* exhibited chromosome condensation and lagging chromosomes phenotypes. Such mutant also had progressive DNA lost upon successive cell divisions¹⁷². In fission yeast, H3S10A mutant had reduced level of H3K9me2 and Swi6 at pericentromeric repeats and displayed lagging chromosomes and a high-lost rate of minichromosomes^{173,174}. Although H3S10A mutant does not affect viability and proliferation rate in budding yeast¹⁷⁰, it is required for so called “adaptive hyper-condensation” of mitotic chromosomes in cells where the two longest chromosomes are artificially joint together¹⁷⁵. More recently through the advancement of chemical genetics, a buddy yeast strain is engineered to incorporate unnatural amino acid that permits direct UV-crosslinking of histone H2A tail to its interacting partners¹⁷⁶. It was found that H2A is highly and reproducibly crosslinked to H4 of the neighboring nucleosomes during mitosis, the authors argued the crosslinking signal as a result of chromosome condensation. Also, since H3S10ph accumulation during mitosis is parallel to the concomitant reduction of H4K16Ac. The authors propose that mitotic H3S10ph is important to recruit HDAC for H4K16Ac deacetylation to promote H2A-H4 contact and hence chromosome condensation¹⁷⁶. Consistent with this idea, H3S10A mutant accumulates more H4K16Ac and reduces H2A-H4 crosslinking signal. These data

collectively seem to suggest an important role for H3S10ph in mitotic chromosome condensation.

The Heterochromatin Protein 1 (HP1) chromodomain specifically recognize H3K9me3 of constitutive heterochromatin including those of pericentromeric regions^{41,42}. During mitosis, Aurora B kinase phosphorylates H3S10 and such H3K9me3S10ph dual modification serve as a phosphor-methyl switch that evicts pre-bound HP1 proteins^{177,178}. It is thought that the clearance of HP1 proteins might facilitate mitotic chromosomes condensation and segregation. However, this prevailing idea is not rigorously tested as discussed in detail in Chapter III, p.137.

Anti-silencing

JIL-1 (the closest *Drosophila* homolog of mammalian MSK1/2 kinase) is the interphase kinase for H3S10ph¹⁷⁹. Genetic evidence identified JIL-1 mutant as an enhancer of PEV¹⁸⁰. And lost of JIL-1, and hence depletion of interphase H3S10ph, leads to genomewide enrichment of H3K9me2. Based on these evidences, it is proposed that JIL-1 mediated H3S10ph is important to counteract H3K9me2-associated repression. This seems to be supported by genomewide study.

To avoid contamination by the huge level of H3S10ph from mitotic cells, ChIP-seq was performed with post-mitotic salivary gland from L3 larvae to profile the distribution pattern of interphase H3S10ph. It was shown that H3S10ph is enriched on active genes as a broad peak slightly downstream of TSS. And lost of H3S10ph in JIL-1 mutant relocated H3K9me2, the genes that gain H3K9me2 showed a significant decrease in expression level¹⁸¹.

Since JIL-1 associates with the Male Specific Lethal (MSL) dosage compensation complex and it is two-fold enriched on the active genes of male chromosomes¹⁸², it has been proposed to be important for dosage compensation¹⁸³. Similarly high level of H3S10ph is particularly enriched along the male X chromosomes, it might be important to counteract H3K9me2 silencing and permit higher transcriptional output from the X-linked genes^{181,182}.

As discussed above, H3S10ph is linked to chromosome condensation. However, studies in interphase nuclei suggest the otherwise. Ectopic induction of H3S10ph at a defined locus by artificial tethering JIL-1 kinase leads to local decondensation of *Drosophila* polytene chromatin¹⁸⁴.

Gene activation

Studies in mammalian model support a role of H3S10ph in gene activation. It is found that the serine/threonine kinase PIM1 form a complex with the transcription factor MYC and is targeted to a subset of MYC target genes to deposit H3S10ph around TSS¹⁸⁵. H3S10ph in turn recruits a HAT complex via 14-3-3, resulting in H4K16ac accumulation. Together with predeposited H3K9ac, the double mark H3K9acS10ph/H4K16ac creates a binding platform for the double bromodomain containing protein BRD4, through which p-TEFb is recruited to promote transcription elongation¹⁸⁶.

2. 10 H3S28ph

Cell cycle regulation & implication in mitotic progression.

Unlike H3S10ph, H3S28ph probably does not exist in primitive eukaryotes like yeasts¹⁷⁰. Interestingly, despite high degree of conservation of histone H3 sequence, the fission yeast H3 is embedded with an alanine at position 28, instead of a serine as in budding yeast and metazoans. Hence, at least in fission yeast histone H3, it does not support H3S28 phosphorylation.

In metazoan, H3S28ph mirrors the cell cycle pattern of H3S10ph which peaks at mitosis¹⁸⁷⁻¹⁸⁹. Mitotic H3S28ph is catalyzed by Aurora B kinase¹⁸¹ and removed by Repo-Man/PP1 γ in chicken and mammalian cells¹⁷¹. The homolog of Repo-man in *Drosophila* has yet to be identified. Unlike mammalian cells where immunostaining of interphase H3S28ph revealed distinct and detectable speckles distribution¹⁸⁹, the existence of interphase H3S28ph in *Drosophila* remained highly controversial as discussed below.

Despite accumulation of high level of H3S28ph during metazoan mitosis, it remains unknown whether it is essential for mitotic progression. Of note, budding mutant with individual H3S28A mutation or in combination with H3S10A are viable with normal proliferation rate¹⁷². H3S28A histone mutant has yet to be studied in other research models.

Role in stimuli-responsive counter-silencing / gene activation

In response to stress, mitogen or differentiation stimuli, the MSK1 and MSK2 kinases are activated to phosphorylate nucleosomal H3 and promote transcription of immediate-early genes such as c-JUN and c-FOS^{189,190}. During this process, the promoter region of polycomb target genes such as ATF3 and c-FOS are accumulated with the H3K27me3S28ph double mark. Analogous to the phosphor-methyl switch of H3K9me3S10ph, H3S28ph abolishes binding of PRC2 and CBX8 to H3K27me3 (¹⁸⁹). Eviction of PcG components from these stress-response genes occurred in parallel to the reduction of H3K27me3 level and a concomitant recruitment of Pol II, accompanied with increased level of H3K4me3. This establishes a cascade of chromatin modifications including H3S28ph in the derepression of PcG targets upon MSK1/2 activation. Similarly, artificial tethering of MSK1 to silenced PcG target genes leads to gene activation accompanied with a reduction of PcG protein occupancies and a reciprocal gain of Pol II binding. Interestingly, these genes also accumulate H3K27AcH3S28ph double mark, it

hints the involvement of demethylation activity against H3K27me3 or active histone exchange in the derepression of PcG target genes¹⁹⁰.

Since H3S28ph is a stress-responsive histone mark, a recent study set out to profile its genomic distribution upon stress induction. To avoid contamination from bulk level of H3S28ph from mitotic cells, serum-deprived mouse Swiss 3T3 fibroblasts arrested in the G0 phase of the cell cycle were used¹⁹¹. Upon stress induction with anisomycin, ~50% of unregulated genes acquired *de novo* H3S28ph which accumulated at promoter and 5'UTR regions. Interestingly, over 50% of H3S28ph targeted region overlapped with CpG islands. Consistent with its stress-responsive role, H3S28ph targets genes covers function from cell signaling, metabolism and cell death¹⁹¹.

Whether similar derepression mechanisms exist in *Drosophila* remains largely untested. *Drosophila* JIL-1 kinase is the closest homolog of MSK1/2, and it does catalyze interphase H3S10ph and function in anti-silencing and dosage compensation as discussed in Chapter I, p.23. However, purified JIL-1 kinase only phosphorylates H3S10 but not H3S28¹⁸². Also, artificial tethering of JIL-1 to a defined genomic locus only leads to *de novo* accumulation of H3S10ph but not H3S28ph. And while H3S10ph is readily detectable as strong bands on the interphasic polytene chromosomes, H3S28ph signal appears to be quite weak¹⁸⁸. Hence it remains to be rigorously tested on whether interphasic H3S28ph exists and to what extent it regulates PcG target genes during interphase of the cell cycle.

2. 11 H3T80ph

Four independent mass-spectrometry studies discovered the phosphorylation of H3T80 located at the globular domain of histone H3^{26,192-194}. H3T80 protrudes from the nucleosome surface and hence modification on this site is unlikely to affect DNA-nucleosome interactions. The development of a specific antibody against H3T80ph confirmed its existence in fruit flies, mouse and human cultured cells. Interestingly, although H3T80 is conserved in both budding and fission yeasts, H3T80ph is undetectable in these primitive eukaryotes¹⁹⁵.

H3T80ph is cell cycle regulated. It is not detectable in interphase and accumulates as cell enters mitosis and reaches a peak level at metaphase. H3T80ph level drops upon mitotic exit and is almost fully dephosphorylated at late anaphase. This is in contrast to the mitotic dynamics of H3S10ph and H3S28ph, since both of them are readily detected in late anaphase^{169,187}.

Importantly, high level of mitotic H3T80ph signal persisted upon AuroraB kinase inhibition by Hesperadin treatment. This indicates that unlike H3S10ph and H3S28ph, H3T80ph is not catalyzed by the AuroraB kinase¹⁸¹. The responsible kinase for H3T80ph remained unknown.

Without knowing the kinase and phosphatase of H3T80ph, perturbation approaches were limited to overexpression of histone mutants. Ectopic expression of the phosphomimetic mutant H3T80E caused a small but significant number of cells restrained in prophase while introducing the non-phosphorylatable mutant H3T80A led to a doubled frequency of anaphase-bridge incidence. Of note, expression of these histone mutants only accounted for less than 8% of total H3, and the bulk H3T80ph level was not mentioned under these conditions¹⁹⁵.

Interestingly, SILAC-based approach identified specific enrichment of H2A and H4 with H3T80ph peptide compared to the non-phosphorylated counterpart. In agreement with this result, H3T80ph was found to be the strongest binder of histone octamers among other phosphopeptides such as H3T3ph, H3S10ph, H3T11ph and H3S28ph¹⁹⁵.

Analysis of the crystal structure of a tetranucleosome¹⁹⁶ suggests that H3T80ph protruding from one nucleosome might interact with H2AK74 of the subsequent nucleosome. Supporting the observed interaction of H3T80ph with H2A and anaphase bridge phenotype associated with H3T80A mutant, it is proposed that H3T80ph might facilitate mitotic chromosome condensation by promoting inter-nucleosomal contacts.

Owing to a lack of specific antibody, it remained uncertain on whether dual modification of H3K79meT80ph exists in mitosis. Although MS studies did not detect such modification, it awaits confirmation with mitosis-enriched samples. Given with known binders of H3K79me2 such as 53BP1¹⁹⁷, it would be interesting to test whether the phosphor-methyl switch binder-eviction model is also applicable to H3K79meT80ph. Besides, it is obvious by co-immunostaining that H3T80ph signal displayed a more confined distribution pattern than H3S10ph on mitotic chromosomes, it would be interesting to know whether only specific genomic regions acquire H3T80ph during mitosis. ChIP-seq with purified mitotic cells would be needed to address this question.

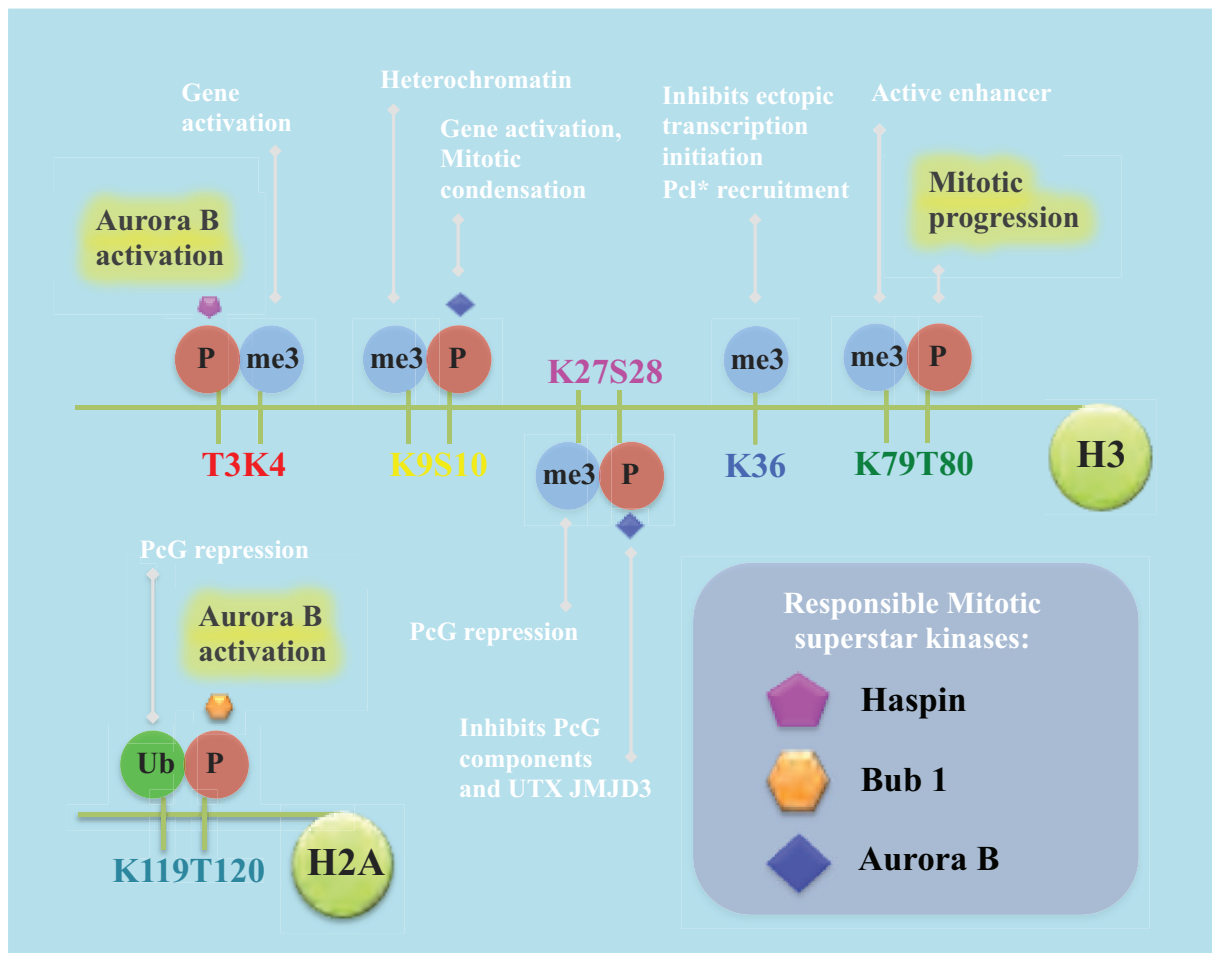


Fig I. Overview of a selection of histone modifications.

A selection of histone modifications and their functions are shown. Of note, many histone marks are juxtaposed to each other as “Phosphor-Methyl” pairs. Of all mitosis-enriched/specific phosphorylations, those essential for mitotic progression are highlighted.

* Mammalian Pcl homologs, not the *Drosophila* counterparts, recognize H3K36me3. The kinase responsible for mitotic H3T80ph remains unknown.

3. PcG Components & Functions

The *Drosophila* polycomb group (PcG) proteins are important epigenetic modifiers essential to maintain gene repression of key developmental regulators (Fig III). Early genetic and biochemical approaches classifies PcG proteins into two canonical polycomb repressive complexes (PRC): PRC1 and PRC2 with different chromatin-modifying activities. Recent advancement reveals novel PcG enzymatic activity such as O-linked N-acetylglucosamine (O-GlcNAc) transferase (OGT) and identified more multimeric assemblies, these include the Pho-Repressive Complex (Pho-RC), dRing Associated Factors (dRAF) and Polycomb Repressive Deubiquitinase (PR-DUB).

3.1 PRC1

Drosophila polycomb repressive complex 1 (PRC1) comprises four core components: Pc, Ph, Psc, and dRing^{198,199}. In the first attempt of affinity purification, FLAG-tagged Ph and Psc transgenic flies were generated and isolated PRC1 complex from *Drosophila* embryo nuclear extracts that accounted for ~ 2 MDa size. Identifications of the subunit components were hampered by antibodies availability. Nonetheless, western blot analysis detected the presence of Ph, Psc, Pc and sub-stoichiometric amounts of Scm but not E(z) as part of the PRC1 components²⁰⁰.

Aided by the availability of the first *Drosophila* genome sequence and better protein-coding gene annotations, together with the advancement of mass-spectrometry, other polypeptides associated with PRC1 were identified, these includes dRing, the DNA-binding factor Zeste and general transcription factor dTAFII. Subsequent biochemical reconstitution defined the core PRC1 particle as Pc, Ph, Psc and dRing¹⁹⁸.

PRC1 is characterized with its ability to stabilize chromatin. Reconstituted PRC1 or recombinant Psc alone counteracts chromatin remodeling mediated by SWI/SNF factors¹⁹⁸ and inhibits transcription *in vitro*²⁰¹. And examination with electron microscope demonstrated that PRC1 (with or without Ph) could compact 12-mer nucleosomal arrays *in vitro*, Psc alone also displayed such compaction activities²⁰².

Recent biochemical purification suggests that Psc-dRing assemble as a core platform on which it can partner with components other than Pc & Ph, as discussed in X (dRAF & Mammalian RYBP-KDM2 PRC1).

3. 1. 1 Pc (Polycomb)

The polycomb mutant was first identified by Pamela Lewis in 1947. As its name implies, such mutant is characterized by the growth of additional comb teeth of the male *Drosophila sex comb*^{203,204}. Besides, Pc mutants displayed classical PcG phenotypes such as cuticular transformation of late embryonic thoracic and abdominal segments into the eighth abdominal segment identity^{204,205}. Mutant clones of Pc in wing disc also derepressed Hox genes such as Ubx and Abd-B²⁰⁵.

Pc, together with another PcG protein polyhomeotic (Ph), accumulates within distinct subnuclear punctate structures known as the polycomb bodies. It is believed that these Pc foci represent the hub of PcG repressions^{105,206-209}. Interestingly, repressed PcG target such as the Hox genes has a higher frequency of colocalizing within the same Pc body than when they are expressed²¹⁰. Recent effort implemented with genomewide RNAi screen identifies novel factors that regulate Pc foci morphology; among these factors are components of the SUMOylation machinery and cohesion ring complex²¹¹.

Pc has a characteristic chromodomain at the N-terminus that recognizes specifically H3K27me3^{90,91,106}. Mutation in chromodomain, such as the I31F mutation in *Pc*¹⁰⁶ allele abolishes Pc binding to polytene chromosomes and disrupts formation of punctate nuclear Pc bodies^{109,111}. Also swapping the chromodomain of Pc with that of heterochromatin protein 1 (HP1) resulted in relocalization of such Pc-chimera to H3K9me2-enriched, DAPI-dense heterochromatin region of *Drosophila* S2 cells¹⁰⁵.

Recognition of H3K27me3 peptide by Pc chromodomain is achieved by the assembly of aromatic cage containing residues, including Y26, W47 and W50, into a complementary fitting groove where the extended methyl-lysine of H3K27 resides^{105,106}.

Base on this chromodomain recognition module, it has been postulated for a hierarchical recruitment model in which depositions of H3K27me3 mark on PcG targets help Pc binding and hence PRC1 targeting^{7,8,212-214}. This one-way recruitment model has been recently challenged, as discussed in Chapters I, p.20.

3. 1. 2 Ph (polyhomeotic)

The *Drosophila* Ph protein is encoded by a tandem-duplication of genes known as ph-d (distal) and ph-p (proximal)²¹⁵. Loss of Ph (maternal and zygotic null) leads to drastic abnormalities that are distinctive from other PcG mutants. Notably, these null mutants failed to complete gastrulation and displayed epidermal developmental defects. Weak hypomorphic alleles developed into later stages of embryogenesis and showed segmental transformation phenotypes similar to other PcG mutants²¹⁵⁻²¹⁷.

Besides, accumulating evidence supports an important role of Ph as a tumor suppressor. Induction of homozygous Ph mutant clones in imaginal discs led to invasive tissue overgrowth phenotypes associated with ectopic Notch and JAK/STAT signaling pathway activities, in addition to Hox gene derepressions^{214,218-221}.

Intriguingly, the C-terminus of Ph harbors a sterile alpha motif (SAM) domain that can polymerize in vitro via a head-to-tail configuration as a left-handed helical structure²²². Functional relevance of such helical structure is unknown, largely because of the lack of in vivo demonstration of the polymer structure. It is postulated that such fibrous and extended structure might help spreading polycomb domain from a chromatin nucleation site. However, this idea was not favored by the sharp ChIP-on-ChIP peaks profile of Ph^{13,14,223}. It still remains possible that such polymer structure might be important for the higher order structure of PcG repressive domains²²⁴. The SAM domain polymerization properties are conserved in mammalian homolog Phc2. Introducing a presumably dominant negative SAM domain mutant of Phc2 disrupted nuclear clustering PRC1 bodies without compromising PRC1 complex integrity, it also led to a reduced H3K27me3 deposition and poor binding of Ring1B to PcG targets^{224,225}. Mice engineered with such mutation even showed skeletal transformation phenotypes²²⁵. In *Drosophila*, tethering WT-Ph, but not the corresponding SAM domain mutant, is capable to repress transcription of a reporter gene. Also, overexpression of SAM mutant, but not WT Ph, leads to Abd-B derepressions in wing discs²²⁶. These data suggest the importance of Ph SAM domain in gene repressions.

3. 1. 3 Psc (Posterior Sexcomb)

Genetics studies suggested that Psc is related to an adjacent gene Su(z)2. Despite their sequence homology is limited to the C-terminal stretch of 200 amino acids²²⁷, Su(z)2 is considered as a functional homolog of Psc²²⁸. In one example, Hox derepression phenotypes in mutant clones deleted for both Psc and Su(z)2 can be rescued by reintroducing either Psc or Su(z)2, suggesting a functional redundancy between the two proteins²⁰⁵. Also they share similar biochemical properties on counteracting SWI/SNF-mediated chromatin remodeling and on compaction of nucleosomal array. Besides, Su(z)2 can substitute Psc on PRC1 assembly²²⁸.

Both Psc and dRing possess RING finger domains that are characteristic of the E3 ubiquitin ligase family²²⁹. When Psc complexes with dRing, the Ring-Ring-heterodimer configuration represents the catalytic core to catalyze H2A ubiquitination^{144,145}. It is important to stress that it is the RING finger of dRing that confer E3 ligase activity in this context. However, the RING finger motif of Psc also confers active E3 ligase activity. Notably, Psc can form an alternative complex with the anaphase-promoting complex (APC) component APC11/LMG to catalyze Cyclin B ubiquitination during mitotic exit²³⁰. Mosaic clones of combined Psc-Su(z)2 mutants display tumor-like phenotype with massive invasion into neighboring tissue, also Ubx is strongly derepressed in the wing disc, even in the hinge and notum regions^{205,218}. Also genetic evidence suggests that, similar to Ph, Psc can function independent of dRing or Pc to repress some of the PRC1 target genes such as *dac*¹⁶. This might be attributed to the chromatin compaction activity of Psc, which does not require other PRC1 components²⁰².

3. 1. 4 dRing / Sce (Sexcomb extra)

dRing (also known as Sce) is an E3-ligase catalytic subunit of dRAF (see p.37) which confers H2A ubiquitination activity^{16,77,142}. It is also a component of canonical PRC1 complex²⁰⁰. Mutation of dRing such as *Sce^l*, which encodes a C-terminus truncated protein, displayed homeotic phenotypes. Maternal and zygotic *Sce^l* mutant derived from germline clones gives rise to defective embryogenesis typical of PcG mutants, with derepressions of canonical PcG target genes, such as Ubx from the Hox cluster. These mutant embryos were characterized by cuticular transformation of thoracic and abdominal segments into the eighth abdominal segment identity^{16,146}. Mutant clones of *Sce^l* induced in wing imaginal disc strongly derepressed Ubx and Abd-B¹⁴⁶. Despite these typical PcG phenotypes, several observations set dRing apart from other PRC1 members. For the non-canonical PcG target genes such as dachshund (*dac*), whose promoter is enriched with all PRC1 components including Pho, it is only derepressed in Psc-Su(z)2 or Ph mutants both at embryonic and larval stages. In contrary, loss of dRing does not affect the expression pattern of *dac*¹⁶. Besides, in the cell-lethal mosaic analysis system where mutant clones were highly enriched in an environment lacking cell-cell competition, all mutant of PRC1 components except dRing, displayed tumorigenic over proliferation phenotype in the eye discs^{16,218,219}.

It remains unclear on the essential role of H2Aub in PcG repression. It is surprising to know that mutation in dRing (I48A), which supposedly hampers its interaction with E2 ubiquitin-conjugating enzyme and hence reduce its E3 ligase activity^{144,145}, can actually support Hox repressions. However, such E3 ligase-dead mutant is lethal. Limited by the availability of a reliable antibody that specifically recognizes H2AK118Ub in *Drosophila*, the E3 ligase dead nature of dRing I48A mutation is yet to be verified¹⁴⁷.

3. 1. 5 Scm (Sexcomb on midleg)

Scm is considered as a sub-stoichiometric component of PRC1²⁰⁰. Similar to other PcG components, late embryos derived from maternal and zygotic null Scm mutant displayed cuticular transformation where the thoracic and abdominal segments acquired features characteristic of the A8 abdominal segment²³¹.

Scm protein consists of two MBT repeats that is implicated in methyl-lysine recognition^{232,233}. Isothermal titration calorimetry (ITC) assay showed that SCM MBT repeats had a modest binding preference on monomethylated lysine on H3K4, H3K9, H3K27, H3K36 and H4K20, when compared to their unmodified or higher methylations states. Structural study confirmed a more stable MBT-monomethyl-lysine binding configuration when compared to their higher order of methylation derivatives²³³.

Hypomorphs carrying missense mutations at the MBT1 domain, such as *Scm*^{KM23}, gave mild derepression phenotype of Hox genes in embryo. Notably these MBT1 mutants showed stronger genetic interaction with other PcG mutants than Scm-null alleles²³². Reintroduction of WT Scm rescued Hox derepression in Scm-null clones in wing discs. In contrary, reintroducing MBT deletion or missense mutant of Scm only partially restored Ubx repression; residual Ubx derepression is readily detectable in the wing pouch²³³.

Similar to Ph, Scm also possesses a SAM domain at the C-terminus end and Scm-SAM can form helical polymers in vitro. Strikingly, Scm-SAM and Ph-SAM can co-polymerize in vitro²³⁴. In line with this result, recombinant Scm can co-assemble with the core PRC1 complex²³⁵. However, only sub-stoichiometric amount of SCM was co-purified with PRC1 complex from *Drosophila* embryo²⁰⁰, indicating that Scm might only interact with a small population of PRC1. Nonetheless, genetics evidence supports the important role of Scm-SAM domain in PcG repressions. Scm-SAM missense mutant that cannot bind full-length Scm failed to rescue Scm-null mutant. Intriguingly, overexpression of a 10-kDa wild type Scm-SAM domain alone can lead to typical PcG transformation phenotypes in adult flies including ectopic sex combs on the second and third legs, antennapedia and wing-to-haltere transformations. It is postulated that the highly abundance SAM domain might compete and titrate interacting partners essential for PcG repressions²³⁵.

As discussed in Chapter I, p.38, Scm was suggested to play a role in PcG recruitment.

3. 2 dRAF (dRing Associated Factors)

Affinity capture of dRing interacting partners using *Drosophila* nuclear extracts immunodepleted of Pc identifies PRC1 subcomplex known as dRAF. Core members of dRAF include Psc, dRing and dKdm2, which harbors H3K36 demethylase activity. Structural studies suggest that the RING fingers from Psc and dRing heterodimerize to confer E3 ligase activity on nucleosomal H2A. Notably, biochemical reconstitution experiment showed that dKdm2, when added to the Psc-dRing complex, strongly stimulated H2A ubiquitination while adding equimolar of Pc-Ph gave limited stimulatory effect on ubiquitination⁷⁷. Consistent with this observation, individual knockdown of dKdm2, Psc and dRing, but not that of Pc and Ph, abolished H2A ubiquitination in S2 cells. These data argue that dRAF, but not canonical PRC1, as the major H2A E3 ligase in *Drosophila*⁷⁷. dRAF-like complex is conserved in mammals. Mammalian Kdm2B complexes with PCGF1 and Ring1B, along with some other factors, as a non-canonical PRC1 complex²³⁶. Interestingly, Kdm2B harbors a CXXC domain that specifically recognizes non-methylated CpG islands and artificial tethering of Kdm2B to a defined genomic locus can nucleate *de novo* H2A ubiquitination and subsequent recruitment of PRC2 and establishment of H3K27me3 domain⁸¹. This suggests a role of H2Aub in PRC2 recruitment. In support of this idea, both flies and mammalian PRC2 components can be affinity captured on H2Aub-containing oligo-nucleosomal array. And together with the auxiliary factors Jarid2 and AEBP2, PRC2 exhibits a stronger HMT activity on H2Aub nucleosomal substrate than unmodified ones¹¹². These observations call for a positive feedback model in which Kdm2B-PRC1 catalyzed H2Aub stimulates PRC2 deposition of H3K27me3, which in turn recruits canonical Pc/CBX containing PRC1 complex. However, to what extent such positive feedback loop is required for PcG silencing is not well defined. In *Drosophila*, loss of dRing abolishes H2Aub, but it seemed not to alter global H3K27me3 level¹⁶. And reintroducing E3-ligase dead mutant of dRing (I48A) can rescue Hox derepression phenotypes of dRing-null mutant¹⁴⁷. Also, knockdown of dKdm2 in S2 cells⁷⁷ and larva homozygous dKdm2 mutants retained normal level of H3K27me3 level²³⁷. It is thus hypothesized that H2Aub might be specifically required during early embryogenesis when H3K27me3 domains are first established. Embryos derived from germline clones with E3 ligase-dead dRing mutant or establishing histone H2A mutant devoided of ubiquitination site would address this question. Also, genomic profile of

H2Aub in *Drosophila* embryos and larval tissues would help to better assess the relevant role of this histone modification in PcG silencing.

3.3 Pho-RC (Pho Repressive Complex)

Pho and Phol encode similar proteins and genetic evidence suggests that they function redundantly in PcG repression²³⁸. Importantly they both have of 4 zinc-finger motifs with overall 80% sequence identity and all the important amino acid residues predicted to contact DNA are fully conserved²³⁸. This is in good agreement with Gel-shift assay where Phol zinc-finger specifically retards the migration of DNA fragment containing Pho-binding site²³⁸. Homozygous mutant of Pho showed subtle Ubx derepression on the wing pouch whereas Ubx remained repressed in homozygous Phol mutant background. However, combined Pho and Phol double homozygous mutant synergized Ubx derepression in the wing discs²³⁸. Pho is the only PcG protein with well-defined DNA binding sequence that is embedded in most PREs^{14,239,240}. Since Pho-binding sites in PRE are essential for PcG repressions²⁴¹⁻²⁴⁴ and given that Pho also physically interacts with PRC1²⁴⁵ and PRC2²⁴⁶ components, and loss of Pho abolishes binding of Pc and E(z) binding to bxd²⁴⁶, it is thus attributed to function as a recruiter to guide binding of PcG components to their target genes²⁴⁷. However, polytene staining of Pho and Phol double mutant revealed substantial retention of PRC1 and PRC2 components on chromatin and only on a few cytological sites where PcG binding is affected²³⁸. It is possible that other factors such as SCM^{247,248}, buffers the loss of Pho/Phol in PcG recruitment. Notably, Ph remained associated to those PcG target sites even when the binding of other PRC1 and PRC2 components are affected in the double mutant background²³⁸.

Proteomics approach using transgenic Pho-TAP as affinity bait identified Scm-related gene containing four mbt domains (dSfmbt) and dINO80 complex. Owing to its important function in PcG repression, Pho-dSfmbt is referred as Pho-repressive complex (Pho-RC). Notably, Pho-RC can be reconstituted as a stable complex that can resist ionic strength in 2M KCl containing buffer²⁴⁹. dSfmbt is structurally related to Scm protein, since it bears four MBT domains and a C-terminus SAM domain. The 4MBT domain displayed a low affinity binding preference to mono or di-methylated histone at H3K9 or H4K20²⁴⁹. Structural data shows that a specialized Pho spacer region binds stably with the 4MBT domains of dSfmbt, and MBT deletion allele or missense mutants of dSfmbt that disrupt

such interaction compromise PcG repression²⁵⁰. Consistent with the observation that dSfmbt and Scm could be reconstituted as a complex in vitro²⁵¹ and their co-occupancy on a candidate collection of PREs^{249,251}, it was found that combined mutations on both Scm and dSfmbt synergized derepressions of PcG targets than individual mutant alone²⁵¹.

Notably, dSfmbt binding to PRE required intact Pho-binding site. Using the PRE bxd as a study model, it was shown that Pho and Scm binding to PRE in S2 cells was independent of each other, but RNAi against either of them abolished binding of PRC1 and PRC2 components²⁴⁸. Together with the genetic interaction between Scm and dSfmbt mentioned above, it is thus hypothesized that Pho-RC and Scm act in parallel for PcG recruitment²⁴⁷. These observations call for the quest of genomewide distribution profile of Scm to better access its role in PcG recruitment.

3. 4 PRC2

Ever since the first discovery of histone methylation catalyzed by the SET-domain containing Su(var)3-9 protein⁴⁰, it paved a way to look for novel histone methyltransferase (HMT) activity on known chromatin regulators. Not surprisingly, E(z) as a SET domain containing protein, is suspected to catalyze histone methylation. Indeed affinity purification of FLAG-Esc in *Drosophila* embryo extracts⁸⁸ and FLAG-EED in human embryonic kidney 293 cell nuclear extracts⁹¹, together with extensive chromatographic purification of HMT activity containing fractions from *Drosophila* embryo extracts⁸⁹ and HeLa cell nuclear pellet⁹⁰ unequivocally identified PRC2 and established its core components as ESC, E(z), Su(z)12 and Nurf55. The Zn-finger containing protein AEBP2⁹⁰ and HDAC Rpd3^{89,136}, was also occasionally copurified with PRC2 components. Studies with immunoprecipitate of PRC2 (91), native chromatographic fraction of PRC2⁹⁰ and reconstitution of the 4-component PRC2⁸⁸ demonstrated its specific HMT activity on H3K27. And guided by the model of HP1 recruitment to Su(var)3-9 catalyzed H3K9me3^{41,42}, it was found that the chromodomain of Pc of the PRC1 component specifically recognized H3K27me3 deposited by PRC2^{90,91,105,106}, hence the field established a one-way model of PRC2-PRC1 recruitment hierarchy, which is recently subjected to revision^{81,252}.

3. 4. 1 Esc (Extra Sexcombs) & Escl (Esc-like)

Embryos derived from parents that were transheterozygous for *esc*-null alleles (*esc*²/*esc*¹⁰) lacked H3K27me3⁹⁴, they also showed strong transformation phenotype typical of other PcG mutants. Notably, cuticle of these late embryos displayed 12 dendritic belts characteristic of the A8 abdominal segment¹⁰³. Similar to the *Psc-Su(z)2* locus, an Esc-like (*Escl*) isoform with 60% sequence identity to *Esc* exists and resides ~150 kb away from the *esc* gene. Similar to *Esc*^{88,89}, *Escl* can assemble with E(z) Su(z)12 and Nurf55 to form PRC2, with the same HMT activity towards H3K27, despite at a reduced efficiency²⁵³. *Escl* also bind to PRE such as *bxl*, and combined mutations of *Esc* and *Escl* resulted in phenotypic enhancement with more severe transformation phenotypes²⁵³⁻²⁵⁵. In *Drosophila* S2 and Kc cells, only simultaneous, but not individual, knockdown of *Esc* and *Escl* would deplete H3K27me3 level^{254,255}. It is thus believed that *Esc* and *Escl* are functionally redundant. In fact, *Esc* expression level peaks at embryogenesis and then dramatically decreased in later stage of development. *Escl* show somewhat a reciprocal expression pattern, in which peak expression is achieved at post-embryonic stage and *Escl* level persist in adulthood^{253,254}. Hence *Escl* may substitute the function of *Esc* in later stages of development.

Early study showed that *Esc*-E(z) interacts with each other²⁵⁶. And based on this observation, subsequent FLAG-*Esc* based affinity purification identified PRC2 components and its HMT activity^{88,91}. *Esc* WD40 forms a beta-propeller structure, and study from the human homolog EED suggests that the bottom of the beta-propeller constitutes a peptide-binding groove for interaction with Ezh2. Owing to good conservation of critical residues at the binding interface, it is predicted that *Drosophila* *Esc*-E(z) adopts a similar interaction mechanism²⁵⁷. More importantly, it is found that EED beta-propeller domain can recognize H3K27me3 and stimulate PRC2 HMT activity. Hence it is proposed that EED-H3K27me3 interaction constitutes a positive feedback loop to enhance the spreading of broad H3K27me3 repression domain, and might serve as an important mechanism to maintain PcG repression during DNA replication¹¹³. Interestingly, transgenic *Esc* carrying mutations that abolish H3K27me3 recognition failed to rescue the loss of H3K27me3 and lethality associated with *esc escl* double null mutant, demonstrating the in vivo functional relevance of *Esc*-H3K27me3 interaction/stimulatory loop¹¹³.

3. 4. 2 E(z) (Enhancer of zeste)

E(z) was classified as a PcG gene based on the loss of function studies of its temperature-sensitive alleles, which derepressed Ubx during embryogenesis and showed cuticular transformation of late embryonic segment acquiring A8 abdominal identity^{258,259}. These E(z) alleles also show adult transformation phenotype when they are raised in semi-permissive temperature. Notably, ectopic sex combs are found on the second and third legs and male anterior abdominal segments acquired patchy pigmentation reminiscent of the posterior counterparts^{90,91}. Similar to other PcG genes, clones of E(z)-null mutants derepressed Hox genes in wing imaginal discs^{100,205}.

Since E(z) is conserved with a SET domain which is also found in Su(var)3-9 and Trithorax protein²⁶⁰. Following the demonstration that Su(var)3-9 as a SET domain-dependent histone methyltransferase⁴⁰, subsequent purification of PRC2 established E(z)/Ezh2 as the catalytic subunit for specific catalysis of H3K27 methylation⁸⁸⁻⁹¹.

E(z)/Ezh2 alone does not possess HMT activity^{40,90,91,94,261}. Crystallography study suggested that the post-SET domain of Ezh2 folds backward and block the substrate-binding site, hence potentially exhibits an auto-inhibitory effect²⁶². Also, cofactor-binding pocket for the methyl-donor SAM is not observed within the Ezh2 SET domain alone, indicating the essential role for other PRC2 subunit interactions to properly assemble correct catalytic site configuration²⁶².

Recently, EM reconstruction of the entire human PRC2-AEBP2 complex at 21Å resolution displayed subunit organization among different components (Fig II)²⁶³. Notably, the SET domain of Ezh2 is in direct contact with the beta-propeller domain of EED and the VEFS (VRN2-EMF2-FIS2-SUZ12) domain of Su(z)12, this might provide mechanistic clue on how these domains integrate the sensing of repressive¹¹³ and active histone marks²⁶⁴ to allosterically alter the HMT activity of PRC2. Besides, the position of individual subunit can be configured in a way that allows PRC2 to interact simultaneously with two adjacent nucleosomes. As such, EED binding to H3K27me3 of one nucleosome can better orientate H3 tail of the subsequent nucleosome in face of the SET domain of PRC2²⁶³. This might explain why PRC2 works more efficiently on dense oligonucleosomes array²⁶⁵.

In *Drosophila*, PRC2 is the sole HMT responsible for H3K27 methylations^{94-96,205}. Since there are accumulating evidence for the existence of Ezh2 non-histone substrates^{266,267}, it might call in to question on whether H3K27 is the key substrate to elicit PRC2-mediated gene repression. Study on *Drosophila* histone mutant provides a neat answer¹⁰⁰. Mosaic

analysis on *Drosophila* histone mutant carrying *H3K27R* mutation depleted H3K27me3 and phenocopied the loss of E(z), hence it strongly suggests that the function of E(z) or PRC2 as a whole is to catalyze H3K27me for gene repressions¹⁰⁰.

In recent years, a number of reports showing oncogenic mutations of Ezh2 SET domain in a variety of cancers with elevated level of H3K27me3²⁶⁸⁻²⁷⁴. WT PRC2 catalyzes efficient monomethylation at H3K27 and exhibit slow conversion of higher methylation states²⁶⁸. The oncogenic mutation hotspot resides at residue Tyrosine 641 of Ezh2 SET domain, and reconstitution of PRC2 using Ezh2 with Y641 mutation showed elevated catalytic activity for converting H3K27me1 into H3K27me2 and H3K27me3. Hence heterozygous cancer patients carrying both WT and Y641 mutant alleles of Ezh2 exhibit marked increase in H3K27me3 level^{268,270,271}. Recent structural data shows that Y641 is positioned to form hydrogen bond with the extended side chain of the substrate lysine (H3K27), mutation such as Y641F would alleviate conformational constraints imposed on the dimethylated state of H3K27 and hence allow better accessibility to the methyl-donor *S*-Adenosyl methionine (SAM)²⁶². Besides, such mutation also allows provide additional space to accommodate trimethylated form of lysine. As such, Ezh2 Y641 mutants are more competent for H3K27 methylations. Similar mutation exists in *Drosophila*. The E(z)^{Trm} (Trithorax-mimic) allele displays hypermorphic activity which deposits high level of H3K27me3 and causes ectopic silencing of PcG targets, hence showing Trithorax-like phenotypes²⁷⁵.

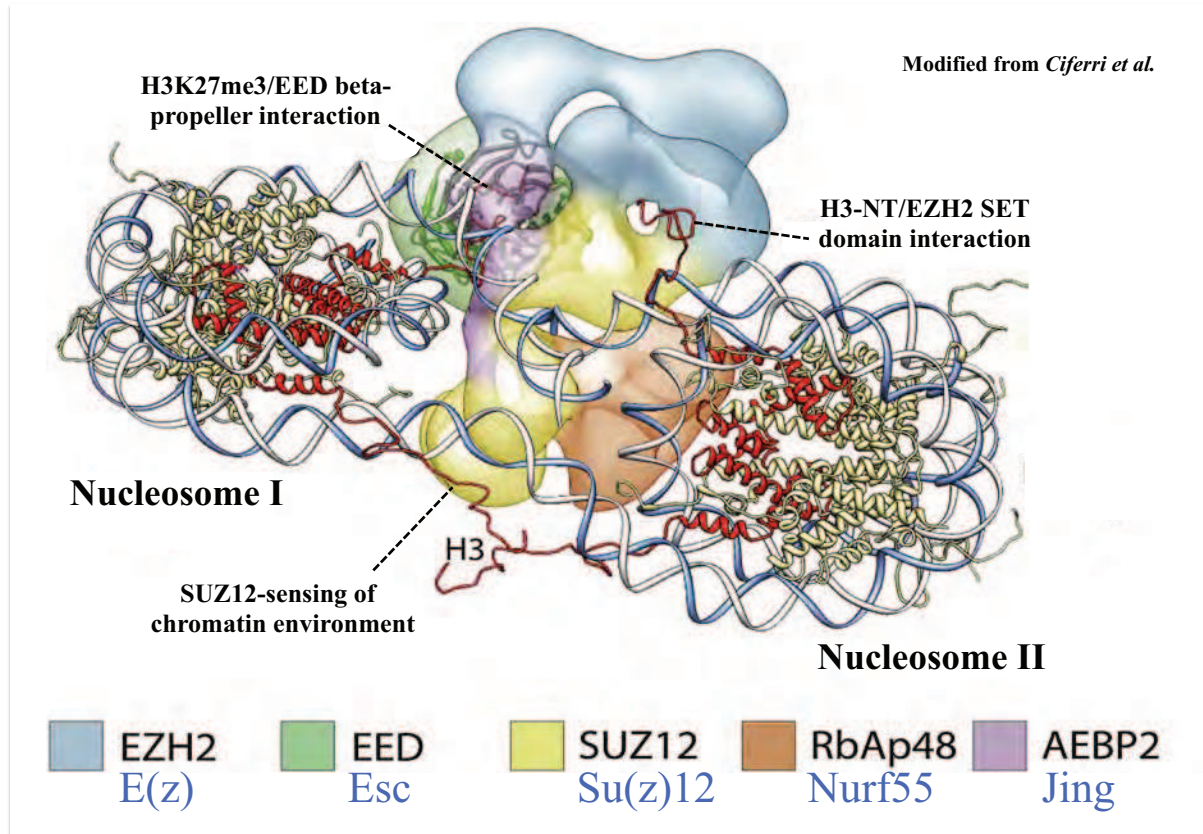


Fig II. A proposed possible model for the binding of the PRC2-AEBP2 complex to a di-nucleosome.

A proposed model based on EM-reconstitution of human PRC2-AEBP2 complex docking on a di-nucleosome. In such configuration, the PRC2 complex is docking on the groove between two adjacent nucleosomes such that EED-H3 interaction from one nucleosome positions EZH2 SET domain in close proximity to the H3 tail from another nucleosome. Please refer to texts for details. *Drosophila* homologs of PRC2 components are highlighted with blue texts. Figure modified from *Ciferri et al*²⁶³.

3. 4. 3 Su(z)12 (Suppressor of zeste 12) & Nurf55 (Nucleosome Remodeling Factors 55)

Su(z)12 is the last core PRC2 components recovered by *Drosophila* genetics. Homozygous Su(z)12 mutants usually died at L1 or L2 larval stage. Maternal and zygotic null mutant embryos strongly derepress Hox genes with late embryos cuticle showing segmental transformation into A8 identity. Combination of transheterozygous Su(z)12 alleles allow development of pharate adults with severe transformation phenotypes as exemplified by the presence of ectopic sexcombs on both second and third legs, growth of haltere-like wings and development of antennapedia²⁷⁶. Biochemical purification identifies Su(z)12 as a core component of PRC2 and it is indispensable for PRC2 HMT activity^{88-91,94}.

Nurf55 is a common components shared by different chromatin modifying complexes such as CAF1, HAT1, NURF and NuRD^{277,278}. In addition, it is also a core PRC2 subunit⁸⁹⁻⁹¹. Notably, *Drosophila* with reduced expression of Nurf55 displayed aristapedia transformation and mosaic clones of Nurf55 mutants in imaginal discs showed reduced H3K27me3 level, supporting its essential role in PcG repression⁹⁷.

Nurf55 possess WD40 repeats that assemble into a 7-blade beta-propeller structure in which an acidic pocket binds the first 14 amino acid residues of H3 N-terminal tail. Such Nurf55-H3 binding module is compatible with the interaction with Su(z)12, this is consistent with the observation that Nurf55 and Su(z)12 are required for PRC2 to bind nucleosome²⁶¹. Importantly, Nurf55-Su(z)12 binding to H3 tail is abolished when H3K4 is methylated²⁶⁴. And H3K4me3 containing nucleosome appeared to be a poor substrate for PRC2, despite PRC2-binding to such modified nucleosome was not affected. Biochemical analysis suggests a reduction of catalytic turnover or processivity when PRC2 acts on H3K4me3 containing nucleosomes²⁶⁴. Similar inhibitory effect is observed with H3K36me2 and H3K36me3 nucleosomes. These active mark inhibitions of PRC2 activities are conserved in fly, human and plants. Interestingly, a variant PRC2 in plants with a another Su(z)12 paralog VRN2 is insensitive to H3K4me3 and H3K36me2,3 inhibition. Hence it is suspected that Su(z)12, likely via its conserved VEFS domain, can sense active chromatin mark to modulate PRC2 activity.

Recently, it is shown that PRC2 favored chromatin substrates with higher nucleosomal density²⁶⁵. And addition of peptide containing H3 31-42 can mimic high nucleosomal density, and stimulate higher PRC2 activity on loosely packed oligonucleosomes. Interestingly, deletion mapping and crosslinking chemistry showed that such stimulatory

peptide directly interacts with a Su(z)12 fragment containing the conserved acidic residues within the VEFS domain. Strikingly, mutation of some of these acidic residues E548A/E550A/D552A abolished PRC2 responsiveness to nucleosome density without compromising complex integrity and stimulation by the EED-H3K27me3 axis²⁶⁵. Also, expression of WT Su(z)12, but not the corresponding allele with the same mutations, rescued H3K27me3 level in a Su(z)12-null ES cell background. It demonstrates the in vivo relevance of the nucleosome-density sensing function of PRC2²⁶⁵.

3.5 PRC2 auxiliary factors

3.5.1 Pcl (Polycomb-like)

Mutation in Pcl caused ectopic growth of sexcombs on both second and third legs, anterior abdominal tergites of these adult flies also gained patchy pigmentation resembling the posterior compartments²⁷⁹. Based on early observations of these homeotic phenotypes, Pcl was classified as a PcG gene.

Pcl has an atypical Tudor domain and two PHD fingers. Subsequent yeast-two-hybrid and in vitro pull down assays suggested direct interactions between Pcl PHD fingers and E(z)²⁸⁰. Indeed reciprocal tandem affinity purifications using Pcl-TAP and E(z)-TAP isolated Pcl-PRC2 complex from *Drosophila* embryo extracts⁹⁵.

Interestingly, both *Drosophila*⁹⁵ and mammalian Pcl-PRC2^{281,282} displayed a higher catalytic activity particularly for H3K27 trimethylation. In agreement with this enzymatic property, mosaic clone of Pcl mutant in wing discs showed marked reduction in H3K27me3 and Hox genes derepressions without affecting H3K27me1⁹⁵. This is in contrary to clones of E(z) or Su(z)12 mutant, in which both methylation states were severely affected. Hence it is proposed that Pcl acts as a PRC2 stimulatory cofactor to specifically boost H3K27 trimethylation⁹⁵.

ChIP assay on Hox PREs demonstrated specific reduction on H3K27me3 in Pcl mutant embryos, while both H3K27me2 and H3K27me1 levels were reciprocally increased. Importantly, PRE-binding of PRC2 components such as Su(z)12 was also decreased in the lack of Pcl, while that of Pho and Ph were unaffected⁹⁵. Similarly, ChIP assay in wing imaginal discs on a PRE element of the Hox gene Ubx (bx) showed that the loss of Pcl only affects PRE-recruitment of E(z) but not Pho²⁸³. While simultaneous loss of both Pho and Ph abolished binding of both E(z) and Pcl. This suggests a role for Pcl to mediate PRC2 recruitment downstream of Pho and Ph. The proposed recruitment function was also supported by polytene staining experiment, in which chromatin binding of E(z) is largely abolished upon the loss of Pcl²⁸³.

Intriguingly, the potential function of Pcl in PRC2 recruitment is elaborated by several studies on mammalian Pcl homologs. All mammalian Pcl homologs including PHF1, PHF19 and MTF2 possess a conserved Tudor domain that specifically interacts with H3K36me3⁷¹⁻⁷⁴. Hence it is proposed that PCL is specifically needed to recruit PRC2 at active genes for de-novo repression during differentiation transitions⁷¹⁻⁷⁴. Since two critical aromatic residues (C361 and S387) within the Tudor domain of *Drosophila* Pcl are not conserved, it lacks an intact binding pocket and does not recognize methylated lysine or arginine²⁸⁴. However, it seems that when including the PHD1 domain, *Drosophila* Pcl Tudor domain can act together to bind to H3K4me3 and H3K36me3⁷¹. Further biochemical studies would be needed to clarify this point.

3. 5. 2 Jarid2 (Jumonji, AT Rich Interactive Domain 2)

Jarid2 belongs to the Jumonji histone demethylase family⁷⁵. Since the amino acid critical for catalyzing demethylation is not conserved within Jarid2 Jumonji C domain, hence it is catalytically inactive for histone demethylation²⁸⁵⁻²⁸⁹.

Affinity purification of different epitope-tagged²⁸⁶⁻²⁸⁹ or in vivo biotinylation of mammalian PRC2 components²⁸⁵ robustly identified Jarid2 as a novel component of PRC2. The presence of PRC2-Jarid2 complex was confirmed by gel filtration where Jarid2 comigrated with PRC2 components²⁸⁵⁻²⁸⁷. Using individually purified recombinant proteins, it was found that Jarid2 can directly interact with Ezh2²⁸⁷ or Suz12 proteins²⁸⁶.

Consistent with the formation of a Jarid2-PRC2 complex, genomewide ChIP assay revealed a striking overlapping (>90%) of Jarid2 occupancy with PcG targets in ES

cells²⁸⁵⁻²⁹⁰. Since the loss of Jarid2 reduced PRC2 binding to target genes and vice versa, such interdependency suggests a cooperative mode of binding between Jarid2 and PRC2 to their target sites. The PRC2-recruitment function of Jarid2 might be mediated by its DNA²⁸⁷ and nucleosome²⁹¹ binding activity.

With the use of a GAL4-tethering luciferase reporter system, artificial targeting of Jarid2 or Ezh2 results in mutual recruitment and productive catalysis of H3K27me3 associating with silencing of the reporter gene^{287,288}. This implies a positive role of Jarid2 in PRC2 activity.

Consistent with the reporter assay, it was shown that Jarid2 could stimulate PRC2 HMT activity²⁸⁷. Ironically, there were also studies demonstrating Jarid2 as an inhibitor on PRC2 catalysis^{285,286}. The reasons for such discrepancy remained unknown, methods of PRC2 reconstitution, the form of histone H3 substrates and other assay conditions might contribute to different results^{123,292}. Similar discrepancy was also reflected on the effect of Jarid2 on H3K27me3 level. Some studies observed reduction of H3K27me3²⁸⁷⁻²⁸⁹ whereas others reported unchanged²⁸⁶ or even increase²⁸⁵ in H3K27me3 on PcG targets upon the loss of Jarid2 in ES cells.

Nonetheless, a subset of PcG target genes were not properly silenced during differentiation upon knock down of Jarid2 or in a heterozygous genetic background with one Jarid2 allele disrupted by gene trap insertion²⁸⁶⁻²⁸⁹.

PRC2 activity is required for ES cells differentiation²⁹³⁻²⁹⁵. Similarly, the loss of Jarid2 impaired ES cells differentiation²⁸⁷⁻²⁸⁹, partly because of delayed silencing of PcG targets involved in pluripotency such as Oct4 and Nanog^{287,288}.

In view of the emerging role of long non-coding RNA (lncRNA) in targeting PcG components^{6,296-298}, the role of Jarid2 in PRC2 recruitment is elaborated by the observation that Jarid2 and Ezh2 share common pool of direct lncRNA interacting partners²⁹⁹. In the case of lncRNA MEG3, which is involved in imprinting³⁰⁰ and pluripotency³⁰¹, Ezh2-MEG3 interaction depends on Jarid2²⁹⁹. Binding studies suggested that Jarid2-Ezh2 interaction is enhanced with the supply of lncRNA.

Despite the role of lncRNA in PcG recruitment, lncRNA and nascent RNA also inhibit PRC2 HMT activity^{123,299}. Based on such “recruitment without activation” function of RNA, it entertained an idea where PRC2 activity remained poised and productive H3K27me3 only follows transcriptional repression elicited by other factors upon differentiation¹²³. Intriguingly, Jarid2 was shown to alleviate RNA-inhibition of PRC2 activity and might be involved to elevate PRC2 activity upon differentiation³⁰².

Study on *Drosophila* Jarid2 (dJarid2) does not fully recapitulate those functions on mammalian models. Despite dJarid2-PRC2 interaction is conserved in *Drosophila*, mosaic clones of dJarid2 in eye disc showed a specific increase of H3K27me3 level while overexpression of dJarid2 conversely led to a global decrease of H3K27me3³⁰³. These results seemed to suggest dJarid2 as a negative regulator on H3K27me3 level. Importantly, like the mammalian homolog, the amino acid residue within the JmjC domain critical for histone demethylation is not conserved in dJarid2³⁰³. And hence dJarid2 should be catalytic inactive for histone demethylation. Biochemical data would need to confirm this idea.

Although dJarid2 overexpression abolished H3K27me3 level and Su(z)12 binding to polytene chromosomes, lost of function studies using Jarid2 mutant did not affect H3K27me3 level nor Su(z)12 binding pattern³⁰³. Also dJarid2 polytene pattern is not affected in E(z) mutant background. As opposed to the mammalian model, these data suggest that chromatin-targeting of dJarid2 and PRC2 are independent of each other despite of their interaction and substantial degree of overlap on genomewide ChIP profile³⁰³. It should be noted that dJarid2 is not enriched in canonical PcG targets such as the Hox clusters³⁰³, and it remained unknown whether any homoeotic transformation phenotypes were detectable in dJarid2 mutant background.

Nonetheless, affinity bait made of oligonucleosomal array assembled with H2Aub can effectively capture PRC2 with dJarid2 and AEBP2/Jing¹¹². And biochemical assay suggested that PRC2 supplemented with both dJarid2 and Jing achieved higher HMT activity than PRC2 alone on H2Aub nucleosomal substrate¹¹². Currently, the physiological role of such enhanced PRC2 activity is not known.

3. 5. 3 Jing/AEBP2 (AE-1-Binding Proteins 2)

From the original identification of HMT activity on mammalian PRC2 activity⁹⁰ to the discovery of mammalian Jarid2²⁸⁵⁻²⁸⁹, affinity-capture of PRC2 components also copurified AEBP2³⁰⁴. (*Drosophila* AEBP2 homolog is known as Jing)

AEBP2 is a zing-finger containing protein that can bind DNA directly³⁰⁵.

ChIP-cloning (similar to regular ChIP protocol except an additional restriction enzyme digestion step is performed after immunoprecipitation, this helps to shorten ChIP fragment size for better prediction of binding motif of chromatin-associating factors) of AEBP2-bound genomic regions showed that >40% AEBP2 enriched peaks mapped closely to

known PcG targets in mouse³⁰⁶. Motif analysis revealed that AEBP2 binding sites were enriched with an unusual bipartite structure³⁰⁶. Whether such DNA-binding property function in PRC2 recruitments awaits further investigations.

AEBP2 also functions as an allosteric activator. It was shown that AEBP2 enhanced mammalian PRC2 HMT activity³⁰⁴. Such stimulatory effect is even more prominent in the presence of Jarid2 on H2Aub-containing oligonucleosomes. Molecular mechanism of such allosteric stimulation is still lacking¹¹². Recent EM-reconstitution of human AEBP2-PRC2 complex showed that AEBP2 interacted extensively with other PRC2 subunits and may help to coordinate and stabilize subunit configurations. Such properties might stimulate productive H3K27 methylation by PRC2²⁶³.

Jing is also copurified with PRC2 and dJarid2 on oligonucleosomal array assembled with H2Aub from *Drosophila* embryos¹¹². Importantly, Jing genetically interacts with Pc, as evident by the enhanced wing-disc Ubx derepression in a transheterozygous *jing*^{22F3/+}; *Pc*^{XT109/+} background³⁰⁷. These data highlight the accessory roles of Jing/AEBP2 in facilitating PcG repression.

3. 6 PR-DUB (Polycomb Repressive Deubiquitinase)

Identification of a novel PcG gene with ubiquitin C-terminal hydrolase (UCH) domain paves the way in understanding the regulation of H2Aub homeostasis²¹⁷. This gene is known as Calypso. Through IP-MS approach, Calypso is found to associate with Additional Sex Comb (Asx) and together they form the Polycomb Repressive Deubiquitinase Complex, PR-DUB, which is conserved from *Drosophila* to mammals¹⁵⁶. Biochemical reconstitution of both human and fly PR-DUB complexes showed that they have robust deubiquitinase activities on H2Aub, but not H2Bub. Loss of PR-DUB led to a bulk increase in H2Aub level in *Drosophila* embryo. Also, mosaic clones of both Calypso and Asx mutant derepressed Hox genes in larval wing discs¹⁵⁶.

These data present a seemingly dilemma on why both positive (dRing) and negative (PR-DUB) regulators of H2Aub are required for efficient PcG silencing. It might suggest an optimal level of H2Aub is essential for gene repression. One could imagine that over ubiquitination of H2A in PR-DUB mutants might titrate away limited readers to elicit its function on specific location. On the other hand, this might suggest a high turnover of H2Aub is required for efficient PcG repression^{147,308}. Similarly, high turn over of H2Bub, achieved by active ubiquitination-deubiquitination cycle, has been proposed for efficient gene activation¹⁵³.

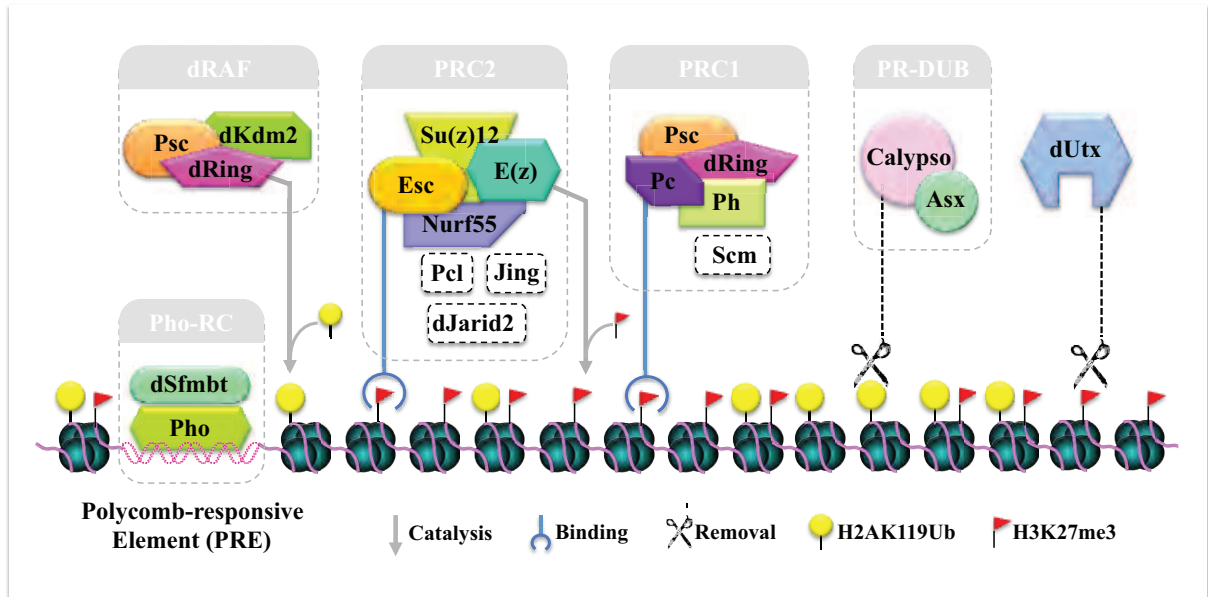


Fig III. *Drosophila* polycomb group proteins and related components.

The five main *Drosophila* PcG complexes are shown. They include Pho-RC which directly binds DNA and recruits other PcG complexes, dRAF which robustly deposits H2A-ubiquitination; PRC2 which catalyzes H3K27 methylations; PRC1 which recognizes H3K27me3 and elicits chromatin compaction and PR-DUB which removes H2A-ubiquitination. dUtx is a trithorax group component which demethylates H3K27me3. Auxiliary factors of PRC1 and PRC2 are highlighted in dotted line. Please refer to text for details.

4. Mechanism of PcG Repression

Despite decades of research in identifying novel PcG components and their associated chromatin-modifying activities, how PcG proteins concertedly elicit gene repression remains a challenging question in the field. In this chapter, potential mechanisms of PcG repressions are discussed, as illustrated in Fig. IV.

4.1 Counteracting chromatin remodeling

PRC1 either purified as immunoprecipitant of FLAG-Ph, FLAG-Psc from *Drosophila* embryo extracts²⁰⁰ or reconstituted from recombinant proteins Pc Ph, Psc and dRing¹⁹⁸, inhibits chromatin remodeling initiated by the SWI/SNF complex on both linear and plasmid nucleosomal arrays. Interestingly, Psc or its paralog Su(z)2 alone also possess such inhibitory function²²⁸. It is postulated that by resisting nucleosome sliding and hence burying the underlining DNA sequence, PRC1 renders promoter sequence inaccessible to transcription factors for gene activation.

Similar study in using mammalian PRC1 components showed that the Pc homolog, M33 (Cbx2) alone or in form of core PRC1 with only Ring1A and Bmi1 was capable of nucleosome remodeling³⁰⁹. Notably, Ring1A and Bmi1 protein alone was inactive in resisting remodeling. Hence it is hypothesized that the chromatin stabilization function of Psc in *Drosophila* is acquired by the Cbx2 subunit in mammals³⁰⁹. Deletion mapping of M33 identified a highly basic region required for counteracting remodeling. Intriguingly, components of PRC1 variants carrying similar basic region such as Pc1 can also inhibit remodeling, indicating that it might be a general function of PRC1³⁰⁹.

4.2 Interference with the transcription machinery

Reconstituted chromatin template assembled with Gal4 binding sites positioned and occupied by nucleosome supports transcription upon sequential addition of GAL4-VP16, ATP, SWI/SNF, HeLa nuclear extracts and NTPs. In the reaction, SWI/SNF remodeling exposes GAL4-binding sites and allows access of GAL4-VP16, which recruits transcriptional machinery from the nuclear extracts²⁰¹. With this in vitro transcription assay, reconstituted PRC1 was shown to efficiently repress transcription even at a low molar ratio to the template, and such repression occurred without affecting GAL4-VP16

binding to the template²⁰¹. Importantly, of all individually purified PRC1 components, only Psc and Ph alone can repress transcription on their own, albeit Ph is less efficient. This fits well with the observation that Psc and Ph belong to the PRC1 mutants that give tumorous phenotype and the most severe Hox derepression phenotype²⁰⁵. Also Psc and Ph are the only necessary factor of PRC1 to repress a class of non-canonical PcG target genes²⁰⁵. With the same assay on chromatin template, subsequent study also showed that reconstituted mammalian PRC1 behave similar inhibitory effect on in vitro transcription³¹⁰. Besides, it was found with, a similar assay, that mammalian PRC2-Ezh1 also repressed transcription, independent of H3K27 methylation activity³¹¹. *Drosophila* PRC2 has yet to be assayed on the same setting. In addition, tethering wild-type Ezh1 and even its SET domain derivative can repress transcription output from a luciferase reporter gene in vivo³¹¹.

More recently, in vitro transcription assay has been revisited using H3K27-MLA¹⁰⁷ assembled nucleosome as a way to recruit PRC1. With this template immobilized on magnetic beads, associating factors can be compared in transcriptionally active vs. repressed states³¹². It was found that incubation with reconstituted PRC1 abolished the assembly of Pre-Initiation complex (PIC) in which TFIID (except TBP) and mediator components were occluded from the transcription template³¹². Given that TFIID components can be co-purified with PRC1 in *Drosophila*¹⁹⁹, perhaps PRC1-TFIID interaction is not compatible with PIC formation.

Study of bivalent genes in mouse ES cells showed that their promoters were enriched with Ser-5 phosphorylated poised RNA Pol II. And upon conditional deletion of Ring1b in a Ring1A-null background, H2Aub drops drastically and these bivalent genes derepressed³¹³. Notably, there were no significant changes in the RNAP phosphorylation profile of these genes. Hence the authors proposed that Ring1b-mediated H2Aub helped to restrain Pol II in a previously unrecognized form that is not processive for active transcription³¹³.

Using the *Drosophila* inducible heat shock promoter hsp26 as a model, transgenic fly carrying ectopic insertion of PRE-hsp26 promoter modules show PcG-dependent repression of downstream reporter genes. Importantly, such repression does not affect binding of TFIID and Pol II. Rather, it restrained Pol II in state refractory to processive transcriptional elongation³¹⁴.

PcG proteins also affect Pol II recruitment. Genomewide nuclear run on (GRO-seq) and ChIP-seq of Pol II in *Drosophila* embryos revealed that, upon perturbation of H3K27me3 in *esc*^{-/-} mutant (obtained by self-crossing *esc*⁶, *b*, *pr* / *CyO*, *esc*²), a large sets of genes

(accounts for ~ 25% of all *Drosophila* genes) acquired significant increase of promoter-proximal Pol II occupancy³¹⁵. When compared to WT, these genes can be divided into two classes. In class I genes, Pol II is recruited already in WT condition and the loss of esc further enhance the binding level. While in class II, Pol II occupancy occurs de-novo. Interestingly, it was found that more class I genes bear signature motifs around their transcription start sites that might favored Pol II binding even in the presence of PcG proteins³¹⁵.

Other than modulation on RNAP, it was shown in macrophages that H2Aub, deposited by another E3 ligase known as hRUL138, is required to repress cytokine genes expressions, potentially by weakening the binding of FACT to H2Aub and hence hamper transcription elongation³¹⁶. Whether polycomb-related H2Aub also counteracts FACT recruitment is yet to be tested.

As discussed above, polycomb repression system could affect the transcription cycle at various stages. These mechanisms might not be generalized and it might vary, depending cell types and structural features of the target genes. Full reconstitution of in vitro transcription reaction on synthetic chromatin template with defined histone marks would be an invaluable tool to dissect the effect of different PcG proteins on transcription.

4.3 Chromatin cross talks –

Inhibition of active chromatin marks

Accumulating evidence demonstrating that PcG repressive activities are very sensitive to local chromatin environment. Likewise, there is a growing appreciation on the inhibitory effect of PcG repressive chromatin on counteracting active chromatin signatures^{4,8,212,317,318}.

H2Aub inhibits H3K4 and H3K36 methylation

Of note, in vitro HMT assays using oligonucleosomes assembled with H2Aub is refractory for H3K36 methylations. Specifically, activities of H3K36 HMTase including Ash1L, HYBP, NSD1 and NSD2 were inhibited, while other HMTase such as PRC2, G9a and Pr-Set7 were not affected¹⁵². Similarly, H2Aub-containing recombinant chromatin inhibits MLL3 for deposition of H3K4me2 and H3K4me3. Treatment of chromatin with H2A-DUB restored MLL3 HMT activity¹⁵¹.

H3K27me3 inhibits H3K4 methylation

Vertebrate H3K4me3 is catalyzed by different HMTases such as Set1A, Set1B and a family of Set1-like complexes containing MLL1-4³¹⁹. All these complexes share common subunits WDR5 and RBBP5, whose binding to H3 tail is strongly inhibited when H3K27 is trimethylated. Consequently, H3K4 methylation activity of Set1A/B and MLL1-containing complexes were attenuated by H3K27me3³²⁰. Hence it suggests that H3K27 demethylation is required to install H3K4me3 by these complexes. Indeed H3K27 demethylase UTX is component of the MLL3/4 Set1-like complex³¹⁹. Whether similar regulation exists in *Drosophila* awaits further investigations.

Counteracting active histone marks

Some PcG components possess histone-modifying activities against active chromatin marks. For example, a component of dRAF, dKdm2 is active for demethylation on H3K36me. Although dKdm2 JmjC mutant did not compromise its stimulatory role for dRAF-mediated H2Aub, the functional relevance of H3K36 demethylation in PcG silencing awaits *in vivo* verification⁷⁷. Similarly, JmjC domain of mammalian Kdm2B is dispensable for the Kdm2B-PRC1-PRC2 recruitment axis⁸¹.

In another case, immunoprecipitates of PRC2 was detected with HDAC activity¹³⁵. Indeed, Rpd3/HDAC1, which is reactive on H3K27 deacetylation, was reported to be co-purified with PRC2 in *Drosophila* embryos^{92,136}. Given the mutually exclusive nature of alternate modified state (methylation/ acetylation) of lysine residues, it is postulated that deacetylation as a prerequisite step for PRC2 methylation on H3K27¹³⁴. Nonetheless, transheterozygous combination of Rpd3 and PcG mutants enhanced Hox derepression and transformation phenotypes^{92,137}.

Mammalian Pcl homologs were shown to recognize H3K36me3 via their Tudor domain⁷¹⁻⁷⁴ (see Chapter I, p.46). Such binding is proposed to recruit PRC2 to active genes to elicit de-novo gene repression. Supporting this idea, PHF19 was shown to interact with the H3K36me3 demethylase NO66³²¹, hence potentially coupling active H3K36 demethylation with productive installment of H3K27me3 during differentiation transitions⁷¹. Similarly in ES cells, PRC2 was shown to recruit RBP2 (JARID1A) for active H3K4me3 demethylation in exchange for robust deposition of H3K27me3 upon commitment in differentiation³²².

4. 4 Chromatin Compaction

As detected by atomic force microscopy, the 12-mer nucleosomal arrays appear to adopt a “beads on the string” conformation. Upon addition of the reconstituted 4-component PRC1, the linear arrays constrict into aggregates in which individual nucleosome cannot be resolved. These compact structures also occupy much less space, as measured by the minimal encircling diameter. Notably, Psc alone or PRC1 lacking Ph can induce such compaction²⁰². Recently characterized self-associating and nucleosome-bridging activities of Psc might be responsible for its compaction function³²³.

In mammalian cells, there are two E(z) homologs known as Ezh2 and Ezh1. Both proteins are interchangeable for PRC2 assembly and possess HMT activity towards H3K27³¹¹. One marked difference between these two mammalian PRC2 variants is that only PRC2-Ezh1 can induce nucleosomal array compaction. And unlike *Drosophila* PRC1 and Psc²⁰², PRC1-Ezh1 compaction required intact histone tails³¹¹. Similar compaction activity for *Drosophila* PRC2 is yet to be determined.

In Ring1b^{-/-} mouse embryonic stem cells, global H2Aub level drops substantially, Hox genes derepress and the Hox locus becomes decompacted, as measured by FISH detection of interprobe distance of the affected locus³²⁴. Intriguingly, reintroduction of WT Ring1b but also the E3-ligase dead allele restores the compact structure of the Hox locus. Hence it supports an H2Aub-independent mode of chromatin compaction effected by the PRC1 complex³²⁴. Nonetheless, H2Aub was shown to facilitate the binding of linker histone H1 to nucleosomal template in vitro³²⁵. Recent study suggests that chromatin compaction function is conserved among different components of PRC1 variants³⁰⁹.

Interestingly, genome-wide profiling of *Drosophila* PRC1 components identify non-canonical PcG targets whose repressions neither require dRing nor Pc. It suggests Psc and Ph alone can repress these genes, which indeed is the case as tested by in-vitro transcription assay²⁰¹. This might be supported by the chromatin compaction activity of Psc. How Ph elicits repression on these genes remained unknown. Especially Ph is dispensable for compaction in reconstituted PRC1²⁰². However, it is well documented that the SAM domain of Ph can form helical polymer^{222,224,225}, and its potential impact on chromatin structure remain untested both in vitro and in vivo.

4.5 3D genome organization – Formation of repressive topologically associating domains (TAD)

The polycomb-responsive element is characterized as the DNA sequence essential and sufficient to elicit polycomb complex recruitment and gene repression^{326,327}. Fab-7 represents one of the best-characterized PRE-containing regulatory elements that control the expression of the Hox gene Abd-B in the bithorax complex (BX-C)^{326,327}. Transgenic fly carrying ectopic insertion of Fab-7 recruits PcG proteins and typically gives variegated repressions of a downstream reporter gene³²⁸. Importantly, as tested on both endogenous and transgenic PREs, silencing of reporter gene is enhanced when the inserted construct is in a homozygous state. This phenomenon is referred as pair-sensitive silencing^{326,327}. Intriguingly, Fab-7 repression on transgene is weakened when the endogenous Fab-7 element is deleted³²⁸. These genetic evidences infer the possibility that PRE elements cluster to act concertedly for synergized PcG repression.

Indeed, with a series of transgenic assays in *Drosophila*, it was shown that two Fab-7 elements separated more than 5kb apart from each other can self-associate and potentially attained a loop conformation³²⁹.

Notably, contacts between PRE-promoters were detected by Dam-ID method. Original design of fusing chromatin protein with the bacterial DAM methyltransferase allows the detection of DNA methylation as readout of protein-DNA interaction³³⁰. By tethering DAM methyltransferase in proximal to the PRE containing Fab-7 element in the BX-C Hox locus, it can profile a collection of loci in contact with the Fab-7 element. With this method, it was found that Fab-7 indeed contact promoter region of Abd-B. Importantly, such Fab-7-promoter contacts occur exclusively in tissue where Abd-B is silenced, indicating its regulatory role in PcG repression³³⁰.

With the technical advance of DNA-FISH and 3C-based technology to detect DNA contacts, it was found that PREs within the BX-C cluster interacted extensively with each other and were postulated to adopt a multi-loop configuration. Importantly, these inter-PRE contacts occurred within Pc bodies when the corresponding Hox genes were repressed. Those PREs associated with active Hox genes were not embedded in Pc bodies^{210,331}.

Remarkably, PRE contacts could occur over long distance²⁹. As exemplified by the *Drosophila* Hox cluster, which is split into the Antennapedia complex (ANT-C) and the Bithorax complex (BX-C), contacts between PREs of Antp and Abd-B are detected even if they were separated 10 Mb apart from each other. With a 4C approach to reveal the “one-to-all” contact profile of the Fab-7 element, it was found that these contacts occurred across the ANT-C and BX-C²⁹. Strikingly, when overlaying the contact map with the ChIP-on-chip profile of Pc, it is prominent that Fab-7 contact hot spots coincided very well with Pc binding peaks²⁹. This echoes the immuno-FISH data showing colocalization of repressed Hox genes within the same Pc body. Importantly, the observed PRE contacts require PcG components. Psc was recently shown to self-associate and bridge nucleosomes in *trans*^{310,323}, and the SAM domains of Scm²³⁴ and Ph^{222,224,225} can polymerize helical structures, these properties might facilitate PRE contacts.

These observations culminate the idea that PcG nuclear bodies act as the hubs of repressions where repressed PcG targets associates. This concept is further elaborated by a plethora of genomewide studies. For instance the number of PcG binding sites outnumbers PcG bodies inside the nucleus, indicating the possibility of different PcG targets sharing the same PcG compartment^{206,208,209}. Of note, principle component analysis based on the genomic distribution profiles of epigenetic regulators and histone marks resolved the *Drosophila* genome into 5 main types of chromatin⁹. And polycomb bound regions, defined as the blue chromatin, represent one of the unique chromatin states that is compositionally distinct from the active chromatin, constitutive heterochromatin and a transcriptionally silent chromatin devoid of known epigenetic features. Applied with 3C-based, high-resolution “all-to-all” chromatin-contact mapping technique known as Hi-C, it becomes clear that the *Drosophila* genome is segmented into topologically associated domain (TAD)³³². Chromosomal contacts are detected throughout the TAD while contact frequency decays towards the domain borders enriched with insulator proteins such as CTCF. Importantly, distribution profile of TAD correlated very well with the underlying epigenetic features along the chromosomes. And homotypic interactions, such as co-association of polycomb-bound repressive chromatin, appear to be a dominant feature of nuclear organization³³². As such, the *Drosophila* genome is spatially partitioned into active and repressive TADs.

The functional significance of nuclear organization in *Drosophila* PcG repression is evidently supported by the initial genetic observation of pair-sensitive silencing of PcG target genes³²⁶⁻³²⁸. Besides, disruption of long-range interaction between Antp and Abd-B by deleting endogenous Fab-7 element results in mild but significant Hox derepression in a sensitized genetic background²¹⁰. In fact, most of the chromatin contacts in ANT-C and BX-C persist in Fab-7 deletion line and supposedly the corresponding repressive TAD architecture is still intact, this might explain the need of a sensitized background to detect derepression phenotype, but it also highlights the possibility that multiple redundant local contacts could reinforce the overall repressive TAD structure to tolerate aberrant loss of specific chromosome contacts. Mechanistically, compartmentalizing PcG repressive TAD could attend a high local density of PREs to facilitate efficient retention of PcG proteins, this might be particularly important for the relatively weak binding affinity of Pc chromodomain to H3K27me3 (¹⁰⁵). It also confers spatial insulation from active transcription machinery. Besides, by spatially confining regulatory elements of PcG targets in a repressive environment, it limits the potential to form alternative chromatin configuration such as enhancer-promoter loop in driving active transcription³³³.

Importantly, the observed PRE co-association requires PcG components^{210,328,331,334}. Recent characterization on a bridging activity of Psc might shed light on how PcG repressive chromosomal contacts can be achieved. As discussed on earlier session, *Drosophila* PRC1 can inhibit transcription on nucleosome template²⁰¹. Remarkably, immobilized nucleosomal array pre-bound with PRC1 or Psc-dRing can inhibit transcription from supernatant templates in *trans*³¹⁰. Thus in vitro data also highlight the capacity of PcG proteins in mediating repressive chromatin interactions.

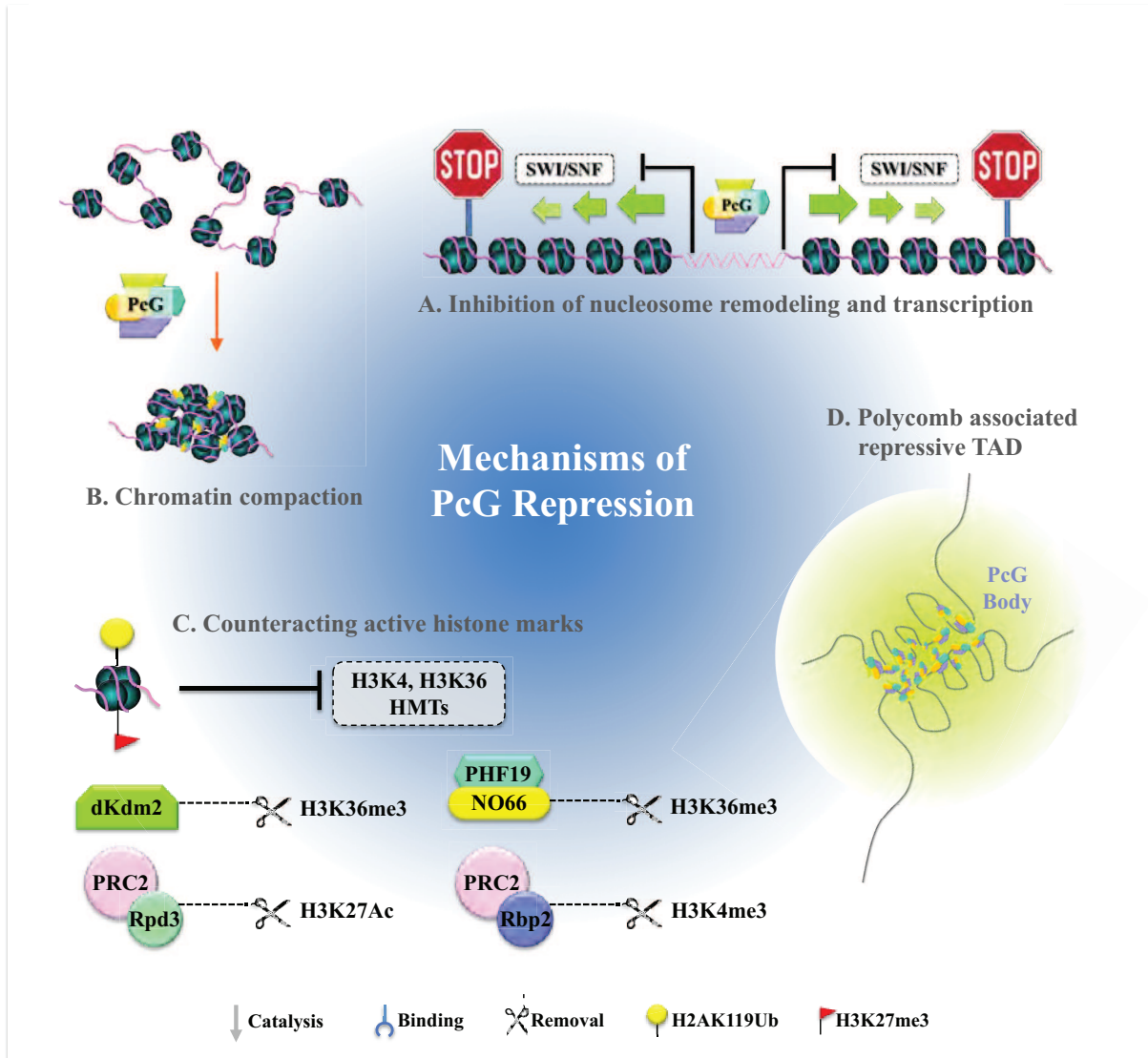


Fig IV. Mechanisms of PcG-mediated gene repression.

Gene repression by PcG proteins are manifested at different levels, from inhibition of nucleosome remodeling and transcription (A), counteracting active histone marks (B), direct compaction of synthetic chromatin (C) to the organization of repressive topologically associating domains (TAD) (D). Please refer to text for details.

5. Mechanisms for Derepression of PcG Target Genes

Guided by comprehensive genomewide studies, it becomes evident that polycomb targets comprise a much broader category beyond the canonical Hox genes. These include signal transduction components, stress-response gene networks, cell cycle regulators and more. Hence there is an emerging idea that in addition to confer stable repression of the Hox clusters, PcG system also contributes to dynamic and switchable gene expressions in response to developmental cues and environmental stimuli³³⁵⁻³³⁷. Central to this regulation is the mechanism of derepressing PcG target genes, which is the key focus of this chapter (Fig V). Of note, mechanism of general active transcription will not be covered.

5.1 ZRF1 (Zuotin-related factor 1)

ZRF1 was identified as a reader of mono-ubiquitinated H2A by affinity purification. Genomewide study revealed that a number of ZRF1 binding sites overlapped with PRC1 and H2Aub target genes, comprising key developmental and differentiation regulators. Importantly, biochemical study suggested that ZRF1 and Ring1b competed to bind H2Aub. Indeed, ZRF1 is recruited to a subset of H2Aub sites during differentiation to displace Ring1b binding, and hence derepresses of PRC1 targets. In addition to PRC1 eviction, in vitro assay showed that ZRF1 also synergized the deubiquitination efficiency of H2A-DUB Ups21^{338,339}.

5.2 Interphasic H3S28ph

Analogous to the first phosphor-methyl switch where H3K9me3S10ph occludes HP1 binding^{177,178,340}, it is found that similar dual modifications such as H3K27me3S28ph could reject binding of PcG components. Notably histone peptide with H3K27me3 can affinity-capture PRC2 and Cbx8 from HeLa cell nuclear extracts¹⁸⁹. But when imposing a juxtaposed phosphorylation in the form of H3K27me3S28ph, the enriched bindings between H3K27me3 to PcG components were lost. It is believed that the huge charge and atomic size of the phosphate group abolish interaction between methylated lysine to the chromodomain of Pc homologs. Similarly, H3S28ph might also interfere binding of EED to H3K27me3.

A vast array of signaling inputs from differentiation, cellular stress and dopamine neurotransmitter activate the MAP kinase-signaling pathway. These signals are funneled to activate MSK1/2, which are recruited to a subset of PcG target genes related to downstream responses^{189-191,341}. MSK1/2 phosphorylates H3S28 and the double mark H3K27me3S28ph evicts both PRC1 and PRC2 from chromatin and leads to derepression of PcG target genes to cope with stress or differentiation^{189,190}. During this process, H3K27me3 level and PcG occupancies decrease while a reciprocal increase in H3K4me3 and Pol II binding occurs on these signaling genes¹⁸⁹⁻¹⁹¹. Of note, prolonged stimulation might lead to acetylation at H3K27 and increased H3K27AcS28ph level¹⁹⁰.

It is important to point out that H3K27me3S28ph is refractory to demethylation by both JMJD3³⁴² and UTX³⁴³. Hence in addition to evict PRC1/2, H3S28ph also protects H3K27me3. Owing to the versatility of phosphorylation kinetics, it is proposed that H3S28ph offers a transient and reversible mode of repression. In this model, removing H3S28ph would allow rapid rebinding of PcG components and robust resumption of repressed chromatin states so that the system retains responsiveness to initial stimuli³⁴³.

Of note, H3S28ph is cell cycle regulated and is highly enriched in mitotic cells^{187-189,344}, its role in modulating chromatin-binding behavior of PcG components during mitosis will be discussed in Chapter III, p.134.

5.3 Aurora B-mediated inhibition of Ring1b-dependent H2Aub.

In resting B cells, Aurora B (AurB) kinase associates with Ring1b and they are required to sustain Pol II occupancy and expressions of a subset of genes. Intriguingly, PRC1 and AurB are enriched at the TSS of these active genes where only low level of Ezh2 and H3K27me3 were detected³⁴⁵. It is proposed that AurB phosphorylates H3S28 and inhibits Ring1b-dependent H2A ubiquitination to enhance Pol II recruitment and transcription. Specifically, AurB enhances the activity of DUB USP16 in H2Aub deubiquitination. Besides, AurB also phosphorylates E2-conjugating enzyme UBE2D3 (UbcH5c) and hampers its activity in Ring1b-dependent H2A ubiquitination³⁴⁵. Whether AurB also directly modulates Ring1b is unknown. It is important to note that H3S28ph does not evict nor recruit Ring1b on these genes³⁴⁵. It is proposed that some unknown transcription factors are required for selective recruitment of Ring1b and H3S28ph might serve to repel PRC2 to facilitate active transcription³⁴⁵.

5. 4 H3K27 demethylation

UTX and JMJD3 belong to the KDM6 demethylase family which specifically remove di- and tri-methylation at H3K27 with the conserved Jumonji C (JmjC)-domain¹²⁵⁻¹²⁸ (see Chapter I, p.14).

UTX is required to sustain expression of active Hox genes^{125,126,128}. RNAi against UTX leads to accumulation of H3K27me2 and H3K27me3 at Hox promoters and enrichment of PRC1 and H2Aub level¹²⁸, resulting in decrease transcriptional repression.

During retinoic acid induction of differentiation, some of the repressed Hox genes such as HOXA1 and HOXB1 become transcriptionally active during which UTX accumulates at their promoter, leading to a decrease in H3K27me3 level. At the same time, PRC2 components are gradually replaced with TrxG proteins and H3K4me3 accumulates at the promoter of these genes^{125,128}. Similar epigenetic changes occur during cardiac differentiation when UTX is recruited to cardiac enhancers to derepress PcG target genes³⁴². Besides differentiation, Utx complexes with transcription factors Oct4, Sox2 and Klf4 to derepress potent pluripotency promoting gene during induced cellular reprogramming³⁴⁶.

Of note, it is demonstrated that the programmed loss of H3K27me3 during early embryonic development can occur independently of Utx and Jmjd3, indicating that other demethylation mechanisms might exist, or passive dilution through cell division might be sufficient for lowering H3K27me3³⁴⁷. Also there is an emerging idea that the catalytic activity of Kdm6 proteins might only play accessory roles. Given the ability to recognize H3K27me3, they might function as a reader to recruit factor essential for gene activation. For example, Utx recruits Brg1, the ATPase subunit of the SWI/SNF remodelers to cardiac enhancer independently of its demethylation activity³⁴². It is thus tempting to speculate that the robust demethylation activity of Utx might be specifically required for a subset of genes such as those required during stress responses.

5.5 DUB (Deubiquitinase)

While PR-DUB complex is essential for PcG repression despite its enzymatic function is to removal H2Aub^{147,156-159}, some DUB enzymes are involved in the derepression of PcG target genes.

In mouse ES cells, the H2A-deubiquitinase USP16 displays an anti-correlated genome-distribution profile with Ring1b. USP16 is enriched with active genes while Ring1b and H2Aub accumulate on repressed genes such as the Hox clusters. ES cells lacking USP16 displayed genomewide increase of H2Aub occupancy and they failed to differentiate. It was found that USP16 is relocated to a number of novel targets during which a global H2A deubiquitination occurs, which is important to activate developmental regulators to commit differentiation³⁴⁸.

Biochemical data showed that H2Aub nucleosomal template did not support H3K4 methylation by MLL3 and it is incompetent for in vitro transcription initiation¹⁵¹. During hepatocyte regeneration, global H2Aub level drops. And gene activations were associated with the lost of H2Aub and a reciprocal gain of H3K4me2 and H3K4me3. Based on differential gene expression data during hepatocyte regeneration, USP21 was identified as the H2A deubiquitinase that specifically acted on nucleosomal H2Aub to promote gene activation¹⁵¹.

2A-DUB/KIAA1915/MYSM1 is yet another H2Aub-specific deubiquitinase. It was identified as a positive regulator for Androgen-signaling genes, which are also subjected to PcG repression³⁴⁹. Interestingly, 2A-DUB forms a complex with a histone acetyltransferase known as p300/CBP-associating factor (p/CAF), and its deubiquitination efficiency is enhanced on acetylated nucleosomal template³⁵⁰. Besides, H2AK119R mutant associates with less linker histone H1 when compared to WT H2A. Hence it is suspected that the lack of H2Aub might favors H1-phosphorylation and eviction from chromatin. Upon addition of androgen-agonist, the downstream signaling target genes PSA is derepressed. During this process, androgen receptor together with 2A-DUB and p/CAF are recruited to PSA promoter, on which the level of H3 acetylation increases with a concomitant drop of H2Aub and H1 occupancy³⁵⁰.

Remarks

As listed from the above examples, it becomes clear that several modes of derepressing PcG target genes exist and such a list would probably keep expanding. This calls for a quest to understand the advantage to have a vast array of mechanisms in overriding PcG silencing. Clearly, we lack the detailed kinetics of each derepression mechanism. Genomewide studies would help to catalog the genes utilizing distinct PcG-counteracting methods, and from the derived gene ontologies we might be able to appreciate more dynamic interplay between PcG repression and derepression.

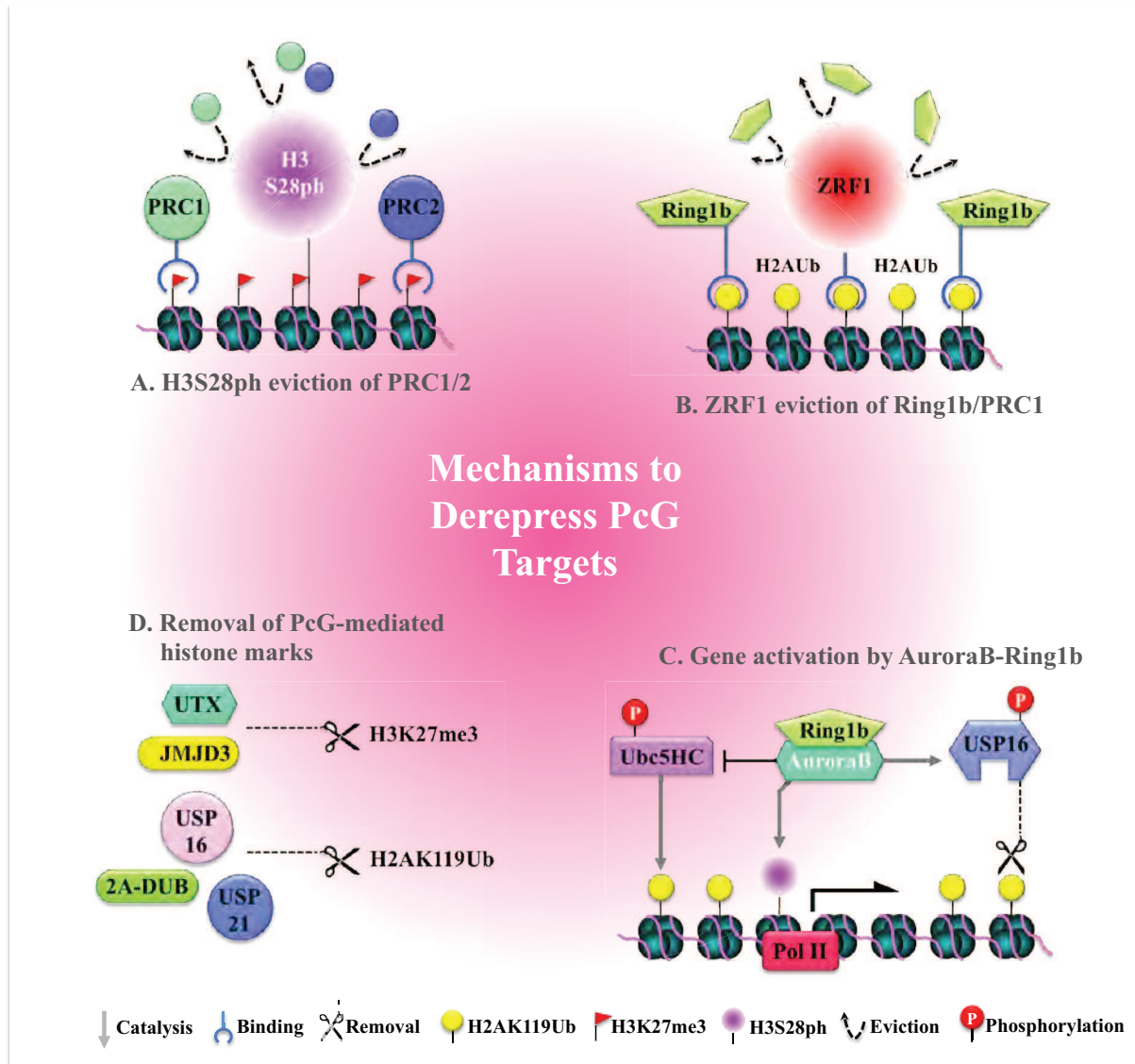


Fig V. Mechanisms for derepression of PcG target genes.

Upon stimulation by environmental factors and developmental cues, PcG targets are derepressed by various mechanisms to trigger downstream responses. H3S28ph evicts pre-bound PRC1 and PRC2 complexes (A). Similarly, ZRF1 displaces Ring1b and hence PRC1 from their target genes (B). In resting B cells, Ring1b is essential to sustain transcription of a subset of genes in collaboration with AuroraB kinase, which phosphorylates key factors to counteract H2A ubiquitination (C). Also, derepression of PcG targets is accompanied by the loss of PcG cognate histone marks (D). Please refer to text for details.

6. Modulation of PcG Repression Activity

Thanks to the advancement of assessing histone-modifying activity using synthetic chromatin template with defined histone marks, we now realize that PcG complexes are very sensitive to local chromatin setting. With the help of structural data, we now have a better understanding on how PcG components integrate and channel chromatin environment to modulate its repressive activity. This chapter mainly focuses on how chromatin features affect PcG activity (Fig VI), and post-translation modification of PcG components will not be discussed.

6.1 H3K27me3

Stimulation on PRC2 HMT activity

PRC2 deposition of H3K27me3 interacts with the seven-bladed beta-propeller structure of Esc/EED WD40 repeats and such interaction stimulates PRC2 HMT activity¹¹³. Hence H3K27me3-Esc/EED stimulatory interaction constitute a positive feedback loop which might be particular important to sustain H3K27me3 repressive domain during DNA replication. Importantly, some phenylalanine residues from the Esc WD40 repeats are critical to contact methylated lysine. Introduction of the corresponding alanine-substitution mutant failed to rescue *esc escl* null mutant and those *Drosophila* larva display diminished amount of global H3K27me2 and H3K27me3 level¹¹³.

Recruitment mark for canonical PRC1

Analogous to the HP1 chromodomain-H3K9me3 binding module^{41,42}, chromodomain of Pc also recognizes H2K27me3^{90,91,105,106}. The prevailing idea is that such interaction contributes to PRC1 recruitment to PcG target genes, despite that H3K27me3-independent mode of recruitment also exists. Apart from this, it is not known whether H3K27me3 can modulate PRC1 activity. At least in *Drosophila*, it is known that dRAF is the dominant form of E3 ligase for H2A ubiquitination and the canonical 4-component PRC1 barely possesses H2A E3 ligase activity⁷⁷. It is known that dRAF and its mammalian paralogous complex prefer to act on nucleosomal H2A^{142,144,145,351}, it would be interesting to test whether H3K27me3 could enhance their E3 ligase activities.

6. 2 H2Aub

Stimulation on PRC2 HMT activity

Nucleosomal arrays assembled with H2Aub affinity-purify PRC2 components and accessory factors AEBP2 (*Drosophila* homolog known as Jing) and Jarid2¹¹². Intriguingly, the 4-component PRC2 displays higher HMT activity when it is supplied with Jarid2 and AEBP2. Remarkably, even stronger H3K27 methylation efficiency is achieved when the 6-component PRC2 is working on H2Aub-containing chromatin template¹¹². Hence in addition to H3K27me₃, H2Aub also stimulates PRC2 HMT activity. In line with this, ectopic nucleation of H2Aub recruits PRC2 components and establishes H3K27me₃ domains *de novo*. These observations suggest an alternative recruitment hierarchy in which H2Aub deposition by PRC1 helps the subsequent binding of PRC2 to PcG target sites.

In addition to PRC2 components, the H2Aub nucleosomal array also captures PRC1¹¹². And indeed H2Aub was found to be associated with Ring1b³³⁹. Hence it is proposed that PRC1-H2Aub binding might also constitute a positive feedback loop to reinforce H2A ubiquitination efficiency.

H2Aub and nucleosome density

Some studies suggested that H2Aub might facilitate the association of linker histone H1 to nucleosomes^{316,325}. Hence H2Aub chromatin might attain a high nucleosomal density configuration that is stimulatory for PRC2 HMT activity, as discussed below.

6. 3 Polycomb-like

Pcl can be co-purified with PRC2^{95,281,282} and it is essential to sustain high activity of PRC2 in catalyzing H3K27me₃^{95,282}. This is consistent with *in vitro* HMT assay, where it is demonstrated that both *Drosophila* Pcl and the corresponding mammalian homolog PHF1 can stimulate high catalytic efficiency of PRC2^{95,281,282}. Notably, all mammalian Pcl homologs including PHF1, PHF19 and MTF2 possess a conserved Tudor domain that specifically interacts with H3Kme₃⁷¹⁻⁷⁴. Hence it raises an attractive model for mammalian PCL to anchor PRC2 at active genes to elicit *de novo* repression during differentiation. In line with this idea, the H3K4 and H3K36 dual specific demethylase NO66³²¹ can complex with PHF19-PRC2. As such, robust removal of active marks alleviates their inhibitions on PRC2 HMT activity and hence permits efficient establishment of H3K27me₃ domains⁷². However, since two critical aromatic residues

within Tudor domain of *Drosophila* Pcl are not conserved, it is not expected to bind H3K36me3^{71,73,284}.

6. 4 Nucleosome density

In vitro HMT assay with oligonucleosomal arrays of defined linker space demonstrated that PRC2 caters more efficient H3K27 methylation on dense chromatin²⁶⁵. As discussed in Chapter I, p.45, the acidic residue within the conserved VEFS motif of Su(z)12 is essential for sensing nucleosome density.

Modeling the EM structure of PRC2-AEBP2 suggests that the complex can adopt a conformation to simultaneously interact with two adjacent nucleosomes without steric hindrance²⁶³. As such, EED binding on one nucleosome can position Ezh2 SET domain in face of the H3 tail of the adjacent nucleosome²⁶³. Having a higher inter-nucleosome density might stabilize such conformation for robust PRC2 HMT activity.

6. 5 H3K4me3 & H3K36me3 inhibit PRC2 activity

Chromatin templates pre-coated with active marks such as H3K4me3 or H3K36me3 are refractory to PRC2 methylation in flies, mammals and plants^{264,352}. Crystallography data suggest that the side chain of H3K4 is engaged in interaction with the Nurf55 beta-propeller domain^{264,353}. Hence increasing the methylation states at H3K4 would progressively introduce steric clashes to the binding pocket in Nurf55. Indeed, the binding of Su(z)12-Nurf55 complex to H3 peptide is abolished upon methylation on H3K4^{264,353}.

Given that VEFS is the main motif of Su(z)12 in contact with E(z)³⁵⁴ and EM structural data reveal its close proximity to the catalytic SET domain of Ezh2²⁶³, it is proposed that the VEFS motif of Su(z)12 can sense and channel chromatin features to modulate PRC2 HMT activity. Consistent with this idea, plant PRC2 with a Su(z)12 variant (VRN2) can remarkably override the inhibitory effect imposed by H3K4me3 and H3K36me3²⁸.

6. 6 H3K27Ac

The side chain of a lysine residue cannot support coexistence of both methylation and acetylation. Owing to this chemical constraint, acetylated lysine occludes the potential of methylation on the same residue. Hence H3K27ac is not a compatible substrate for PRC2 HMT activity. Besides, it remains possible that H3K27ac might have a mild inhibitory effect on PRC2¹⁰².

6. 7 H3S28ph

Since the first discovery of dually modified H3K9me3S10ph histone mark^{177,178}, there are growing examples of phosphor-methyl switches in the eviction of pre-bound chromatin effectors (Chapter I, p.30; Chapter III, p.137). As discussed in Chapter I, p.26, various signaling inputs can activate MSK1/2 to phosphorylate H3S28 on PcG targets^{189-191,341}. The resulting H3K27me3S28ph double mark evicts PRC1 and PRC2 components and leads to derepression of PcG target genes. Of note the binding affinity of EED beta-propeller domain¹¹³ and Pc Chromodomain^{105,106} to H3K27me3 is relatively weak (5-36 uM), and hence these interactions are believed to be disrupted by the huge charge and atomic size imposed by the phosphate group^{189,190}.

6. 8 H3.3

A study from *Drosophila* cultured cells estimates that H3.3 variants account for 25% of total histone H3³⁵⁵. HPLC isolation of H3.3 and MS analysis showed that it is enriched with active histone marks, which is consistent with its enriched genomic distributions over active chromatin and its established mode of incorporation via transcription¹⁰¹. As demonstrated by a recent study in plants, the activities of H3K27 mono-methyltransferases ATXR5 and ATXR6 are inhibited by the Thr31 residue unique to H3.3. It is believed that such substrate preference can prevent aberrant deposition of repressive H3K27 methylation on transcription-coupled H3.3⁹⁹. Although *Drosophila* H3.3 is conserved with a hydrophilic serine residue at position 31, PRC2 does not seem to be refractory to act on H3.3, as discussed in Chapter I, p.10.

6. 9 CpG methylation

Mammalian Kdm2B-RYBP containing PRC1 variant can nucleate *de novo* H2A ubiquitination to establish a chromatin platform for PRC2 recruitment and formation of H3K27me3 domain^{81,155}. Central to this alternative recruitment hierarchy is the Kdm2B protein, which possess a CXXC domain whose binding to CpG island is sensitive to cytosine methylation^{79,80}. Indeed genomewide distribution of Kdm2B is highly enriched at unmethylated CpG islands in ES cells and is inversely correlated to methylated CpG in differentiated cells⁸⁰.

Given the wide distribution of CpG islands over gene promoters, dKM2B-PRC1-PRC2 may represent a versatile recruitment axis subjected to regulation by CpG methylation in mammalian cells^{81,356}. In fact, mouse somatic cells severely compromised in DNA methylation displayed drastic redistribution of global H3K27me3. It is proposed that DNA hypomethylation increases accessible CpG island that titrate PRC2 away from its native targets, resulting in the loss of H3K27me3 and their derepression^{155,357}.

6.10 RNA inhibition of PRC2 activity

In mouse ES cells model, it was found that PRC2 also occupy promoter regions of active genes with low level of H3K27me3^{358,359}. In addition, the use of photo-activatable ribonucleoside-enhanced cross-linking and immunoprecipitation (PAR-CLIP) documented a catalogue of Ezh2-associating nascent RNA³⁵⁹. These observations culminate an idea that PRC2 occupancies at active genes are inhibited by their nascent transcripts. Indeed, in vitro assay showed that PRC2-interacting lncRNA such as HOTAIR and RepA inhibits PRC2 HMT activity in a length dependent manner^{123,302,358}. Similar observation was made for *Drosophila* PRC2³⁶⁰. Interestingly, RNA lacking secondary structures such as the extended polyA stretches did not possess inhibitory effect. Using *Ntn1* as a model of PRC2-bound active gene, introduction of premature polyadenylation site downstream proximal to *Ntn1* transcription start site (TSS) effectively reduced transcription output and committedly increased H3K27me3 level at promoter region¹²³. As such, PRC2 activity can be regulated at a post-recruitment level. A recent report showing genomewide de-novo recruitment of PRC2 upon transcription inhibition³⁶¹, it would be interesting to know whether H3K27me3 also increases in those active genes pre-bound by PRC2.

Remarks: Emerging concepts on regulating PcG repression

The growing knowledge in how chromatin features affect PcG components begins to culminate the idea that, apart from the regulation by binding compatibility, PcG proteins activities can also be modulated at a post-recruitment level.

For example, it was found that during DNA replication, PcG proteins remained associated with nascent chromatin without apparent activity on catalyzing histone methylations³⁶². Besides, by isolating tissues with differential expression states of the Hox gene *Ubx*, it was shown that PRC1 and PRC2 components bind to PRE of *Ubx* disregarded of its expression status¹²². Similarly, FACS-sorting parasegment-specific nuclei from *Drosophila* embryos with differential Hox expression states demonstrated the presence of Su(z)12 at active Hox genes without apparent level of H3K27me3¹¹⁴. More recently, it was shown in mouse ES cells that nascent RNA transcripts emanating from PcG binding site can inhibits PRC2 HMT activity without affecting their binding¹²³. As such, it becomes evident that the PcG occupancy at target sites might not necessarily coincide with the presence of their cognate histone modifications. It is thus proposed that, like RNA polymerase, PcG complexes can be held in a poised state competent for robust establishment of repressive chromatin states upon the presence of transcriptional repressors¹²³.

Another important concept is to interpret chromatin signal in context. Given the vast number of PcG complex variants, one rule might not apply to all. This is so far best demonstrated by the plants PRC2 variants, whereby assembling PRC2 with an alternative Su(z)12 paralog can override the otherwise inhibitory effect of active chromatin²⁶⁴. This highlights the functional diversity of PcG complex variants.

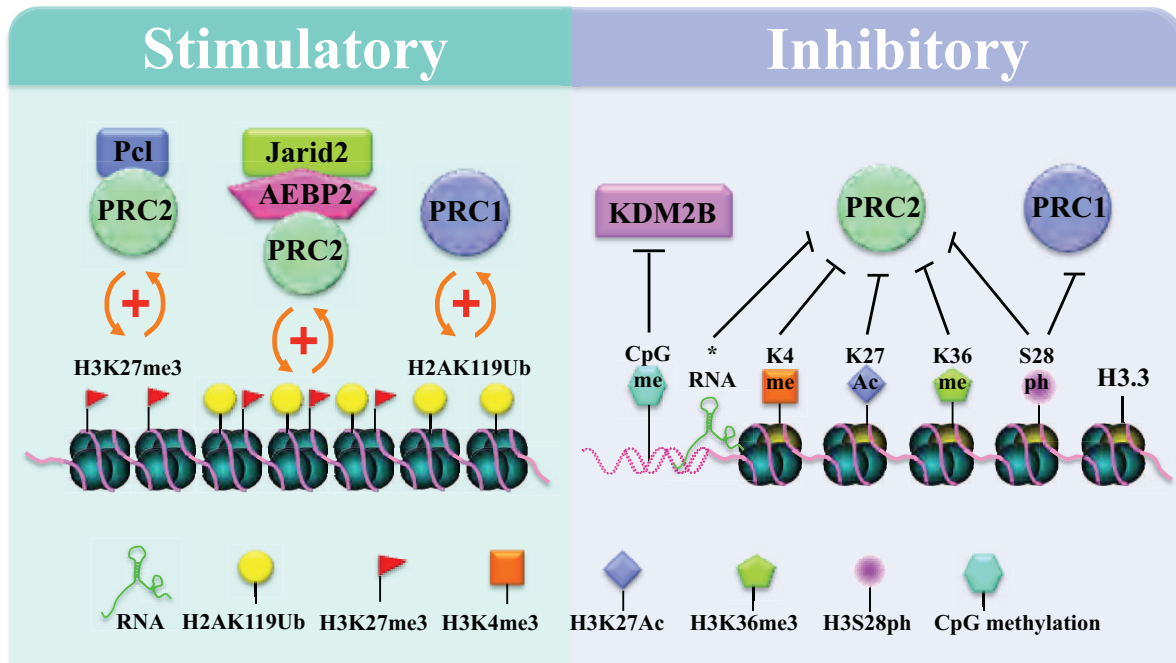


Fig VI. Modulating the repressive activity of PcG components.

The activities of PcG complexes are very sensitive to local chromatin environment. PcG complexes possess components to detect both active and repressive histone marks. In general, cognate repressive histone marks such as H2Aub and H3K27me3 are stimulatory to PcG complex activities. Active histone modifications, on the other hand, present a binding barrier against the establishment of PcG-repressive domains. Please refer to text for details. * RNA includes lncRNA and nascent RNA transcripts.

7. Epigenetic Inheritance of PcG-mediated Gene Repression

Polycomb-mediated repression of Hox genes represents a classical epigenetic phenomenon in which the Hox expression pattern established during early embryogenesis were maintained throughout later developmental stages in the absence of initial transcription repressors^{8,298,363-365}.

Such epigenetic memory entails mechanisms to preserve repressive chromatin states from one cell cycle to the next. In this Chapter, potential epigenetic inheritance mechanisms in cope with DNA replication (Fig VII) and mitotic chromosomes condensation (Fig IX) will be discussed.

7.1 DNA replication

During DNA replication, transversal of replication fork can evict pre-bound chromatin factors and de-novo chromatinization inevitably dilutes pre-existing histone modifications. These factors impose immense challenge to maintain PcG repressive chromatin³⁶⁶⁻³⁶⁸.

Persistence of PcG proteins during DNA replication

As demonstrated with in vitro SV40 replication system, reconstituted *Drosophila* PRC1 or Psc alone remains associated with nascent chromatin³⁶⁹. The same result is obtained when using a simple reconstituted T7 bacteriophage replication system devoided of endogenous eukaryotic proteins³⁷⁰; hence it highlights the intrinsic persistent-binding properties of PRC1 and Psc during the course of replication. Given that Psc can self associates and bridge nucleosomal templates³²³, a model is proposed in which the potentially displaced Psc proteins during replication fork traversal are retained by self-association to those Psc molecules on the parental chromatin. These retained pools of Psc would reassociate with nascent daughter chromatin once they are emerged from the replication fork. This elegant model emphasizes retention of Psc/PRC1 on chromatin template while allowing the passage of replication fork^{323,363}. The SAM domain containing PcG protein Ph is capable of oligomerization²²⁵, such property may act similarly to PSC to accommodate replication fork passage. Supporting this persistent binding model, both PRC1 and PRC2 components

are detected on nascent chromatin by both mass-spectrometry³⁷¹ and microscopy approaches³⁶².

Restoration of H3K27me3 repressive chromatin

Several observations support the idea that parental histones are partitioned randomly over daughter chromatin, together with the pre-existing histone modifications. Notably, H3K27me3 is detected on nascent chromatin even in the presence of translation inhibitors³⁷¹.

Since H3/H4 is inherited as intact tetramer (no splitting) and over 40% of global H3K27me3 exist as asymmetrically modified nucleosomes^{119,121}, it does not favor a semi-conservative mode of duplicating histone modifications. Hence it is likely that H3K27me3 is not restored in a nucleosome-resolution fashion³⁶⁵. Nonetheless, the inheritance of parental histone and their associated modifications can act as seeding sites that guide the propagation of pre-existing chromatin features^{363,365}. In the case of PcG targets, the inherited H3K27me3 can be recognized by the EED subunit of PRC2¹¹³. Such interaction not only helps PRC2 retention but also allosterically stimulates PRC2 HMT activity, hence it constitutes a positive feedback loop to catalyze robust deposition of H3K27me3¹¹³ (See Chapter I, p.41). In line with the “seeding model”, it is observed in *Drosophila* culture cells that there is an increase in H3K27me3 level at PcG target just before DNA replication. Such predeposition of H3K27me3 is proposed to alleviate the effect of passive dilution during DNA replication^{372,373}.

SILAC (Stable Isotope Labeling of Amino Acids in Cell Culture)-based approaches represent exceptional tool to track dynamic changes of site-specific histone methylation status. Since mammalian cells are incapable of synthesizing methionine, which is the metabolic precursor of SAM (S-adenosyl methionine), the sole methyl-group donor for histone methylations, the use of isotopic methionine in defined cell culture medium can eventually label histone methylations with different atomic masses at different time course of interest. When coupled with quantitative mass-spectrometry, detail changes of histone methylation status can be traced³⁷⁴.

Thanks to SILAC approaches, we now know that the kinetics of H3K27me3 restoration can be divided into two phases. Most H3K27dimethylations are restored during S-phase but H3K27 trimethylation on new histones occur much slower and are not fully restored during DNA replication³⁷⁵. Most of the H3K27me3 is catalyzed in a post-replication

manner and full restoration is achieved in the next G1 phase. The H3K27 methylation kinetics across the cell cycle is in good agreement with proteomics analysis of nascent chromatin composition in which PRC1 and PRC2 are further enriched in maturing chromatin³⁷¹.

These studies highlight the fact that PcG targets remain repressed despite cell-cycle fluctuation of H3K27me3 level. Hence a buffer model of gene repression is proposed³⁶⁵ (Fig VIII) where a certain degree in the drop of H3K27me3 is well tolerated and not until a critically low level would permit gene derepression. The broad domain of H3K27me3 might facilitate efficient seeding of parental histone modification over daughter chromatin and also help to maintain overall repressive chromatin features despite passive dilution of histone marks during replication³⁶⁵.

The observed imprecise restoration of repressive chromatin might challenge the fidelity in maintaining epigenetic information. Importantly, PRC2 activity is restrained over active chromatin as discussed in Chapter I, p.70. Hence gene activity and chromatin features also play an important role to guide fidelity in reestablishing PcG epigenome without excessive spreading of H3K27me3 and ectopic repressions.

Outlook and remarks

Despite decades of research, the fundamental question on the epigenetic mechanism of PcG repression remained largely unknown. Notably, we have no idea about change of enzymatic activity, complex integrity, component stability of the PcG repression system across the cell cycle. Also, experiments aim to testify the buffering capacity of PcG repressive chromatin is still lacking. With the advancement of fast-acting small molecule inhibitors against Ezh2³⁷⁶, one could now ask how many rounds of cell-cycle passive dilution of PcG chromatin features is enough to trigger derepression. In *Drosophila* embryo, it was found that only PcG components, but not their cognate histone methylations, were detected on nascent chromatin³⁶². Hence it argues against the role of H3K27me3 as the epigenetic information carrier over DNA replication and suggests *de novo* establishment of H3K27me3 over newly replication template. Despite the apparent discrepancies with the “seeding” model, it highlights the possibility that active histone methylation might not be mechanistically compatible with *de novo* histone deposition. In particular, PRC2 activity might be inactivated by chemical modifications associated with newly deposited histones.

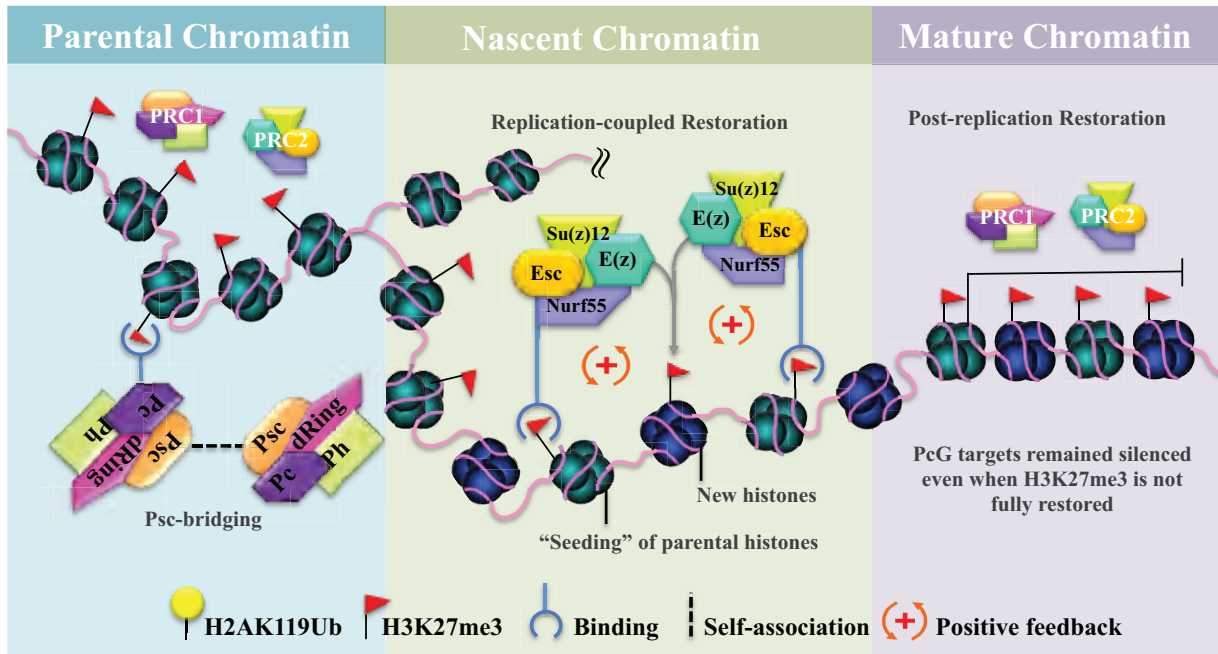


Fig VII. Epigenetic inheritance of PcG repression through DNA replication.

Traversal of replication fork and de novo chromatinization dilutes parental histone modifications. The figure highlights the self-association / bridging activity of Psc, which might facilitate rebinding of PRC1 complex to nascent chromatin. Transfers of parental histones to nascent chromatin serve as a seed to nucleate and guide restoration of PcG repressive domain by positive feedback loops between H3K27me3 and PRC2. Full restoration of H3K27me3 is not achieved during S-phase, and post-replication catalysis of H3K27me3 continues until next G1 for complete restoration of H3K27me3 level. * Figure modified from *Campos et al*³⁶³.

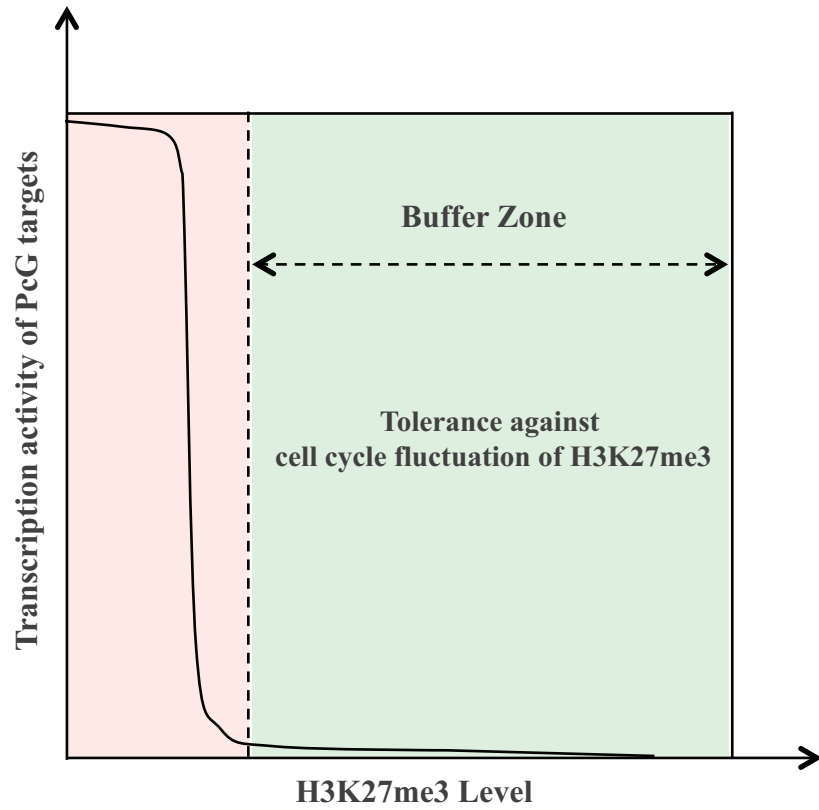


Fig VIII. Buffer model of H3K27me3 levels for effective gene repression despite cell cycle fluctuation.

The model suggests that cell cycle dilution of H3K27me3 is not sufficient to trigger derepression so that it permits post-replication full restoration of parental H3K27me3 level.

* Figure modified from *Huang et al*³⁶⁵.

7. 2 Mitosis

To ensure faithful segregation of the replicated genome, systemic chromatin condensation is achieved during mitosis so that sister chromatids are gradually resolved to facilitate pole-ward separation. To facilitate proper condensation, global transcriptions are shut down³⁷⁷ and even rDNA activity is halted^{378,379}. And persistent rDNA transcription would lead to segregation defects such as anaphase bridges, potentially due to entanglement of the active rDNA locus³⁷⁹. Notably, H2A.Z-containing +1 nucleosomes of active genes are upshifted to cover the transcription start sites during mitosis, rendering them incompetent to support transcription^{380,381}.

Owing to tremendous shrinkage of the chromatin volume, lots of chromatin-bound molecules such as RNA polymerase II, transcription factors and even non-coding RNA are mostly evicted. This presents a challenge to preserve epigenetic information and cellular identity³⁸²⁻³⁸⁴.

Mitotic bookmarking as a way to preserve transcription status

Early observations revealed the persistence of DNase hypersensitive sites during mitosis³⁸⁵ and it is now clear that a subset of transcription factors or chromatin effectors remain associated with mitotic chromosomes despite immense chromatin condensation. They are referred to as mitotic bookmarking factors and their persistent binding serves to robustly reactivate specific target genes in early G1 phase of the next cell cycle, and help to restore cell type specific transcriptome³⁸²⁻³⁸⁴. Importantly, repressive chromatin structures are also disrupted during mitosis, and an example of bookmarking repressed genes is also reported^{386,387}.

Examples of different mitotic bookmarking mechanisms

Among the growing examples of mitotic bookmarking, it was shown that mitotic retention of Brd4³⁸⁸⁻³⁹⁰ and MLL³⁹¹ on chromatin is required for robust reactivation of their target genes in next G1. Besides, the TATA-box binding protein (TBP) helped to recruit PP2A to keep condensin at a hypo-phosphorylated and inactive state. As such a local decompacted region can be maintained at TBP-bookmarked sites to facilitate subsequent gene reactivation^{392,393}.

Recent ChIP-seq analyses of over a hundred transcription factors identified clustered binding sites with over 100 transcription factor occupancies³⁹⁴. Interestingly, these clusters

are always anchored with cohesin whose binding persisted during mitosis^{394,395}. Normally, bulk cohesin rings are removed from chromosome arms starting from prophase under the control of Aurora B kinase³⁹⁶. How cohesin at clustered site counteract such removal pathway is not know, but it is proposed that such cohesion retention help to maintain DNA accessibility to facilitate rebinding of transcription factors during mitotic exit^{394,395}.

In one elegant study of the pioneering factor GATA1, which is a hematopoietic transcription factor essential for establishment and maintenance of erythroid lineage, live-cell imaging and ChIP-seq of FACS-sorted mitotic cells detected GATA1 persistent binding on mitotic chromosomes³⁸⁷. Importantly, the bookmarked GATA1 targets included important hematopoietic regulators and they showed a more robust reactivation kinetics compared to unbound targets. The functional relevance of bookmarking was elegantly demonstrated by fusing GATA1 to the degradation box of Cyclin B to achieve mitosis-specific degradation of GATA1. It was found that GATA1 depletion during mitosis resulted in slower reactivation kinetics of GATA1 bookmarked genes in the next G1 phase, highlighting the essential role of mitotic bookmarking^{386,387}. Similar bookmarking function is observed for another pioneering factor FOXA1³⁹⁷.

Are PcG targets bookmarked during mitosis? If so, how?

Although the majority of known bookmarking examples come from active genes, preserving epigenetic features of repressive chromatin states during mitosis are also important.

As exemplified by the pioneering factor GATA1, which also functions as a repressor, depletion of GATA1 during mitosis also leads to partial derepression of its target genes³⁸⁷. It demonstrates that despite global transcription inhibition during mitosis, silenced genes were also susceptible to ectopic reactivation if their associated repressive chromatin features are not preserved.

As for *Drosophila* PcG proteins, whether they bind to mitotic chromosomes are somewhat controversial, largely because of the varied methods of detection. Early observation with indirect immunofluorescence on formaldehyde-fixed embryo showed that virtually bulk proportion of PRC1 components such as Pc, Ph and Psc were dissociated from metaphase chromosomes, and Psc is the only component which begins robust rebinding in anaphase³⁹⁸. In contrary, pre-extracting culture cells with detergent-containing buffer followed by methanol/acetone fixation robustly detected substantial amount of dRing, Pc

and Psc on mitotic chromosomes³⁹⁹. Similarly, squashed samples from *Drosophila* larval brains also readily detect strong retention of Pc, Ph, Psc and E(z) on mitotic chromosomes⁴⁰⁰.

In addition to microscopy approaches on fixed samples, western blot analysis of chromatin-pellet, defined as the insoluble fraction after cell lysis by non-ionic detergent buffer, detect ~ 10-30% of PcG proteins are retained on mitotic chromatin³⁹⁸, although the nocodazole-treated cells only show a mitotic index of ~ 68%. Hence some of the chromatin-bound proteins should come from a G2 population.

Owing to potential bias introduced to the immunostaining protocol, live-cell imaging is regarded as the golden standard for detecting chromatin-retention of PcG factors during mitosis. Until now several PcG-GFP fusion lines were established, and all of these fusions rescue their corresponding null mutants, indicating that GFP-fusion does not interfere with the protein function.

Pc-GFP fusion rescues the chromodomain mutant of Pc but not the corresponding null mutant, nonetheless, Pc-GFP shares same polytene staining pattern as endogenous Pc and hence it is considered that the GFP-fusion can reflect cellular distribution of Pc⁴⁰¹. With these GFP-fusion lines, Pho, Pc, Ph, E(z) and Esc (unpublished) were found dissociated from chromatin during the course of entire mitosis in syncytial blastoderm⁴⁰². Of note, the Hox gene expression patterns are not yet specified at such early embryonic stage. FRAP study of Pc-GFP showed that the residence time of Pc on mitotic chromosomes increase in later stage of development³⁴⁴.

Recently a series of inducible PcG-GFP fusion stably cell lines were analyzed in mammalian model⁴⁰³, and unlike the tested *Drosophila* homologs, canonical PRC1 components Cbx2-GFP, Ring1b-GFP, Phc1-GFP (*Drosophila* Ph homolog) and Mel18-GFP (*Drosophila* Psc homolog) showed striking association on mitotic chromosomes with a long residence time⁴⁰³. Of note, among other Pc homologs, only Cbx2 show exclusive mitotic retention with long residence time. Other Cbx components show much faster exchange rate on mitotic chromosomes. Importantly, mitotic association of Cbx2 does not rely on other PRC1 components or H3K27me3, as persistent binding is still detected even in Rinb1a^{-/-} Ring1b^{-/-}, Bmi1^{-/-} Mel18^{-/-} and Eed^{-/-} mouse ES cell knockout backgrounds⁴⁰³. In contrary, other PRC1 components binding to mitotic chromosomes are disrupted in Cbx2^{-/-} knockout line, demonstrating the pioneering role of Cbx2 in mitotic binding of mammalian PRC1⁴⁰³. Given that such mitotic PRC1 retention is not dependent on H3K27me3, it would be interesting to know if it reflects a non-specific binding property of

PRC1. ChIP-seq of PRC1 with mitotic samples would be needed to address this question. Finally whether Cbx2-mediated anchoring of PRC1 on mitotic chromosomes is essential for preserving PcG repressive chromatin awaits further loss of function studies.

Other than microscopy approach, ChIP assay is also used to detect and locate mitotic binding of PcG proteins. Taking advantage of specific enrichment of H3S10ph during mitosis, a FACS-sorting procedure was optimized to isolate large quantities of H3S10ph-positive mitotic cells from colchicine-treated cell culture³⁹⁹. ChIP-seq on Psc using asynchronized (H3-sorted) and purified mitotic samples (H3S10ph-sorted) revealed that majority of Psc bindings were lost during mitosis, while a selection of them persisted, despite at a lower enrichment than in the asynchronized sample. No novel Psc-binding sites were detected in the mitotic sample³⁹⁹. Importantly, canonical PcG targets such as the Hox clusters showed dramatic reduction of Psc occupancy during mitosis. For those mitotic-retention targets of Psc, they are enriched with genes involved in cell cycle regulation. Strikingly, 84-94% of mitotic Psc sites overlapped with insulator binding sites, these included CP190, CTCF, BEAF and chromator³⁹⁹. Consistent with this finding, it was found that almost half of the Psc mitotic sites overlapped with domain borders, which is defined as the genomic regions lacking long-range chromatin contacts³³². Although there are no Psc mitotic sites within the Hox clusters, ChIP-qPCR detects similar enrichment of H3K27me3 in Hox PREs in both asynchronized and G2/M cells, suggesting that H3K27me3 might serve as a bookmark to guide rebinding of PcG protein during mitotic exit³⁹⁹. Based on these data, it was proposed that the majority of Psc is dissociated from its target sites during mitosis, and those retained on domain borders could serve as mitotic reservoir which facilitates robust relocation of Psc and other PcG proteins to their targets in the following G1 phase³⁹⁹.

Outlook and remarks

The golden standards to testify a mitotic bookmarking function reply on at least three important approaches. First, live imaging of potential bookmarking factors is needed to determine chromatin-binding kinetics during the sub-phases of mitosis. FRAP experiments would also be informative on the change of chromatin residence time between interphase and mitosis. Second, ChIP-seq profiling of mitotic chromosome occupancies. With the increasing ease of FACS-sorting H3S10ph-containing mitotic cells⁴⁰⁴, it is important to compare if specific targets are bookmarked, these data would also guide later lost of function studies. Third, selective ablation of bookmarking factors during mitosis ultimately addresses the necessity of their mitotic retention in the resumption of target genes expression status in the subsequent cell cycle.

Unfortunately, previous studies on PcG mitotic bookmarking have yet to incorporate all the above approaches. Particularly, owing to a diversified method of detection, there is a lack of consensus on the mitotic binding behavior of PcG components on *Drosophila* fixed samples. And although live imaging is more reliable, a comprehensive PcG-GFP fusion lines are still lacking. Despite the observation that a subset of Psc binding sites are retained on mitotic chromosomes, their essential role in maintaining PcG repression awaits further lost of function study. Finally, despite the fact that FACS-sorting mitotic cells are getting more and more efficient, ChIP-seq profiles of any histone modifications during mitosis are still awaiting³⁸⁴. This is particularly interesting since mitotic chromosomes are highly enriched with H3S28ph, and H3K27me3S28ph double mark is shown to evict PcG components and refractory to UTX-mediated demethylation^{342,343}, it would be of great interest to see how their function interplay is reflected on a genomic scale.

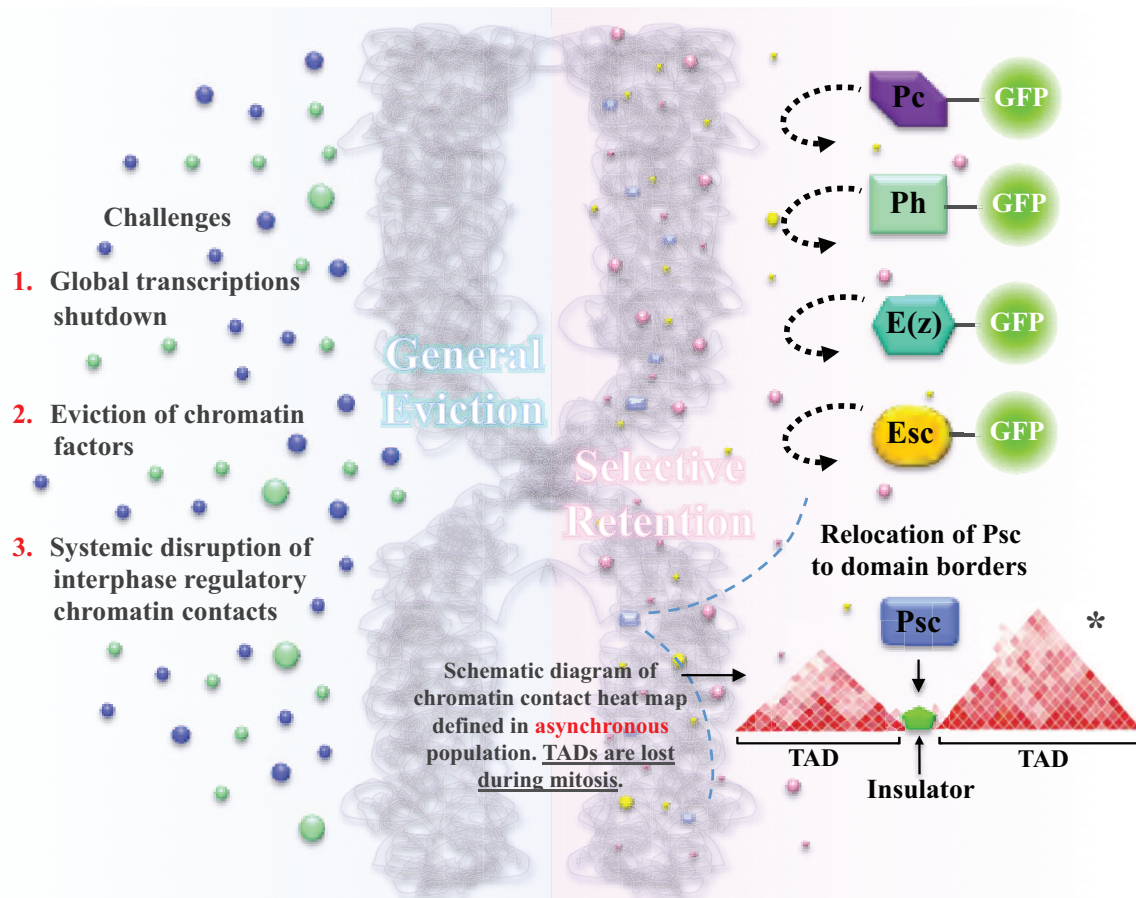


Fig IX. Epigenetic inheritance of PcG repression through mitosis.

During mitosis, global transcription is halted and the massive mitotic chromosome condensation evicts numerous chromatin factors and abolished regulatory chromatin contacts established during interphase. These inevitably impose distortion of cell-type specific transcription network. A selection of transcription factors and epigenetic regulators are specifically retained on mitotic chromosomes to serve as “bookmarks” to instruct robust restoration of the transcription programs upon entry to the next cell cycle. Live imaging studies of most PcG-GFP fusions in *Drosophila* argue their dissociation from mitotic chromatin. Nonetheless, ChIP-seq of mitotic cells detects a subpopulation of Psc is enriched on domain borders. Please refer to text for details. * Schematic diagram of chromatin contact heat map modified from Ong & Corces⁴⁰⁵.

Chapter II

Results

1. **Cell cycle Dynamics of H3S28ph, H3K27me3 and Pc in *Drosophila* S2 Cells**
2. ***In vivo* RNAi against Aurora B kinase in *Drosophila***
3. **Principle of the histone replacement system in *Drosophila***
4. **Principle of mosaic analysis of histone mutants in *Drosophila* larval tissues**
5. **H3S28 is required for efficient PcG-mediated Gene Repression (Submitted Manuscript)**
6. **Extended Results: Phenotyping *H3S28A* mutant in *dUtxA* background**

Results

Guided by the studies in mammalian models, interphase H3S28ph deposited as H3K27me3S28ph dual modification was shown to counteract chromatin binding of both PRC1 and PRC2 components^{189,190}. This serves as a mechanism to derepress PcG targets in response to stress or developmental signalings. Meanwhile, biochemical data suggested that H3K27me3S28ph is resistant to demethylation and hence H3S28ph might shield H3K27me3 from demethylases^{342,343}. Since H3S28ph is highly enriched during mitosis, I wonder if mitotic H3S28ph might modulate PcG-mediated epigenetic inheritance in a cell cycle context. To address this question, I documented the cell cycle dynamics of H3S28ph along with H3K27me3 and Pc in *Drosophila* S2 cells. Secondly, I checked if the PcG system is misregulated upon RNAi against Aurora B, the kinase responsible for mitotic H3S28ph.

1. Cell cycle dynamics of H3S28ph, H3K27me3 and Pc in *Drosophila* S2 cells

As shown in Fig 1 & 2, both H3S10ph and H3S28ph shared similar cell-cycle dynamics, with peak level of phosphorylation achieved during the course of mitosis, from prophase to anaphase. Dephosphorylations of H3S10ph and H3S28ph occurred in telophase. Interphase H3S28ph was undetectable in the experiment condition, which was consistent with a previous report¹⁸⁸. H3K27me3 was detected throughout the cell cycle. A previous study suggested that H3S28ph would impede antibody recognition of H3K27me3 on the same histone tail¹⁸⁹. Despite potential epitope masking by H3S28ph, high level of H3K27me3 was detected during the course of mitosis. As for PcG proteins, the majority of Pc proteins were displaced from mitotic chromosomes and reassociation began in telophase. This is consistent with previous observations in fixed cells³⁹⁸ and live-imaging⁴⁰².

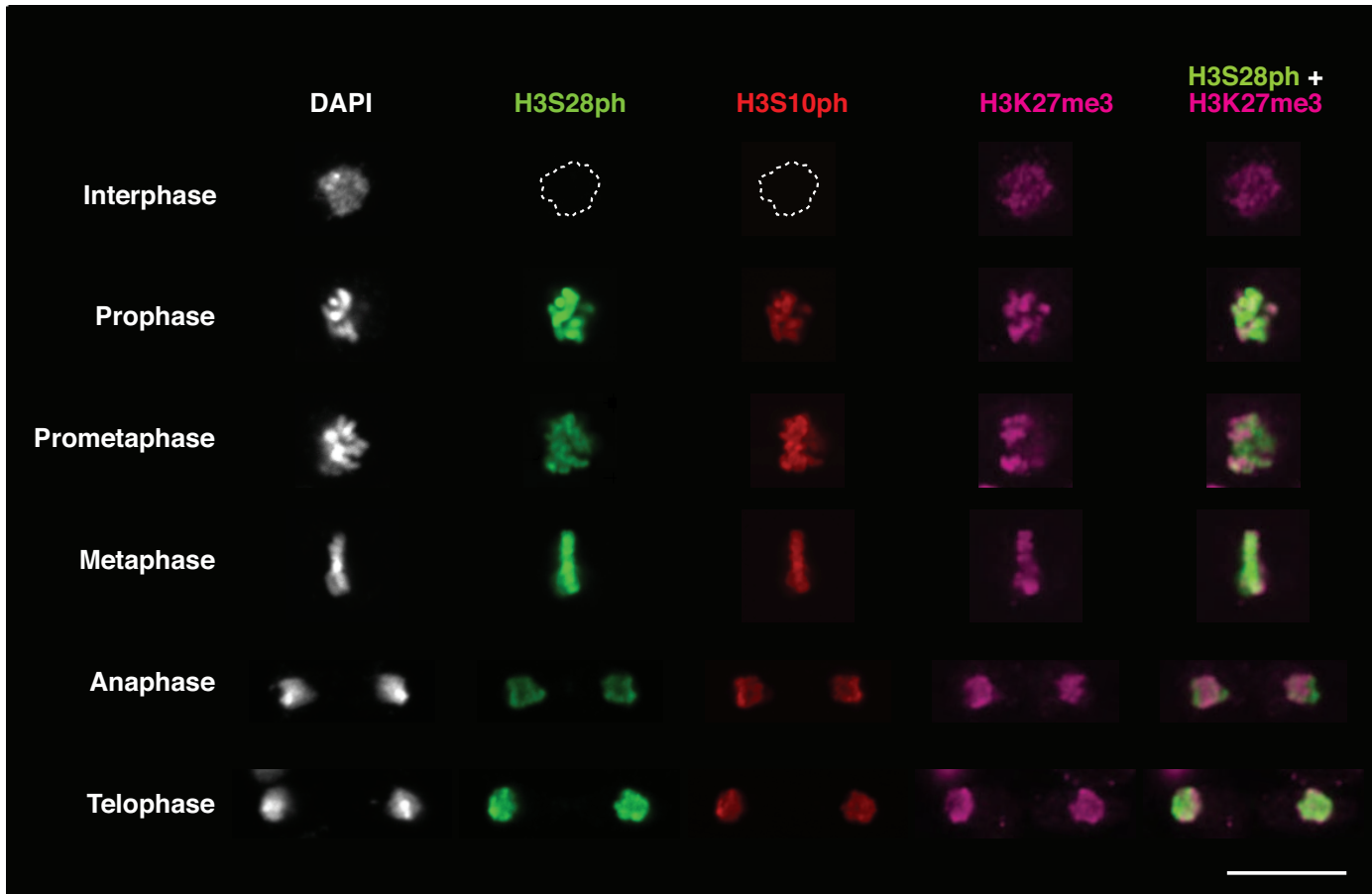


Fig 1 | Cell cycle dynamics of H3S10ph, H3S28ph and H3K27me3.

Immunostaining of H3S10ph, H3S28ph and H3K27me3 of *Drosophila* S2 cells during interphase and mitosis. Since H3S10ph and H3S28ph are undetectable in interphase, the nuclei boundaries of both channels are highlighted with dotted line. Scale bar = 10 μ m.

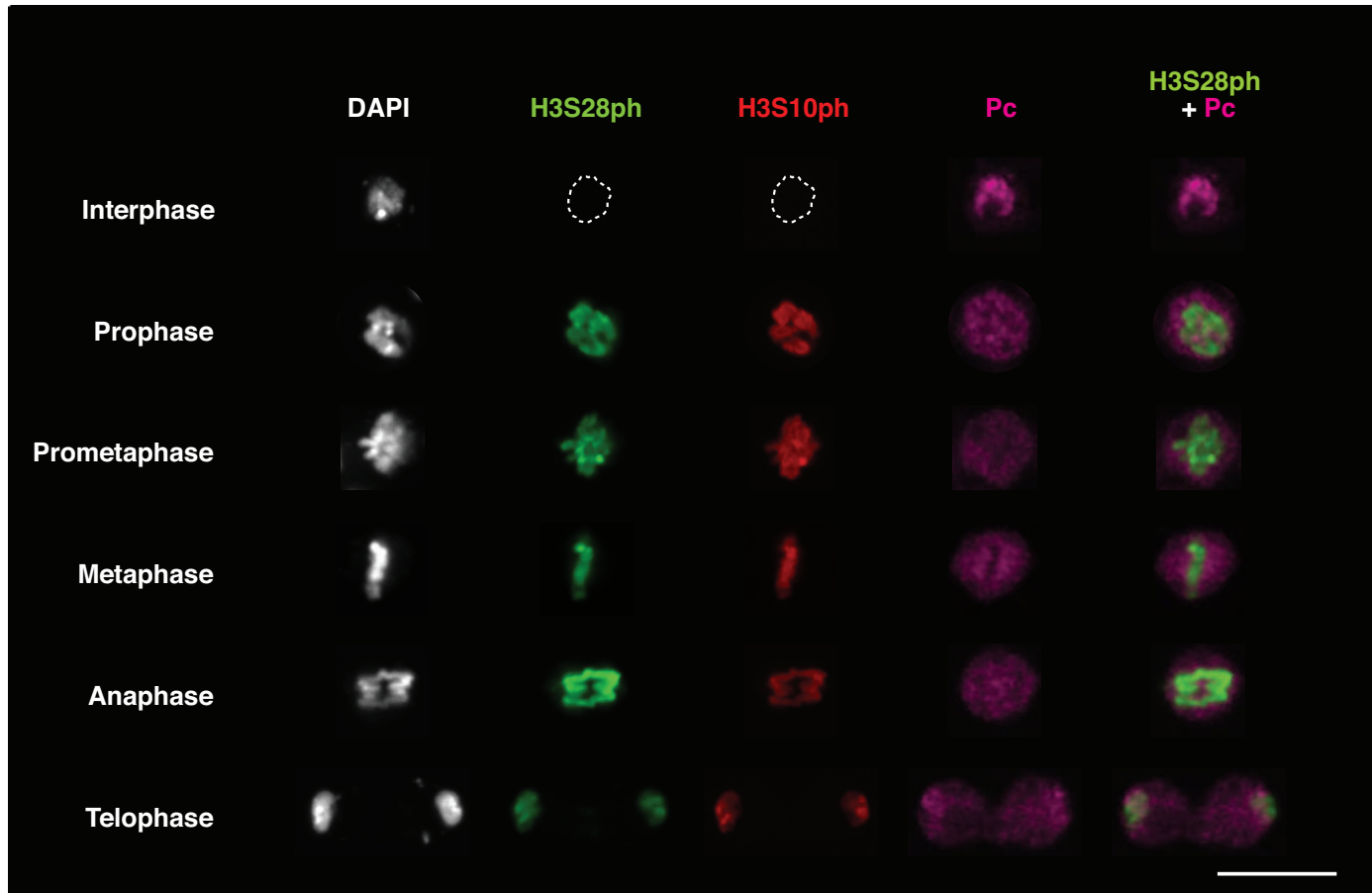


Fig 2 | Cell cycle dynamics of H3S10ph, H3S28ph and Pc.

Immunostaining of H3S10ph, H3S28ph and Pc of *Drosophila* S2 cells during interphase and mitosis. Since H3S10ph and H3S28ph are undetectable in interphase, the nucleus boundaries of both channels are highlighted with dotted line. Scale bar = 10 μ m.

2. *In vivo* RNAi against Aurora B kinase in *Drosophila*

RNAi against Aurora B kinase was performed in *Drosophila* to probe for potential deregulation in PcG repression. Nub-GAL4-UAS-driven expression of hairpin against Aurora B in the wing pouch region of wing imaginal disc effectively reduced the kinase level (Fig 3A). The RNAi-effective area lost both H3S10ph and H3S28ph signals, as shown Fig 3B. This confirms observations made in cultured cells that Aurora B is the responsible kinase for these mitotic histone phosphorylations¹⁸⁷. As expected H3K27me3S28ph was also compromised upon knock down of Aurora B (Fig 3C).

Having validated the effectiveness of RNAi against Aurora B, we used en-GAL4 to knockdown Aurora B in the posterior compartment of imaginal disc. Consistent with the well-established role of Aurora B in mitotic progression, lost of the kinase lead to aneuploidy, as evident by the increase of nuclear volume in the RNAi-affected cells (Fig 4). However, it seems that the repressive mark H3K27me3 and active mark H3K27ac and gross staining pattern of Pc were not affected in Aurora B RNAi cells. Canonical PcG repression targets such as Ubx remained silenced in the wing disc. Native Ubx expression in the haltere disc was not affected either (Fig 4). However, RNAi against Aurora B in the eye-antenna disc gave rise to flies with severely deformed heads, most commonly represented by eyes with reduced size, eye-missing, rough and hairy eyes (data not shown). Also some of the flies display different degree of antenna duplication as shown in Fig 5. Since Aurora B kinase phosphorylate numerous substrates essential for mitosis progression, it is difficult to specifically attribute the observed pleiotropic phenotypes upon AurB-depletion to the lost of H3S28ph. Hence, a *Drosophila* model of non-phosphorylatable histone mutant (*H3S28A*), carrying a serine to alanine substitution was established to pinpoint the potential effect of H3S28ph in PcG repression.

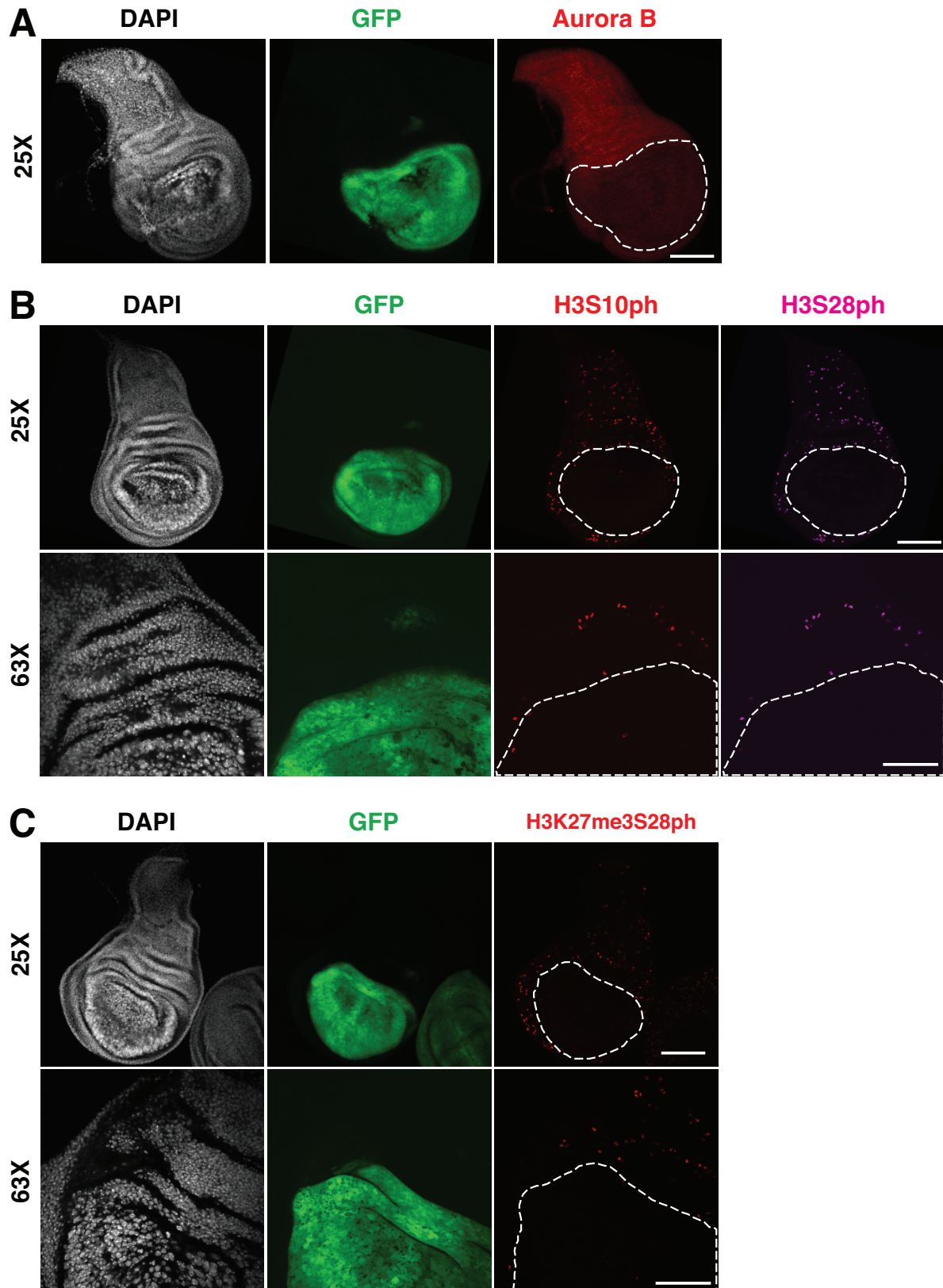


Fig 3 | In vivo RNAi against *Drosophila* Aurora B.

(A-C) *Drosophila* wing imaginal discs of L3 larva with nub-GAL4 directed RNAi against Aurora B at the wing pouch compartment marked by GFP and dotted lines. Wing discs were immunostained with DAPI and antibodies against (A) Aurora B, (B) H3S10ph and H3S28ph and (C) H3K27me3S28ph. Scale bar (25X) = 100 μ m, Scale bar (63X) = 50 μ m.

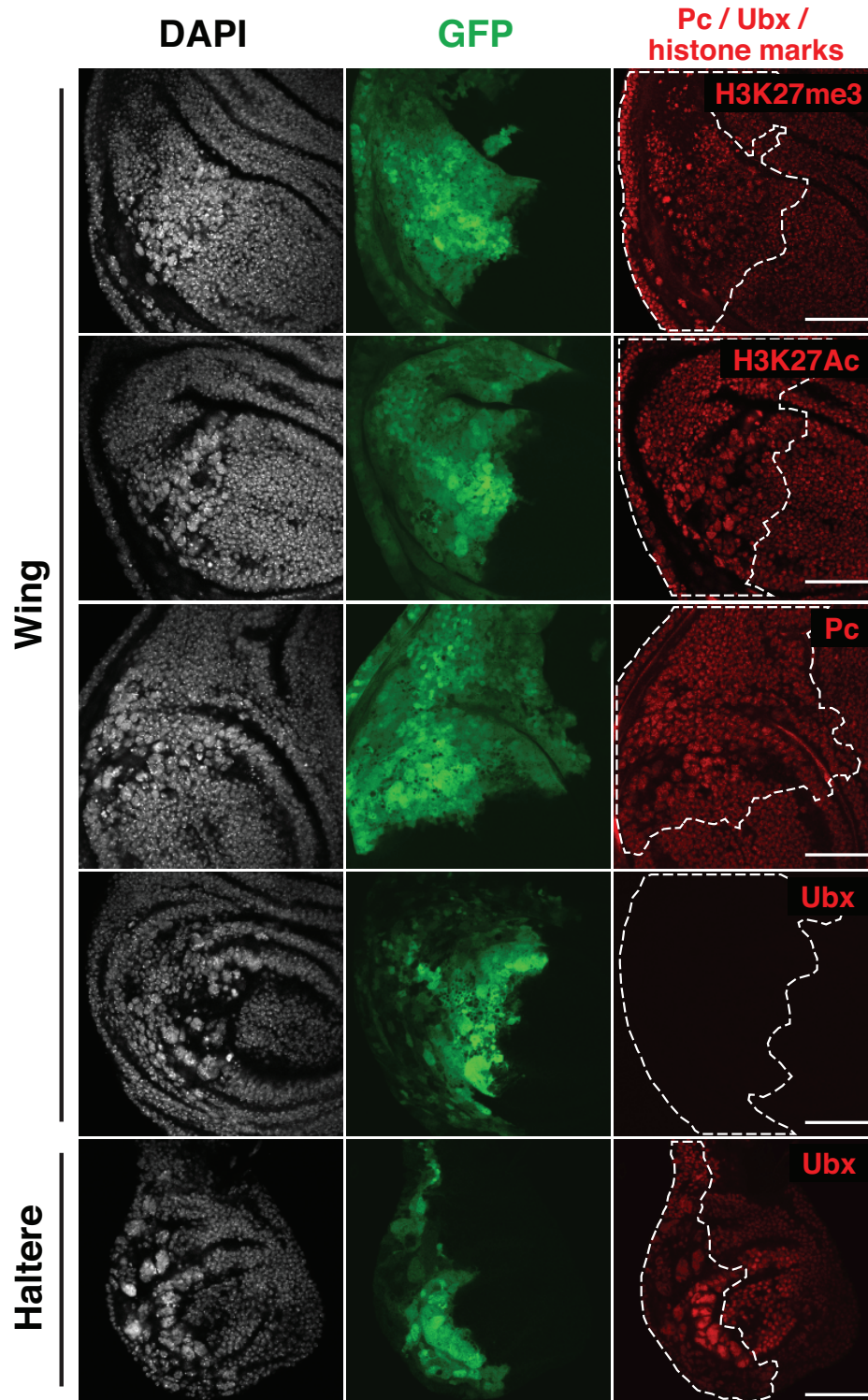


Fig 4 | H3K27me3, H3K27Ac, Pc and Ubx immunostaining patterns were unaffected upon RNAi against Aurora B.

Drosophila wing and haltere imaginal discs of L3 larva with en-GAL4 directed RNAi against Aurora B at the posterior compartment marked by GFP and dotted lines were immunostained with DAPI and antibodies against H3K27me3, H3K27Ac, Pc and Ubx. Loss of Aurora B leads to aneuploidy evident by the swelling of nuclear volume indicated by DAPI staining, but expression level of Ubx and staining pattern of H3K27me3, H3K27Ac and Pc were not affected. Scale bar = 100 μ m.

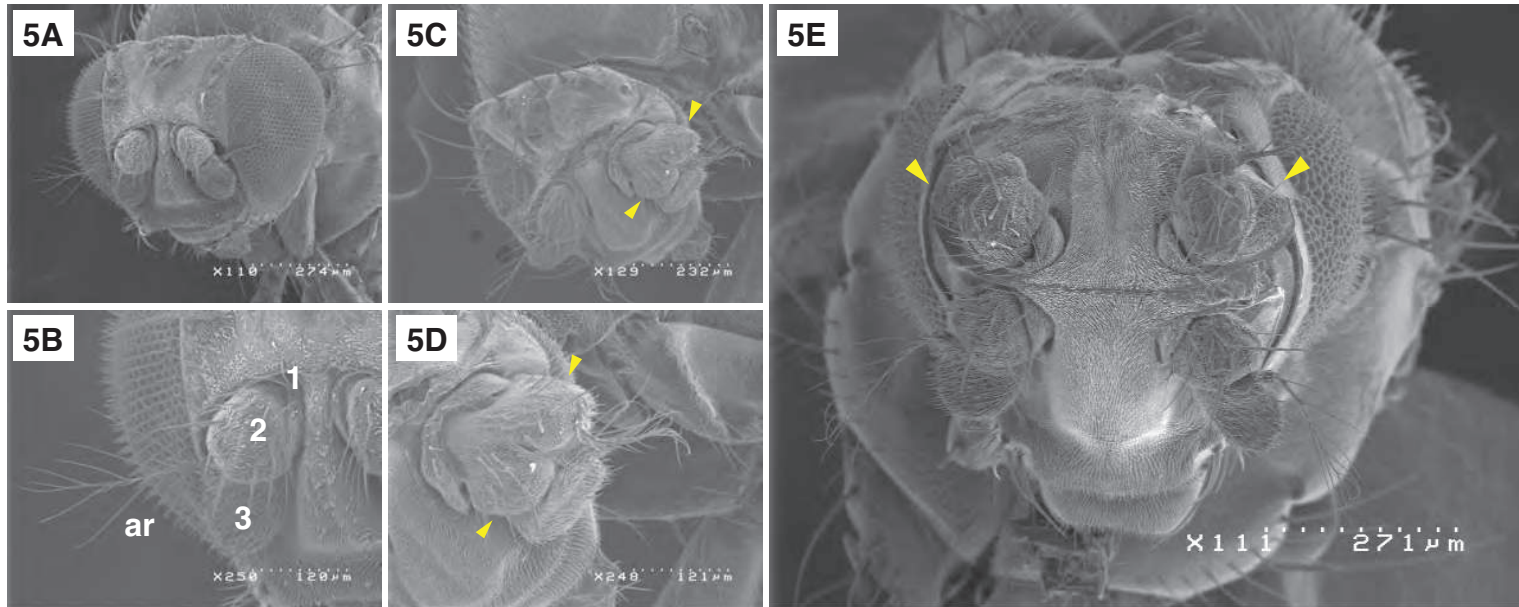


Fig 5 | Antenna duplication defects in flies upon Aurora B knockdown.

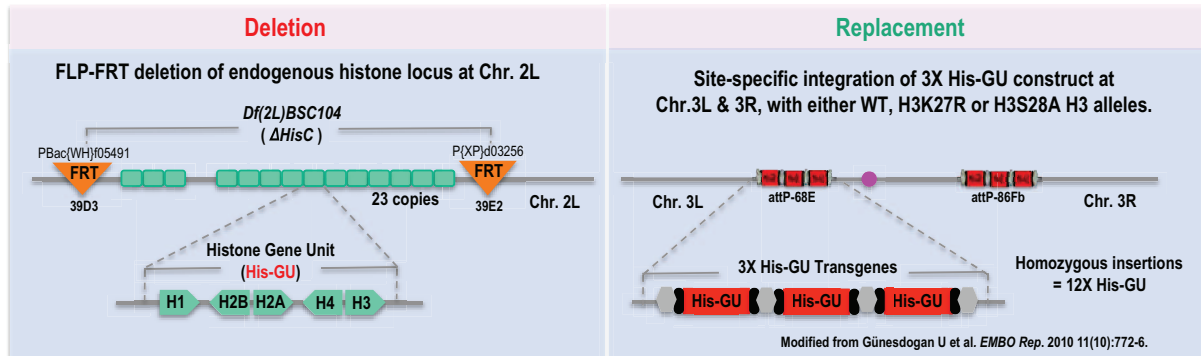
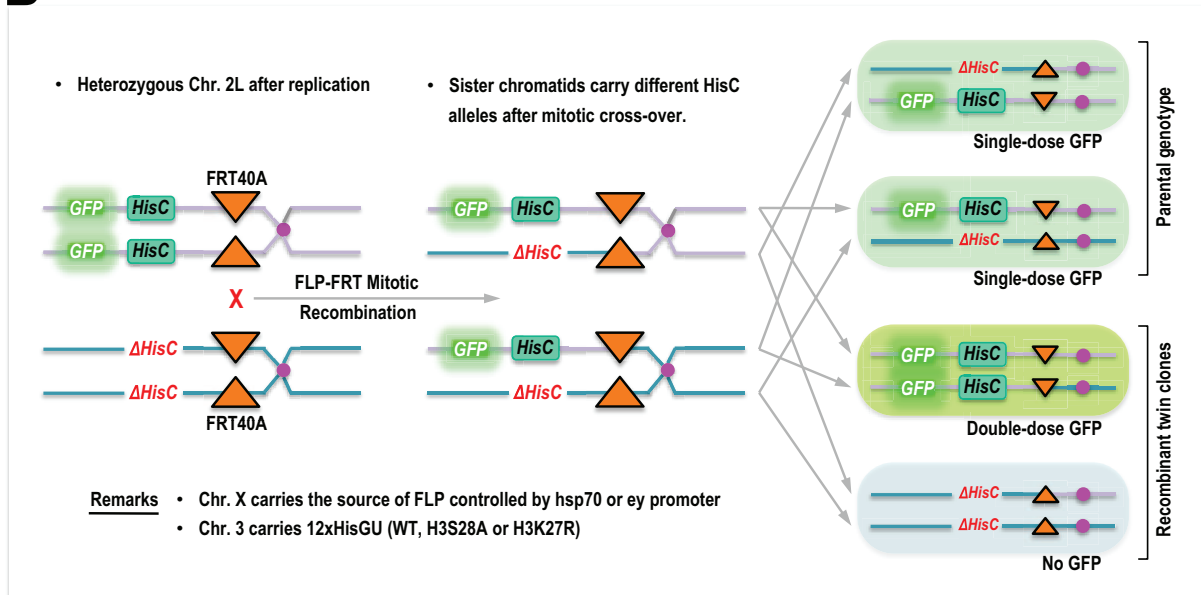
(A) & (B), Wild type *Drosophila* with 4 well-defined antenna segments, labeled as 1-3 and arista (ar) (C) & (D) *ey-GAL4/UAS-RNAi-Aurora B* flies with partial duplication of antenna. Notably, segment 2 (arrowheads) is branched as a bi-lobule structure that gave rise to two individual segment 3. In the most extreme case, complete 4-segment antenna duplication is observed, as shown in (E, arrowheads). Scale bars are annotated in each micrograph.

3. Principle of the histone replacement system in *Drosophila*

The *Drosophila* histone genes encoding canonical nucleosomal and linker histones are organized as a histone gene unit (*His-GU*) as shown in Fig 6A. There are 23 annotated *His-GU* in the haploid *Drosophila* genome, all of them cluster at a single locus at chromosome 2L, known as the Histone complex (*HisC*). With the availability of two FRT-containing p-element transposable insertions flanking *HisC*, the entire histone cluster is deleted via FLP-FRT recombination, resulting the histone deficiency (Δ *HisC*) allele known as *Df(2L)BSC104*³⁶. Homozygous Δ *HisC* mutant dies during embryogenesis after exhaustion of maternally deposited histone pools¹⁰⁴. However it has been shown that a total of 12 copies of wild-type *His-GU* transgenes are sufficient to rescue lethality associated with histone deficiency¹⁰⁴. Using site-specific plasmid integration with the Φ C31 integrase system⁴⁰⁶, the transgenesis was achieved by inserting plasmid with *3xHisGU* into two genomic loci on chromosome III. One located on chromosome 3L at 68E, and the other resides at 86Fb. Hence recombinant carrying *3xHisGU* at both 68E and 86Fb would attain *12xHisGU* at homozygous state. With the same transgenesis scheme, transgene carrying wild type or mutant *HisGU* can generate the corresponding histone replacement lines¹⁰⁴.

4. Principle of mosaic analysis of histone mutants in *Drosophila* larval tissues

Previous report on *Drosophila H3K27R* mutant showed that the limited number of cell division after cellularization of blastoderm failed to completely replace the chromatinized maternal core histones¹⁰⁰. Hence a mosaic analysis platform of histone mutant was established in larval imaginal discs where typically larva were dissected 3-4 days after clone induction^{36,100}. With the use of this system, it was shown that H3K27me3 and H3K4me3 were drastically reduced in larval *H3K27R*¹⁰⁰ and *H3K4R*³⁶ mutant clones respectively. Fig 6B illustrates the molecular events underlying the mosaic clone induction. First of all, parent cells are heterozygous on chromosome 2L. Both homologous Chr. 2L carry centromere-proximal *FRT40A* for recombination. The chromosome with endogenous intact *HisC* is linked and marked with ubiquitous GFP expression, whereas the Δ *HisC* allele is unmarked. With the supply of FLP, mitotic recombination occurs via *FRT40A* of both the heterozygous chromosomes, such that for each replicated homologous Chr. 2L, one of the sister chromatids would carry intact *HisC*, while the other would have the Δ *HisC* allele. Through independent assortment at the metaphase plate, heterozygous alleles facing the same side of the metaphase plate would regenerate progenies with parental genotype. For the case when the same alleles segregate to the same pole, homozygous GFP, *HisC* with doubled GFP expression and homozygous Δ *HisC* without GFP expression would coemerge as twins' clones.

A**B****Fig 6 | Principle of the *Drosophila* histone replacement system.**

(A) The *Drosophila* genome encodes canonical nucleosomal and linker histones from a single locus (*HisC*) at chromosome 2L. Homozygous histone deficiency mutant ($\Delta HisC$) is not viable, but it can be rescued by introducing 12 copies of transgenic histone gene units (*His-GU*) in chromosome 3. (B) Mosaic analysis of histone mutant begins with parental cells that are heterozygous for the histone locus. Mitotic crossover occurs at FRT40A with the supply of FLP such that homozygous *HisC* alleles, either in WT or deficiency forms, can be generated. Homozygous $\Delta HisC$ clones are marked by the lack of GFP, while that of WT *HisC* have double GFP expression. Since chromosome 3 is integrated with 12x*HisGU*, the endogenous source of H3 can be replacement by different H3 alleles in the $\Delta HisC$ clones.

5. Submitted Manuscript

Histone H3 Serine 28 is essential for efficient Polycomb-mediated gene repression in *Drosophila*.

Philip Yuk Kwong Yung¹, Alexandra Stuetzer², Anne-Marie Martinez¹, Wolfgang Fischle², Giacomo Cavalli¹

¹Institute of Human Genetics, UPR1142 CNRS, 141 Rue de la Cardonille, 34396, Montpellier Cedex 5, France.

²Laboratory of Chromatin Biochemistry, Max Planck Institute for Biophysical Chemistry, 37077 Göttingen, Germany.

Abstract

Central to the polycomb repression system is the deposition of the histone mark H3K27me₃, which can be regulated by the juxtaposed phosphorylation on H3S28. To assess the importance of H3S28ph, we have generated a *Drosophila* histone mutant with a non-phosphorylatable form of H3 (H3S28A). *H3S28A* mutant cells lack H3S28ph on mitotic chromosomes but support normal bulk H3 and H3S10ph levels. Strikingly, all methylation states of H3K27 dropped drastically in *H3S28A* cells, while active chromatin mark H3K4me₃ was unaffected. *H3S28A* clones derepressed Hox genes and adult tissues developed homeotic transformation. Biochemical assay suggested that recombinant H3S28A nucleosomes appeared to be a suboptimal substrate for PRC2. Hence the observed phenotypes in *H3S28A* mutant *in vivo* could be in part caused by structural defects introduced by the alanine substitution, in addition to the loss of H3S28ph. Collectively, our data indicate an essential role of H3S28 in the catalysis of H3K27 methylation.

Introduction

Polycomb group (PcG) proteins are epigenetic regulators essential for repression of key developmental genes. Canonical targets of PcG proteins include the Hox genes, which specify body segments identities along the anterior to posterior axis. Mutations in PcG proteins fail to maintain repressive chromatin states, which lead to Hox derepression and cause homeotic transformation⁴⁻⁸. *Drosophila* PcG proteins assemble into at least five complexes, namely Polycomb Repressive Complex 1 (PRC1)²⁰⁰, PRC2⁸⁸⁻⁹¹, Pho-Repressive Complex (Pho-RC)²⁴⁹, dRing Associated Factor (dRAF)⁷⁷ and Polycomb Repressive Deubiquitinase (PR-DUB)¹⁵⁶. Enhancer of zeste, E(z), the catalytic subunit of PRC2 deposits H3K27me3 on target genes and dRing is an active E3 ligase subunit in dRAF that monoubiquitinates nucleosomal H2A. In the canonical model, H3K27me3-binding by the chromodomain of polycomb (Pc) helps to recruit PRC1^{90,91,105,106}. Recent studies suggest an alternative recruitment hierarchy whereby H2Aub initiates PRC2 chromatin targeting and the establishment of H3K27me3 domain^{81,112,155}. PcG repressive activity is modulated by local chromatin environment^{212,317}. For example, both H3K27me3¹¹³ and H2Aub¹¹² stimulate PRC2 activity, while active histone marks such as H3K4me3 and H3K36me3²⁶⁴ show inhibitory effects. Notably, the serine residue juxtaposed to H3K27 can be phosphorylated¹⁸⁷, and interphase H3S28ph was shown to counteract mammalian PRC1 and PRC2 chromatin binding to derepress PcG target genes in response to stress and developmental signalings^{189,190}, as well as to activate stress response genes via displacement of HDAC corepressor complexes⁴⁰⁷. Equally important, biochemical studies showed that H3K27me3S28ph was refractory to UTX³⁴³ and JMJD3³⁴² demethylations. Hence it seems that H3S28ph on one hand evicts PcG proteins and on the other hand preserves H3K27me3. More intriguingly, H3S28ph is deposited by the mitotic Aurora B kinase and, like H3S10ph, it is highly enriched during the course of mitosis¹⁸⁷. As such, H3S28ph might represent a cell-cycle link to PcG repression and epigenetic inheritance. To assess the importance of the highly conserved H3S28 residue and the physiological relevance of mitotic H3S28ph in modulating PcG repression, we have established an *in vivo Drosophila* model where the endogenous source of histone H3 is replaced by a non-phosphorylatable H3S28A mutant with a serine to alanine mutation.

Results & Discussion

Establishment of *Drosophila H3S28A* and *H3K27R* histone mutants

The endogenous source of canonical nucleosomal and linker histones are encoded from the histone gene unit (His-GU), which is organized as a multicopy array residing at a single genetic locus in the *Drosophila* genome known as the histone gene cluster (*HisC*). Previous studies showed that embryos carrying homozygous *HisC* deletion ($\Delta HisC$) died in late blastoderm, after exhaustion of maternally deposited histones reserves¹⁰⁴. A histone replacement genetic platform is developed based on the fact that reintroduction of $\Delta HisC$ mutant with 12 copies of wild-type transgenic His-GU is sufficient to rescue lethality. Likewise, His-GU carrying different point mutations can be introduced to replace endogenous histones to study the biological functions of specific histone modifications¹⁰⁴. In the previous study of *H3K27R* mutant¹⁰⁰, it was reported that the limited number of cell divisions during late embryogenesis was not sufficient to completely replace wild-type chromatinized maternal histones, resulting in chromatin with a mixture of wild-type and mutant histones. To circumvent this limitation, mosaic analysis systems of histone mutants were developed, such as FLP-FRT mediated recombination which generates homozygous $\Delta HisC$ clones that can be supplemented with 12xHis-GU of either WT or mutated histones in larval tissues^{36,100}. We adopted the same system to generate clonal histone mutants in larval imaginal discs. In this study, we generate *H3S28A* mutant with an alanine substitution over the native serine residue, rendering it unable to be phosphorylated. In parallel, histone replacement lines carrying *WT* and *H3K27R* histone mutants were established as controls. To simplify the nomenclature, homozygous $\Delta HisC$ clones supplemented with different transgenic 12xHis-GU are referred as *WT*, *H3S28A* and *H3K27R* lines, unless otherwise stated.

Consistent with previous reports^{36,100}, homozygous $\Delta HisC$ clones induced with a heat shock pulse of FLP died and were replaced by neighboring tissues (Supplementary Fig S1). This is evident by the presence of cells with double GFP staining levels, while the twin clones lacking GFP that would correspond to $\Delta HisC$ mutant did not develop. Reintroducing 12xHisGU in the form of WT-H3, H3S28A or H3K27R mutants rescued $\Delta HisC$ clone development. As shown in Fig M1A, these histone replacement clones displayed similar DAPI and H3 staining patterns to the neighboring GFP +ve tissues. Importantly, *H3S28A* clones specifically lost mitotic H3S28ph signal, while retained

normal level of H3S10ph (Fig M1B). Likewise and as previously reported ¹⁰⁰, *H3K27R* clones almost depleted H3K27me3 level, without affecting juxtaposed mitotic phosphorylation at H3S28 (Fig M1C). This indicates that the native pool of histone variant H3.3 neither supports mitotic H3S28ph nor H3K27me3. This may be linked to the transcription-coupled deposition pathway of H3.3, which restricts its distribution on active promoters, resulting in genomic distributions that might not be compatible with PRC2 catalysis. With a similar logic, it might be inferred that mitotic H3S28ph is not randomly distributed on a global genomic scale and the responsible Aurora B kinase might not overlap with H3.3 over active chromatin. As a control, in WT clones, mitotic H3S10ph, H3S28ph and H3K27me3 were not affected (Fig M1B & C).

Strong reduction of all H3K27 methylation states in the *H3S28A* mutant

Owing to the close proximity between H3K27me3 and H3S28, and because H3S28ph is shown to both evict PcG components ^{190,264} and prevent H3K27me demethylations ^{342,343}, we asked if the lost of H3S28ph in *H3S28A* clones would affect H3K27 methylation. Strikingly, H3K27me3 and H3K27me1 dropped drastically in *H3S28A* clones (Fig M2A). Considerable reduction in H3K27me2 was also detected. This is in contrast to active chromatin marks, where H3K27ac is only mildly decreased and H3K4me3 is unaffected in *H3S28A* clones. For all histone marks examined, *WT* clones showed normal staining levels indistinguishable from neighboring tissues (Fig M2B).

***H3S28A* and *H3K27R* mutants shared similar Hox gene derepression profiles**

It has been shown that in various PRC2 mutants ^{88,205,276} and *H3K27R* histone mutant ¹⁰⁰ clones where H3K27me3 level is compromised, canonical PcG targets such as Hox genes are derepressed. Hence we probed for Hox gene derepression in *H3S28A* mutant, together with *H3K27R* mutant as a positive control.

Endogenous expression of *Scr* is limited to a patch of cells located at the base of antennal discs (arterisks) and is absent within the antennal disc proper ⁴⁰⁸. As shown in Fig. M3A, *Scr* was derepressed across the entire antennal disc in both *H3S28A* and *H3K27R* clones. Low level of *Scr* expression were reported in the ad epithelial cells of the 2nd and 3rd leg

discs (arterisks) ⁴⁰⁹. Similar to PcG mutants, Scr was strongly derepressed in *H3S28A* and *H3K27R* clones of these tissues (Supplementary Fig S3). Also, in both histone mutant clones, relatively weak notum-restricted Scr derepression was occasionally detected in the wing discs, which was in agreement with a previous report in *Pc³/+* heterozygous mutant background ⁴⁰⁹. Strong Ubx derepression was also detected in both *H3S28A* and *H3K27R* mutant clones in antennal and wing discs (Supplementary Fig S3). In both mutants, Ubx derepression tended to be zonally confined within the wing pouch region at a level comparable to its native expression in the haltere disc. Intriguingly, strong Abd-B derepression was only detected in *H3K27R* clones across the entire wing ¹⁰⁰ and eye-antennal discs while *H3S28A* clones showed no obvious derepression in the same tissues (Fig M3A & Supplementary Fig S3). Hox derepressions were undetectable in *WT* clones in all the imaginal discs examined.

Similar to the *Antp^{Ns}* mutant with ectopic expression of Antp in the antennal disc (Supplementary Fig S7), GAL4-driven overexpression of various Hox genes in the antennal disc were known to silence the antennal selector gene Hth and caused antenna-to-leg transformation ⁴¹⁰. In the antennal discs carrying *H3S28A* and *H3K27R* clones, we observed Antp derepression in addition to the aforementioned Hox genes. These clones also showed Hth silencing, most prominent in the *H3K27R* mutant (Fig M3B). Consistent with the Hox derepression and Hth silencing phenotypes in the larval tissues, adult flies developing from clonal *H3S28A* and *H3K27R* mutant backgrounds displayed antenna-to-leg transformation. Wild-type *Drosophila* adults show distinct antenna segmentation into a1-a3 and arista, as exemplified by *w1118* in Fig M3C. Notably, *H3K27R* mutant displayed enlarged a3 antennal segment, from which massive outgrowth developed with leg-like features resembling the antennapedia phenotype of the *Antp^{Ns}* mutant. *H3S28A* mutant showed milder transformations, with smaller a3 segment protrusions and thickening of arista resembling the aristapedia phenotype. In contrast, WT histone replacement flies showed normal antenna structures (Fig M3C).

H3S28A nucleosomes are suboptimal substrates for PRC2-catalysis of H3K27 methylation

In vitro PRC2 HMT assay was performed by our collaborator - Alexandra Stuetzer* & Wolfgang Fischle*

* Laboratory of Chromatin Biochemistry, Max Planck Institute for Biophysical Chemistry, 37077 Göttingen, Germany.

Because *H3S28A* mutant phenotypes closely resemble *H3K27R* homeotic transformations, we wondered if the serine-to-alanine substitution per se would affect PRC2 activity. To address this question, *in vitro* histone methyltransferase (HMT) assay was performed with reconstituted 4-component *Drosophila* PRC2 complex that includes Esc, Su(z)12, E(z) and Nurf55. As shown by previous reports^{113,264}, when assayed on WT nucleosomes supplied with trans-acting histone peptide carrying H3K27me₃, PRC2 activity was robustly enhanced in a dose-dependent manner (Fig M4). On the other hand, basal HMT activities were detected when H3S28ph, unmodified or no histone peptides were added in the reaction mixture. Interestingly, the stimulatory effect of H3K27me₃ was retained when combined with H3S28A mutation but was abolished in the form of H3K27me₃S28ph “double mark” (Fig M4A). Since the stimulatory effect of H3K27me₃ relies on its binding to the beta-propeller structure of Esc¹¹³, this indicates that the lost of hydroxyl group in the serine-to-alanine substitution in H3K27me₃S28A does not affect Esc-H3K27me₃ recognition while juxtaposed phosphorylation as H3K27me₃S28ph does. Structural data seem to support this idea, since the side chain of H3S28 is pointing away from, and hence does not contribute to, the interaction with the Esc beta-propeller domain^{113,212}.

However, when the same assay was performed with H3S28A mutant nucleosomes, PRC2 HMT activities were considerably reduced, with or without supplementation of stimulatory H3K27me₃-containing peptides (Fig M4B). Similar to WT nucleosomal substrates, the PRC2-stimulatory effects of H3K27me₃ and H3K27me₃S28A were similar on H3S28A nucleosomes. As such, it appears that H3S28A mutation introduces structural intolerance that renders it a suboptimal substrate. Although crystal structure of human Ezh2 SET domain is available⁴¹¹, the exact contribution from the hydroxyl group of H3S28 for H3K27 methylation remains unknown.

In this report, we have established a *H3S28A* histone mutant in *Drosophila* in which mitotic H3S28ph is depleted. H3S28A nucleosomes appear to be a suboptimal substrate for *in vitro* PRC2 HMT activity. Consistent with this, *H3S28A* mutant exhibits defects in H3K27 methylation and shows similar but milder Hox derepression profiles and transformation phenotypes to that of *H3K27R* mutant flies. Currently, we cannot segregate the differential contributions from the structural intolerance versus the lack of H328 phosphorylation associated with the *H3S28A* mutant to the observed *in vivo* phenotypes. The structural role of H3S28 in PRC2 catalysis remains to be determined. A likely possibility is that the hydroxyl group of the serine residue might be needed to interact with the SET domain of E(z) for efficient K27 methylation.

Previous immunostaining detections of *Drosophila* PcG proteins on mitotic chromosomes showed discrepancies depending on staining protocols and tissue types^{344,398-400}. Nonetheless, live imaging of Pc-GFP, Ph-GFP and E(z)-GFP in early *Drosophila* embryos^{402,412} all suggested that majority of these PcG components were dissociated from mitotic chromosomes. Since stress-induced interphase H3S28ph evicts PcG complexes^{190,264}, one might expect rebinding of PcG proteins on mitotic chromosomes depleted of H3S28ph. However, both Pc and Ph remained largely dissociated from mitotic chromosomes of *H3S28A* mutant (Supplementary Fig S8E & F). This might be caused by the reduced level of H3K27me3 in *H3S28A* mutant. Alternatively, other mechanisms might operate to dissociate the majority of PcG proteins during mitosis. As for interphase cells, Pc and Ph in both *H3S28A* and *H3K27R* clones displayed similar staining patterns to the neighboring tissues as well as to *WT* clones (Supplementary Fig S8A-D). ChIP experiments on FACS-sorted cells would better address the effect of H3K27me3 alternations on the genomic distribution of PRC1 proteins in both *H3S28A* and *H3K27R* mutant cells.

Despite the similarities between *H3S28A* and *H3K27R* phenotypes, there are notable differences between them. First of all, among the Hox genes tested, Abd-B was only derepressed in *H3K27R* clones (Fig M3A & Supplementary Fig S3). Similar to the reported mosaic clones of PcG mutants^{91,205,276}, *H3K27R* clones¹⁰⁰ typically showed round or smooth edge boundaries excluded from the neighboring GFP +ve tissues (Fig M1, 3 and Supplementary Fig S1-5). One explanation might be that the change of cellular identity of *H3K27R* clones renders them incapable to maintain cell-cell contacts with native tissues. Similarly, island of cells ectopically expressing Antp in *Antp^{Ns}* antennal discs are also “sorted out” from other cells without Antp expression and the resulting tissue resembles an internal imaginal disc (Supplementary Fig S7). However, clone borders of

H3S28A mutant maintained a typical zigzag shape resembling that of the *WT* clones. Besides, Antp and En were not derepressed in both *H3S28A* and *H3K27R* clones (Supplementary Fig S4), and only *H3K27R* clones cause silencing of endogenous Antp and En expression (Supplementary Fig S5). This might be an effect of posterior dominance⁴¹³ accompanied by Abd-B derepression in *H3K27R* clones. Intriguingly, not every cell within *H3S28A* clones in the wing pouch derepressed Ubx while *H3K27R* clones display a more homogenous Ubx derepression (Supplementary Fig S6). Currently, the reason for this is unclear. Whether this variegated pattern of Ubx derepression correlates with specific cell cycle stages remains to be investigated.

In our experimental conditions, we were not able to detect interphase H3S28ph (Fig M1). Consistent with previous report¹⁸⁸, interphase H3S28ph is not detectable in *Drosophila* S2 cells. And JIL-1, the closest homolog of mammalian interphase H3S28 kinase MSK1/2, does not phosphorylate H3S28 *in vitro*¹⁸² and *in vivo*¹⁸⁸. Although H3S28ph is tightly coupled with mitosis, we did not observe obvious mitotic defects in *H3S28A* mutant. Live imaging experiments might help to clarify potential mitotic progression abnormalities associated with the *H3S28A* mutant.

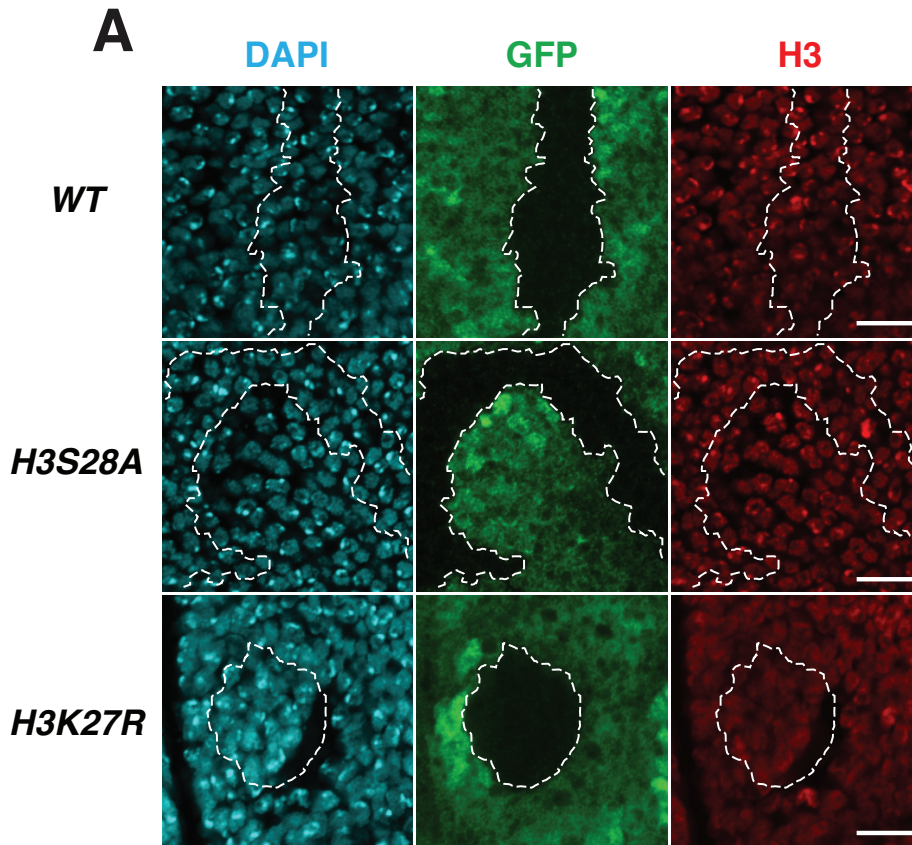
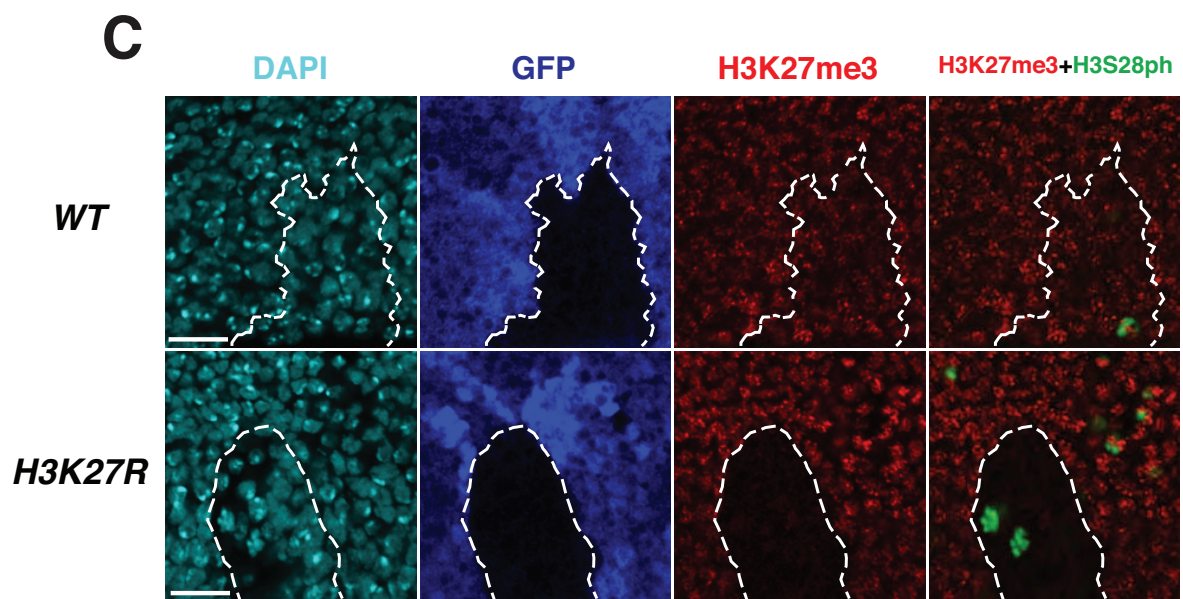
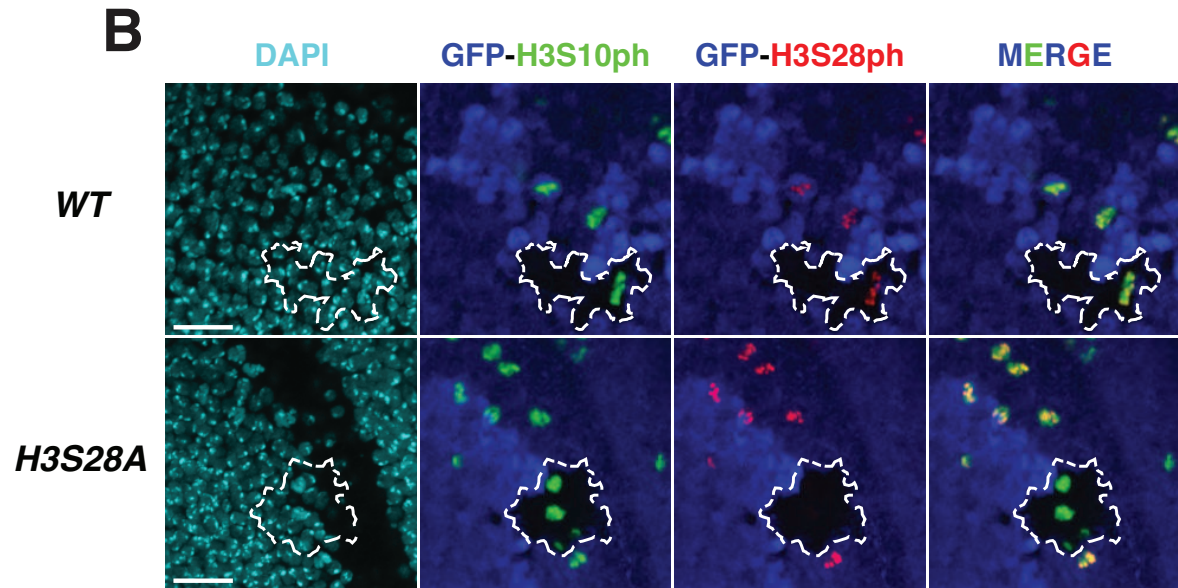


Fig M1 | Validation of the mosaic histone replacement system.

(A&C) Wing and (B) eye-antenna imaginal discs with homozygous $\Delta HisC$ clones supplemented with $12xHisGU$ transgenes carrying either *WT*, *H3S28A* or *H3K27R* H3 alleles were immunostained with DAPI and the indicated antibodies. Clones of interest were marked by the lack of GFP and were indicated by dotted lines. (A) All histone replacement clones displayed normal H3 staining level similar to the surrounding GFP +ve cells. (B) Mitotic cells within *H3S28A* clone (bottom row) displayed high level of mitotic H3S10ph but were depleted of H3S28ph. *WT* clones (top row) supported both mitotic histone phosphorylation marks. (C) *H3K27R* mutant cells (bottom row) were depleted of H3K27me3 despite having normal mitotic H3S28ph signal. *WT* clone supported robust H3K27me3 level indistinguishable from the surrounding GFP +ve cells. For the clarity of composite micrograph, GFP is pseudocolored to blue in (B) & (C). In order to capture mitotic cells at different focal planes, a Z-projection is applied in (B). Full-scale imaginal discs were shown in Supplementary Fig S2. Scale bar = 10 μ m.



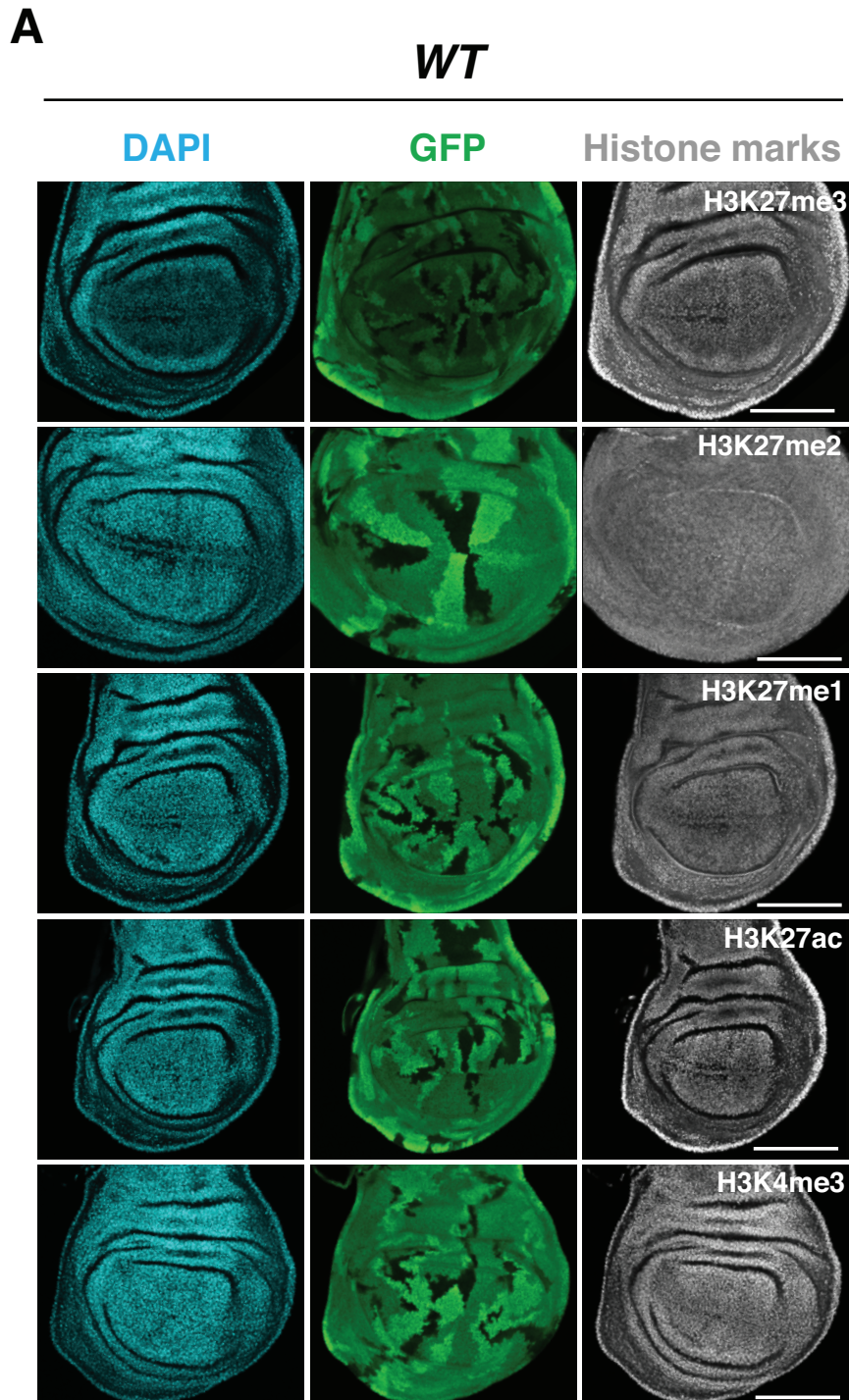


Fig M2 | Strong reduction of H3K27 methylations in *H3S28A* mutant.

Wing imaginal disc carrying (A) *WT* or (B) *H3S28A* clones were immunostained with DAPI and the indicated histone marks antibodies. Clones were marked by the lack of GFP. *H3S28A* clones showed strong reduction of all H3K27 methylation states (arrowheads) while active histone mark H3K27ac was mildly decreased and H3K4me3 was unaffected. *WT* clones showed normal levels of all indicated histone marks, which were indistinguishable from the surrounding GFP +ve tissues. Scale bar = 100 μ m.

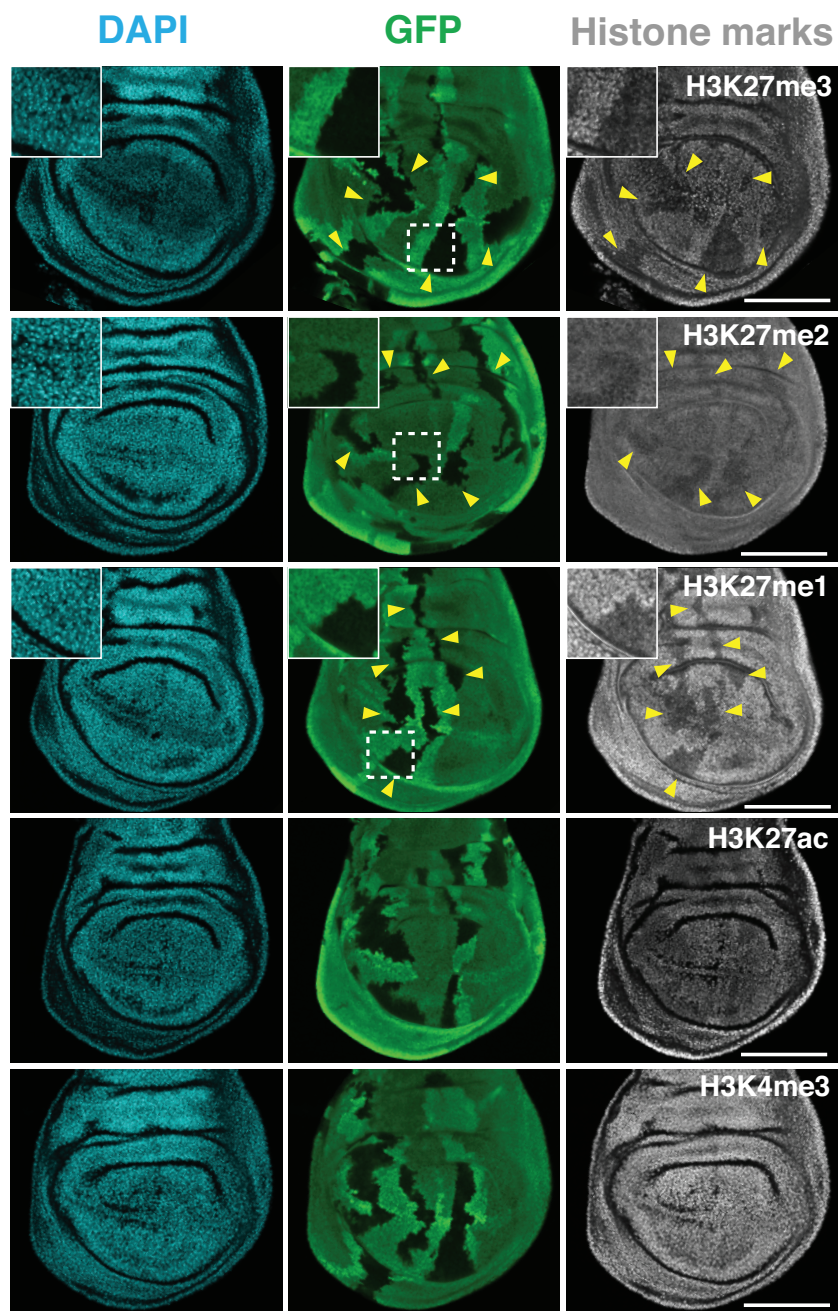
B***H3S28A***

Fig M2 | Strong reduction of H3K27 methylations in *H3S28A* mutant.

Wing imaginal disc carrying (A) *WT* or (B) *H3S28A* clones were immunostained with DAPI and the indicated histone marks antibodies. Clones were marked by the lack of GFP. *H3S28A* clones showed strong reduction of all H3K27 methylation states (arrowheads) while active histone mark H3K27ac was mildly decreased and H3K4me3 was unaffected. *WT* clones showed normal levels of all indicated histone marks, which were indistinguishable from the surrounding GFP +ve tissues. Scale bar = 100 μ m.

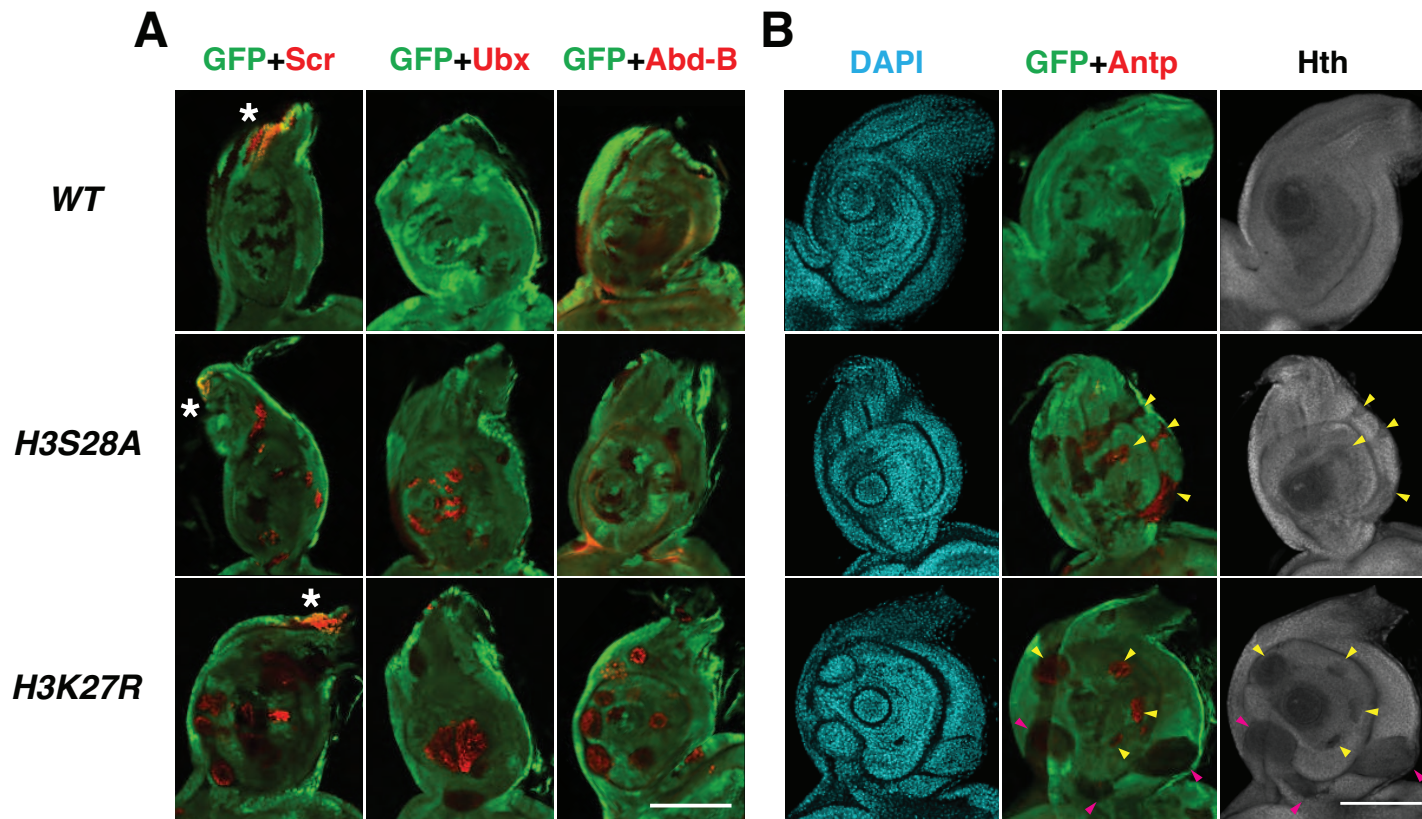


Fig M3 | Deregulation of Hox and antenna selector genes in *H3K27R* and *H3S28A* mutants and their associating transformation phenotypes. (A&B) Antennal discs with *WT*, *H3S28A* and *H3K27R* clones were immunostained with anti-GFP and the indicated Hox antibodies. Clone areas were marked by the absence of GFP. (A) *H3K27R* clones derepressed Scr, Antp, Ubx and Abd-B in the antenna disc. *H3S28A* clones showed similar derepression profiles except for Abd-B, which remained silenced in the antennal disc. Endogenous expression of Hox genes was marked by asterisks. (B) Most of the *H3S28A* and *H3K27R* clones derepressed Antp (yellow arrowheads) and silenced endogenous Hth expression. The silencing effect is less obvious but significant and reproducible in *H3S28A* clones. In some *H3K27R* clones (magenta arrowheads), Hth is silenced without Antp derepression. Hox derepression was not detected in *WT* clones in both (A) and (B), and Hth showed uniform eccentric expression pattern in (B). Scale bars in antennal discs represent 100 μ m. Micrographs showing full-scale imaginal discs are shown in Supplementary Fig S3.

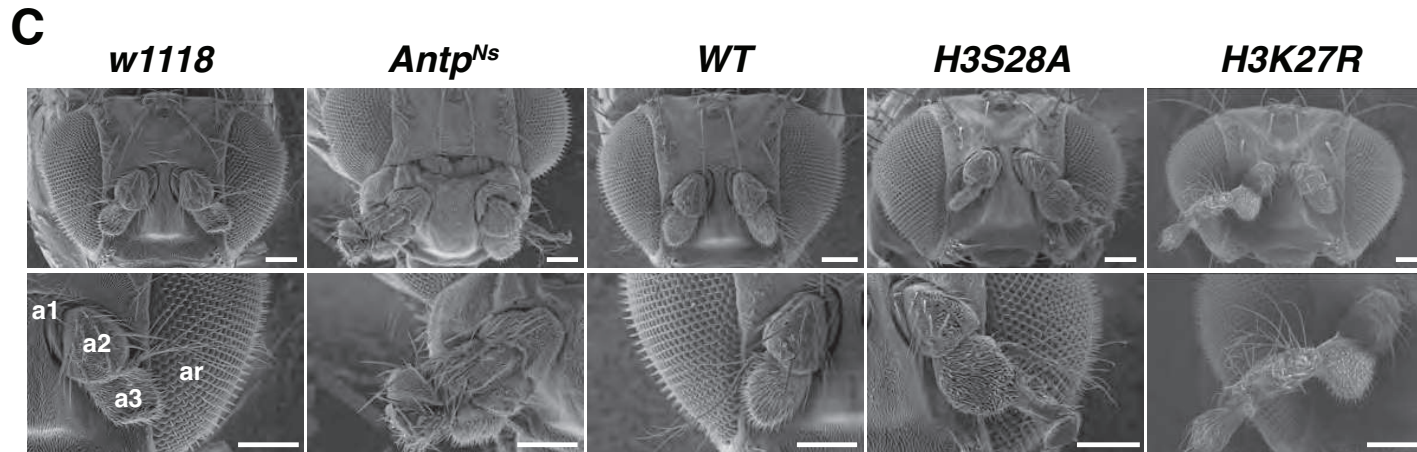


Fig M3 | Deregulation of Hox and antenna selector genes in *H3K27R* and *H3S28A* mutants and their associating transformation phenotypes.

(C) Electron micrographs of adult *Drosophila* heads derived from *w1118*, *Antp^{Ns}* and the indicated mosaic histone replacement lines. *H3K27R* mutant displayed antennapedia transformation while *H3S28A* mutant showed milder transformation resembling aristapedia. *WT* histone replacement line and *w1118* showed normal segmented antenna structures. *Antp^{Ns}* was shown as a positive control for antenna-to-leg transformation. Scale bars = 100 μ m.

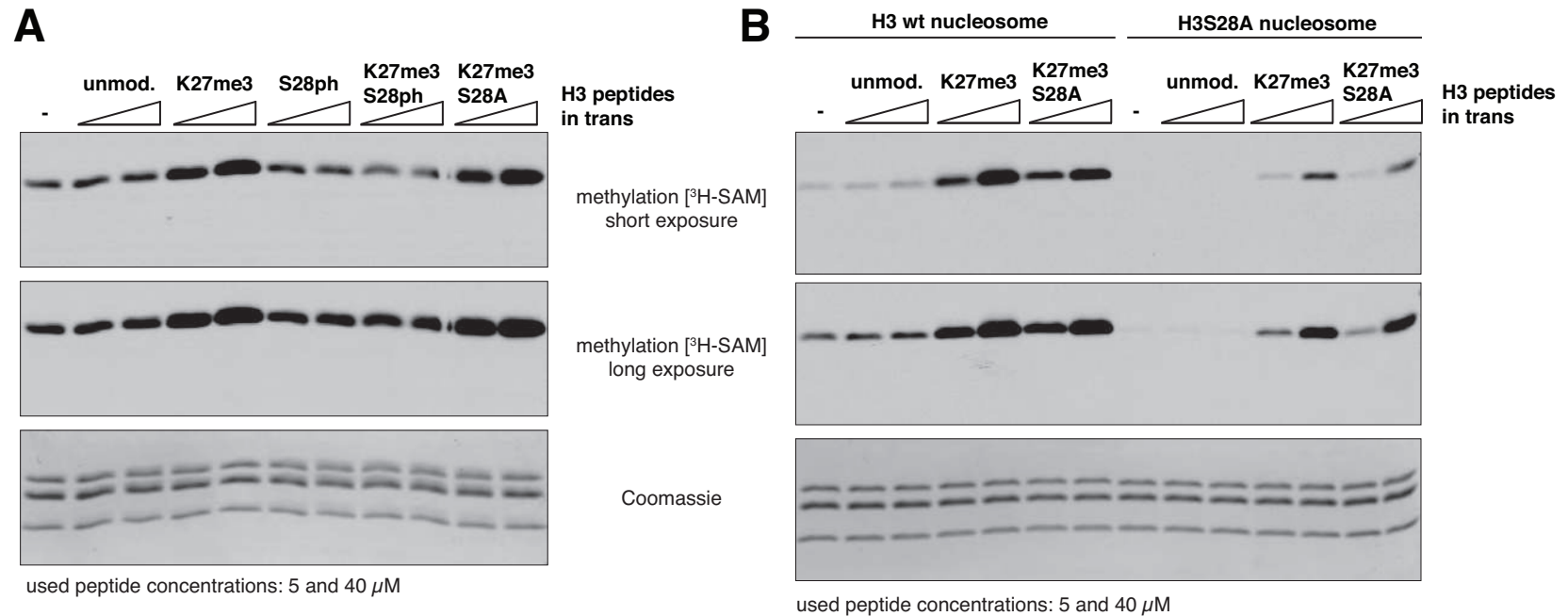


Fig M4 | H3S28A nucleosome is a suboptimal substrate for PRC2 activity.

(A) *In vitro* HMT assay using reconstituted *Drosophila* PRC2 complex and WT nucleosomes supplied with different trans-acting histone peptides. Consistent with previous reports, the H3K27me3 peptide stimulates PRC2 activity. Such stimulatory effect is unaffected in H3K27me3S28A, but is lost in H3K27me3S28ph. (B) *In vitro* PRC2 HMT assay using nucleosomal substrates assembled with either WT-H3 or H3S28A mutant. PRC2 activity is reduced on H3S28A nucleosomes even when it is supplied with stimulatory trans-acting H3K27me3 peptides. Coomassie stainings of histones were used as loading controls.

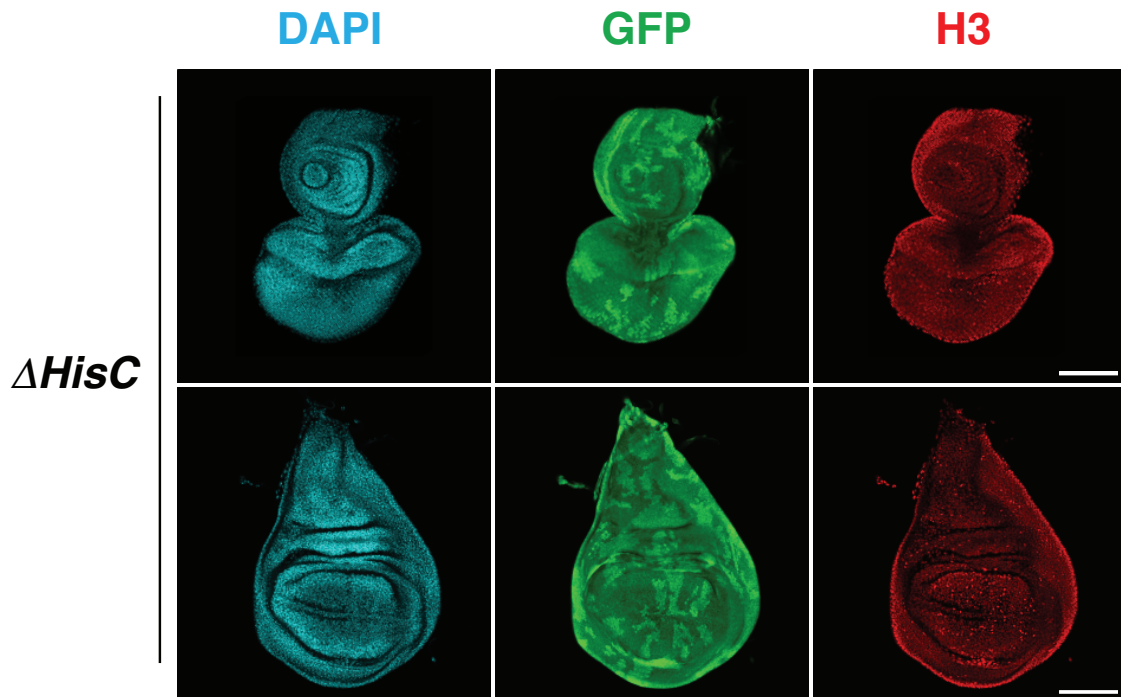


Fig S1. Homozygous $\Delta HisC$ clones are not viable in larval tissues.

Mosaic clones carrying homozygous $\Delta HisC$ (GFP -ve) were induced in eye-antennal (upper row) and wing imaginal discs (lower row). Samples were immunostained with DAPI and the indicated antibodies. Twin clones that co-emerged with $\Delta HisC$ clones were marked with double expression levels of GFP. Scale bar = 100 μm .

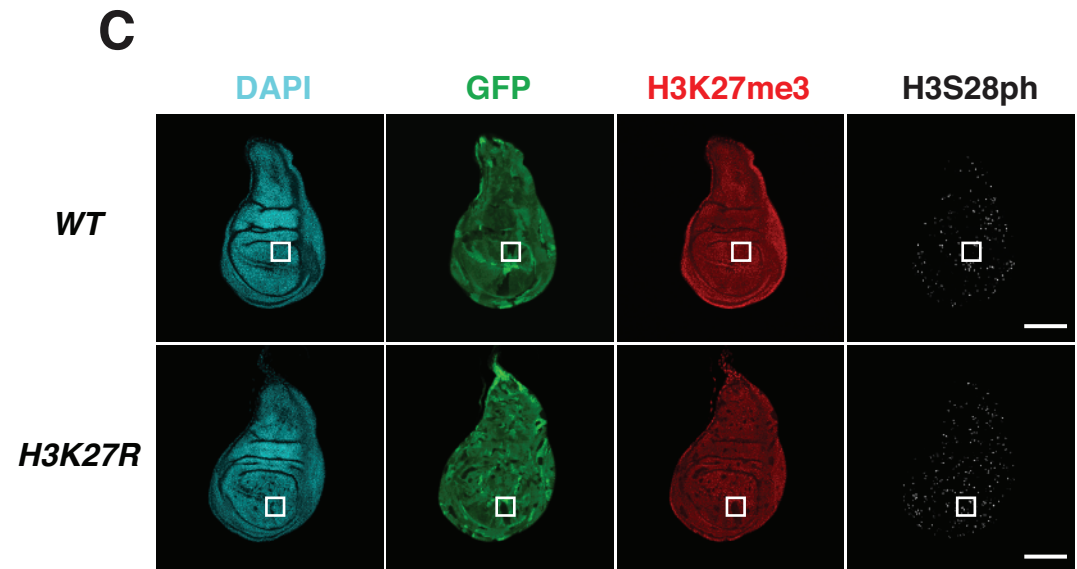
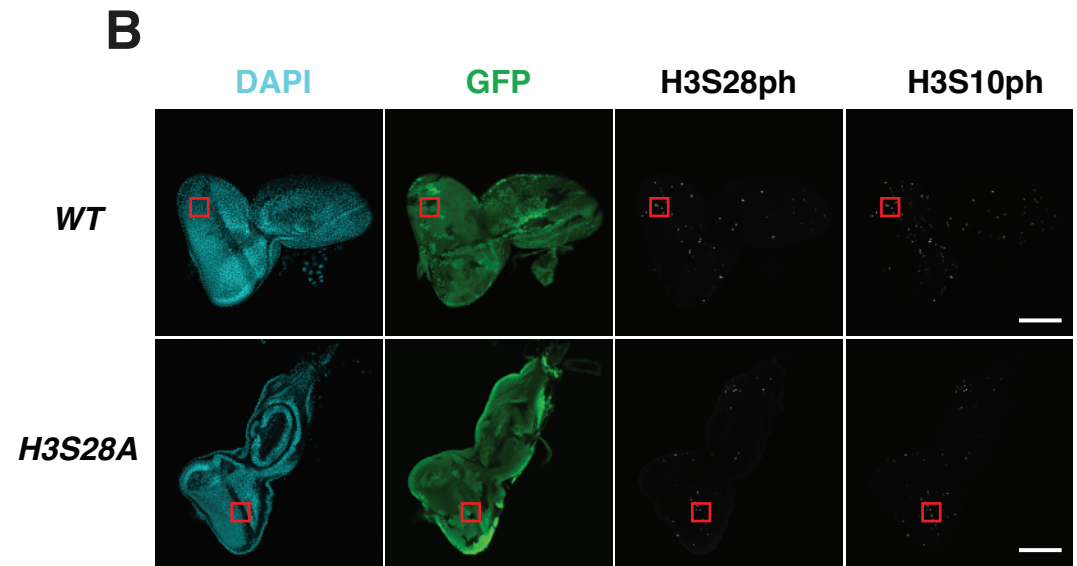
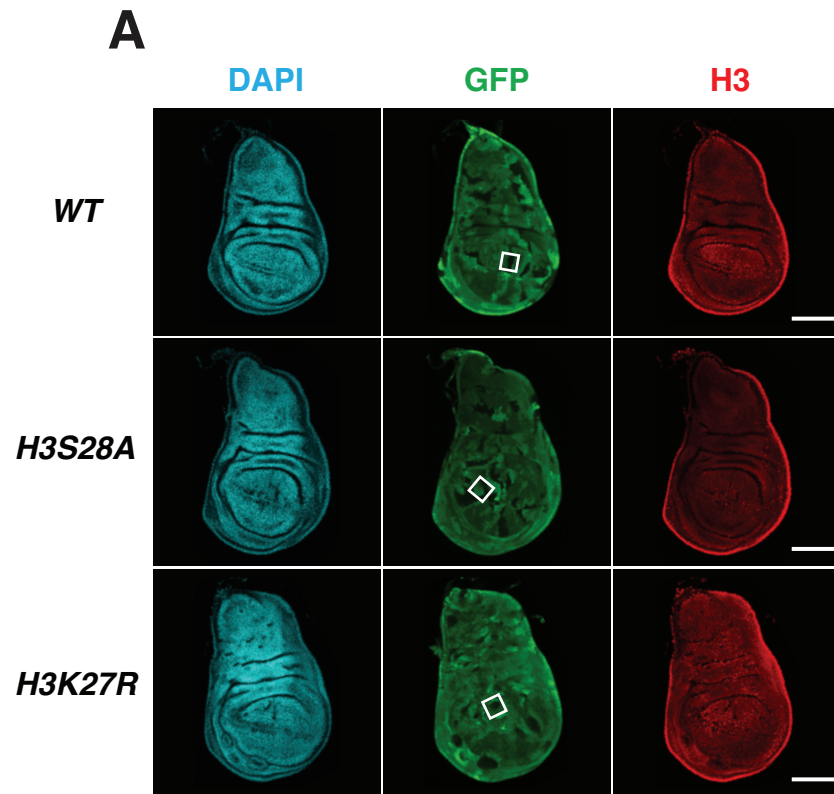


Fig S2. Validation of the mosaic histone replacement system.

(A-C) Micrographs showing full-scale imaginal discs used for staining showed in Fig M1. White/Red squares indicate the regions that were magnified and displayed in Fig M1. Scale bar = 100 μ m.

Fig. S3

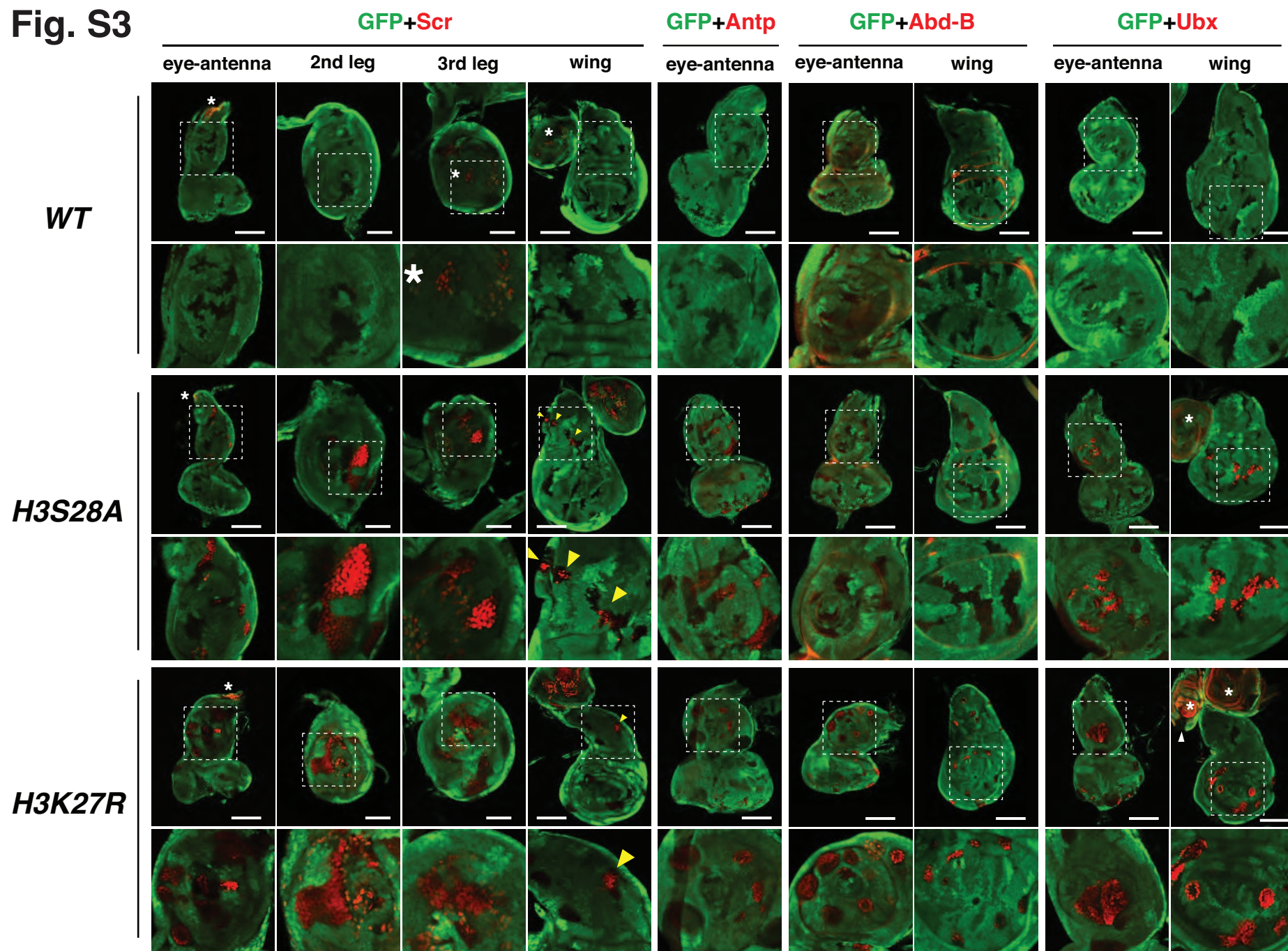


Fig S3. Hox gene derepression profiles in *H3S28A* and *H3K27R* clones.

Micrographs showing full-scale imaginal discs described in Fig M3 and texts. For each imaginal disc, a selected region (squared by dotted line) is magnified and displayed below the corresponding micrograph. In addition to the endogenous expression (asterisks), Scr was strongly derepressed in the antenna and both the 2nd and 3rd leg discs with *H3S28A* or *H3K27R* clones. Weak Scr derepression was occasionally detected in the notum region of wing discs in both mutant clones (yellow arrowheads). Antp staining described in Fig M3B is shown in full eye-antennal discs. Of note, Antp derepression was also detectable in *H3S28A* and *H3K27R* clones within the eye discs. Abd-B was strongly derepressed in *H3K27R* clones across both the eye-antenna and wing discs, while *H3S28A* clones did not show derepression in any of these tissues. Both *H3S28A* and *H3K27R* mutants strongly derepressed Ubx at both the antennal and the wing discs. Ubx derepression in both mutants was limited to the pouch region of wing discs at a level comparable to the endogenous Ubx expression in the haltere disc. Unlike *H3S28A* mutant, *H3K27R* clones strongly silenced endogenous Ubx expression in the haltere disc (white arrowhead). Endogenous expressions of Hox genes were marked by asterisks. Scale bars of both wing and eye-antenna discs represent 100 μm and those of leg discs represent 50 μm .

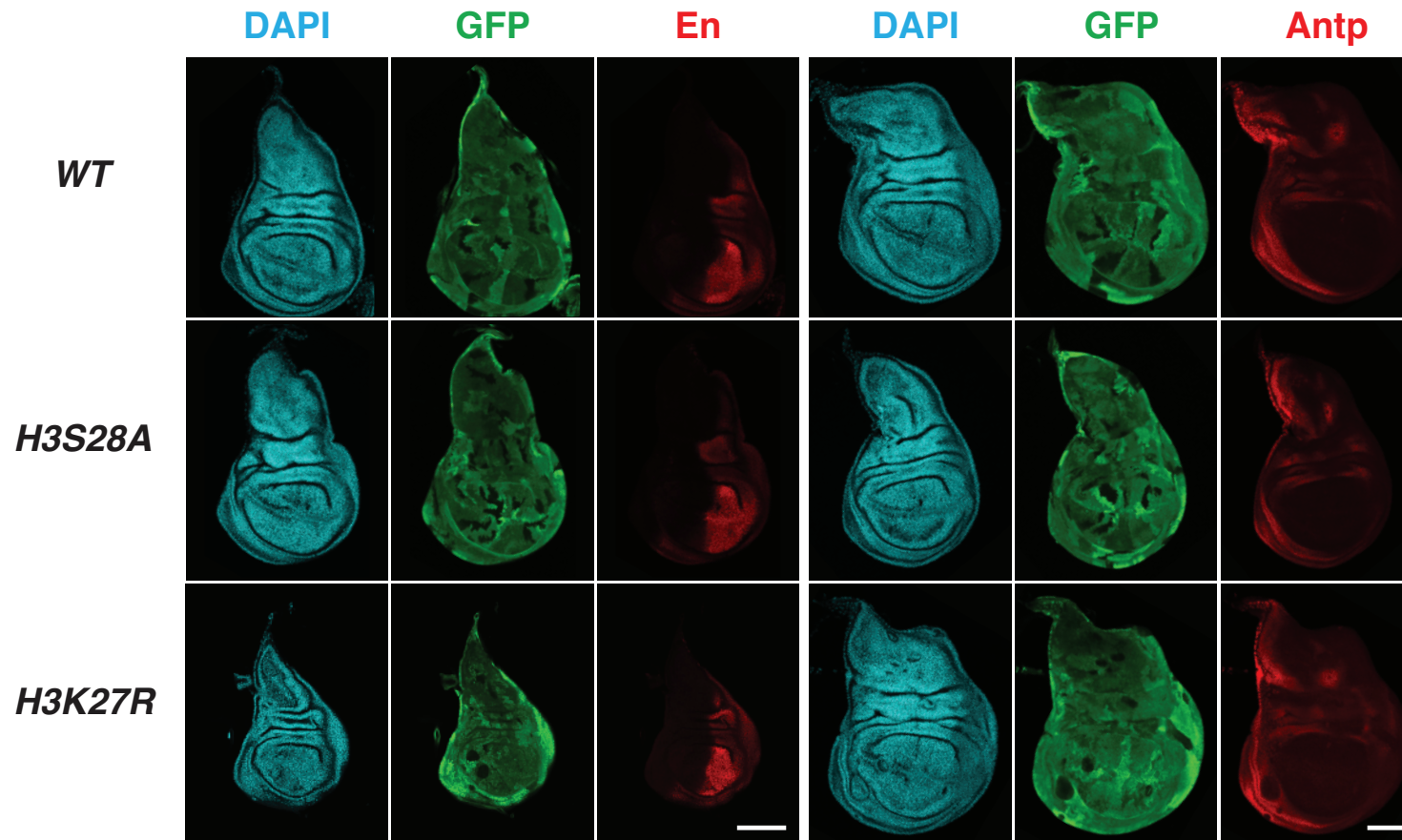


Fig S4. En and Antp were not derepressed in *WT*, *H3S28A* and *H3K27R* clones.

Wing imaginal discs with *WT*, *H3S28A* and *H3K27R* clones were immunostained with DAPI and indicated antibodies. Clone areas were marked by the absence of GFP. En derepression was not detected in *WT*, *H3S28A* and *H3K27R* clones located at the anterior compartment of the wing discs. Similarly Antp derepression was not detectable in all clones located in regions outside of its endogenous expression zone, such as the wing pouch region. Scale bar = 100 μ m.

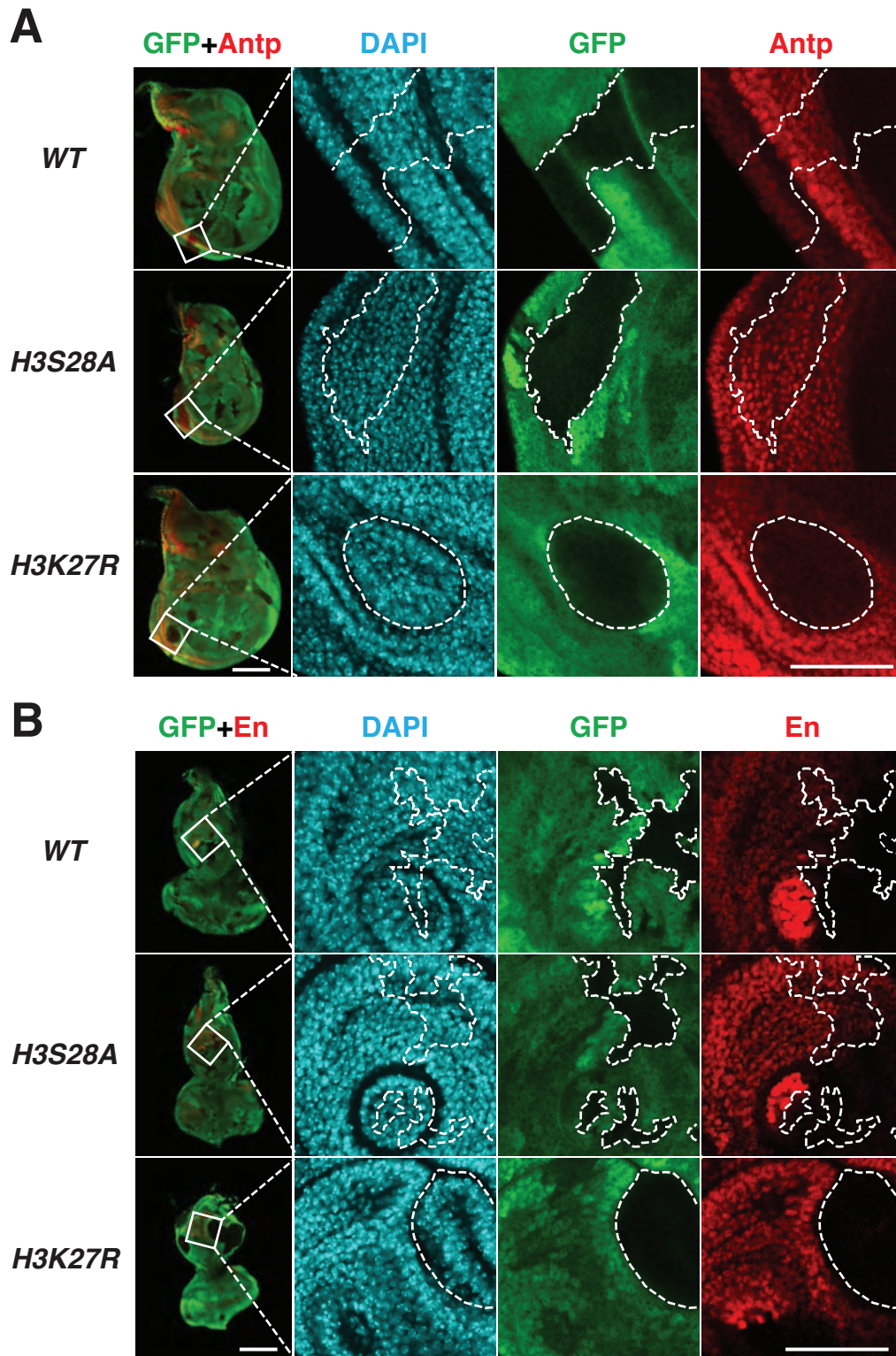


Fig S5. Ectopic silencing of endogenous expression of PcG target genes in *H3K27R* clones. (A) Wing discs and (B) eye-antenna discs with *WT*, *H3S28A* and *H3K27R* clones were immunostained with DAPI and indicated antibodies. Clone areas were marked by the absence of GFP and are indicated by dotted lines. (A) *H3K27R* clones located at the anterior rim of wing discs silenced the endogenous expression of *Antp*. (B) Similarly, *H3K27R* clones repressed endogenous *En* expression at the posterior compartment of the eye-antennal disc. *WT* and *H3S28A* clones located at similar regions did not affect endogenous (A) *Antp* or (B) *En* expression levels. Scale bar of full-disc micrograph represents 100 μm and those of magnified regions represents 40 μm .

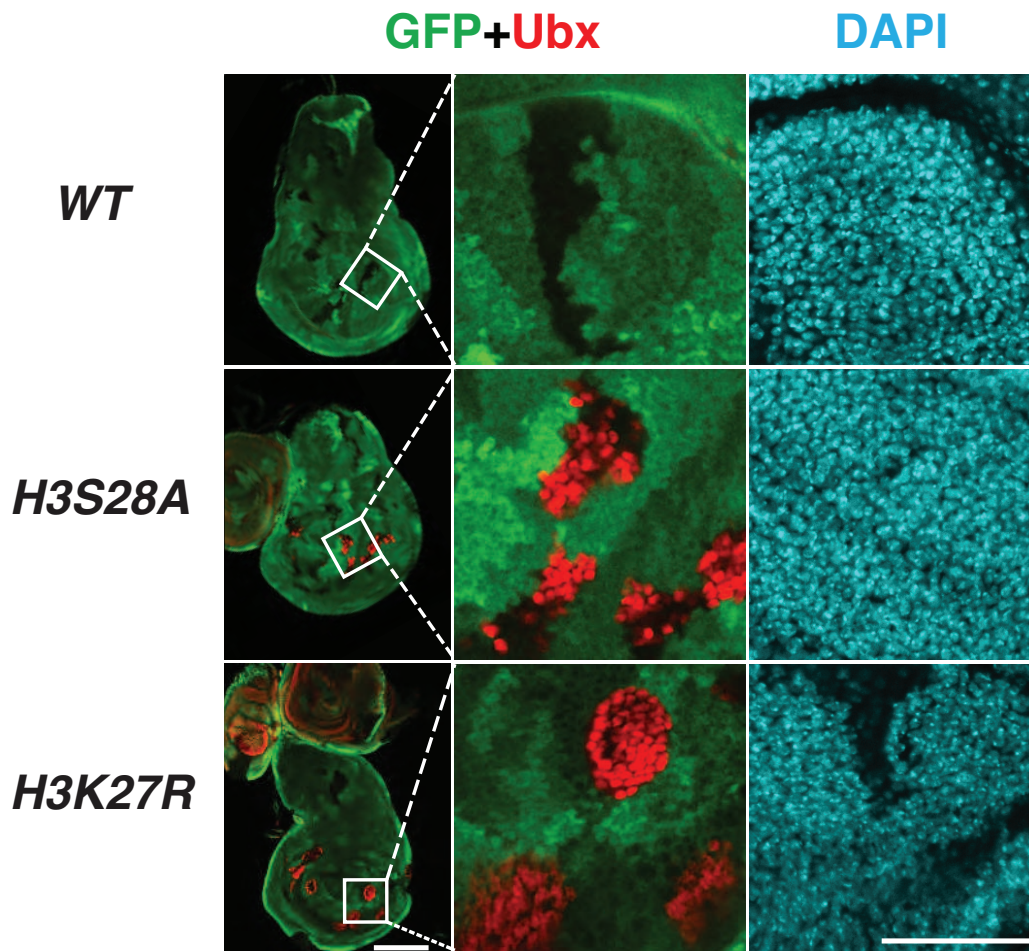


Fig S6. Heterogeneous Ubx derepression in *H3S28A* clones.

Wing imaginal discs with *WT*, *H3S28A* and *H3K27R* clones were marked by the absence of GFP and immunostained with DAPI and the indicated antibodies. Both *H3S28A* and *H3K27R* clones showed strong derepression of Ubx in the wing pouch. Unlike *H3K27R* mutant, not all *H3S28A* mutant cells within the same clone derepressed Ubx. Scale bar of full-disc micrograph represents 100 μm and those of magnified regions represents 40 μm .

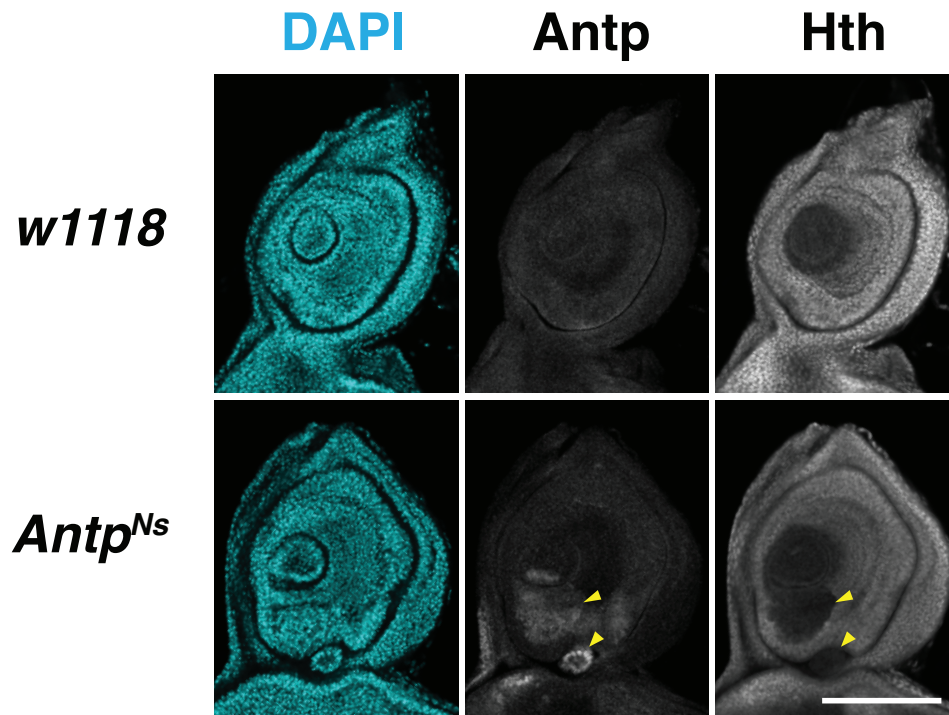


Fig S7. Ectopic expression of Antp repressed of Hth in *Antp^{Ns}* antenna disc. Antennal discs of *w1118* (top row) and *Antp^{Ns}* (bottom row) were immunostained with DAPI and the indicated antibodies. In *Antp^{Ns}* antennal discs, ectopic expression of Antp silenced endogenous expression of the antennal selector gene Hth, as indicated by arrowheads. Scale bar = 100 μ m.

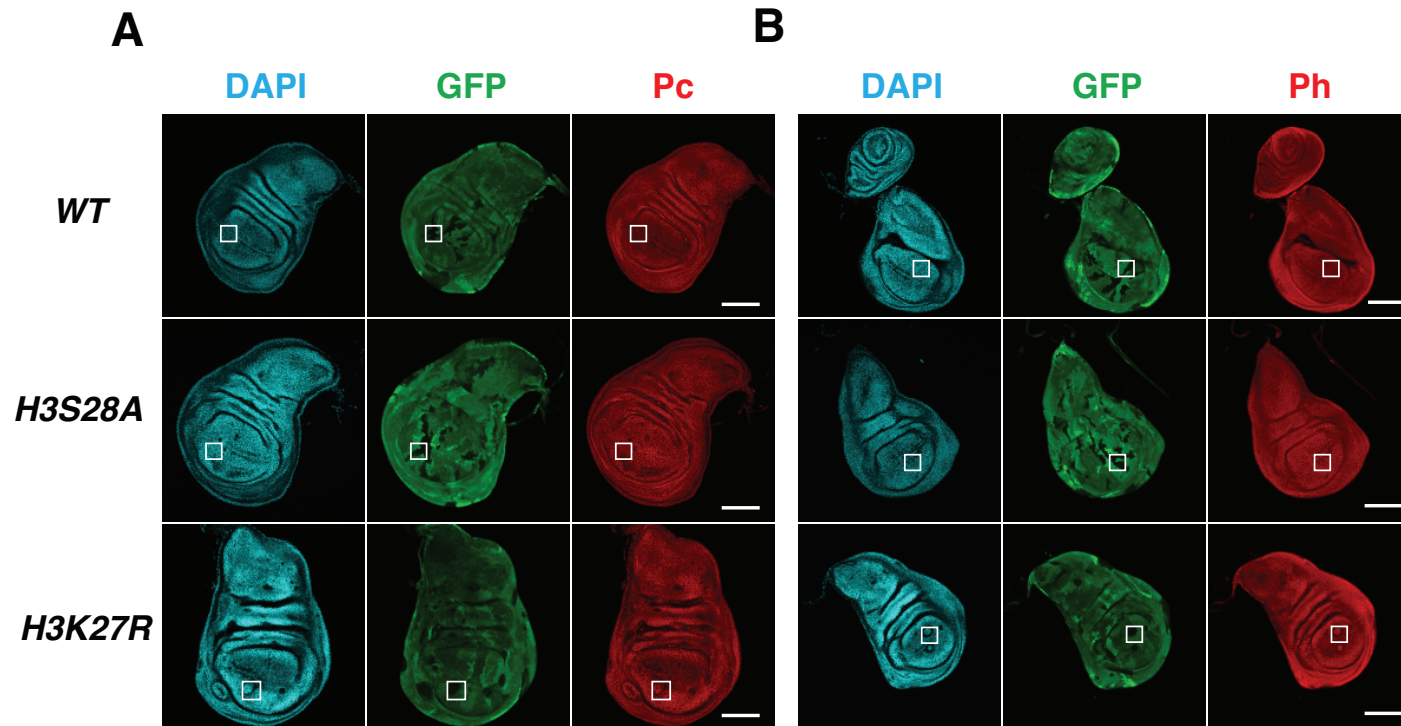


Fig S8. Nuclear staining pattern of Pc and Ph remained unchanged in *H3S28A* and *H3K27R* mutant. (A-D) Wing imaginal discs with either *WT* (top row), *H3S28A* (middle row) or *H3K27R* (bottom row) clones were marked by the lack of GFP and were indicated by dotted lines. Full-scale wing discs were shown in (A&B) and the inset white squares represent cropped regions magnified and displayed in (C&D). Samples were stained with DAPI and the indicated antibodies. Nuclear distribution of (C) Pc and (D) Ph was not affected in any of the histone replacement lines, which showed similar staining pattern to the surrounding GFP +ve cells. Regions at the clone borders were further cropped and magnified. Scale bars = 100 μ m.

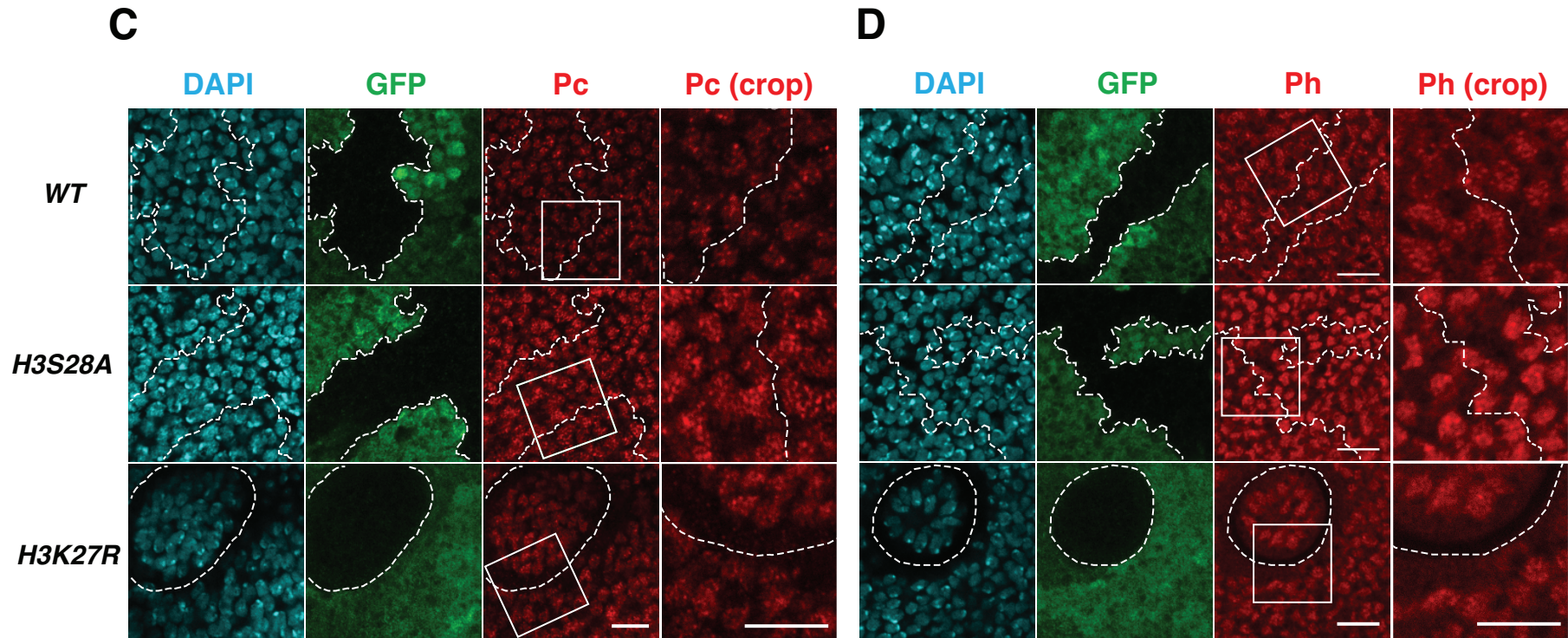


Fig S8. Nuclear staining pattern of Pc and Ph remained unchanged in *H3S28A* and *H3K27R* mutant.

(A-D) Wing imaginal discs with either *WT* (top row), *H3S28A* (middle row) or *H3K27R* (bottom row) clones were marked by the lack of GFP and were indicated by dotted lines. Full-scale wing discs were shown in (A&B) and the inset white squares represent cropped regions magnified and displayed in (C&D). Samples were stained with DAPI and the indicated antibodies. Nuclear distribution of (C) Pc and (D) Ph was not affected in any of the histone replacement lines, which showed similar staining pattern to the surrounding GFP +ve cells. Regions at the clone borders were further cropped and magnified. Scale bar = 10 μ m.

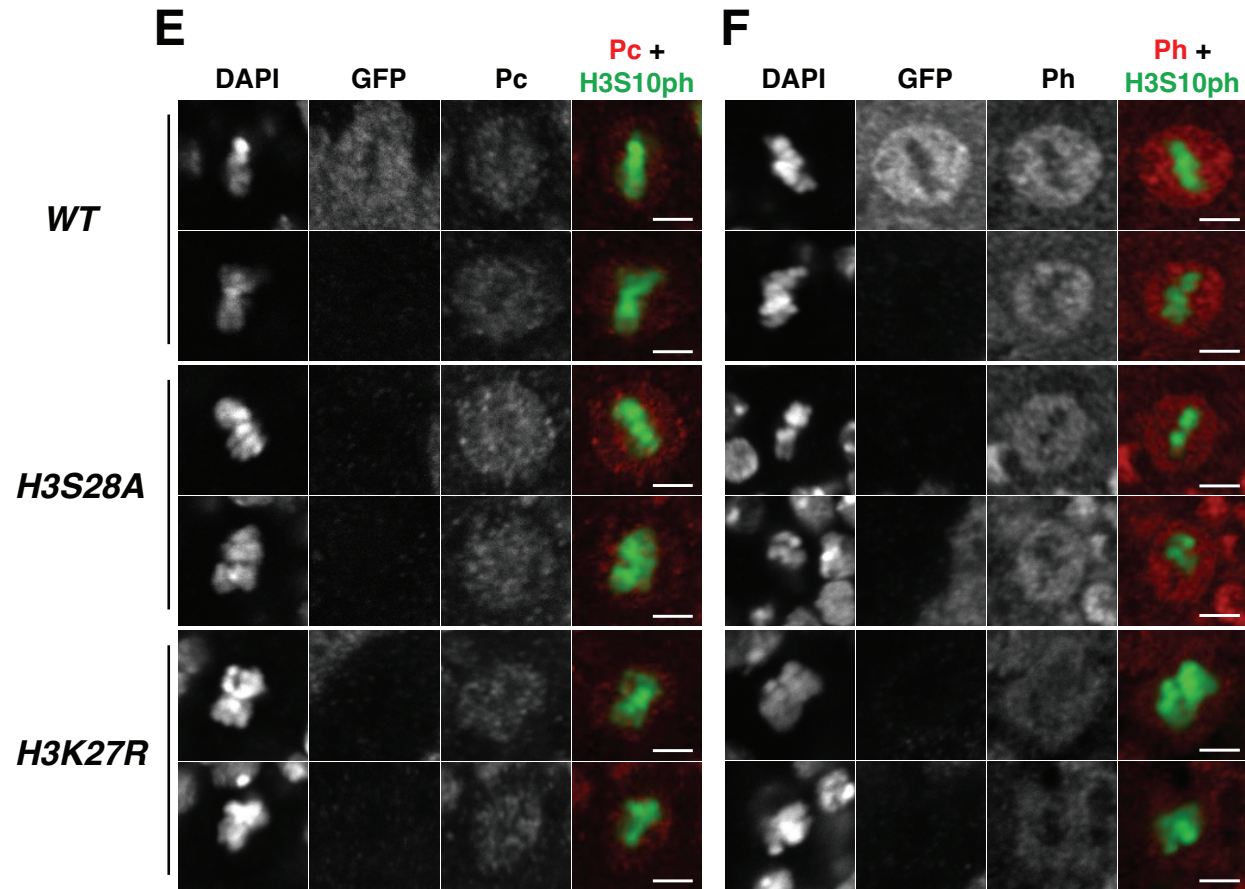


Fig S8. Nuclear staining pattern of Pc and Ph remained unchanged in *H3S28A* and *H3K27R* mutant. Selections of mitotic cells from *WT*, *H3S28A* and *H3K27R* clones in wing imaginal discs were compiled to show the distribution of (E) Pc and (F) Ph during mitosis in the corresponding histone replacement backgrounds. Only GFP +ve internal controls of *WT* clones were shown. As in mitotic cells of *WT* clones, Pc and Ph remained largely dissociated from mitotic chromosomes in *H3S28A* and *H3K27R* clones. Scale bars = 2.5 μm .

6. Extended results

Phenotyping *H3S28A* mutant in *dUtxΔ* background

As mentioned previously, H3S28ph blocks both mammalian PcG components^{189,190} and demethylases^{342,343} from accessing H3K27me3. Since *H3S28A* shows PcG phenotypes that are similar but milder to that of *H3K27R* mutant, I wonder if the lack of H3S28ph might render H3K27me3 more susceptible to excessive demethylation. This is in line with the in vitro result showing *H3S28A* nucleosome is a suboptimal substrate of PRC2. Since both factors could, in principle, lead the drop of H3K27 methylation levels observed in larval *H3S28A* clones. To test this idea, I recombine a molecular null allele of dUtx (*dUtxΔ*, 2L-31C)¹³² into $\Delta HisC$ background. Since both deficiency alleles reside on chromosome 2L, a single *FRT40A* recombination element can be used to generate double homozygous mutant via canonical mosaic analysis technique. As such *H3S28A* mutant can be assayed in *dUtxΔ* background. As verified in Fig 7A, *H3S28A* clones (marked by the lack of GFP) combined with homozygous *dUtxΔ* (molecular null mutant) or *dUtx^{PB}* (*PiggyBac* transposon inserted mutant) both displayed drastic reduction in *dUtx* immunostaining signal. Owing to similar results obtained with *dUtxΔ* and *dUtx^{PB}*, only *dUtxΔ* allele was used in further experiments. As for histone marks, it appeared that for all methylation states of H3K27, there were no notable differences between *H3S28A* and combined *dUtxΔ*, *H3S28A* clones (Fig 7B). Surprisingly, adult flies derived from *dUtxΔ*, *H3S28A* mutant displayed more severe antenna-to-leg transformation than *H3S28A* mutant alone (Fig 7C), they showed larger ectopic tissue outgrowth from antennal segment 3. At present, it is not known if dUtx is the only H3K27me3 demethylase in *Drosophila*. And as discussed in the Chapter I, p.14, its demethylation function in larval stage is yet to be confirmed. Currently there is no explanation for the phenotypic enhancement in *H3S28A*, *dUtxΔ* double mutant, it would be informative to know whether similar or even stronger additive effect is observed in *H3K27R*, *dUtxΔ* background.

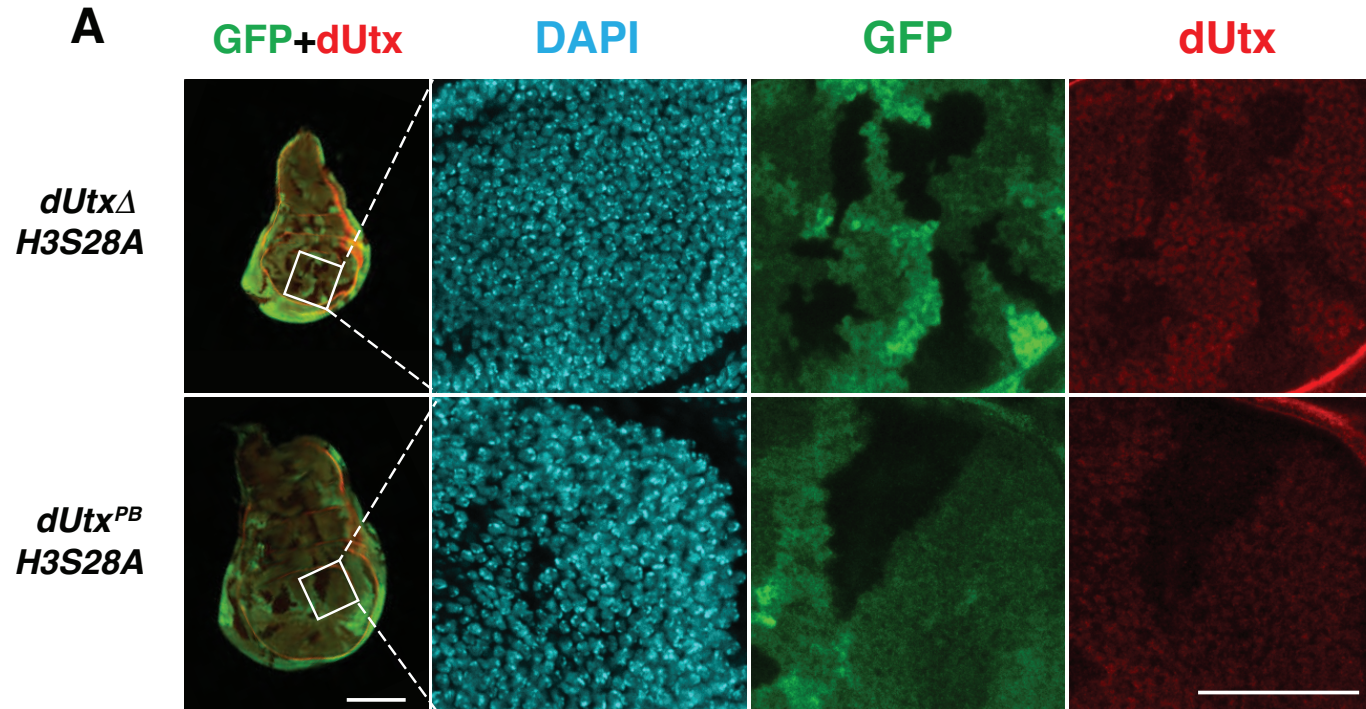


Fig 7 | Combining *dUtx* Δ with *H3S28A* mutant did not rescue reduction of H3K27 methylations.
 (A) Validation of the lost of dUtx in *dUtx* Δ , *H3S28A* and *dUtx*^{PB}, *H3S28A* clones. Wing imaginal discs with clones homozygous of the combined *dUtx*, *H3S28A* mutants were stained with DAPI and the indicated antibodies. Clones were marked by the absence of GFP, which correspond to a drastic reduction of dUtx signal in both *dUtx* Δ , *H3S28A* and *dUtx*^{PB}, *H3S28A* genetic backgrounds. Scale bar of full-disc micrograph represents 100 μ m and those of magnified regions represents 40 μ m.

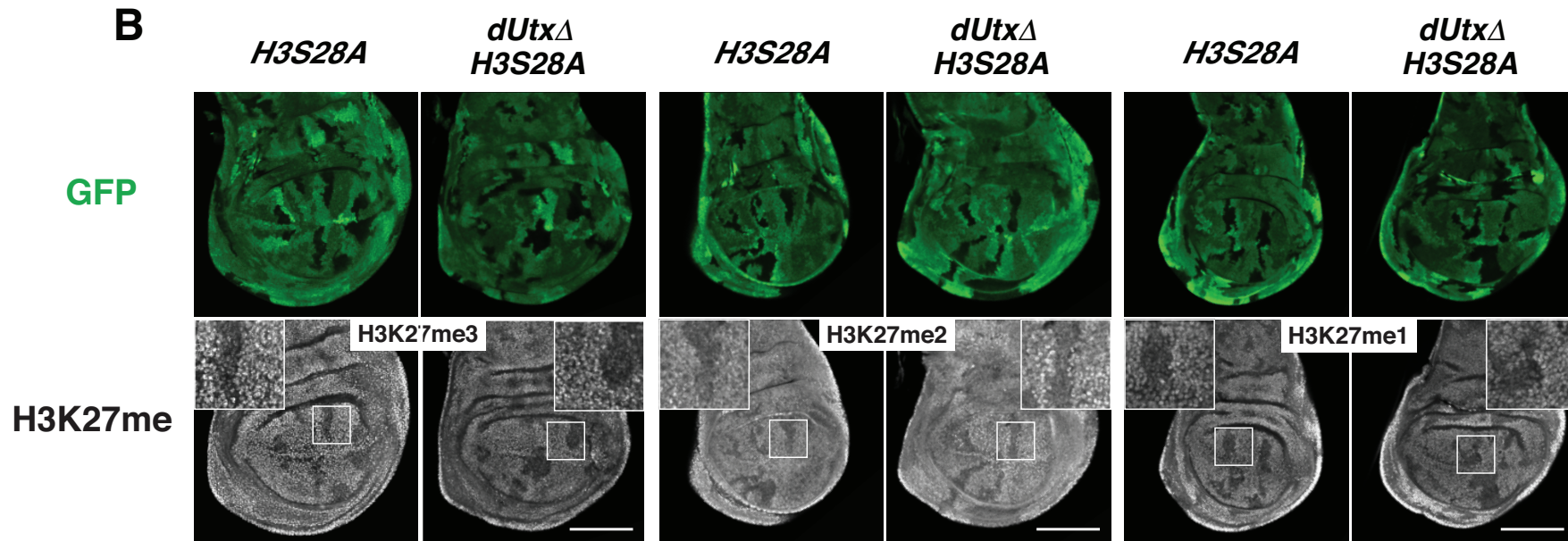


Fig 7 | Combining *dUtxΔ* with *H3S28A* mutant did not rescue reduction of H3K27 methylations.

(B) Wing disc carrying either *H3S28A* clone alone or in combination with *dUtxΔ* were immunostained with the indicated antibodies. Reductions of different H3K27 methylation states in *H3S28A* mutant clones were not rescued in *dUtxΔ*, *H3S28A* background. Scale bar = 100 μ m.

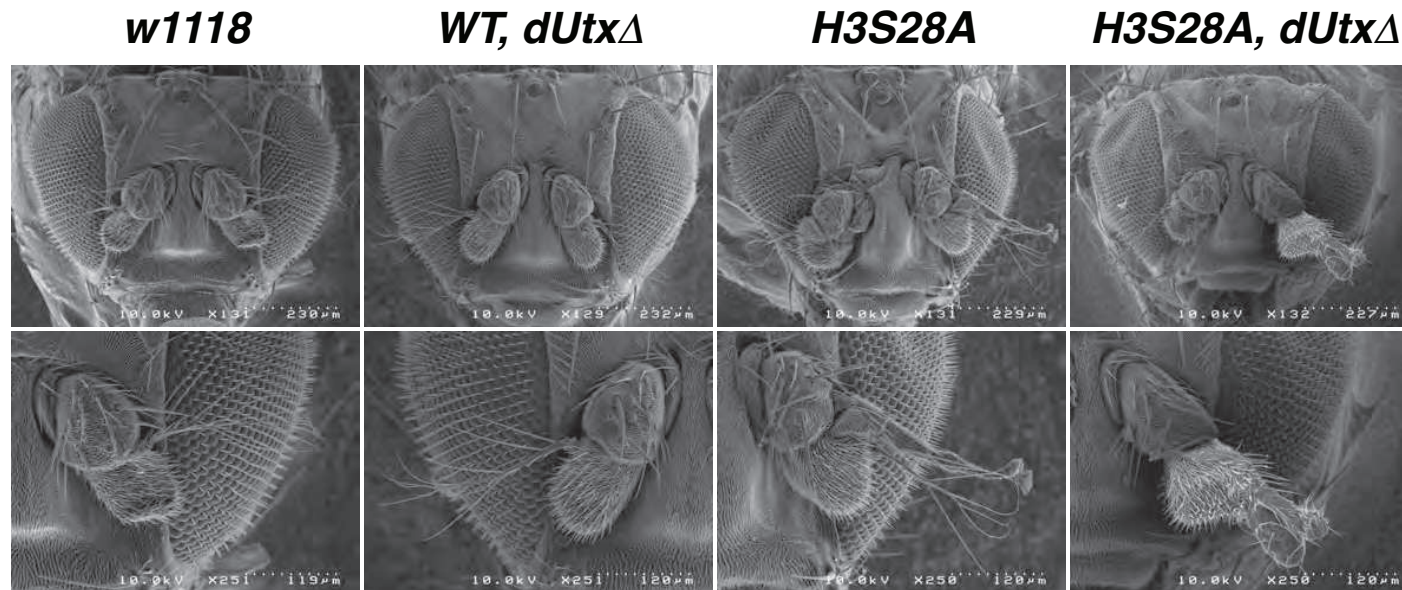
C

Fig 7 | Combining *dUtxΔ* with *H3S28A* mutant did not rescue reduction of H3K27 methylations.

(C) Electron micrographs of adult *Drosophila* heads derived from *w1118*, the indicated mosaic histone replacement lines. Combined *dUtxΔ*, *H3S28A* mutant displayed more severe antenna-to-leg transformation than *H3S28A* mutant alone. *WT* histone replacement line and *w1118* showed normal segmented antenna structures. Scale bar of full-head and magnified fields were annotated in the figures.

Chapter III

Extended Discussions

- 1. Future Plans**
- 2. Potential role of H3S28ph in the epigenetic inheritance of PcG repression through mitosis**
- 3. Transcription-independent role of PcG proteins in mitotic progression**
- 4. Phospho-methyl switches and mitotic progression**
- 5. Alternative method to address the function of mitotic H3S28ph**

Extended Discussion

1. Further experiments

Probing for cell cycle and mitotic defects in *H3S28A* mutant.

Given the H3S28ph is tightly coupled with mitosis, loss of H3S28ph might hamper normal cell cycle progression. RNAi against Aurora B, the mitotic kinase for H3S28ph, leads to aneuploidy nucleus with enlarged volume (Chapter I, p. 26). This is not observed in *H3S28A* mutant clones, which appeared to grow normally and large clone size can be obtained. To document cell cycle defects, the following experiments can be done:

Cell cycle profile of isolated histone mutant cells

H3S28A clones and other histone replacement clones can be sorted as GFP negative populations from larval tissue after cell dissociation by enzymatic treatment. Multicolor-FACS analysis on isolated cells stained with anti-GFP, DAPI, EDU labeling and H3S10ph can provide detail cell cycle profile of *H3S28A* mutant. As shown in Fig. S6, not all *H3S28A* mutant cells within the same clone derepress Ubx in the wing pouch region; this is in contrast to the relatively homogenous derepression state of Ubx in *H3K27R* mutant. It would be interesting to know if the variegated Ubx derepression pattern is associated with different cell cycle state of *H3S28A* mutant cells. Overlaying cell cycle (DAPI or other DNA stain) profile with Ubx derepression level (anti-Ubx immunostaining) might shed light on this question.

Detection of potential mitotic defects in *H3S28A* mutant cells

By means of immunostaining, no obvious mitotic defects were detected. However, it appeared that *H3S28A* clones occasionally displayed abnormally high mitotic index. As shown in Fig 8, a confined *H3S28A* clones located at the post-mitotic region of the eye disc showing intense H3S10ph signal from condensed chromosomes. High mitotic index can be a result of slow mitotic progression or checkpoint activation. To closely examine mitotic progression phenotypes, I have assembled histone replacement lines (see fly stock) compatible with live imaging of chromosome dynamics with the use of H2Av-mRFP transgene. As such, *H3S28A* mutant cells can be identified by the lack of GFP and their chromosomes can be followed by H2Av-mRFP. Ideally clone would be induced in the

larval brain neuroblasts, which has high cell division rate and live imaging of mitotic progression is well documented and established. As such the duration of mitoses and chromosome dynamics can be compared between different histone replacement clones. In parallel, mitotic chromosome squashes can be prepared using wing imaginal discs; this might provide higher resolution analysis of mitotic chromosome morphology and scoring of metaphase/ anaphase ratio. GFP expression states will not be a useful marker to identify histone deficiency clones. Markers specific for endogenous *HisC* at chromosome 2L such as MPM-2⁴¹⁴, Mute-LS⁴¹⁵, Lsm10⁴¹⁶ and HERS⁴¹⁷ can be considered. Alternatively, FISH probes specific for endogenous *HisC* can be used to identify $\Delta HisC$ clones.

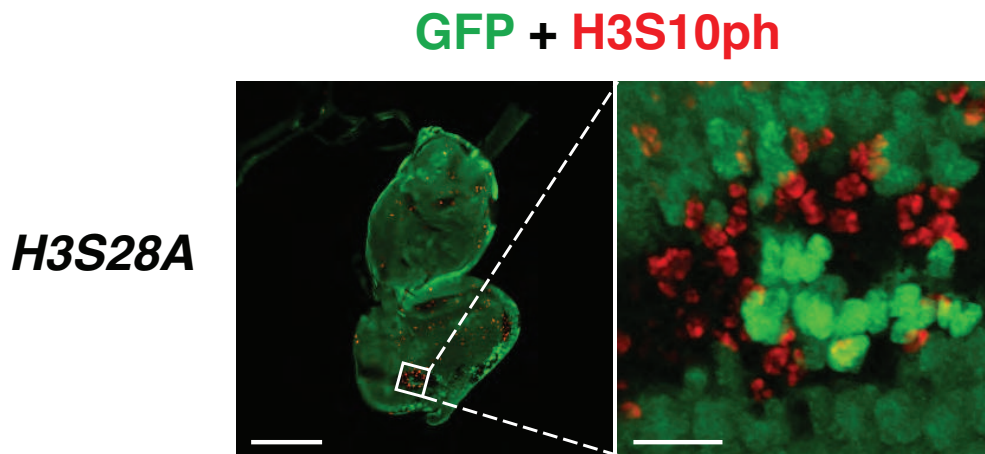


Fig 8 | Mitotic abnormality in *H3S28A* mutant clones.

Eye-antenna disc with *H3S28A* clones were marked by the lack of GFP and immunostained with the indicated antibodies. Z-projection of the magnified region revealed high frequency of *H3S28A* mutant cells undergoing mitosis (H3S10ph +ve) in the post-mitotic region of the eye disc. Scale bar of full-disc micrograph represents 100 μm and those of magnified regions represents 10 μm .

FACS-sorting mitotic cells for ChIP-seq analysis

SILAC-based proteomics approach in mammalian cell culture mode suggests that H3K27me3 level fluctuates throughout the cell cycle with notable decrease by passive dilution during replication and gradual restoration of methylation states during and after S-phase³⁷⁵. However, the changes in the genomics level is not known, this is particularly true in mitosis. In both *H3S28A* and *H3K27R*¹⁰⁰ mutant clones, the endogenous sources of H3.3 variants are intact but do not support H3S28ph and H3K27me3 modifications. However, this is not the case for active chromatin mark H3K4me3. For the *H3K4R* mutant clones³⁶, endogenous wild-type H3.3 can robustly support H3K4me3. This indicates that H3S28ph, similar to H3K27me3, might not overlap with active gene regions covered by H3.3. Hence the mitotic genomic distribution of H3S28ph, in the form of H3K27me3S28ph, would be very important to assess its functional relevance to the PcG repression system¹⁹¹ during the course of mitosis. To achieve this, FACS-sorting fixed mitotic cells based on H3S10ph labeling is required and detailed procedures are described in the material and methods section. According to the optimized protocol and as shown in Fig 9, starting with asynchronous *Drosophila* S2 cell culture of ~1% mitotic index can yield ~ 1 x 10⁶ mitotic cells (> 95% purity) within 4 hours continuous sorting.

As illustrated in Fig 10, FACS-sorted mitotic populations contain mouse anti-H3S10ph antibody on the chromosomes, which will contaminated ChIP-seq samples if general Protein A or Protein G beads are used to recover immunoprecipitated chromatin fragments. Since most of the ChIP-seq antibodies (e.g. anti-H3K27me3, anti-H3K27me3S28ph, anti-Pc ...etc) are raised from rabbit or animal hosts other than mouse, the used of secondary antibody coated beads, such as donkey anti-rabbit beads, can specifically recover ChIP-seq antibody immunoprecipitated chromatin fragments.

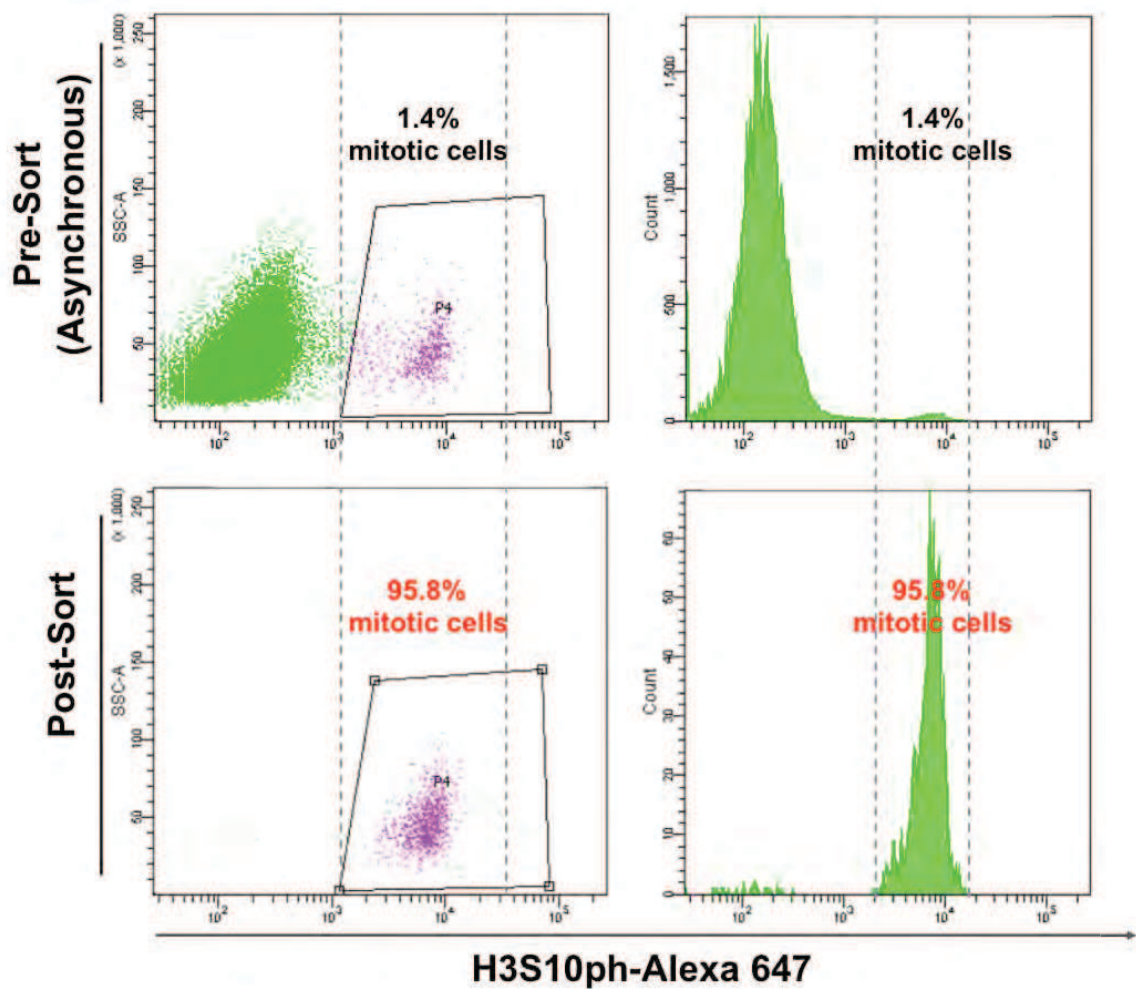


Fig 9 | FACS-sorting of mitotic populations from asynchronous *Drosophila* S2 cell culture.

H3S10ph-Alexa 647 is used as mitotic marker for FACS-sorting. Under asynchronous conditions, mitotic S2 cells account for around 1% of the population. Re-FACS analysis of sorted cells indicates > 95% of pure mitotic cells. SCC, side scattering.

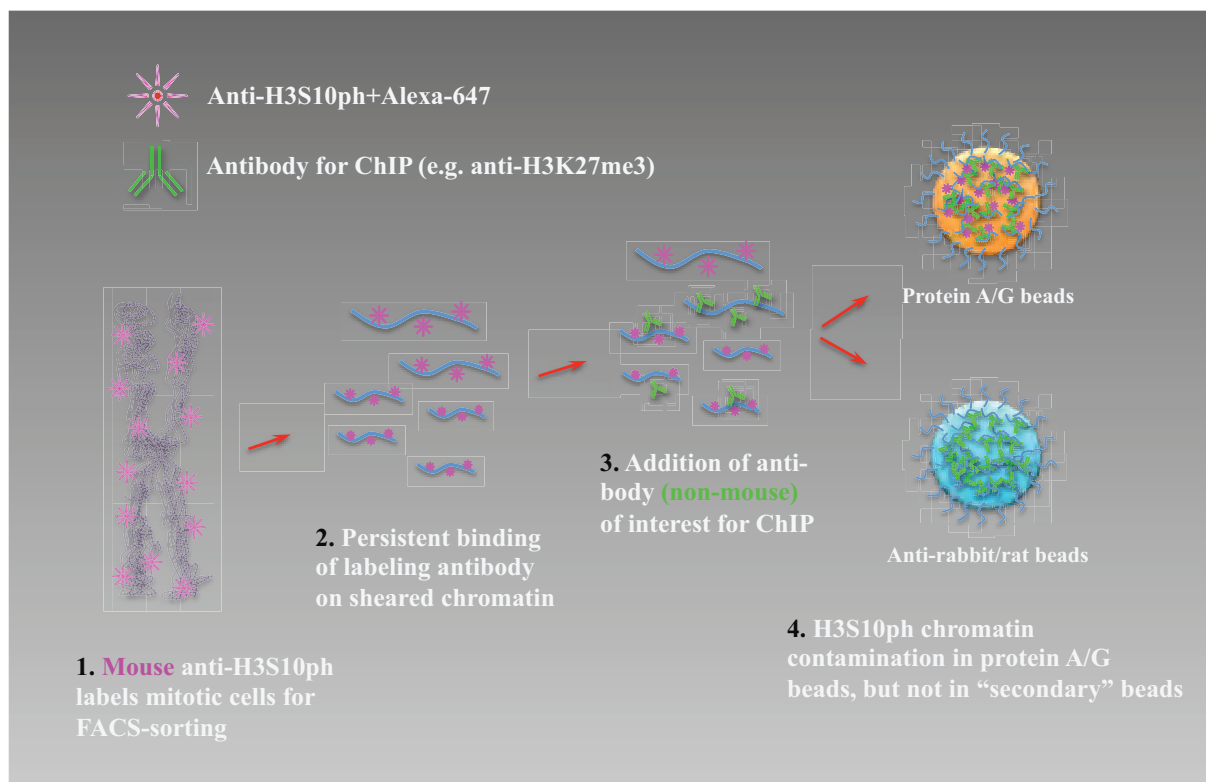


Fig 10 | Using secondary antibodies to prevent H3S10ph contamination of ChIP-seq samples.

FACS-sorted mitotic cells contain mitotic chromosomes coated with mouse anti-H3S10ph antibody, which will contaminate with ChIP-seq antibody if Protein A or Protein G beads are used. Highly adsorbed, species-specific secondary antibody can specifically recover ChIP-seq chromatin fragments.

Potential role of H3S28ph in the epigenetic inheritance of PcG repression through mitosis

Studies from mammalian cells showed that interphase H3S28ph on one hand repelled PcG proteins from binding chromatin^{189,190} while on the other hand shielded H3K27me3 from demethylases^{342,343}. How are these seemingly contrasting properties channeled with epigenetic inheritance?

Also, the emerging functions of mitotic bookmarking stress the importance of mitotic retention of transcription factor to re-establish transcription program in early G1 phase of the next cell cycle³⁸²⁻³⁸⁴. Since majority of *Drosophila* PcG proteins are dissociated from mitotic chromosomes (see Chapter I, p.81), it begs the question on how PcG repressive chromatin states are maintained during mitosis? In fact the lack of PcG proteins on their canonical target sites during mitosis might leaves a time window where H3K27me3 could be susceptible to negatively regulator such as demethylases. Hence the demethylation-resistant property of H3K27me3S28ph^{342,343} might serve to protect H3K27me3 *in-cis* during the course of mitosis.

A related question would be how essential PcG eviction is during mitosis? Analogous to another phospho-methyl switch, H3K9me3S10ph eviction of HP1 is proposed to be important for mitotic chromosome condensation^{177,178}. This idea remained to be rigorously tested, since it would be important to have an experimental condition to track mitotic progression when HPI persists on mitotic chromosomes. Similarly to PcG proteins, it remains unknown what happen to mitosis if PcG protein persist on mitotic chromosomes.

Recently, Hi-C mapping of chromosome contacts on mitotic mammalian cells has been published⁴¹⁸. Polymer physics simulation based on such Hi-C data suggest that mitotic chromosomes are assembled as longitudinally compressed consecutive arrays of chromatin loops devoided of interphase nuclear organization features such as chromosome compartments and TADs^{418,419}. This raises an intriguing question as how the extensive and labyrinth network of interphase chromosome contacts are systemically demolished into neatly condensed mitotic chromosomes. In addition to condensin action, phosphor-methyl switch evictions of their native binders might assist such process. As described in Chapter I and illustrated in Fig I, there are at least 5 groups of phosphor-methyl switches, that each of them has documented functions in chromosome organizations. Hence by evicting the binders, it may alleviate their role in sustaining interphase chromosome organization and facilitate mitotic chromosome condensation. Following this logic, persistent PcG binding

might misguide mitotic chromosome condensation. Since we did not observe rebinding of Pc and Ph on *H3S28A* mitotic chromosomes and tools to enforce PcG mitotic retention are not available, this idea remains to be tested in the future.

Transcription-independent role of PcG proteins in mitotic progression

The intimate link between PcG proteins and the cell cycle machinery has just begun to unfold in recent years. Notably, Psc was found to complex with an anaphase-promoting complex (APC) component, Lemming (LMG/Apc11), to degrade cyclin B for anaphase onset²³⁰. Unlike dRAF complex whose E3 ligase activity is contributed by dRing⁷⁷, the RING finger motif of Psc is required for cyclin B ubiquitination²³⁰. Lack of Psc accumulates cyclin B and leads to misalignment and segregation defects of mitotic chromosomes. Since Psc is a subunit component of PRC1, dRAF and Psc-Apc11, it raises the question of how Psc is partitioned over these complexes, particularly if Psc is a limiting factor. In fact, such novel function of Psc provides an attractive model in epigenetic inheritance of PcG repression during mitosis, as depicted in Fig 11. In this model, gross dissociation of Psc from mitotic chromosomes might liberate Psc availability to complex with Apc11 and hence progressively engage for cyclin B degradation. PcG repressive loops are not sustained as PcG proteins including Psc are evicted from their target sites, and this may facilitate mitotic chromosome condensation. Up to a threshold where sufficient Psc-Apc11 complex is formed, cyclin B is degraded to permit chromosomes segregation. As such, it could constitute a fail-safe mechanism to ensure chromatin-eviction of Psc occurs before anaphase onset. This mechanism is particularly important if persistent PcG bindings and retention of their associated chromatin loops misguide mitotic chromosome condensation with tangled chromatin fibers. Since subsequent anaphase would results in chromosome breakages. (Examples!!)

Of note, *Drosophila* cyclin B can be phosphorylated by Aurora B kinase⁴²⁰, it would be interesting to compare with canonical APC/CDC20 and assess whether Psc-LMG is required for degradation such a specific population of cyclin B.

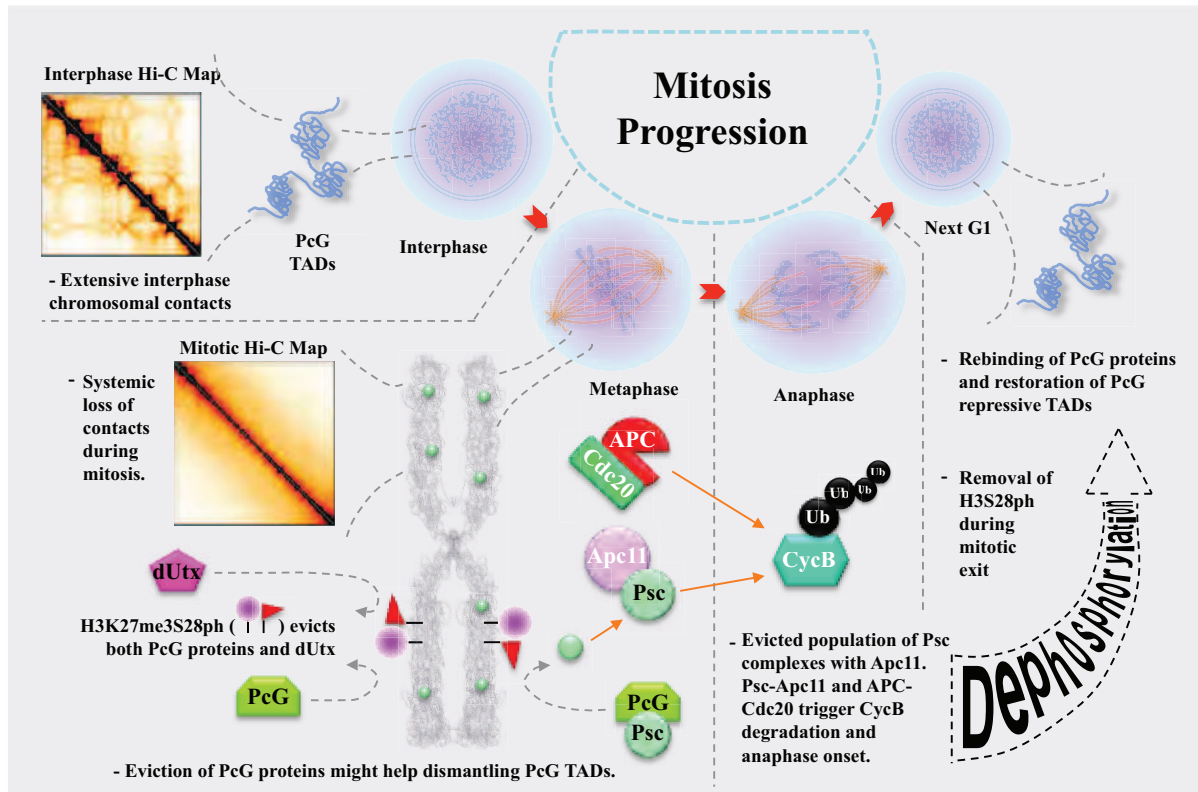


Fig 11 | Potential role of H3S28ph in the epigenetic inheritance of PcG repression through mitosis.

Extensive chromosomal contacts including polycomb-related topologically associated domains (TAD) are systemically dismantled during the mitosis, as shown in the comparison between interphase and mitotic Hi-C chromosomal contact heat maps⁴¹⁸. The repulsive property of H3S28ph against PcG-H3K27me3 interaction might facilitate the lost of PcG proteins from mitotic chromosomes and resolution of their associated chromatin looping structures. At the same time, the lost of PcG proteins at their target sites, such as the Hox clusters, during mitosis might render them susceptible to negative regulators. Hence the demethylase-resistant nature of H3K27me3S28ph might help to preserve H3K27me3 level during mitosis. Besides, the displaced population of Psc might make it available to form alternative complex with Apc11, which act together with APC/Cdc20 to ubiquitinate cyclin B and trigger anaphase onset. As such, chromosome segregation is initiated in a condition when sufficient Psc-Apc11 complex is formed. Although a subpopulation of Psc is retained on mitotic chromosomes, their enrichment at domain borders might indicate a less engagement in mediating chromatin contacts. Global histone dephosphorylations along mitotic exit resume H3K27me3-PcG bindings and gradual restoration of their repressive TADs structures in the next G1 phase. * Hi-C maps are modified from *Naumova et al.*

Phospho-methyl switches and mitotic progression

As exemplified by the case of H3K27me3S28ph, addition of a phosphate group renders the methylated lysine irresponsive to both positive^{189,190} and negative^{342,343} regulators. This property is yet to be generalized to other mitotic “phospho-methyl” dual modifications, particularly on its role in resisting demethylations.

It was shown that H3T3ph repelled binding of TFIID (TAF3)⁴²¹, MLL5^{166,422} and CHD1²⁷ to H3K4me3. H3S10ph blocks HP binding to H3K9me3^{177,178}. H3S28ph shields H3K27me3 away from PcG components^{189,190} and demethylases^{342,343}. H2AK119ub and H2AT120 exists individually, but their presences as dually modified form on the same tail remained to be verified. Similarly, H3K79me3S80ph coexistence remained to be confirmed. Except for H3T3ph and H2AT120ph¹⁶²⁻¹⁶⁴, which has proved to activate Aurora B kinase for mitotic progression, the necessity of other mitotic phosphorylations has yet to be verified. Lack of H3S10ph in budding yeast *H3S10A* mutant is viable with no mitotic defects¹⁷⁰; it only displays condensation phenotype for an artificially lengthened chromosome. This is different for eukaryotes that support H3K9me3. In the case of fission yeast^{173,174} and *Tetrahymena*¹⁷², *H3S10A* mutation led to various mitotic defects. Notably, pericentromeric occupancy of H3K9me3 dropped significantly in fission yeast *H3S10A* mutant¹⁷⁴, it would be interesting to know if it is caused by excessive demethylation or inefficient catalysis by Clr4, homolog of Su(var)3-9, on *H3S10A* nucleosome. Interestingly, primitive eukaryotes that lack H3K27me3 seem not to support H3S28ph. There are no reports on the existence of H3S28ph in budding yeast so far, and the combined *H3S10A*, *H3S28A* mutant is viable with no defects in mitosis and meiosis¹⁶⁹. It is more extreme in the case fission yeast, whose native genome encodes histone H3 with an alanine at position 28. Hence the endogenous wild type H3 is not phosphorylatable for H3S28ph. Sophisticated histone mutagenesis and mitotic chromatin-tethering tools would be needed to systematically address the roles of these dual modifications in mitosis.

Alternative method to address the function of mitotic H3S28ph

Since *H3S28A* mutant introduces structural intolerance that hampers PRC2 HMT activity, it is difficult to explain the observed phenotype as a result of the lack of H3S28ph or reduced H3K27me₃-deposition efficiency on *H3S28A* mutant. If we know exactly how H3S28 contributes in PRC2 catalysis, it might be possible to design complementing suppressor mutation on E(z) to override H3S28A inhibitory effect. Assuming the hydroxyl group of H3S28 is essential for hydrogen bonding, the best amino-acid substitute that ablates phosphorylation potential by serine/threonine kinase while retaining side-chain polarity would be 2, 3-diaminopropanoic acid (Dap). Of note, DAP differ from a serine residue by replacing the side chain hydroxyl group with an amino group. In fact Dap exists as non-proteinogenic amino acid in cellular metabolites. It can be incorporated during artificial peptide synthesis and hence compatible with *in vitro* studies. However, tools for *in vivo* orthogonal labeling of Dap is not yet available. Apart from optimizing the mutation on histones, lost of function approaches can still be applied to Aurora B kinase. Since Aurora B kinase was shown to tethering to subcellular compartments by different factors¹⁶⁰, it remains possible that specific components are required for chromatin-targeting of Aurora B. If this is the case, lost of function approach against such factor might uncouple histone phosphorylations from other essential Aurora B-dependent mitotic functions without the need of histone mutation.

Chapter IV

Materials & Methods

1. **Plasmids constructions**
2. ***Drosophila* transgenesis**
3. **Generation of the histone locus deficiency line**
4. ***Drosophila* Genetics**
5. **Mosaic analysis and immunostaining**
6. **Scanning electron microscope**
7. **in vitro PRC2 histone methyltransferase assay**
8. **FACS-sorting of mitotic population from *Drosophila* S2 cell culture**
9. **Primer list**
10. ***E.coli* stock**
11. **Fly stocks**

Materials & Methods

Plasmid constructions

Molecular cloning for histone replacement system largely follows a previous report¹⁰⁴. Generation of **Integration plasmid** carrying *3xHisGU* requires recombineering of three different **entry vectors** into a **destination vector** carrying an attB site. Recombineering follows the instructions of the commercial kit (Invitrogen 12537-023, MultiSite Gateway Three-Fragment Vector Construction Kit)

Entry vectors:

- pENTR221-*HisGU* (7602 bp)
- pENTRL4R1-*HisGU* (7701 bp)
- pENTRR2L3-*HisGU* (7697 bp)

Destination vectors:

- pDESTR3R4-fC31attB (9216 bp)

Integration plasmid:

- pfC31attB3xHisGU

Since WT-H3 and H3K27R mutant derivatives of His-GU is requested from Alf Herzig lab, only the molecular cloning of H3S28A is described as follow:

1. Gene Synthesis

The following histone H3 fragment is synthesized by Eurofins Scientific to exchange the codon AGT->GCC for H3S28A serine to alanine substitution. This fragment is 815 bp and is flanked by two restrictions site for subsequent subcloning steps. 5' restriction site: NcoI, 3' restriction site: SacI. Coding region of histone H3, start codon and the introduced mutation codon is highlighted in grey, blue and red respectively.

ccatggctgtaactgtctctctcttggcgtgtccgtgtaggtcacggcatcacgaattacgttctccaagaaaaccttcagaacgccacgcgttcc
ctcgatatgagtcagatatgcgcttcacaccgcctcgacgggccaacggcgtagcaggcttcgtgataaccttgatgttatcacgcagc
actttgcatgacgcttggcgcacccttccaagccttgcctcctttaccacgaccagtcattttcactgttctatactattatacacgcacagc
acgaaagtcactaaagaactaattcaacgtttctgtgtgccctattataggtaaaacgacaaaaacccgagagagtacgaacgatatgttcgtt
cgcttttcgctcgtcaaatgaaatggcctctgttttctctctctctctctctcttccacgtccacgattgctatataagtaggtagcaaatgctctga
tcgtttattgtgtttcaaacgtgaagtagtgaacgtgaactttagtgaacccaaatcggag**atg**gctcgtaccaagcaaacgtcgcgcaaatcg
actggtggaaggcggccacgcaacaactggctactaaggccgctcgcaag**GCC**gctccagccaccggaggtgtaagaagccccacc
gctatgccctggaaccgtggccttgcgtgaaattcgtcgtaccaaaagagaccgagcttctaataccgcaagctgcctttccagcgtctggtg
cgtgaaatcgtcaggacttaagacggacttgcgattccagagctc**3**

The fragment is synthesized and cloned into pEX-A vector for amplification.

2. Construction of pENTR221-*HisGU-H3S28A*

NcoI-SacI digestion is applied to pENTR221-*HisGU* to release the WT 815 bp fragment. Vector backbone is gel-purified and ligated to the corresponding H3S28A 815 bp fragment released from the gene synthesis pEX-A vector. This gives rise to **pENTR221-*HisGU-H3S28A***.

3. Construction of pENTRL4R1-*HisGU-H3S28A* and pENTRR2L3-*HisGU-H3S28A*

AgeI-Acc65I sequential digestion is applied to pENTRL4R1-*HisGU* to release the WT-*HisGU* fragment (~5 kb), the resulting vector backbone (~2.7 kb) is gel-purified and ready for ligation. Similarly, the vector backbone of pENTRR2L3-*HisGU* with AgeI-Acc65I ends is prepared. To prepare the *HisGU-H3S28A* insert (~5kb), the same restriction digestion is applied to pENTR221-*HisGU-H3S28A*, and in this case, the vector backbone is discarded, while the *HisGU-H3S28A* fragment is gel-purified and ligated to pENTRL4R1 and pENTRR2L3 vector backbones.

4. Recombineering

Recombineering follows the instructions of the commercial kit (Invitrogen 12537-023, MultiSite Gateway Three-Fragment Vector Construction Kit). The following integration plasmids are generated:

- *pfC31attB3xHisGU* (~23 kb)
- *pfC31attB3xHisGU-H3S28A* (~23 kb)
- *pfC31attB3xHisGU-H3K27R* (~23 kb)

Because of their large sizes, it is difficult to verify plasmid purification by midi- or maxipreps. Hence it is useful to verify plasmid identity by restriction digestion with NcoI-BstXI, which yield restriction fragments of 8370 bp, 2x 5082 bp, 3603 bp and 641 bp.

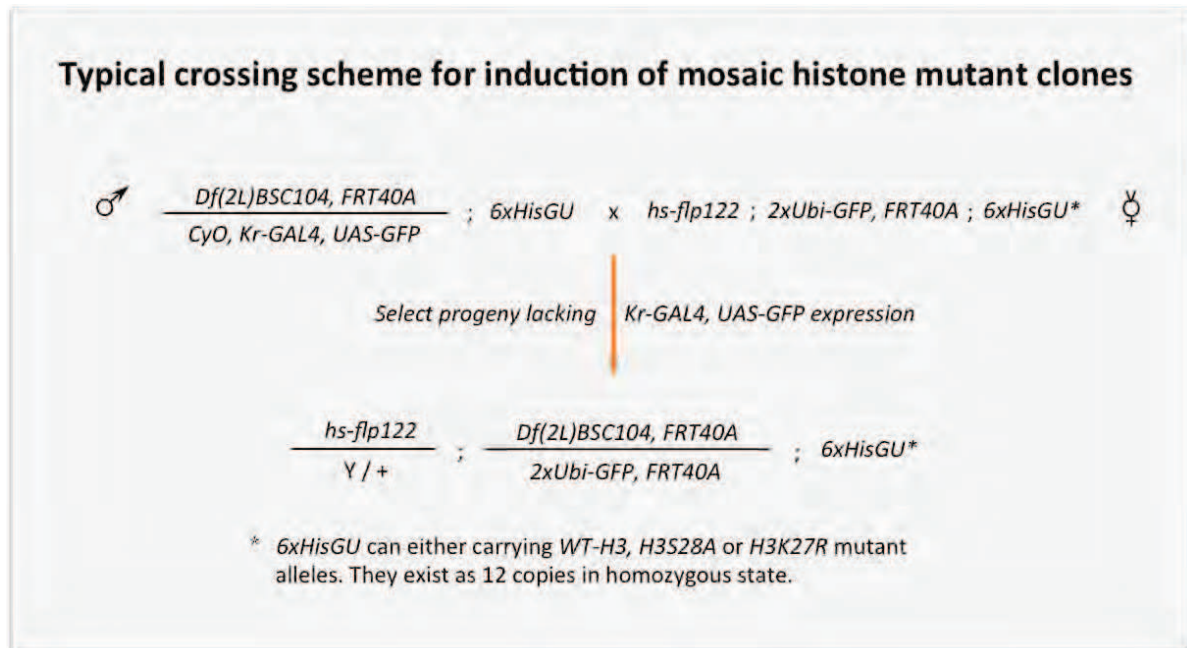
***Drosophila* Transgenesis**

ϕ C31-mediated site-specific transgenesis is performed by the BestGene Inc. company, using the *attP* landing sites reside at cytological location 68E and 86Fb. Positive and stable transformants are selected based on the *mini-white* marker, which is subsequently removed using Cre-Lox recombination. Hence the resulting *3xHisGU* transgenic lines at both 68E and 86Fb lack phenotypic markers, detection of transgenes insertions require PCR. 68E and 86Fb transgenic lines carrying the same HisGU alleles are recombined (confirmed by PRC) and balanced. The resulting line would have *12xHisGU* on chromosome III at homozygous state.

Generation of the histone locus deficiency line

The histone deficiency alleles used in this study is *Df(2L)BSC104* (BL#8670). It is generated via FLP-FRT mediated recombination between P elements PBac(WH)f05491 and P(XP) d03256. The resulting *Df(2L)BSC104* lack *mini-white* marker. The *Df(2L)BSC104* line is requested from Konrad Basler lab in the form of *BSC104, FRT40A* recombinant to facilitate mosaic analysis.

Drosophila Genetics



Mosaic analysis and Immunostaining

Egg depositions were allowed over a 24 hr time window at 25°C. Larva developed for two days before they were heat shocked at 37°C for 1 hr. L3 larva emerged 3 days after heat shock, and they were selected for the lack of green balancer before dissection. Inverted larva heads were fixed in 4% formaldehyde/PBS for 20 min at room temperature. After washing with PBS, the samples were permeabilized twice with 0.3% TritonX-100/PBS for 30 min at room temperature. After blocking with 3% BSA 0.03% TritonX-100/PBS for 1 hr, the samples were incubated with primary antibodies in 0.03% Triton X-100/PBS overnight at 4°C. Samples were then incubated with Alexa (Invitrogen) fluorophores conjugated secondary antibodies before DAPI staining. Thorough washes were applied in between incubations. Imaginal discs were carefully removed and mounted with ProLong Gold (Invitrogen) antifade reagent. Micrographs were acquired from the Zeiss LSM 780 inverted confocal microscope. Raw micrographs were processed with ImageJ and assembled with Adobe Illustrator.

Primary antibodies used for immunostaining in this study:

Hox antibodies were purchased from the Developmental Studies Hybridoma Bank (DSHB). Mouse anti-Scr (DSHB 6H4.1, 1:20), mouse anti-Antp (DSHB 8C11, 1:20), mouse anti-Ubx (DSHB FP3.38, 1:20), mouse anti-Abd-B (DSHB 1A2E9, 1:10), mouse

anti-En (DSHB 4D9, 1:20), mouse anti-H3 (ActiveMotif 39763, 1:500), mouse anti-H3S10ph (Millipore 05-806, 1:1000), rat anti-H3S28ph (Millipore MABE76, 1:1000), rabbit anti-H3K27me3 (Millipore 07-449, 1:500), rabbit anti-H3K27me2 (Upstate 07-452, 1:500), rabbit anti-H3K27me1 (Millipore 07-448, 1: 250), rabbit anti-H3K27ac (Abcam Ab4729, 1:500), rabbit anti-H34me3 (Millipore 04-745, 1:500), rabbit anti-Pc (³³⁴, 1:500), rabbit anti-Ph (³³⁴, 1:500), guinea pig anti-Hth (a gift from Ginés Morata, 1:200), rabbit anti-dUtx (a gift from Feng Tie, 1:100), rabbit anti *Drosophila* Aurora B kinase (a gift from David Glover, 1:200), rabbit anti-H3K27me3S28ph (a gift from Klaus Hansen, 1:500), chicken anti-GFP (Invitrogen A10262, 1:500).

Scanning electron microscopy

Adult fly heads were fixed as described⁴²³ using the critical-point-dried method. Briefly, dissected heads were fixed at 1% glutaraldehyde, 1% formaldehyde and 1 M sodium cacodylate (pH 7.2) for 2 hr at room temperature. Samples were washed once in water and dehydrated through incubations at increasing ethanol concentrations, starting from 25%, 50%, 75% and twice in 100%. Each incubation step lasted for at least 4 hr. After critical-point-dried, the samples were then sputter-coated with a 10 nm thick gold film and examined under a scanning electron microscope (Hitachi S4000) using a lens detector with an acceleration voltage of 10 kV at calibrated magnifications.

***In vitro* PRC2 histone methyltransferase assay**

In vitro PRC2 HMT assay was performed by our collaborator - Alexandra Stuetzer* & Wolfgang Fischle*

*Laboratory of Chromatin Biochemistry, Max Planck Institute for Biophysical Chemistry, 37077 Göttingen, Germany.

Nucleosome and Chromatin Reconstitution

Nucleosomes and chromatin arrays were reconstituted by salt gradient dialysis as described⁴²⁴, using recombinant *Xenopus laevis* core histones. Nucleosomes contained a 187bp long DNA fragment with the 601 DNA sequence at its center⁴²⁵. Histones mutant H3S28A/C110A and was generated by site-directed mutagenesis. All reconstitutions were analyzed by native gel electrophoresis.

H3 Peptides Synthesis

H3 peptides corresponding to H3 amino acids 21-33 were synthesized according to standard procedures. A non-natural tyrosine was added at the C-terminus for quantification. Peptides carrying no modification (H3 unmod), H3S28ph, H3K27me3, H3K27me3S28ph and H3K27me3S28A were generated.

HMT Assays

Histone methyltransferase (HMT) reactions were performed using 1 µg nucleosomes in a total volume of 15 µl for 1 h at 30°C. HMT reactions were carried out in presence of 0.8 µCi [methyl-³H]-S-Adenosyl-L-methionine (³H-SAM) and 325 ng PRC2 (75 nM) in HMT buffer (50 mM Tris-HCl pH 8.8, 5 mM MgCl₂, 4 mM DTT). Recombinant *Drosophila melanogaster* PRC2 complex, comprised of Su(z)12, E(z), Nurf55 and ESC, was a kind gift of Nico Thomä (FMI Basel) and was purified as described²⁶⁴. PRC2 HMT assays in presence of H3₂₁₋₃₃ peptides *in trans* contained 5 or 40 µM of peptide. Reactions were stopped by addition of SDS sample buffer followed by separation by SDS-PAGE. Reactions were analyzed by fluorography.

FACS-sorting of mitotic population from S2 cell culture

Drosophila S2 cell culture conditions follow standard guidelines from the *Drosophila* RNAi Screening Center (DRSC, Harvard Medical School). S2 cells are cultured in Schneider's medium (Sigma S0146) supplemented with heat-inactivated 10% Fetal Bovine Serum (Life technologies, 10500064) and Penicillin-Streptomycin (Invitrogen, 15070-063).

S2 culture is kept at a cell density within $1-5 \times 10^6$ /ml in order to attain relatively higher mitotic index (1-2%) from asynchronous population. Prepare sufficient culture accounts for $120-200 \times 10^6$ cells. Harvest cells by scrapping and resuspend them in aliquots. Fix cells in medium at final 1% formaldehyde (Thermo Scientific, 28908) for 10 min at room temperature. Quench fixation by adding glycine to a final concentration of 130mM, incubate for 5 min at room temperature. Wash cells with ice-cold PBS and permeabilize at 0.5% saponin/PBS for 15 min at 4°C. Block cells with 1% BSA/0.5% saponin/PBS for 30 min at 4°C. Pellet cells and adjust cell density at 20×10^6 cells/ml with 0.5% saponin/PBS and add anti-H3S10ph (Millipore, Mouse Monoclonal, 05-806) at 0.5ug/ml, incubation for 1 hr at 4°C. Similarly, add secondary antibody donkey anti-mouse Alexa-647 at 2ug/ml incubation for 1 hr at 4°C. Allow thorough washes with 0.5% saponin/PBS after incubation of primary and secondary antibodies. Adjust sample to 20×10^6 cells/ml, protect them from light and set on ice before use. When the cell sorter is ready, pass sample 10 times through 18-20G needle and pass them through 40 μ m cell strainer (BD Falcon, 352340) to disrupt cell clumps.

The following inhibitors are applied after fixation: Complete Protease inhibitor, EDTA Free (Roche, 04693132001), 1 mM PMSF, 2 mM EDTA, PhosSTOP phosphatase inhibitors (Roche, 04906837001).

Primer List

Purpose	Primer Name	Sequence (5'→3')	Amplicon size
Detection of <i>68E-HisGU</i>	attL.For 68E1.Rev	GGGCGTGCCCTTGAGTTCTCTC GCCGGAAGTGTTGCAATAGATGCC	~ 600 bp
Detection of <i>86Fb-HisGU</i>	attL.For 86F8.Rev	GGGCGTGCCCTTGAGTTCTCTC AGGATGGGGGACAGAAGCAGCC	~ 650 bp
Detection of <i>FRT40A</i>	(F)70 (R)738	GAGAGGCTATTCGGCTATGACT GATACCGTAAAGCACGAGGAAG	~ 690 bp
Detection of <i>Df(2L)BSC104</i>	WH5' plus XP5' minus	GACGCATGATTATCTTTTACGTGAC AATGATTTCGCAGTGGGAAGGCT	~ 1.5 kb

E. coli Stocks

Stock no.	Plasmid Name	Antibiotics resistance	Host	Remarks
36	pENTR221- <i>HisGU</i>	Kan ^R	TOP10	
37	pENTRL4R1- <i>HisGU</i>	Kan ^R	TOP10	
38	pENTRR2L3- <i>HisGU</i>	Kan ^R	TOP10	Requested from Alf Herzig
39	pENTR221- <i>HisGU-H3K27R</i>	Kan ^R	TOP10	
40	pENTRL4R1- <i>HisGU-H3K27R</i>	Kan ^R	TOP10	
41	pENTRR2L3- <i>HisGU-H3K27R</i>	Kan ^R	TOP10	
42	pDESTR3R4-fC31attB	Amp ^R Chl ^R	DB3.1	
73	pφC31attB3xHisGU #1	Amp ^R	Omni Max 2-T1R	Chl-sensitive
74	pφC31attB3xHisGU #2	Amp ^R	Omni Max 2-T1R	Chl-sensitive
75	pφC31attB3xHisGU-H3K27R #1	Amp ^R	Omni Max 2-T1R	Chl-sensitive
76	pφC31attB3xHisGU-H3K27R #2	Amp ^R	Omni Max 2-T1R	Chl-sensitive
82	pEX-A-H3S28A	Amp ^R	TOP10	
83	pEX-A-H3S28D	Amp ^R	TOP10	
84	pEX-A-H3K27RS28A	Amp ^R	TOP10	
85	pEX-A-H1-Null	Amp ^R	TOP10	
86	pENTR221- <i>HisGU-H3S28A</i> #1	Kan ^R	TOP10	
87	pENTR221- <i>HisGU-H3S28A</i> #2	Kan ^R	TOP10	
88	pENTR221- <i>HisGU-H3S28D</i> #1	Kan ^R	TOP10	
89	pENTR221- <i>HisGU-H3S28D</i> #2	Kan ^R	TOP10	
90	pENTR221- <i>HisGU-H3K27RS28A</i> #1	Kan ^R	TOP10	
91	pENTR221- <i>HisGU-H3K27RS28A</i> #2	Kan ^R	TOP10	
92	pENTR221- <i>HisGU-H1-Null</i> #1	Kan ^R	TOP10	
93	pENTR221- <i>HisGU-H1-Null</i> #2	Kan ^R	TOP10	
94	pENTR221- <i>HisGU-H2AK119R</i> #1	Kan ^R	TOP10	
95	pENTR221- <i>HisGU-H2AK119R</i> #2	Kan ^R	TOP10	
96	pENTRL4R1- <i>HisGU-H3S28A</i> #1	Kan ^R	TOP10	
97	pENTRL4R1- <i>HisGU-H3S28A</i> #2	Kan ^R	TOP10	
98	pENTRR2L3- <i>HisGU-H3S28A</i> #1	Kan ^R	TOP10	
99	pENTRR2L3- <i>HisGU-H3S28A</i> #2	Kan ^R	TOP10	
100	pφC31attB3xHisGU-H3S28A #1	Amp ^R	Omni Max 2-T1R	Chl-sensitive
101	pφC31attB3xHisGU-H3S28A #2	Amp ^R	Omni Max 2-T1R	Chl-sensitive

Fly Stocks

The following fly lines were used in this study

Miscellaneous starter lines for the mosaic histone replacement system

y, w, hsp70-flp; FRT40A; TM2/TM6B (Erika Bach)

y, w; P{Ubi-GFP.D}h33, P{Ubi-GFP.D}38, FRT40A (Bloomington #BL5189)

y, w, hsp70-flp; Df(2L) BSC104, FRT40A/CyO, twis-Gal4, UAS-GFP; MKRS/TM6B (Konrad Basler)

Parental lines for mosaic analysis of histone mutants

y, w, hsp70-flp122; P{Ubi-GFP.D}33, P{Ubi-GFP.D}38, FRT40A; 6xHisGU

y, w, hsp70-flp122; P{Ubi-GFP.D}33, P{Ubi-GFP.D}38, FRT40A; 6xHisGU^{H3S28A}

y, w, hsp70-flp122; P{Ubi-GFP.D}33, P{Ubi-GFP.D}38, FRT40A; 6xHisGU^{H3K27R}

w; Df(2L) BSC104, FRT40A /CyO, Kr-Gal4, UAS-GFP; 6xHisGU

w; Df(2L) BSC104, FRT40A /CyO, Kr-Gal4, UAS-GFP; 6xHisGU^{H3S28A}

w; Df(2L) BSC104, FRT40A /CyO, Kr-Gal4, UAS-GFP; 6xHisGU^{H3K27R}

Mosaic analysis of histone mutants with *ey-FLP1*

y, w, ey-FLP1; P{Ubi-GFP.D}33, P{Ubi-GFP.D}38, FRT40A; 6xHisGU

y, w, ey-FLP1; P{Ubi-GFP.D}33, P{Ubi-GFP.D}38, FRT40A; 6xHisGU^{H3S28A}

y, w ey-FLP1; P{Ubi-GFP.D}33, P{Ubi-GFP.D}38, FRT40A; 6xHisGU^{H3K27R}

Mosaic analysis of histone mutants in *dUtxA* background

w; dUtxA, Df(2L) BSC104, FRT40A /CyO, Kr-Gal4, UAS-GFP; 6xHisGU

w; dUtxA, Df(2L) BSC104, FRT40A /CyO, Kr-Gal4, UAS-GFP; 6xHisGU^{H3S28A}

Mosaic analysis of histone mutants compatible with live-imaging

y, w, hsp70-flp122; P{Ubi-GFP.D}33, P{Ubi-GFP.D}38, FRT40A; 6xHisGU

y, w, hsp70-flp122; P{Ubi-GFP.D}33, P{Ubi-GFP.D}38, FRT40A; 6xHisGU^{H3S28A}

y, w, hsp70-flp122; P{Ubi-GFP.D}33, P{Ubi-GFP.D}38, FRT40A; 6xHisGU^{H3K27R}

Controls

Antp^{Ns}/TM3, Ser (Walter Gehring)

w¹¹¹⁸

References

- 1 Allis, C. D., Jenuwein, T. & Reinberg, D. *Epigenetics*. 23-61 (Cold Spring Harbor Laboratory Press, 2007).
- 2 Kouzarides, T. Chromatin modifications and their function. *Cell* **128**, 693-705, doi:10.1016/j.cell.2007.02.005 (2007).
- 3 Strahl, B. D. & Allis, C. D. The language of covalent histone modifications. *Nature* **403**, 41-45, doi:10.1038/47412 (2000).
- 4 Di Croce, L. & Helin, K. Transcriptional regulation by Polycomb group proteins. *Nat Struct Mol Biol* **20**, 1147-1155, doi:10.1038/nsmb.2669 (2013).
- 5 Grossniklaus, U. & Paro, R. Transcriptional Silencing by Polycomb-Group Proteins. *Cold Spring Harb Perspect Biol* **6**, doi:10.1101/cshperspect.a019331 (2014).
- 6 Margueron, R. & Reinberg, D. The Polycomb complex PRC2 and its mark in life. *Nature* **469**, 343-349, doi:10.1038/nature09784 (2011).
- 7 Schuettengruber, B., Chourrout, D., Vervoort, M., Leblanc, B. & Cavalli, G. Genome regulation by polycomb and trithorax proteins. *Cell* **128**, 735-745, doi:10.1016/j.cell.2007.02.009 (2007).
- 8 Simon, J. A. & Kingston, R. E. Occupying chromatin: Polycomb mechanisms for getting to genomic targets, stopping transcriptional traffic, and staying put. *Mol Cell* **49**, 808-824, doi:10.1016/j.molcel.2013.02.013 (2013).
- 9 Fillion, G. J. *et al.* Systematic protein location mapping reveals five principal chromatin types in *Drosophila* cells. *Cell* **143**, 212-224, doi:10.1016/j.cell.2010.09.009 (2010).
- 10 Kharchenko, P. V. *et al.* Comprehensive analysis of the chromatin landscape in *Drosophila melanogaster*. *Nature* **471**, 480-485, doi:10.1038/nature09725 (2011).
- 11 Bonn, S. *et al.* Tissue-specific analysis of chromatin state identifies temporal signatures of enhancer activity during embryonic development. *Nat Genet* **44**, 148-156, doi:10.1038/ng.1064 (2012).
- 12 Yin, H., Sweeney, S., Raha, D., Snyder, M. & Lin, H. A high-resolution whole-genome map of key chromatin modifications in the adult *Drosophila melanogaster*. *PLoS Genet* **7**, e1002380, doi:10.1371/journal.pgen.1002380 (2011).
- 13 Schuettengruber, B. *et al.* Cooperativity, specificity, and evolutionary stability of polycomb targeting in *Drosophila*. *Cell Rep* **9**, 219-233, doi:10.1016/j.celrep.2014.08.072 (2014).
- 14 Schuettengruber, B. *et al.* Functional anatomy of polycomb and trithorax chromatin landscapes in *Drosophila* embryos. *PLoS Biol* **7**, e13, doi:10.1371/journal.pbio.1000013 (2009).
- 15 Tie, F. *et al.* Trithorax monomethylates histone H3K4 and interacts directly with CBP to promote H3K27 acetylation and antagonize Polycomb silencing. *Development* **141**, 1129-1139, doi:10.1242/dev.102392 (2014).
- 16 Gutierrez, L. *et al.* The role of the histone H2A ubiquitinase Sce in Polycomb repression. *Development* **139**, 117-127, doi:10.1242/dev.074450 (2012).
- 17 Ardehali, M. B. *et al.* *Drosophila* Set1 is the major histone H3 lysine 4 trimethyltransferase with role in transcription. *Embo J* **30**, 2817-2828, doi:10.1038/emboj.2011.194 (2011).
- 18 Mohan, M. *et al.* The COMPASS family of H3K4 methylases in *Drosophila*. *Mol Cell Biol* **31**, 4310-4318, doi:10.1128/MCB.06092-11 (2011).

- 19 Hallson, G. *et al.* dSet1 is the main H3K4 di- and tri-methyltransferase throughout Drosophila development. *Genetics* **190**, 91-100, doi:10.1534/genetics.111.135863 (2012).
- 20 Wood, A. *et al.* Bre1, an E3 ubiquitin ligase required for recruitment and substrate selection of Rad6 at a promoter. *Mol Cell* **11**, 267-274 (2003).
- 21 Wu, M. *et al.* Molecular regulation of H3K4 trimethylation by Wdr82, a component of human Set1/COMPASS. *Mol Cell Biol* **28**, 7337-7344, doi:10.1128/MCB.00976-08 (2008).
- 22 Bray, S., Musisi, H. & Bienz, M. Bre1 is required for Notch signaling and histone modification. *Dev Cell* **8**, 279-286, doi:10.1016/j.devcel.2004.11.020 (2005).
- 23 Santos-Rosa, H. *et al.* Methylation of histone H3 K4 mediates association of the Isw1p ATPase with chromatin. *Mol Cell* **12**, 1325-1332 (2003).
- 24 Wysocka, J. *et al.* A PHD finger of NURF couples histone H3 lysine 4 trimethylation with chromatin remodelling. *Nature* **442**, 86-90, doi:10.1038/nature04815 (2006).
- 25 Taverna, S. D. *et al.* Yng1 PHD finger binding to H3 trimethylated at K4 promotes NuA3 HAT activity at K14 of H3 and transcription at a subset of targeted ORFs. *Mol Cell* **24**, 785-796, doi:10.1016/j.molcel.2006.10.026 (2006).
- 26 Vermeulen, M. *et al.* Selective anchoring of TFIID to nucleosomes by trimethylation of histone H3 lysine 4. *Cell* **131**, 58-69, doi:10.1016/j.cell.2007.08.016 (2007).
- 27 Flanagan, J. F. *et al.* Double chromodomains cooperate to recognize the methylated histone H3 tail. *Nature* **438**, 1181-1185, doi:10.1038/nature04290 (2005).
- 28 Sims, R. J., 3rd *et al.* Human but not yeast CHD1 binds directly and selectively to histone H3 methylated at lysine 4 via its tandem chromodomains. *J Biol Chem* **280**, 41789-41792, doi:10.1074/jbc.C500395200 (2005).
- 29 Sims, R. J., 3rd *et al.* Recognition of trimethylated histone H3 lysine 4 facilitates the recruitment of transcription postinitiation factors and pre-mRNA splicing. *Mol Cell* **28**, 665-676, doi:10.1016/j.molcel.2007.11.010 (2007).
- 30 Shi, X. *et al.* ING2 PHD domain links histone H3 lysine 4 methylation to active gene repression. *Nature* **442**, 96-99, doi:10.1038/nature04835 (2006).
- 31 Di Stefano, L., Ji, J. Y., Moon, N. S., Herr, A. & Dyson, N. Mutation of Drosophila Lsd1 disrupts H3-K4 methylation, resulting in tissue-specific defects during development. *Curr Biol* **17**, 808-812, doi:10.1016/j.cub.2007.03.068 (2007).
- 32 Rudolph, T. *et al.* Heterochromatin formation in Drosophila is initiated through active removal of H3K4 methylation by the LSD1 homolog SU(VAR)3-3. *Mol Cell* **26**, 103-115, doi:10.1016/j.molcel.2007.02.025 (2007).
- 33 Secombe, J., Li, L., Carlos, L. & Eisenman, R. N. The Trithorax group protein Lid is a trimethyl histone H3K4 demethylase required for dMyc-induced cell growth. *Genes Dev* **21**, 537-551, doi:10.1101/gad.1523007 (2007).
- 34 Lee, N., Erdjument-Bromage, H., Tempst, P., Jones, R. S. & Zhang, Y. The H3K4 demethylase lid associates with and inhibits histone deacetylase Rpd3. *Mol Cell Biol* **29**, 1401-1410, doi:10.1128/MCB.01643-08 (2009).
- 35 Eissenberg, J. C. *et al.* The trithorax-group gene in Drosophila little imaginal discs encodes a trimethylated histone H3 Lys4 demethylase. *Nat Struct Mol Biol* **14**, 344-346, doi:10.1038/nsmb1217 (2007).
- 36 Hodl, M. & Basler, K. Transcription in the absence of histone H3.2 and H3K4 methylation. *Curr Biol* **22**, 2253-2257, doi:10.1016/j.cub.2012.10.008 (2012).

- 37 Girton, J. R. & Johansen, K. M. Chromatin structure and the regulation of gene expression: the lessons of PEV in *Drosophila*. *Adv Genet* **61**, 1-43, doi:10.1016/S0065-2660(07)00001-6 (2008).
- 38 Ebert, A., Lein, S., Schotta, G. & Reuter, G. Histone modification and the control of heterochromatic gene silencing in *Drosophila*. *Chromosome Res* **14**, 377-392, doi:10.1007/s10577-006-1066-1 (2006).
- 39 Elgin, S. C. & Reuter, G. Position-effect variegation, heterochromatin formation, and gene silencing in *Drosophila*. *Cold Spring Harb Perspect Biol* **5**, a017780, doi:10.1101/cshperspect.a017780 (2013).
- 40 Rea, S. *et al.* Regulation of chromatin structure by site-specific histone H3 methyltransferases. *Nature* **406**, 593-599, doi:10.1038/35020506 (2000).
- 41 Bannister, A. J. *et al.* Selective recognition of methylated lysine 9 on histone H3 by the HP1 chromo domain. *Nature* **410**, 120-124, doi:10.1038/35065138 (2001).
- 42 Lachner, M., O'Carroll, D., Rea, S., Mechtler, K. & Jenuwein, T. Methylation of histone H3 lysine 9 creates a binding site for HP1 proteins. *Nature* **410**, 116-120, doi:10.1038/35065132 (2001).
- 43 Mis, J., Ner, S. S. & Grigliatti, T. A. Identification of three histone methyltransferases in *Drosophila*: dG9a is a suppressor of PEV and is required for gene silencing. *Mol Genet Genomics* **275**, 513-526, doi:10.1007/s00438-006-0116-x (2006).
- 44 Seum, C., Bontron, S., Reo, E., Delattre, M. & Spierer, P. *Drosophila* G9a is a nonessential gene. *Genetics* **177**, 1955-1957, doi:10.1534/genetics.107.078220 (2007).
- 45 Kato, Y., Kato, M., Tachibana, M., Shinkai, Y. & Yamaguchi, M. Characterization of *Drosophila* G9a in vivo and identification of genetic interactants. *Genes Cells* **13**, 703-722, doi:10.1111/j.1365-2443.2008.01199.x (2008).
- 46 Yoon, J. *et al.* dSETDB1 and SU(VAR)3-9 sequentially function during germline-stem cell differentiation in *Drosophila melanogaster*. *PLoS One* **3**, e2234, doi:10.1371/journal.pone.0002234 (2008).
- 47 Lejeune, E., Bayne, E. H. & Allshire, R. C. On the connection between RNAi and heterochromatin at centromeres. *Cold Spring Harbor symposia on quantitative biology* **75**, 275-283, doi:10.1101/sqb.2010.75.024 (2010).
- 48 Pal-Bhadra, M. *et al.* Heterochromatic silencing and HP1 localization in *Drosophila* are dependent on the RNAi machinery. *Science* **303**, 669-672, doi:10.1126/science.1092653 (2004).
- 49 Allshire, R. C. & Karpen, G. H. Epigenetic regulation of centromeric chromatin: old dogs, new tricks? *Nat Rev Genet* **9**, 923-937, doi:10.1038/nrg2466 (2008).
- 50 Castel, S. E. & Martienssen, R. A. RNA interference in the nucleus: roles for small RNAs in transcription, epigenetics and beyond. *Nat Rev Genet* **14**, 100-112, doi:10.1038/nrg3355 (2013).
- 51 Hall, I. M., Noma, K. & Grewal, S. I. RNA interference machinery regulates chromosome dynamics during mitosis and meiosis in fission yeast. *Proc Natl Acad Sci U S A* **100**, 193-198, doi:10.1073/pnas.232688099 (2003).
- 52 Bloom, K. S. Centromeric Heterochromatin: The Primordial Segregation Machine. *Annu Rev Genet*, doi:10.1146/annurev-genet-120213-092033 (2014).
- 53 Lin, C. H. *et al.* Heterochromatin protein 1a stimulates histone H3 lysine 36 demethylation by the *Drosophila* KDM4A demethylase. *Mol Cell* **32**, 696-706, doi:10.1016/j.molcel.2008.11.008 (2008).

- 54 Lin, C. H., Paulson, A., Abmayr, S. M. & Workman, J. L. HP1a targets the Drosophila KDM4A demethylase to a subset of heterochromatic genes to regulate H3K36me3 levels. *PLoS One* **7**, e39758, doi:10.1371/journal.pone.0039758 (2012).
- 55 Lu, X. *et al.* Drosophila H1 regulates the genetic activity of heterochromatin by recruitment of Su(var)3-9. *Science* **340**, 78-81, doi:10.1126/science.1234654 (2013).
- 56 Lloret-Llinares, M., Carre, C., Vaquero, A., de Olano, N. & Azorin, F. Characterization of Drosophila melanogaster JmjC+N histone demethylases. *Nucleic Acids Res* **36**, 2852-2863, doi:10.1093/nar/gkn098 (2008).
- 57 Tsurumi, A., Dutta, P., Shang, R., Yan, S. J. & Li, W. X. Drosophila Kdm4 demethylases in histone H3 lysine 9 demethylation and ecdysteroid signaling. *Sci Rep* **3**, 2894, doi:10.1038/srep02894 (2013).
- 58 Wagner, E. J. & Carpenter, P. B. Understanding the language of Lys36 methylation at histone H3. *Nat Rev Mol Cell Biol* **13**, 115-126, doi:10.1038/nrm3274 (2012).
- 59 Bell, O. *et al.* Localized H3K36 methylation states define histone H4K16 acetylation during transcriptional elongation in Drosophila. *Embo J* **26**, 4974-4984, doi:10.1038/sj.emboj.7601926 (2007).
- 60 Stabell, M., Larsson, J., Aalen, R. B. & Lambertsson, A. Drosophila dSet2 functions in H3-K36 methylation and is required for development. *Biochem Biophys Res Commun* **359**, 784-789, doi:10.1016/j.bbrc.2007.05.189 (2007).
- 61 Tanaka, Y., Katagiri, Z., Kawahashi, K., Kioussis, D. & Kitajima, S. Trithorax-group protein ASH1 methylates histone H3 lysine 36. *Gene* **397**, 161-168, doi:10.1016/j.gene.2007.04.027 (2007).
- 62 Lhoumaud, P. *et al.* Insulators recruit histone methyltransferase dMes4 to regulate chromatin of flanking genes. *Embo J* **33**, 1599-1613, doi:10.15252/embj.201385965 (2014).
- 63 Beisel, C., Imhof, A., Greene, J., Kremmer, E. & Sauer, F. Histone methylation by the Drosophila epigenetic transcriptional regulator Ash1. *Nature* **419**, 857-862, doi:10.1038/nature01126 (2002).
- 64 Byrd, K. N. & Shearn, A. ASH1, a Drosophila trithorax group protein, is required for methylation of lysine 4 residues on histone H3. *Proc Natl Acad Sci U S A* **100**, 11535-11540, doi:10.1073/pnas.1933593100 (2003).
- 65 Keogh, M. C. *et al.* Cotranscriptional set2 methylation of histone H3 lysine 36 recruits a repressive Rpd3 complex. *Cell* **123**, 593-605, doi:10.1016/j.cell.2005.10.025 (2005).
- 66 Joshi, A. A. & Struhl, K. Eaf3 chromodomain interaction with methylated H3-K36 links histone deacetylation to Pol II elongation. *Mol Cell* **20**, 971-978, doi:10.1016/j.molcel.2005.11.021 (2005).
- 67 Venkatesh, S. *et al.* Set2 methylation of histone H3 lysine 36 suppresses histone exchange on transcribed genes. *Nature* **489**, 452-455, doi:10.1038/nature11326 (2012).
- 68 Smolle, M. *et al.* Chromatin remodelers Isw1 and Chd1 maintain chromatin structure during transcription by preventing histone exchange. *Nat Struct Mol Biol* **19**, 884-892, doi:10.1038/nsmb.2312 (2012).
- 69 Butler, J. S. & Dent, S. Y. Chromatin 'resetting' during transcription elongation: a central role for methylated H3K36. *Nat Struct Mol Biol* **19**, 863-864, doi:10.1038/nsmb.2370 (2012).
- 70 Dhayalan, A. *et al.* The Dnmt3a PWWP domain reads histone 3 lysine 36 trimethylation and guides DNA methylation. *J Biol Chem* **285**, 26114-26120, doi:10.1074/jbc.M109.089433 (2010).

- 71 Ballare, C. *et al.* Phf19 links methylated Lys36 of histone H3 to regulation of Polycomb activity. *Nat Struct Mol Biol* **19**, 1257-1265, doi:10.1038/nsmb.2434 (2012).
- 72 Brien, G. L. *et al.* Polycomb PHF19 binds H3K36me3 and recruits PRC2 and demethylase NO66 to embryonic stem cell genes during differentiation. *Nat Struct Mol Biol* **19**, 1273-1281, doi:10.1038/nsmb.2449 (2012).
- 73 Abed, J. A. & Jones, R. S. H3K36me3 key to Polycomb-mediated gene silencing in lineage specification. *Nat Struct Mol Biol* **19**, 1214-1215, doi:10.1038/nsmb.2458 (2012).
- 74 Musselman, C. A. *et al.* Molecular basis for H3K36me3 recognition by the Tudor domain of PHF1. *Nat Struct Mol Biol* **19**, 1266-1272, doi:10.1038/nsmb.2435 (2012).
- 75 Tsukada, Y. *et al.* Histone demethylation by a family of JmjC domain-containing proteins. *Nature* **439**, 811-816, doi:10.1038/nature04433 (2006).
- 76 He, J., Kallin, E. M., Tsukada, Y. & Zhang, Y. The H3K36 demethylase Jhdm1b/Kdm2b regulates cell proliferation and senescence through p15(Ink4b). *Nat Struct Mol Biol* **15**, 1169-1175, doi:10.1038/nsmb.1499 (2008).
- 77 Lagarou, A. *et al.* dKDM2 couples histone H2A ubiquitylation to histone H3 demethylation during Polycomb group silencing. *Genes Dev* **22**, 2799-2810, doi:10.1101/gad.484208 (2008).
- 78 Farcas, A. M. *et al.* KDM2B links the Polycomb Repressive Complex 1 (PRC1) to recognition of CpG islands. *Elife* **1**, e00205, doi:10.7554/eLife.00205 (2012).
- 79 He, J. *et al.* Kdm2b maintains murine embryonic stem cell status by recruiting PRC1 complex to CpG islands of developmental genes. *Nat Cell Biol* **15**, 373-384, doi:10.1038/ncb2702 (2013).
- 80 Wu, X., Johansen, J. V. & Helin, K. Fbxl10/Kdm2b recruits polycomb repressive complex 1 to CpG islands and regulates H2A ubiquitylation. *Mol Cell* **49**, 1134-1146, doi:10.1016/j.molcel.2013.01.016 (2013).
- 81 Blackledge, N. P. *et al.* Variant PRC1 complex-dependent H2A ubiquitylation drives PRC2 recruitment and polycomb domain formation. *Cell* **157**, 1445-1459, doi:10.1016/j.cell.2014.05.004 (2014).
- 82 Shanower, G. A. *et al.* Characterization of the grappa gene, the *Drosophila* histone H3 lysine 79 methyltransferase. *Genetics* **169**, 173-184, doi:10.1534/genetics.104.033191 (2005).
- 83 Nguyen, A. T. & Zhang, Y. The diverse functions of Dot1 and H3K79 methylation. *Genes Dev* **25**, 1345-1358, doi:10.1101/gad.2057811 (2011).
- 84 Mueller, D. *et al.* Misguided transcriptional elongation causes mixed lineage leukemia. *PLoS Biol* **7**, e1000249, doi:10.1371/journal.pbio.1000249 (2009).
- 85 Shilatifard, A. Chromatin modifications by methylation and ubiquitination: implications in the regulation of gene expression. *Annu Rev Biochem* **75**, 243-269, doi:10.1146/annurev.biochem.75.103004.142422 (2006).
- 86 Mohan, M. *et al.* Linking H3K79 trimethylation to Wnt signaling through a novel Dot1-containing complex (DotCom). *Genes Dev* **24**, 574-589, doi:10.1101/gad.1898410 (2010).
- 87 Kim, W., Choi, M. & Kim, J. E. The histone methyltransferase Dot1/DOT1L as a critical regulator of the cell cycle. *Cell Cycle* **13**, 726-738, doi:10.4161/cc.28104 (2014).
- 88 Muller, J. *et al.* Histone methyltransferase activity of a *Drosophila* Polycomb group repressor complex. *Cell* **111**, 197-208 (2002).

- 89 Czermin, B. *et al.* Drosophila enhancer of Zeste/ESC complexes have a histone H3 methyltransferase activity that marks chromosomal Polycomb sites. *Cell* **111**, 185-196 (2002).
- 90 Cao, R. *et al.* Role of histone H3 lysine 27 methylation in Polycomb-group silencing. *Science* **298**, 1039-1043, doi:10.1126/science.1076997 (2002).
- 91 Kuzmichev, A., Nishioka, K., Erdjument-Bromage, H., Tempst, P. & Reinberg, D. Histone methyltransferase activity associated with a human multiprotein complex containing the Enhancer of Zeste protein. *Genes Dev* **16**, 2893-2905, doi:10.1101/gad.1035902 (2002).
- 92 Tie, F., Prasad-Sinha, J., Birve, A., Rasmuson-Lestander, A. & Harte, P. J. A 1-megadalton ESC/E(Z) complex from Drosophila that contains polycomblike and RPD3. *Mol Cell Biol* **23**, 3352-3362 (2003).
- 93 LaJeunesse, D. & Shearn, A. E(z): a polycomb group gene or a trithorax group gene? *Development* **122**, 2189-2197 (1996).
- 94 Ketel, C. S. *et al.* Subunit contributions to histone methyltransferase activities of fly and worm polycomb group complexes. *Mol Cell Biol* **25**, 6857-6868, doi:10.1128/MCB.25.16.6857-6868.2005 (2005).
- 95 Nekrasov, M. *et al.* Pcl-PRC2 is needed to generate high levels of H3-K27 trimethylation at Polycomb target genes. *Embo J* **26**, 4078-4088, doi:10.1038/sj.emboj.7601837 (2007).
- 96 Chen, S., Birve, A. & Rasmuson-Lestander, A. In vivo analysis of Drosophila SU(Z)12 function. *Mol Genet Genomics* **279**, 159-170, doi:10.1007/s00438-007-0304-3 (2008).
- 97 Anderson, A. E. *et al.* The enhancer of trithorax and polycomb gene Caf1/p55 is essential for cell survival and patterning in Drosophila development. *Development* **138**, 1957-1966, doi:10.1242/dev.058461 (2011).
- 98 Jacob, Y. *et al.* ATXR5 and ATXR6 are H3K27 monomethyltransferases required for chromatin structure and gene silencing. *Nat Struct Mol Biol* **16**, 763-768, doi:10.1038/nsmb.1611 (2009).
- 99 Jacob, Y. *et al.* Selective methylation of histone H3 variant H3.1 regulates heterochromatin replication. *Science* **343**, 1249-1253, doi:10.1126/science.1248357 (2014).
- 100 Pengelly, A. R., Copur, O., Jackle, H., Herzig, A. & Muller, J. A histone mutant reproduces the phenotype caused by loss of histone-modifying factor Polycomb. *Science* **339**, 698-699, doi:10.1126/science.1231382 (2013).
- 101 Mito, Y., Henikoff, J. G. & Henikoff, S. Genome-scale profiling of histone H3.3 replacement patterns. *Nat Genet* **37**, 1090-1097, doi:10.1038/ng1637 (2005).
- 102 Lewis, P. W. *et al.* Inhibition of PRC2 activity by a gain-of-function H3 mutation found in pediatric glioblastoma. *Science* **340**, 857-861, doi:10.1126/science.1232245 (2013).
- 103 Struhl, G. A gene product required for correct initiation of segmental determination in Drosophila. *Nature* **293**, 36-41 (1981).
- 104 Gunesdogan, U., Jackle, H. & Herzig, A. A genetic system to assess in vivo the functions of histones and histone modifications in higher eukaryotes. *EMBO Rep* **11**, 772-776, doi:10.1038/embor.2010.124 (2010).
- 105 Fischle, W. *et al.* Molecular basis for the discrimination of repressive methyl-lysine marks in histone H3 by Polycomb and HP1 chromodomains. *Genes Dev* **17**, 1870-1881, doi:10.1101/gad.1110503 (2003).

- 106 Min, J., Zhang, Y. & Xu, R. M. Structural basis for specific binding of Polycomb chromodomain to histone H3 methylated at Lys 27. *Genes Dev* **17**, 1823-1828, doi:10.1101/gad.269603 (2003).
- 107 Simon, M. D. *et al.* The site-specific installation of methyl-lysine analogs into recombinant histones. *Cell* **128**, 1003-1012, doi:10.1016/j.cell.2006.12.041 (2007).
- 108 Jacob, Y. *et al.* Regulation of heterochromatic DNA replication by histone H3 lysine 27 methyltransferases. *Nature* **466**, 987-991, doi:10.1038/nature09290 (2010).
- 109 Messmer, S., Franke, A. & Paro, R. Analysis of the functional role of the Polycomb chromo domain in *Drosophila melanogaster*. *Genes Dev* **6**, 1241-1254 (1992).
- 110 Franke, A. *et al.* Polycomb and polyhomeotic are constituents of a multimeric protein complex in chromatin of *Drosophila melanogaster*. *Embo J* **11**, 2941-2950 (1992).
- 111 Franke, A., Messmer, S. & Paro, R. Mapping functional domains of the polycomb protein of *Drosophila melanogaster*. *Chromosome Res* **3**, 351-360 (1995).
- 112 Kalb, R. *et al.* Histone H2A monoubiquitination promotes histone H3 methylation in Polycomb repression. *Nat Struct Mol Biol* **21**, 569-571, doi:10.1038/nsmb.2833 (2014).
- 113 Margueron, R. *et al.* Role of the polycomb protein EED in the propagation of repressive histone marks. *Nature* **461**, 762-767, doi:10.1038/nature08398 (2009).
- 114 Bowman, S. K. *et al.* H3K27 modifications define segmental regulatory domains in the *Drosophila bithorax* complex. *Elife* **3**, e02833, doi:10.7554/eLife.02833 (2014).
- 115 Schwartz, Y. B. *et al.* Genome-wide analysis of Polycomb targets in *Drosophila melanogaster*. *Nat Genet* **38**, 700-705, doi:10.1038/ng1817 (2006).
- 116 Tolhuis, B. *et al.* Genome-wide profiling of PRC1 and PRC2 Polycomb chromatin binding in *Drosophila melanogaster*. *Nat Genet* **38**, 694-699, doi:10.1038/ng1792 (2006).
- 117 Bernstein, B. E. *et al.* A bivalent chromatin structure marks key developmental genes in embryonic stem cells. *Cell* **125**, 315-326, doi:10.1016/j.cell.2006.02.041 (2006).
- 118 Vastenhouw, N. L. & Schier, A. F. Bivalent histone modifications in early embryogenesis. *Curr Opin Cell Biol* **24**, 374-386, doi:10.1016/j.ceb.2012.03.009 (2012).
- 119 Chen, X., Xiong, J., Xu, M., Chen, S. & Zhu, B. Symmetrical modification within a nucleosome is not required globally for histone lysine methylation. *EMBO Rep* **12**, 244-251, doi:10.1038/embor.2011.6 (2011).
- 120 van Rossum, B., Fischle, W. & Selenko, P. Asymmetrically modified nucleosomes expand the histone code. *Nat Struct Mol Biol* **19**, 1064-1066, doi:10.1038/nsmb.2433 (2012).
- 121 Voigt, P. *et al.* Asymmetrically modified nucleosomes. *Cell* **151**, 181-193, doi:10.1016/j.cell.2012.09.002 (2012).
- 122 Papp, B. & Muller, J. Histone trimethylation and the maintenance of transcriptional ON and OFF states by trxG and PcG proteins. *Genes Dev* **20**, 2041-2054, doi:10.1101/gad.388706 (2006).
- 123 Kaneko, S., Son, J., Bonasio, R., Shen, S. S. & Reinberg, D. Nascent RNA interaction keeps PRC2 activity poised and in check. *Genes Dev* **28**, 1983-1988, doi:10.1101/gad.247940.114 (2014).
- 124 Swigut, T. & Wysocka, J. H3K27 demethylases, at long last. *Cell* **131**, 29-32, doi:10.1016/j.cell.2007.09.026 (2007).

- 125 Agger, K. *et al.* UTX and JMJD3 are histone H3K27 demethylases involved in HOX gene regulation and development. *Nature* **449**, 731-734, doi:10.1038/nature06145 (2007).
- 126 Lan, F. *et al.* A histone H3 lysine 27 demethylase regulates animal posterior development. *Nature* **449**, 689-694, doi:10.1038/nature06192 (2007).
- 127 Hong, S. *et al.* Identification of JmjC domain-containing UTX and JMJD3 as histone H3 lysine 27 demethylases. *Proc Natl Acad Sci U S A* **104**, 18439-18444, doi:10.1073/pnas.0707292104 (2007).
- 128 Lee, M. G. *et al.* Demethylation of H3K27 regulates polycomb recruitment and H2A ubiquitination. *Science* **318**, 447-450, doi:10.1126/science.1149042 (2007).
- 129 Smith, E. R. *et al.* Drosophila UTX is a histone H3 Lys27 demethylase that colocalizes with the elongating form of RNA polymerase II. *Mol Cell Biol* **28**, 1041-1046, doi:10.1128/MCB.01504-07 (2008).
- 130 Herz, H. M. *et al.* The H3K27me3 demethylase dUTX is a suppressor of Notch- and Rb-dependent tumors in Drosophila. *Mol Cell Biol* **30**, 2485-2497, doi:10.1128/MCB.01633-09 (2010).
- 131 Tarayrah, L., Herz, H. M., Shilatifard, A. & Chen, X. Histone demethylase dUTX antagonizes JAK-STAT signaling to maintain proper gene expression and architecture of the Drosophila testis niche. *Development* **140**, 1014-1023, doi:10.1242/dev.089433 (2013).
- 132 Copur, O. & Muller, J. The histone H3-K27 demethylase Utx regulates HOX gene expression in Drosophila in a temporally restricted manner. *Development* **140**, 3478-3485, doi:10.1242/dev.097204 (2013).
- 133 Griffin, R., Binari, R. & Perrimon, N. Genetic odyssey to generate marked clones in Drosophila mosaics. *Proc Natl Acad Sci U S A* **111**, 4756-4763, doi:10.1073/pnas.1403218111 (2014).
- 134 Tie, F. *et al.* CBP-mediated acetylation of histone H3 lysine 27 antagonizes Drosophila Polycomb silencing. *Development* **136**, 3131-3141, doi:10.1242/dev.037127 (2009).
- 135 van der Vlag, J. & Otte, A. P. Transcriptional repression mediated by the human polycomb-group protein EED involves histone deacetylation. *Nat Genet* **23**, 474-478, doi:10.1038/70602 (1999).
- 136 Tie, F., Furuyama, T., Prasad-Sinha, J., Jane, E. & Harte, P. J. The Drosophila Polycomb Group proteins ESC and E(Z) are present in a complex containing the histone-binding protein p55 and the histone deacetylase RPD3. *Development* **128**, 275-286 (2001).
- 137 Chang, Y. L. *et al.* Essential role of Drosophila Hdac1 in homeotic gene silencing. *Proc Natl Acad Sci U S A* **98**, 9730-9735, doi:10.1073/pnas.171325498 (2001).
- 138 Kehle, J. *et al.* dMi-2, a hunchback-interacting protein that functions in polycomb repression. *Science* **282**, 1897-1900 (1998).
- 139 Reynolds, N. *et al.* NuRD-mediated deacetylation of H3K27 facilitates recruitment of Polycomb Repressive Complex 2 to direct gene repression. *Embo J* **31**, 593-605, doi:10.1038/emboj.2011.431 (2012).
- 140 Schwartz, Y. B. *et al.* Alternative epigenetic chromatin states of polycomb target genes. *PLoS Genet* **6**, e1000805, doi:10.1371/journal.pgen.1000805 (2010).
- 141 Pasini, D. *et al.* Characterization of an antagonistic switch between histone H3 lysine 27 methylation and acetylation in the transcriptional regulation of Polycomb group target genes. *Nucleic Acids Res* **38**, 4958-4969, doi:10.1093/nar/gkq244 (2010).

- 142 Wang, H. *et al.* Role of histone H2A ubiquitination in Polycomb silencing. *Nature* **431**, 873-878, doi:10.1038/nature02985 (2004).
- 143 de Napoles, M. *et al.* Polycomb group proteins Ring1A/B link ubiquitylation of histone H2A to heritable gene silencing and X inactivation. *Dev Cell* **7**, 663-676, doi:10.1016/j.devcel.2004.10.005 (2004).
- 144 Buchwald, G. *et al.* Structure and E3-ligase activity of the Ring-Ring complex of polycomb proteins Bmi1 and Ring1b. *Embo J* **25**, 2465-2474, doi:10.1038/sj.emboj.7601144 (2006).
- 145 Li, Z. *et al.* Structure of a Bmi-1-Ring1B polycomb group ubiquitin ligase complex. *J Biol Chem* **281**, 20643-20649, doi:10.1074/jbc.M602461200 (2006).
- 146 Fritsch, C., Beuchle, D. & Muller, J. Molecular and genetic analysis of the Polycomb group gene Sex combs extra/Ring in *Drosophila*. *Mech Dev* **120**, 949-954 (2003).
- 147 Scheuermann, J. C., Gutierrez, L. & Muller, J. Histone H2A monoubiquitination and Polycomb repression: the missing pieces of the puzzle. *Fly (Austin)* **6**, 162-168, doi:10.4161/fly.20986 (2012).
- 148 Bhatnagar, S. *et al.* TRIM37 is a new histone H2A ubiquitin ligase and breast cancer oncoprotein. *Nature* **516**, 116-120, doi:10.1038/nature13955 (2014).
- 149 Kallin, E. M. *et al.* Genome-wide uH2A localization analysis highlights Bmi1-dependent deposition of the mark at repressed genes. *PLoS Genet* **5**, e1000506, doi:10.1371/journal.pgen.1000506 (2009).
- 150 Endoh, M. *et al.* Histone H2A mono-ubiquitination is a crucial step to mediate PRC1-dependent repression of developmental genes to maintain ES cell identity. *PLoS Genet* **8**, e1002774, doi:10.1371/journal.pgen.1002774 (2012).
- 151 Nakagawa, T. *et al.* Deubiquitylation of histone H2A activates transcriptional initiation via trans-histone cross-talk with H3K4 di- and trimethylation. *Genes Dev* **22**, 37-49, doi:10.1101/gad.1609708 (2008).
- 152 Yuan, G. *et al.* Histone H2A ubiquitination inhibits the enzymatic activity of H3 lysine 36 methyltransferases. *J Biol Chem* **288**, 30832-30842, doi:10.1074/jbc.M113.475996 (2013).
- 153 Zhang, Y. Transcriptional regulation by histone ubiquitination and deubiquitination. *Genes Dev* **17**, 2733-2740, doi:10.1101/gad.1156403 (2003).
- 154 Jason, L. J., Moore, S. C., Ausio, J. & Lindsey, G. Magnesium-dependent association and folding of oligonucleosomes reconstituted with ubiquitinated H2A. *J Biol Chem* **276**, 14597-14601, doi:10.1074/jbc.M011153200 (2001).
- 155 Cooper, S. *et al.* Targeting polycomb to pericentric heterochromatin in embryonic stem cells reveals a role for H2AK119u1 in PRC2 recruitment. *Cell Rep* **7**, 1456-1470, doi:10.1016/j.celrep.2014.04.012 (2014).
- 156 Scheuermann, J. C. *et al.* Histone H2A deubiquitinase activity of the Polycomb repressive complex PR-DUB. *Nature* **465**, 243-247, doi:10.1038/nature08966 (2010).
- 157 Baskind, H. A. *et al.* Functional conservation of Asxl2, a murine homolog for the *Drosophila* enhancer of trithorax and polycomb group gene *Asx*. *PLoS One* **4**, e4750, doi:10.1371/journal.pone.0004750 (2009).
- 158 Lai, H. L. & Wang, Q. T. Additional sex combs-like 2 is required for polycomb repressive complex 2 binding at select targets. *PLoS One* **8**, e73983, doi:10.1371/journal.pone.0073983 (2013).
- 159 Abdel-Wahab, O. *et al.* ASXL1 mutations promote myeloid transformation through loss of PRC2-mediated gene repression. *Cancer Cell* **22**, 180-193, doi:10.1016/j.ccr.2012.06.032 (2012).

- 160 Carmena, M., Wheelock, M., Funabiki, H. & Earnshaw, W. C. The chromosomal passenger complex (CPC): from easy rider to the godfather of mitosis. *Nat Rev Mol Cell Biol* **13**, 789-803, doi:10.1038/nrm3474 (2012).
- 161 Musacchio, A. Molecular biology. Surfing chromosomes (and Survivin). *Science* **330**, 183-184, doi:10.1126/science.1197261 (2010).
- 162 Wang, F. *et al.* Histone H3 Thr-3 phosphorylation by Haspin positions Aurora B at centromeres in mitosis. *Science* **330**, 231-235, doi:10.1126/science.1189435 (2010).
- 163 Yamagishi, Y., Honda, T., Tanno, Y. & Watanabe, Y. Two histone marks establish the inner centromere and chromosome bi-orientation. *Science* **330**, 239-243, doi:10.1126/science.1194498 (2010).
- 164 Kelly, A. E. *et al.* Survivin reads phosphorylated histone H3 threonine 3 to activate the mitotic kinase Aurora B. *Science* **330**, 235-239, doi:10.1126/science.1189505 (2010).
- 165 Shintomi, K. & Hirano, T. Sister chromatid resolution: a cohesin releasing network and beyond. *Chromosoma* **119**, 459-467, doi:10.1007/s00412-010-0271-z (2010).
- 166 Ali, M. *et al.* Molecular basis for chromatin binding and regulation of MLL5. *Proc Natl Acad Sci U S A* **110**, 11296-11301, doi:10.1073/pnas.1310156110 (2013).
- 167 Aihara, H. *et al.* Nucleosomal histone kinase-1 phosphorylates H2A Thr 119 during mitosis in the early *Drosophila* embryo. *Genes Dev* **18**, 877-888, doi:10.1101/gad.1184604 (2004).
- 168 Brittle, A. L., Nanba, Y., Ito, T. & Ohkura, H. Concerted action of Aurora B, Polo and NHK-1 kinases in centromere-specific histone 2A phosphorylation. *Exp Cell Res* **313**, 2780-2785, doi:10.1016/j.yexcr.2007.04.038 (2007).
- 169 Wang, F. & Higgins, J. M. Histone modifications and mitosis: countermarks, landmarks, and bookmarks. *Trends Cell Biol* **23**, 175-184, doi:10.1016/j.tcb.2012.11.005 (2013).
- 170 Hsu, J. Y. *et al.* Mitotic phosphorylation of histone H3 is governed by Ipl1/aurora kinase and Glc7/PP1 phosphatase in budding yeast and nematodes. *Cell* **102**, 279-291 (2000).
- 171 Vagnarelli, P. *et al.* Repo-Man coordinates chromosomal reorganization with nuclear envelope reassembly during mitotic exit. *Dev Cell* **21**, 328-342, doi:10.1016/j.devcel.2011.06.020 (2011).
- 172 Wei, Y., Yu, L., Bowen, J., Gorovsky, M. A. & Allis, C. D. Phosphorylation of histone H3 is required for proper chromosome condensation and segregation. *Cell* **97**, 99-109 (1999).
- 173 Mellone, B. G. *et al.* Centromere silencing and function in fission yeast is governed by the amino terminus of histone H3. *Curr Biol* **13**, 1748-1757 (2003).
- 174 Kloc, A., Zaratiegui, M., Nora, E. & Martienssen, R. RNA interference guides histone modification during the S phase of chromosomal replication. *Curr Biol* **18**, 490-495, doi:10.1016/j.cub.2008.03.016 (2008).
- 175 Neurohr, G. *et al.* A midzone-based ruler adjusts chromosome compaction to anaphase spindle length. *Science* **332**, 465-468, doi:10.1126/science.1201578 (2011).
- 176 Wilkins, B. J. *et al.* A cascade of histone modifications induces chromatin condensation in mitosis. *Science* **343**, 77-80, doi:10.1126/science.1244508 (2014).
- 177 Hirota, T., Lipp, J. J., Toh, B. H. & Peters, J. M. Histone H3 serine 10 phosphorylation by Aurora B causes HP1 dissociation from heterochromatin. *Nature* **438**, 1176-1180, doi:10.1038/nature04254 (2005).

- 178 Fischle, W. *et al.* Regulation of HP1-chromatin binding by histone H3 methylation and phosphorylation. *Nature* **438**, 1116-1122, doi:10.1038/nature04219 (2005).
- 179 Wang, Y., Zhang, W., Jin, Y., Johansen, J. & Johansen, K. M. The JIL-1 tandem kinase mediates histone H3 phosphorylation and is required for maintenance of chromatin structure in *Drosophila*. *Cell* **105**, 433-443 (2001).
- 180 Wang, C. *et al.* The epigenetic H3S10 phosphorylation mark is required for counteracting heterochromatic spreading and gene silencing in *Drosophila melanogaster*. *J Cell Sci* **124**, 4309-4317, doi:10.1242/jcs.092585 (2011).
- 181 Cai, W. *et al.* Genome-wide analysis of regulation of gene expression and H3K9me2 distribution by JIL-1 kinase mediated histone H3S10 phosphorylation in *Drosophila*. *Nucleic Acids Res* **42**, 5456-5467, doi:10.1093/nar/gku173 (2014).
- 182 Regnard, C. *et al.* Global analysis of the relationship between JIL-1 kinase and transcription. *PLoS Genet* **7**, e1001327, doi:10.1371/journal.pgen.1001327 (2011).
- 183 Jin, Y., Wang, Y., Johansen, J. & Johansen, K. M. JIL-1, a chromosomal kinase implicated in regulation of chromatin structure, associates with the male specific lethal (MSL) dosage compensation complex. *J Cell Biol* **149**, 1005-1010 (2000).
- 184 Deng, H. *et al.* Ectopic histone H3S10 phosphorylation causes chromatin structure remodeling in *Drosophila*. *Development* **135**, 699-705, doi:10.1242/dev.015362 (2008).
- 185 Zippo, A., De Robertis, A., Serafini, R. & Oliviero, S. PIM1-dependent phosphorylation of histone H3 at serine 10 is required for MYC-dependent transcriptional activation and oncogenic transformation. *Nat Cell Biol* **9**, 932-944, doi:10.1038/ncb1618 (2007).
- 186 Zippo, A. *et al.* Histone crosstalk between H3S10ph and H4K16ac generates a histone code that mediates transcription elongation. *Cell* **138**, 1122-1136, doi:10.1016/j.cell.2009.07.031 (2009).
- 187 Giet, R. & Glover, D. M. *Drosophila* aurora B kinase is required for histone H3 phosphorylation and condensin recruitment during chromosome condensation and to organize the central spindle during cytokinesis. *J Cell Biol* **152**, 669-682 (2001).
- 188 Wang, C. *et al.* Evidence against a role for the JIL-1 kinase in H3S28 phosphorylation and 14-3-3 recruitment to active genes in *Drosophila*. *PLoS One* **8**, e62484, doi:10.1371/journal.pone.0062484 (2013).
- 189 Gehani, S. S. *et al.* Polycomb group protein displacement and gene activation through MSK-dependent H3K27me3S28 phosphorylation. *Mol Cell* **39**, 886-900, doi:10.1016/j.molcel.2010.08.020 (2010).
- 190 Lau, P. N. & Cheung, P. Histone code pathway involving H3 S28 phosphorylation and K27 acetylation activates transcription and antagonizes polycomb silencing. *Proc Natl Acad Sci U S A* **108**, 2801-2806, doi:10.1073/pnas.1012798108 (2011).
- 191 Sawicka, A. *et al.* H3S28 phosphorylation is a hallmark of the transcriptional response to cellular stress. *Genome Res*, doi:10.1101/gr.176255.114 (2014).
- 192 Tweedie-Cullen, R. Y. *et al.* Identification of combinatorial patterns of post-translational modifications on individual histones in the mouse brain. *PLoS One* **7**, e36980, doi:10.1371/journal.pone.0036980 (2012).
- 193 Tweedie-Cullen, R. Y., Reck, J. M. & Mansuy, I. M. Comprehensive mapping of post-translational modifications on synaptic, nuclear, and histone proteins in the adult mouse brain. *J Proteome Res* **8**, 4966-4982, doi:10.1021/pr9003739 (2009).
- 194 Huttlin, E. L. *et al.* A tissue-specific atlas of mouse protein phosphorylation and expression. *Cell* **143**, 1174-1189, doi:10.1016/j.cell.2010.12.001 (2010).
- 195 Hammond, S. L. *et al.* Mitotic phosphorylation of histone H3 threonine 80. *Cell Cycle* **13**, 440-452, doi:10.4161/cc.27269 (2014).

- 196 Schalch, T., Duda, S., Sargent, D. F. & Richmond, T. J. X-ray structure of a tetranucleosome and its implications for the chromatin fibre. *Nature* **436**, 138-141, doi:10.1038/nature03686 (2005).
- 197 Huyen, Y. *et al.* Methylated lysine 79 of histone H3 targets 53BP1 to DNA double-strand breaks. *Nature* **432**, 406-411, doi:10.1038/nature03114 (2004).
- 198 Francis, N. J., Saurin, A. J., Shao, Z. & Kingston, R. E. Reconstitution of a functional core polycomb repressive complex. *Mol Cell* **8**, 545-556 (2001).
- 199 Saurin, A. J., Shao, Z., Erdjument-Bromage, H., Tempst, P. & Kingston, R. E. A *Drosophila* Polycomb group complex includes Zeste and dTAFII proteins. *Nature* **412**, 655-660, doi:10.1038/35088096 (2001).
- 200 Shao, Z. *et al.* Stabilization of chromatin structure by PRC1, a Polycomb complex. *Cell* **98**, 37-46, doi:10.1016/S0092-8674(00)80604-2 (1999).
- 201 King, I. F., Francis, N. J. & Kingston, R. E. Native and recombinant polycomb group complexes establish a selective block to template accessibility to repress transcription in vitro. *Mol Cell Biol* **22**, 7919-7928 (2002).
- 202 Francis, N. J., Kingston, R. E. & Woodcock, C. L. Chromatin compaction by a polycomb group protein complex. *Science* **306**, 1574-1577, doi:10.1126/science.1100576 (2004).
- 203 Lewis, P. H. *Drosophila* new mutants: report of Pamela H. Lewis. *Drosophila Information Service* **21** (1947).
- 204 Lipshitz, H. D. From fruit flies to fallout: Ed Lewis and his science. *J Genet* **83**, 201-218 (2004).
- 205 Beuchle, D., Struhl, G. & Muller, J. Polycomb group proteins and heritable silencing of *Drosophila* Hox genes. *Development* **128**, 993-1004 (2001).
- 206 Bantignies, F. & Cavalli, G. Polycomb group proteins: repression in 3D. *Trends Genet* **27**, 454-464, doi:10.1016/j.tig.2011.06.008 (2011).
- 207 Cavalli, G. Chromosome kissing. *Curr Opin Genet Dev* **17**, 443-450, doi:10.1016/j.gde.2007.08.013 (2007).
- 208 Delest, A., Sexton, T. & Cavalli, G. Polycomb: a paradigm for genome organization from one to three dimensions. *Curr Opin Cell Biol* **24**, 405-414, doi:10.1016/j.ceb.2012.01.008 (2012).
- 209 Cheutin, T. & Cavalli, G. Polycomb silencing: from linear chromatin domains to 3D chromosome folding. *Curr Opin Genet Dev* **25**, 30-37, doi:10.1016/j.gde.2013.11.016 (2014).
- 210 Bantignies, F. *et al.* Polycomb-dependent regulatory contacts between distant Hox loci in *Drosophila*. *Cell* **144**, 214-226, doi:10.1016/j.cell.2010.12.026 (2011).
- 211 Gonzalez, I., Mateos-Langerak, J., Thomas, A., Cheutin, T. & Cavalli, G. Identification of regulators of the three-dimensional polycomb organization by a microscopy-based genome-wide RNAi screen. *Mol Cell* **54**, 485-499, doi:10.1016/j.molcel.2014.03.004 (2014).
- 212 O'Meara, M. M. & Simon, J. A. Inner workings and regulatory inputs that control Polycomb repressive complex 2. *Chromosoma* **121**, 221-234, doi:10.1007/s00412-012-0361-1 (2012).
- 213 Muller, J. & Kassis, J. A. Polycomb response elements and targeting of Polycomb group proteins in *Drosophila*. *Curr Opin Genet Dev* **16**, 476-484, doi:10.1016/j.gde.2006.08.005 (2006).
- 214 Gonzalez, I., Simon, R. & Busturia, A. The Polyhomeotic protein induces hyperplastic tissue overgrowth through the activation of the JAK/STAT pathway. *Cell Cycle* **8**, 4103-4111 (2009).

- 215 Dura, J. M. *et al.* A complex genetic locus, polyhomeotic, is required for segmental specification and epidermal development in *D. melanogaster*. *Cell* **51**, 829-839 (1987).
- 216 Dura, J. M., Brock, H. W. & Santamaria, P. Polyhomeotic: a gene of *Drosophila melanogaster* required for correct expression of segmental identity. *Mol Gen Genet* **198**, 213-220 (1985).
- 217 Gaytan de Ayala Alonso, A. *et al.* A genetic screen identifies novel polycomb group genes in *Drosophila*. *Genetics* **176**, 2099-2108, doi:10.1534/genetics.107.075739 (2007).
- 218 Classen, A. K., Bunker, B. D., Harvey, K. F., Vaccari, T. & Bilder, D. A tumor suppressor activity of *Drosophila* Polycomb genes mediated by JAK-STAT signaling. *Nat Genet* **41**, 1150-1155, doi:10.1038/ng.445 (2009).
- 219 Martinez, A. M. *et al.* Polyhomeotic has a tumor suppressor activity mediated by repression of Notch signaling. *Nat Genet* **41**, 1076-1082, doi:10.1038/ng.414 (2009).
- 220 Feng, S., Huang, J. & Wang, J. Loss of the Polycomb group gene polyhomeotic induces non-autonomous cell overproliferation. *EMBO Rep* **12**, 157-163, doi:10.1038/embor.2010.188 (2011).
- 221 Feng, S., Thomas, S. & Wang, J. Diverse tumor pathology due to distinctive patterns of JAK/STAT pathway activation caused by different *Drosophila* polyhomeotic alleles. *Genetics* **190**, 279-282, doi:10.1534/genetics.111.135442 (2012).
- 222 Kim, C. A., Gingery, M., Pilpa, R. M. & Bowie, J. U. The SAM domain of polyhomeotic forms a helical polymer. *Nat Struct Biol* **9**, 453-457, doi:10.1038/nsb802 (2002).
- 223 Gambetta, M. C., Oktaba, K. & Muller, J. Essential role of the glycosyltransferase *sxc/Ogt* in polycomb repression. *Science* **325**, 93-96, doi:10.1126/science.1169727 (2009).
- 224 Sievers, C. & Paro, R. Polycomb group protein bodybuilding: working out the routines. *Dev Cell* **26**, 556-558, doi:10.1016/j.devcel.2013.09.012 (2013).
- 225 Isono, K. *et al.* SAM domain polymerization links subnuclear clustering of PRC1 to gene silencing. *Dev Cell* **26**, 565-577, doi:10.1016/j.devcel.2013.08.016 (2013).
- 226 Robinson, A. K. *et al.* The growth-suppressive function of the polycomb group protein polyhomeotic is mediated by polymerization of its sterile alpha motif (SAM) domain. *J Biol Chem* **287**, 8702-8713, doi:10.1074/jbc.M111.336115 (2012).
- 227 Brunk, B. P., Martin, E. C. & Adler, P. N. *Drosophila* genes Posterior Sex Combs and Suppressor two of zeste encode proteins with homology to the murine *bmi-1* oncogene. *Nature* **353**, 351-353, doi:10.1038/353351a0 (1991).
- 228 Lo, S. M., Ahuja, N. K. & Francis, N. J. Polycomb group protein Suppressor 2 of zeste is a functional homolog of Posterior Sex Combs. *Mol Cell Biol* **29**, 515-525, doi:10.1128/MCB.01044-08 (2009).
- 229 Deshaies, R. J. & Joazeiro, C. A. RING domain E3 ubiquitin ligases. *Annu Rev Biochem* **78**, 399-434, doi:10.1146/annurev.biochem.78.101807.093809 (2009).
- 230 Mohd-Sarip, A. *et al.* Transcription-independent function of Polycomb group protein PSC in cell cycle control. *Science* **336**, 744-747, doi:10.1126/science.1215927 (2012).
- 231 Breen, T. R. & Duncan, I. M. Maternal expression of genes that regulate the bithorax complex of *Drosophila melanogaster*. *Dev Biol* **118**, 442-456 (1986).

- 232 Bornemann, D., Miller, E. & Simon, J. Expression and properties of wild-type and mutant forms of the *Drosophila* sex comb on midleg (SCM) repressor protein. *Genetics* **150**, 675-686 (1998).
- 233 Grimm, C. *et al.* Structural and functional analyses of methyl-lysine binding by the malignant brain tumour repeat protein Sex comb on midleg. *EMBO Rep* **8**, 1031-1037, doi:10.1038/sj.embor.7401085 (2007).
- 234 Kim, C. A., Sawaya, M. R., Cascio, D., Kim, W. & Bowie, J. U. Structural organization of a Sex-comb-on-midleg/polyhomeotic copolymer. *J Biol Chem* **280**, 27769-27775, doi:10.1074/jbc.M503055200 (2005).
- 235 Peterson, A. J. *et al.* Requirement for sex comb on midleg protein interactions in *Drosophila* polycomb group repression. *Genetics* **167**, 1225-1239, doi:10.1534/genetics.104.027474 (2004).
- 236 Gil, J. & O'Loughlen, A. PRC1 complex diversity: where is it taking us? *Trends Cell Biol*, doi:10.1016/j.tcb.2014.06.005 (2014).
- 237 Zheng, Y. *et al.* A developmental genetic analysis of the lysine demethylase KDM2 mutations in *Drosophila melanogaster*. *Mech Dev* **133**, 36-53, doi:10.1016/j.mod.2014.06.003 (2014).
- 238 Brown, J. L., Fritsch, C., Mueller, J. & Kassis, J. A. The *Drosophila* pho-like gene encodes a YY1-related DNA binding protein that is redundant with pleiohomeotic in homeotic gene silencing. *Development* **130**, 285-294 (2003).
- 239 Mihaly, J., Mishra, R. K. & Karch, F. A conserved sequence motif in Polycomb-response elements. *Mol Cell* **1**, 1065-1066 (1998).
- 240 Oktaba, K. *et al.* Dynamic regulation by polycomb group protein complexes controls pattern formation and the cell cycle in *Drosophila*. *Dev Cell* **15**, 877-889, doi:10.1016/j.devcel.2008.10.005 (2008).
- 241 Fritsch, C., Brown, J. L., Kassis, J. A. & Muller, J. The DNA-binding polycomb group protein pleiohomeotic mediates silencing of a *Drosophila* homeotic gene. *Development* **126**, 3905-3913 (1999).
- 242 Shimell, M. J., Peterson, A. J., Burr, J., Simon, J. A. & O'Connor, M. B. Functional analysis of repressor binding sites in the *iab-2* regulatory region of the abdominal-A homeotic gene. *Dev Biol* **218**, 38-52, doi:10.1006/dbio.1999.9576 (2000).
- 243 Busturia, A. *et al.* The MCP silencer of the *Drosophila* Abd-B gene requires both Pleiohomeotic and GAGA factor for the maintenance of repression. *Development* **128**, 2163-2173 (2001).
- 244 Mishra, R. K. *et al.* The *iab-7* polycomb response element maps to a nucleosome-free region of chromatin and requires both GAGA and pleiohomeotic for silencing activity. *Mol Cell Biol* **21**, 1311-1318, doi:10.1128/MCB.21.4.1311-1318.2001 (2001).
- 245 Mohd-Sarip, A., Venturini, F., Chalkley, G. E. & Verrijzer, C. P. Pleiohomeotic can link polycomb to DNA and mediate transcriptional repression. *Mol Cell Biol* **22**, 7473-7483 (2002).
- 246 Wang, L. *et al.* Hierarchical recruitment of polycomb group silencing complexes. *Mol Cell* **14**, 637-646, doi:10.1016/j.molcel.2004.05.009 (2004).
- 247 Kassis, J. A. & Kennison, J. A. Recruitment of polycomb complexes: a role for SCM. *Mol Cell Biol* **30**, 2581-2583, doi:10.1128/MCB.00231-10 (2010).
- 248 Wang, L. *et al.* Comparative analysis of chromatin binding by Sex Comb on Midleg (SCM) and other polycomb group repressors at a *Drosophila* Hox gene. *Mol Cell Biol* **30**, 2584-2593, doi:10.1128/MCB.01451-09 (2010).

- 249 Klymenko, T. *et al.* A Polycomb group protein complex with sequence-specific DNA-binding and selective methyl-lysine-binding activities. *Genes Dev* **20**, 1110-1122, doi:10.1101/gad.377406 (2006).
- 250 Alfieri, C. *et al.* Structural basis for targeting the chromatin repressor Sfm1b to Polycomb response elements. *Genes Dev* **27**, 2367-2379, doi:10.1101/gad.226621.113 (2013).
- 251 Grimm, C. *et al.* Molecular recognition of histone lysine methylation by the Polycomb group repressor dSfm1b. *Embo J* **28**, 1965-1977, doi:10.1038/emboj.2009.147 (2009).
- 252 Comet, I. & Helin, K. Revolution in the Polycomb hierarchy. *Nat Struct Mol Biol* **21**, 573-575, doi:10.1038/nsmb.2848 (2014).
- 253 Wang, L. *et al.* Alternative ESC and ESC-like subunits of a polycomb group histone methyltransferase complex are differentially deployed during Drosophila development. *Mol Cell Biol* **26**, 2637-2647, doi:10.1128/MCB.26.7.2637-2647.2006 (2006).
- 254 Kurzhals, R. L., Tie, F., Stratton, C. A. & Harte, P. J. Drosophila ESC-like can substitute for ESC and becomes required for Polycomb silencing if ESC is absent. *Dev Biol* **313**, 293-306, doi:10.1016/j.ydbio.2007.10.025 (2008).
- 255 Ohno, K., McCabe, D., Czermin, B., Imhof, A. & Pirrotta, V. ESC, ESCL and their roles in Polycomb Group mechanisms. *Mech Dev* **125**, 527-541, doi:10.1016/j.mod.2008.01.002 (2008).
- 256 Jones, C. A. *et al.* The Drosophila esc and E(z) proteins are direct partners in polycomb group-mediated repression. *Mol Cell Biol* **18**, 2825-2834 (1998).
- 257 Han, Z. *et al.* Structural basis of EZH2 recognition by EED. *Structure* **15**, 1306-1315, doi:10.1016/j.str.2007.08.007 (2007).
- 258 Jones, R. S. & Gelbart, W. M. Genetic analysis of the enhancer of zeste locus and its role in gene regulation in Drosophila melanogaster. *Genetics* **126**, 185-199 (1990).
- 259 Phillips, M. D. & Shearn, A. Mutations in polycomb, a Drosophila polycomb-group gene, cause a wide range of maternal and zygotic phenotypes. *Genetics* **125**, 91-101 (1990).
- 260 Tschiersch, B. *et al.* The protein encoded by the Drosophila position-effect variegation suppressor gene Su(var)3-9 combines domains of antagonistic regulators of homeotic gene complexes. *Embo J* **13**, 3822-3831 (1994).
- 261 Nekrasov, M., Wild, B. & Muller, J. Nucleosome binding and histone methyltransferase activity of Drosophila PRC2. *EMBO Rep* **6**, 348-353, doi:10.1038/sj.embor.7400376 (2005).
- 262 Wu, H. *et al.* Structure of the catalytic domain of EZH2 reveals conformational plasticity in cofactor and substrate binding sites and explains oncogenic mutations. *PLoS One* **8**, e83737, doi:10.1371/journal.pone.0083737 (2013).
- 263 Ciferri, C. *et al.* Molecular architecture of human polycomb repressive complex 2. *Elife* **1**, e00005, doi:10.7554/eLife.00005 (2012).
- 264 Schmitges, F. W. *et al.* Histone methylation by PRC2 is inhibited by active chromatin marks. *Mol Cell* **42**, 330-341, doi:10.1016/j.molcel.2011.03.025 (2011).
- 265 Yuan, W. *et al.* Dense chromatin activates Polycomb repressive complex 2 to regulate H3 lysine 27 methylation. *Science* **337**, 971-975, doi:10.1126/science.1225237 (2012).
- 266 He, A. *et al.* PRC2 directly methylates GATA4 and represses its transcriptional activity. *Genes Dev* **26**, 37-42, doi:10.1101/gad.173930.111 (2012).

- 267 Lee, J. M. *et al.* EZH2 generates a methyl degron that is recognized by the DCAF1/DDB1/CUL4 E3 ubiquitin ligase complex. *Mol Cell* **48**, 572-586, doi:10.1016/j.molcel.2012.09.004 (2012).
- 268 Sneeringer, C. J. *et al.* Coordinated activities of wild-type plus mutant EZH2 drive tumor-associated hypertrimethylation of lysine 27 on histone H3 (H3K27) in human B-cell lymphomas. *Proc Natl Acad Sci U S A* **107**, 20980-20985, doi:10.1073/pnas.1012525107 (2010).
- 269 Chase, A. & Cross, N. C. Aberrations of EZH2 in cancer. *Clin Cancer Res* **17**, 2613-2618, doi:10.1158/1078-0432.CCR-10-2156 (2011).
- 270 Wigle, T. J. *et al.* The Y641C mutation of EZH2 alters substrate specificity for histone H3 lysine 27 methylation states. *FEBS Lett* **585**, 3011-3014, doi:10.1016/j.febslet.2011.08.018 (2011).
- 271 Yap, D. B. *et al.* Somatic mutations at EZH2 Y641 act dominantly through a mechanism of selectively altered PRC2 catalytic activity, to increase H3K27 trimethylation. *Blood* **117**, 2451-2459, doi:10.1182/blood-2010-11-321208 (2011).
- 272 Majer, C. R. *et al.* A687V EZH2 is a gain-of-function mutation found in lymphoma patients. *FEBS Lett* **586**, 3448-3451, doi:10.1016/j.febslet.2012.07.066 (2012).
- 273 McCabe, M. T. *et al.* Mutation of A677 in histone methyltransferase EZH2 in human B-cell lymphoma promotes hypertrimethylation of histone H3 on lysine 27 (H3K27). *Proc Natl Acad Sci U S A* **109**, 2989-2994, doi:10.1073/pnas.1116418109 (2012).
- 274 Ott, H. M. *et al.* A687V EZH2 is a driver of histone H3 lysine 27 (H3K27) hypertrimethylation. *Mol Cancer Ther*, doi:10.1158/1535-7163.MCT-13-0876 (2014).
- 275 Stepanik, V. A. & Harte, P. J. A mutation in the E(Z) methyltransferase that increases trimethylation of histone H3 lysine 27 and causes inappropriate silencing of active Polycomb target genes. *Dev Biol* **364**, 249-258, doi:10.1016/j.ydbio.2011.12.007 (2012).
- 276 Birve, A. *et al.* Su(z)12, a novel Drosophila Polycomb group gene that is conserved in vertebrates and plants. *Development* **128**, 3371-3379 (2001).
- 277 Migliori, V., Mapelli, M. & Guccione, E. On WD40 proteins: propelling our knowledge of transcriptional control? *Epigenetics* **7**, 815-822, doi:10.4161/epi.21140 (2012).
- 278 Suganuma, T., Pattenden, S. G. & Workman, J. L. Diverse functions of WD40 repeat proteins in histone recognition. *Genes Dev* **22**, 1265-1268, doi:10.1101/gad.1676208 (2008).
- 279 Duncan, I. M. Polycomblike: a gene that appears to be required for the normal expression of the bithorax and antennapedia gene complexes of *Drosophila melanogaster*. *Genetics* **102**, 49-70 (1982).
- 280 O'Connell, S. *et al.* Polycomblike PHD fingers mediate conserved interaction with enhancer of zeste protein. *J Biol Chem* **276**, 43065-43073, doi:10.1074/jbc.M104294200 (2001).
- 281 Cao, R. *et al.* Role of hPHF1 in H3K27 methylation and Hox gene silencing. *Mol Cell Biol* **28**, 1862-1872, doi:10.1128/MCB.01589-07 (2008).
- 282 Sarma, K., Margueron, R., Ivanov, A., Pirrotta, V. & Reinberg, D. Ezh2 requires PHF1 to efficiently catalyze H3 lysine 27 trimethylation in vivo. *Mol Cell Biol* **28**, 2718-2731, doi:10.1128/MCB.02017-07 (2008).
- 283 Savla, U., Benes, J., Zhang, J. & Jones, R. S. Recruitment of Drosophila Polycomb-group proteins by Polycomblike, a component of a novel protein complex in larvae. *Development* **135**, 813-817, doi:10.1242/dev.016006 (2008).

- 284 Friberg, A., Oddone, A., Klymenko, T., Muller, J. & Sattler, M. Structure of an atypical Tudor domain in the Drosophila Polycomb-like protein. *Protein Sci* **19**, 1906-1916, doi:10.1002/pro.476 (2010).
- 285 Shen, X. *et al.* Jumonji modulates polycomb activity and self-renewal versus differentiation of stem cells. *Cell* **139**, 1303-1314, doi:10.1016/j.cell.2009.12.003 (2009).
- 286 Peng, J. C. *et al.* Jarid2/Jumonji coordinates control of PRC2 enzymatic activity and target gene occupancy in pluripotent cells. *Cell* **139**, 1290-1302, doi:10.1016/j.cell.2009.12.002 (2009).
- 287 Li, G. *et al.* Jarid2 and PRC2, partners in regulating gene expression. *Genes Dev* **24**, 368-380, doi:10.1101/gad.1886410 (2010).
- 288 Pasini, D. *et al.* JARID2 regulates binding of the Polycomb repressive complex 2 to target genes in ES cells. *Nature* **464**, 306-310, doi:10.1038/nature08788 (2010).
- 289 Landeira, D. *et al.* Jarid2 is a PRC2 component in embryonic stem cells required for multi-lineage differentiation and recruitment of PRC1 and RNA Polymerase II to developmental regulators. *Nat Cell Biol* **12**, 618-624, doi:10.1038/ncb2065 (2010).
- 290 Landeira, D. & Fisher, A. G. Inactive yet indispensable: the tale of Jarid2. *Trends Cell Biol* **21**, 74-80, doi:10.1016/j.tcb.2010.10.004 (2011).
- 291 Son, J., Shen, S. S., Margueron, R. & Reinberg, D. Nucleosome-binding activities within JARID2 and EZH1 regulate the function of PRC2 on chromatin. *Genes Dev* **27**, 2663-2677, doi:10.1101/gad.225888.113 (2013).
- 292 Zhang, Z. *et al.* PRC2 complexes with JARID2, MTF2, and esPRC2p48 in ES cells to modulate ES cell pluripotency and somatic cell reprogramming. *Stem Cells* **29**, 229-240, doi:10.1002/stem.578 (2011).
- 293 Pasini, D., Bracken, A. P., Hansen, J. B., Capillo, M. & Helin, K. The polycomb group protein Suz12 is required for embryonic stem cell differentiation. *Mol Cell Biol* **27**, 3769-3779, doi:10.1128/MCB.01432-06 (2007).
- 294 Chamberlain, S. J., Yee, D. & Magnuson, T. Polycomb repressive complex 2 is dispensable for maintenance of embryonic stem cell pluripotency. *Stem Cells* **26**, 1496-1505, doi:10.1634/stemcells.2008-0102 (2008).
- 295 Shen, X. *et al.* EZH1 mediates methylation on histone H3 lysine 27 and complements EZH2 in maintaining stem cell identity and executing pluripotency. *Mol Cell* **32**, 491-502, doi:10.1016/j.molcel.2008.10.016 (2008).
- 296 Beisel, C. & Paro, R. Silencing chromatin: comparing modes and mechanisms. *Nat Rev Genet* **12**, 123-135, doi:10.1038/nrg2932 (2011).
- 297 Brockdorff, N. Noncoding RNA and Polycomb recruitment. *Rna* **19**, 429-442, doi:10.1261/rna.037598.112 (2013).
- 298 Steffen, P. A. & Ringrose, L. What are memories made of? How Polycomb and Trithorax proteins mediate epigenetic memory. *Nat Rev Mol Cell Biol* **15**, 340-356, doi:10.1038/nrm3789 (2014).
- 299 Kaneko, S. *et al.* Interactions between JARID2 and noncoding RNAs regulate PRC2 recruitment to chromatin. *Mol Cell* **53**, 290-300, doi:10.1016/j.molcel.2013.11.012 (2014).
- 300 Stadtfeld, M. *et al.* Aberrant silencing of imprinted genes on chromosome 12qF1 in mouse induced pluripotent stem cells. *Nature* **465**, 175-181, doi:10.1038/nature09017 (2010).
- 301 da Rocha, S. T., Edwards, C. A., Ito, M., Ogata, T. & Ferguson-Smith, A. C. Genomic imprinting at the mammalian Dlk1-Dio3 domain. *Trends Genet* **24**, 306-316, doi:10.1016/j.tig.2008.03.011 (2008).

- 302 Cifuentes-Rojas, C., Hernandez, A. J., Sarma, K. & Lee, J. T. Regulatory interactions between RNA and polycomb repressive complex 2. *Mol Cell* **55**, 171-185, doi:10.1016/j.molcel.2014.05.009 (2014).
- 303 Herz, H. M. *et al.* Polycomb repressive complex 2-dependent and -independent functions of Jarid2 in transcriptional regulation in *Drosophila*. *Mol Cell Biol* **32**, 1683-1693, doi:10.1128/MCB.06503-11 (2012).
- 304 Cao, R. & Zhang, Y. SUZ12 is required for both the histone methyltransferase activity and the silencing function of the EED-EZH2 complex. *Mol Cell* **15**, 57-67, doi:10.1016/j.molcel.2004.06.020 (2004).
- 305 He, G. P., Kim, S. & Ro, H. S. Cloning and characterization of a novel zinc finger transcriptional repressor. A direct role of the zinc finger motif in repression. *J Biol Chem* **274**, 14678-14684 (1999).
- 306 Kim, H., Kang, K. & Kim, J. AEBP2 as a potential targeting protein for Polycomb Repression Complex PRC2. *Nucleic Acids Res* **37**, 2940-2950, doi:10.1093/nar/gkp149 (2009).
- 307 Culi, J., Aroca, P., Modolell, J. & Mann, R. S. jing is required for wing development and to establish the proximo-distal axis of the leg in *Drosophila melanogaster*. *Genetics* **173**, 255-266, doi:10.1534/genetics.106.056341 (2006).
- 308 Schuettengruber, B. & Cavalli, G. The DUBle life of polycomb complexes. *Dev Cell* **18**, 878-880, doi:10.1016/j.devcel.2010.06.001 (2010).
- 309 Grau, D. J. *et al.* Compaction of chromatin by diverse Polycomb group proteins requires localized regions of high charge. *Genes Dev* **25**, 2210-2221, doi:10.1101/gad.17288211 (2011).
- 310 Lavigne, M., Francis, N. J., King, I. F. & Kingston, R. E. Propagation of silencing; recruitment and repression of naive chromatin in trans by polycomb repressed chromatin. *Mol Cell* **13**, 415-425 (2004).
- 311 Margueron, R. *et al.* Ezh1 and Ezh2 maintain repressive chromatin through different mechanisms. *Mol Cell* **32**, 503-518, doi:10.1016/j.molcel.2008.11.004 (2008).
- 312 Lehmann, L. *et al.* Polycomb repressive complex 1 (PRC1) disassembles RNA polymerase II preinitiation complexes. *J Biol Chem* **287**, 35784-35794, doi:10.1074/jbc.M112.397430 (2012).
- 313 Stock, J. K. *et al.* Ring1-mediated ubiquitination of H2A restrains poised RNA polymerase II at bivalent genes in mouse ES cells. *Nat Cell Biol* **9**, 1428-1435, doi:10.1038/ncb1663 (2007).
- 314 Dellino, G. I. *et al.* Polycomb silencing blocks transcription initiation. *Mol Cell* **13**, 887-893 (2004).
- 315 Chopra, V. S. *et al.* The polycomb group mutant esc leads to augmented levels of paused Pol II in the *Drosophila* embryo. *Mol Cell* **42**, 837-844, doi:10.1016/j.molcel.2011.05.009 (2011).
- 316 Zhou, W. *et al.* Histone H2A monoubiquitination represses transcription by inhibiting RNA polymerase II transcriptional elongation. *Mol Cell* **29**, 69-80, doi:10.1016/j.molcel.2007.11.002 (2008).
- 317 Muller, J. & Verrijzer, P. Biochemical mechanisms of gene regulation by polycomb group protein complexes. *Curr Opin Genet Dev* **19**, 150-158, doi:10.1016/j.gde.2009.03.001 (2009).
- 318 Morey, L. & Helin, K. Polycomb group protein-mediated repression of transcription. *Trends Biochem Sci* **35**, 323-332, doi:10.1016/j.tibs.2010.02.009 (2010).

- 319 Shilatifard, A. Molecular implementation and physiological roles for histone H3 lysine 4 (H3K4) methylation. *Curr Opin Cell Biol* **20**, 341-348, doi:10.1016/j.ceb.2008.03.019 (2008).
- 320 Kim, D. H. *et al.* Histone H3K27 trimethylation inhibits H3 binding and function of SET1-like H3K4 methyltransferase complexes. *Mol Cell Biol* **33**, 4936-4946, doi:10.1128/MCB.00601-13 (2013).
- 321 Sinha, K. M., Yasuda, H., Coombes, M. M., Dent, S. Y. & de Crombrughe, B. Regulation of the osteoblast-specific transcription factor Osterix by NO66, a Jumonji family histone demethylase. *Embo J* **29**, 68-79, doi:10.1038/emboj.2009.332 (2010).
- 322 Pasini, D. *et al.* Coordinated regulation of transcriptional repression by the RBP2 H3K4 demethylase and Polycomb-Repressive Complex 2. *Genes Dev* **22**, 1345-1355, doi:10.1101/gad.470008 (2008).
- 323 Lo, S. M. *et al.* A bridging model for persistence of a polycomb group protein complex through DNA replication in vitro. *Mol Cell* **46**, 784-796, doi:10.1016/j.molcel.2012.05.038 (2012).
- 324 Eskeland, R. *et al.* Ring1B compacts chromatin structure and represses gene expression independent of histone ubiquitination. *Mol Cell* **38**, 452-464, doi:10.1016/j.molcel.2010.02.032 (2010).
- 325 Jason, L. J., Finn, R. M., Lindsey, G. & Ausio, J. Histone H2A ubiquitination does not preclude histone H1 binding, but it facilitates its association with the nucleosome. *J Biol Chem* **280**, 4975-4982, doi:10.1074/jbc.M410203200 (2005).
- 326 Kassis, J. A. Pairing-sensitive silencing, polycomb group response elements, and transposon homing in *Drosophila*. *Adv Genet* **46**, 421-438 (2002).
- 327 Kassis, J. A. & Brown, J. L. Polycomb group response elements in *Drosophila* and vertebrates. *Adv Genet* **81**, 83-118, doi:10.1016/B978-0-12-407677-8.00003-8 (2013).
- 328 Bantignies, F., Grimaud, C., Lavrov, S., Gabut, M. & Cavalli, G. Inheritance of Polycomb-dependent chromosomal interactions in *Drosophila*. *Genes Dev* **17**, 2406-2420, doi:10.1101/gad.269503 (2003).
- 329 Kyrchanova, O., Toshchakov, S., Podstreshnaya, Y., Parshikov, A. & Georgiev, P. Functional interaction between the Fab-7 and Fab-8 boundaries and the upstream promoter region in the *Drosophila* Abd-B gene. *Mol Cell Biol* **28**, 4188-4195, doi:10.1128/MCB.00229-08 (2008).
- 330 Cleard, F., Moshkin, Y., Karch, F. & Maeda, R. K. Probing long-distance regulatory interactions in the *Drosophila melanogaster* bithorax complex using Dam identification. *Nat Genet* **38**, 931-935, doi:10.1038/ng1833 (2006).
- 331 Lanzuolo, C., Roure, V., Dekker, J., Bantignies, F. & Orlando, V. Polycomb response elements mediate the formation of chromosome higher-order structures in the bithorax complex. *Nat Cell Biol* **9**, 1167-1174, doi:10.1038/ncb1637 (2007).
- 332 Sexton, T. *et al.* Three-dimensional folding and functional organization principles of the *Drosophila* genome. *Cell* **148**, 458-472, doi:10.1016/j.cell.2012.01.010 (2012).
- 333 Ghavi-Helm, Y. *et al.* Enhancer loops appear stable during development and are associated with paused polymerase. *Nature* **512**, 96-100, doi:10.1038/nature13417 (2014).
- 334 Grimaud, C. *et al.* RNAi components are required for nuclear clustering of Polycomb group response elements. *Cell* **124**, 957-971, doi:10.1016/j.cell.2006.01.036 (2006).

- 335 Arzate-Mejia, R. G., Valle-Garcia, D. & Recillas-Targa, F. Signaling epigenetics: novel insights on cell signaling and epigenetic regulation. *IUBMB Life* **63**, 881-895, doi:10.1002/iub.557 (2011).
- 336 Schwartz, Y. B. & Pirrotta, V. A new world of Polycombs: unexpected partnerships and emerging functions. *Nat Rev Genet* **14**, 853-864, doi:10.1038/nrg3603 (2013).
- 337 Sawarkar, R. & Paro, R. Interpretation of developmental signaling at chromatin: the Polycomb perspective. *Dev Cell* **19**, 651-661, doi:10.1016/j.devcel.2010.10.012 (2010).
- 338 Richly, H. & Di Croce, L. The flip side of the coin: role of ZRF1 and histone H2A ubiquitination in transcriptional activation. *Cell Cycle* **10**, 745-750 (2011).
- 339 Richly, H. *et al.* Transcriptional activation of polycomb-repressed genes by ZRF1. *Nature* **468**, 1124-1128, doi:10.1038/nature09574 (2010).
- 340 Fischle, W., Wang, Y. & Allis, C. D. Binary switches and modification cassettes in histone biology and beyond. *Nature* **425**, 475-479, doi:10.1038/nature02017 (2003).
- 341 Stojic, L. *et al.* Chromatin regulated interchange between polycomb repressive complex 2 (PRC2)-Ezh2 and PRC2-Ezh1 complexes controls myogenin activation in skeletal muscle cells. *Epigenetics Chromatin* **4**, 16, doi:10.1186/1756-8935-4-16 (2011).
- 342 Kruidenier, L. *et al.* A selective jumonji H3K27 demethylase inhibitor modulates the proinflammatory macrophage response. *Nature* **488**, 404-408, doi:10.1038/nature11262 (2012).
- 343 Sengoku, T. & Yokoyama, S. Structural basis for histone H3 Lys 27 demethylation by UTX/KDM6A. *Genes Dev* **25**, 2266-2277, doi:10.1101/gad.172296.111 (2011).
- 344 Fonseca, J. P. *et al.* In vivo Polycomb kinetics and mitotic chromatin binding distinguish stem cells from differentiated cells. *Genes Dev* **26**, 857-871, doi:10.1101/gad.184648.111 (2012).
- 345 Frangini, A. *et al.* The aurora B kinase and the polycomb protein ring1B combine to regulate active promoters in quiescent lymphocytes. *Mol Cell* **51**, 647-661, doi:10.1016/j.molcel.2013.08.022 (2013).
- 346 Mansour, A. A. *et al.* The H3K27 demethylase Utx regulates somatic and germ cell epigenetic reprogramming. *Nature* **488**, 409-413, doi:10.1038/nature11272 (2012).
- 347 Shpargel, K. B., Starmer, J., Yee, D., Pohlars, M. & Magnuson, T. KDM6 demethylase independent loss of histone H3 lysine 27 trimethylation during early embryonic development. *PLoS Genet* **10**, e1004507, doi:10.1371/journal.pgen.1004507 (2014).
- 348 Yang, W. *et al.* The histone H2A deubiquitinase Usp16 regulates embryonic stem cell gene expression and lineage commitment. *Nat Commun* **5**, 3818, doi:10.1038/ncomms4818 (2014).
- 349 Zhao, J. C. *et al.* Cooperation between Polycomb and androgen receptor during oncogenic transformation. *Genome Res* **22**, 322-331, doi:10.1101/gr.131508.111 (2012).
- 350 Zhu, P. *et al.* A histone H2A deubiquitinase complex coordinating histone acetylation and H1 dissociation in transcriptional regulation. *Mol Cell* **27**, 609-621, doi:10.1016/j.molcel.2007.07.024 (2007).
- 351 McGinty, R. K., Henrici, R. C. & Tan, S. Crystal structure of the PRC1 ubiquitylation module bound to the nucleosome. *Nature* **514**, 591-596, doi:10.1038/nature13890 (2014).
- 352 Yuan, W. *et al.* H3K36 methylation antagonizes PRC2-mediated H3K27 methylation. *J Biol Chem* **286**, 7983-7989, doi:10.1074/jbc.M110.194027 (2011).

- 353 Nowak, A. J. *et al.* Chromatin-modifying complex component Nurf55/p55 associates with histones H3 and H4 and polycomb repressive complex 2 subunit Su(z)12 through partially overlapping binding sites. *J Biol Chem* **286**, 23388-23396, doi:10.1074/jbc.M110.207407 (2011).
- 354 Rai, A. N. *et al.* Elements of the polycomb repressor SU(Z)12 needed for histone H3-K27 methylation, the interface with E(Z), and in vivo function. *Mol Cell Biol* **33**, 4844-4856, doi:10.1128/MCB.00307-13 (2013).
- 355 McKittrick, E., Gafken, P. R., Ahmad, K. & Henikoff, S. Histone H3.3 is enriched in covalent modifications associated with active chromatin. *Proc Natl Acad Sci U S A* **101**, 1525-1530, doi:10.1073/pnas.0308092100 (2004).
- 356 Klose, R. J., Cooper, S., Farcas, A. M., Blackledge, N. P. & Brockdorff, N. Chromatin sampling--an emerging perspective on targeting polycomb repressor proteins. *PLoS Genet* **9**, e1003717, doi:10.1371/journal.pgen.1003717 (2013).
- 357 Reddington, J. P. *et al.* Redistribution of H3K27me3 upon DNA hypomethylation results in de-repression of Polycomb target genes. *Genome Biol* **14**, R25, doi:10.1186/gb-2013-14-3-r25 (2013).
- 358 Davidovich, C., Zheng, L., Goodrich, K. J. & Cech, T. R. Promiscuous RNA binding by Polycomb repressive complex 2. *Nat Struct Mol Biol* **20**, 1250-1257, doi:10.1038/nsmb.2679 (2013).
- 359 Kaneko, S., Son, J., Shen, S. S., Reinberg, D. & Bonasio, R. PRC2 binds active promoters and contacts nascent RNAs in embryonic stem cells. *Nat Struct Mol Biol* **20**, 1258-1264, doi:10.1038/nsmb.2700 (2013).
- 360 Herzog, V. A. *et al.* A strand-specific switch in noncoding transcription switches the function of a Polycomb/Trithorax response element. *Nat Genet* **46**, 973-981, doi:10.1038/ng.3058 (2014).
- 361 Riising, E. M. *et al.* Gene silencing triggers polycomb repressive complex 2 recruitment to CpG islands genome wide. *Mol Cell* **55**, 347-360, doi:10.1016/j.molcel.2014.06.005 (2014).
- 362 Petruk, S. *et al.* TrxG and PcG proteins but not methylated histones remain associated with DNA through replication. *Cell* **150**, 922-933, doi:10.1016/j.cell.2012.06.046 (2012).
- 363 Campos, E. I., Stafford, J. M. & Reinberg, D. Epigenetic inheritance: histone bookmarks across generations. *Trends Cell Biol*, doi:10.1016/j.tcb.2014.08.004 (2014).
- 364 Lanzuolo, C. & Orlando, V. Memories from the polycomb group proteins. *Annu Rev Genet* **46**, 561-589, doi:10.1146/annurev-genet-110711-155603 (2012).
- 365 Huang, C., Xu, M. & Zhu, B. Epigenetic inheritance mediated by histone lysine methylation: maintaining transcriptional states without the precise restoration of marks? *Philos Trans R Soc Lond B Biol Sci* **368**, 20110332, doi:10.1098/rstb.2011.0332 (2013).
- 366 Budhavarapu, V. N., Chavez, M. & Tyler, J. K. How is epigenetic information maintained through DNA replication? *Epigenetics Chromatin* **6**, 32, doi:10.1186/1756-8935-6-32 (2013).
- 367 Alabert, C. & Groth, A. Chromatin replication and epigenome maintenance. *Nat Rev Mol Cell Biol* **13**, 153-167, doi:10.1038/nrm3288 (2012).
- 368 Margueron, R. & Reinberg, D. Chromatin structure and the inheritance of epigenetic information. *Nat Rev Genet* **11**, 285-296, doi:10.1038/nrg2752 (2010).
- 369 Francis, N. J., Follmer, N. E., Simon, M. D., Aghia, G. & Butler, J. D. Polycomb proteins remain bound to chromatin and DNA during DNA replication in vitro. *Cell* **137**, 110-122, doi:10.1016/j.cell.2009.02.017 (2009).

- 370 Lengsfeld, B. M., Berry, K. N., Ghosh, S., Takahashi, M. & Francis, N. J. A Polycomb complex remains bound through DNA replication in the absence of other eukaryotic proteins. *Sci Rep* **2**, 661, doi:10.1038/srep00661 (2012).
- 371 Alabert, C. *et al.* Nascent chromatin capture proteomics determines chromatin dynamics during DNA replication and identifies unknown fork components. *Nat Cell Biol* **16**, 281-293, doi:10.1038/ncb2918 (2014).
- 372 Lanzuolo, C., Lo Sardo, F. & Orlando, V. Concerted epigenetic signatures inheritance at PcG targets through replication. *Cell Cycle* **11**, 1296-1300, doi:10.4161/cc.19710 (2012).
- 373 Lanzuolo, C., Lo Sardo, F., Diamantini, A. & Orlando, V. PcG complexes set the stage for epigenetic inheritance of gene silencing in early S phase before replication. *PLoS Genet* **7**, e1002370, doi:10.1371/journal.pgen.1002370 (2011).
- 374 Xu, M., Chen, S. & Zhu, B. Investigating the cell cycle-associated dynamics of histone modifications using quantitative mass spectrometry. *Methods Enzymol* **512**, 29-55, doi:10.1016/B978-0-12-391940-3.00002-0 (2012).
- 375 Xu, M., Wang, W., Chen, S. & Zhu, B. A model for mitotic inheritance of histone lysine methylation. *EMBO Rep* **13**, 60-67, doi:10.1038/embor.2011.206 (2012).
- 376 Tan, J. Z., Yan, Y., Wang, X. X., Jiang, Y. & Xu, H. E. EZH2: biology, disease, and structure-based drug discovery. *Acta Pharmacol Sin* **35**, 161-174, doi:10.1038/aps.2013.161 (2014).
- 377 Parsons, G. G. & Spencer, C. A. Mitotic repression of RNA polymerase II transcription is accompanied by release of transcription elongation complexes. *Mol Cell Biol* **17**, 5791-5802 (1997).
- 378 Klein, J. & Grummt, I. Cell cycle-dependent regulation of RNA polymerase I transcription: the nucleolar transcription factor UBF is inactive in mitosis and early G1. *Proc Natl Acad Sci U S A* **96**, 6096-6101 (1999).
- 379 Clemente-Blanco, A. *et al.* Cdc14 inhibits transcription by RNA polymerase I during anaphase. *Nature* **458**, 219-222, doi:10.1038/nature07652 (2009).
- 380 Kelly, T. K. & Jones, P. A. Role of nucleosomes in mitotic bookmarking. *Cell Cycle* **10**, 370-371 (2011).
- 381 Kelly, T. K. *et al.* H2A.Z maintenance during mitosis reveals nucleosome shifting on mitotically silenced genes. *Mol Cell* **39**, 901-911, doi:10.1016/j.molcel.2010.08.026 (2010).
- 382 Zaidi, S. K. *et al.* Mitotic bookmarking of genes: a novel dimension to epigenetic control. *Nat Rev Genet* **11**, 583-589, doi:10.1038/nrg2827 (2010).
- 383 Kadauke, S. & Blobel, G. A. Mitotic bookmarking by transcription factors. *Epigenetics Chromatin* **6**, 6, doi:10.1186/1756-8935-6-6 (2013).
- 384 Zaret, K. S. Genome reactivation after the silence in mitosis: recapitulating mechanisms of development? *Dev Cell* **29**, 132-134, doi:10.1016/j.devcel.2014.04.019 (2014).
- 385 Martinez-Balbas, M. A., Dey, A., Rabindran, S. K., Ozato, K. & Wu, C. Displacement of sequence-specific transcription factors from mitotic chromatin. *Cell* **83**, 29-38 (1995).
- 386 Kadauke, S. & Blobel, G. A. "Remembering" tissue-specific transcription patterns through mitosis. *Cell Cycle* **11**, 3911-3912, doi:10.4161/cc.22237 (2012).
- 387 Kadauke, S. *et al.* Tissue-specific mitotic bookmarking by hematopoietic transcription factor GATA1. *Cell* **150**, 725-737, doi:10.1016/j.cell.2012.06.038 (2012).

- 388 Zhao, R., Nakamura, T., Fu, Y., Lazar, Z. & Spector, D. L. Gene bookmarking accelerates the kinetics of post-mitotic transcriptional re-activation. *Nat Cell Biol* **13**, 1295-1304, doi:10.1038/ncb2341 (2011).
- 389 Follmer, N. E. & Francis, N. J. Speed reading for genes: bookmarks set the pace. *Dev Cell* **21**, 807-808, doi:10.1016/j.devcel.2011.10.020 (2011).
- 390 Dey, A., Nishiyama, A., Karpova, T., McNally, J. & Ozato, K. Brd4 marks select genes on mitotic chromatin and directs postmitotic transcription. *Mol Biol Cell* **20**, 4899-4909, doi:10.1091/mbc.E09-05-0380 (2009).
- 391 Blobel, G. A. *et al.* A reconfigured pattern of MLL occupancy within mitotic chromatin promotes rapid transcriptional reactivation following mitotic exit. *Mol Cell* **36**, 970-983, doi:10.1016/j.molcel.2009.12.001 (2009).
- 392 Xing, H., Vanderford, N. L. & Sarge, K. D. The TBP-PP2A mitotic complex bookmarks genes by preventing condensin action. *Nat Cell Biol* **10**, 1318-1323, doi:10.1038/ncb1790 (2008).
- 393 Sarge, K. D. & Park-Sarge, O. K. Mitotic bookmarking of formerly active genes: keeping epigenetic memories from fading. *Cell Cycle* **8**, 818-823 (2009).
- 394 Yan, J. *et al.* Transcription factor binding in human cells occurs in dense clusters formed around cohesin anchor sites. *Cell* **154**, 801-813, doi:10.1016/j.cell.2013.07.034 (2013).
- 395 Blobel, G. A. & Hardison, R. C. A cluster to remember. *Cell* **154**, 718-720, doi:10.1016/j.cell.2013.07.041 (2013).
- 396 Wang, X. & Dai, W. Shugoshin, a guardian for sister chromatid segregation. *Exp Cell Res* **310**, 1-9, doi:10.1016/j.yexcr.2005.07.018 (2005).
- 397 Caravaca, J. M. *et al.* Bookmarking by specific and nonspecific binding of FoxA1 pioneer factor to mitotic chromosomes. *Genes Dev* **27**, 251-260, doi:10.1101/gad.206458.112 (2013).
- 398 Buchenau, P., Hodgson, J., Strutt, H. & Arndt-Jovin, D. J. The distribution of polycomb-group proteins during cell division and development in *Drosophila* embryos: impact on models for silencing. *J Cell Biol* **141**, 469-481 (1998).
- 399 Follmer, N. E., Wani, A. H. & Francis, N. J. A polycomb group protein is retained at specific sites on chromatin in mitosis. *PLoS Genet* **8**, e1003135, doi:10.1371/journal.pgen.1003135 (2012).
- 400 Fanti, L. *et al.* The trithorax group and Pc group proteins are differentially involved in heterochromatin formation in *Drosophila*. *Chromosoma* **117**, 25-39, doi:10.1007/s00412-007-0123-7 (2008).
- 401 Dietzel, S., Niemann, H., Bruckner, B., Maurange, C. & Paro, R. The nuclear distribution of Polycomb during *Drosophila melanogaster* development shown with a GFP fusion protein. *Chromosoma* **108**, 83-94 (1999).
- 402 Steffen, P. A. *et al.* Quantitative in vivo analysis of chromatin binding of Polycomb and Trithorax group proteins reveals retention of ASH1 on mitotic chromatin. *Nucleic Acids Res* **41**, 5235-5250, doi:10.1093/nar/gkt217 (2013).
- 403 Zhen, C. Y., Duc, H. N., Kokotovic, M., Phiel, C. J. & Ren, X. Cbx2 stably associates with mitotic chromosomes via a PRC2 or PRC1-independent mechanism and is needed for recruiting PRC1 complex to mitotic chromosomes. *Mol Biol Cell*, doi:10.1091/mbc.E14-06-1109 (2014).
- 404 Campbell, A. E., Hsiung, C. C. & Blobel, G. A. Comparative analysis of mitosis-specific antibodies for bulk purification of mitotic populations by fluorescence-activated cell sorting. *Biotechniques* **56**, 90-91, 93-94, doi:10.2144/000114137 (2014).

- 405 Ong, C. T. & Corces, V. G. CTCF: an architectural protein bridging genome
topology and function. *Nat Rev Genet* **15**, 234-246, doi:10.1038/nrg3663 (2014).
- 406 Bischof, J., Maeda, R. K., Hediger, M., Karch, F. & Basler, K. An optimized
transgenesis system for *Drosophila* using germ-line-specific phiC31 integrases.
Proc Natl Acad Sci U S A **104**, 3312-3317, doi:10.1073/pnas.0611511104 (2007).
- 407 Sawicka, A. *et al.* H3S28 phosphorylation is a hallmark of the transcriptional
response to cellular stress. *Genome Res* **24**, 1808-1820, doi:10.1101/gr.176255.114
(2014).
- 408 Abzhanov, A., Holtzman, S. & Kaufman, T. C. The *Drosophila* proboscis is
specified by two Hox genes, proboscipedia and Sex combs reduced, via repression
of leg and antennal appendage genes. *Development* **128**, 2803-2814 (2001).
- 409 Pattatucci, A. M. & Kaufman, T. C. The homeotic gene Sex combs reduced of
Drosophila melanogaster is differentially regulated in the embryonic and imaginal
stages of development. *Genetics* **129**, 443-461 (1991).
- 410 Yao, L. C., Liaw, G. J., Pai, C. Y. & Sun, Y. H. A common mechanism for
antenna-to-Leg transformation in *Drosophila*: suppression of homothorax
transcription by four HOM-C genes. *Dev Biol* **211**, 268-276,
doi:10.1006/dbio.1999.9309 (1999).
- 411 Antonysamy, S. *et al.* Structural context of disease-associated mutations and
putative mechanism of autoinhibition revealed by X-ray crystallographic analysis
of the EZH2-SET domain. *PLoS One* **8**, e84147, doi:10.1371/journal.pone.0084147
(2013).
- 412 Cheutin, T. & Cavalli, G. Progressive polycomb assembly on H3K27me3
compartments generates polycomb bodies with developmentally regulated motion.
PLoS Genet **8**, e1002465, doi:10.1371/journal.pgen.1002465 (2012).
- 413 Duboule, D. & Morata, G. Colinearity and functional hierarchy among genes of the
homeotic complexes. *Trends Genet* **10**, 358-364 (1994).
- 414 White, A. E., Leslie, M. E., Calvi, B. R., Marzluff, W. F. & Duronio, R. J.
Developmental and cell cycle regulation of the *Drosophila* histone locus body. *Mol
Biol Cell* **18**, 2491-2502, doi:10.1091/mbc.E06-11-1033 (2007).
- 415 Bulchand, S., Menon, S. D., George, S. E. & Chia, W. Muscle wasted: a novel
component of the *Drosophila* histone locus body required for muscle integrity. *J
Cell Sci* **123**, 2697-2707, doi:10.1242/jcs.063172 (2010).
- 416 Godfrey, A. C., White, A. E., Tatomer, D. C., Marzluff, W. F. & Duronio, R. J. The
Drosophila U7 snRNP proteins Lsm10 and Lsm11 are required for histone pre-
mRNA processing and play an essential role in development. *Rna* **15**, 1661-1672,
doi:10.1261/rna.1518009 (2009).
- 417 Ito, S. *et al.* Epigenetic silencing of core histone genes by HERS in *Drosophila*.
Mol Cell **45**, 494-504, doi:10.1016/j.molcel.2011.12.029 (2012).
- 418 Naumova, N. *et al.* Organization of the mitotic chromosome. *Science* **342**, 948-953,
doi:10.1126/science.1236083 (2013).
- 419 Dekker, J. Two ways to fold the genome during the cell cycle: insights obtained
with chromosome conformation capture. *Epigenetics Chromatin* **7**, 25,
doi:10.1186/1756-8935-7-25 (2014).
- 420 Mathieu, J. *et al.* Aurora B and cyclin B have opposite effects on the timing of
cytokinesis abscission in *Drosophila* germ cells and in vertebrate somatic cells. *Dev
Cell* **26**, 250-265, doi:10.1016/j.devcel.2013.07.005 (2013).
- 421 Varier, R. A. *et al.* A phospho/methyl switch at histone H3 regulates TFIID
association with mitotic chromosomes. *Embo J* **29**, 3967-3978,
doi:10.1038/emboj.2010.261 (2010).

- 422 Lemak, A. *et al.* Solution NMR structure and histone binding of the PHD domain of human MLL5. *PLoS One* **8**, e77020, doi:10.1371/journal.pone.0077020 (2013).
- 423 Wolff, T. Preparation of Drosophila eye specimens for scanning electron microscopy. *Cold Spring Harb Protoc* **2011**, 1383-1385, doi:10.1101/pdb.prot066506 (2011).
- 424 Luger, K., Rechsteiner, T. J. & Richmond, T. J. Expression and purification of recombinant histones and nucleosome reconstitution. *Methods Mol Biol* **119**, 1-16, doi:10.1385/1-59259-681-9:1 (1999).
- 425 Munari, F. *et al.* Methylation of lysine 9 in histone H3 directs alternative modes of highly dynamic interaction of heterochromatin protein hHP1beta with the nucleosome. *J Biol Chem* **287**, 33756-33765, doi:10.1074/jbc.M112.390849 (2012).

Appendix I

Accepted Manuscript in *Cell Reports*:

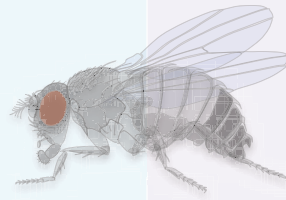
**” Histone H3 Serine 28 is essential for efficient
Polycomb-mediated gene repression in *Drosophila* ”**

Cell Reports

Histone H3 Serine 28 is essential for efficient Polycomb-mediated gene repression in *Drosophila*

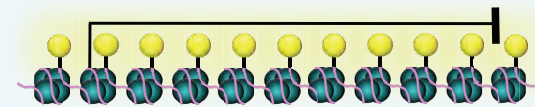
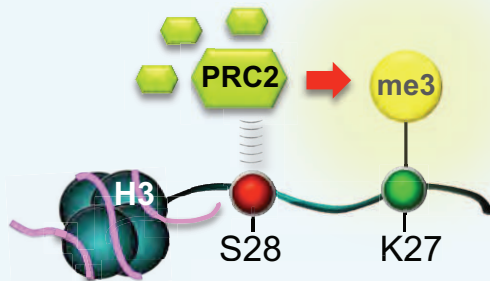
--Manuscript Draft--

Manuscript Number:	CELL-REPORTS-D-15-00635R1
Full Title:	Histone H3 Serine 28 is essential for efficient Polycomb-mediated gene repression in <i>Drosophila</i>
Article Type:	Research Article
Keywords:	Histone, H3S28, Polycomb, <i>Drosophila</i> , phosphorylation, development
Corresponding Author:	Giacomo Cavalli Centre National de la Recherche Scientifique Montpellier, Cedex 5 FRANCE
First Author:	Philip Yuk Kwong Yung, PhD
Order of Authors:	Philip Yuk Kwong Yung, PhD Alexandra Stuetzer, PhD Wolfgang Fischle, PhD Anne-Marie Martinez, PhD Giacomo Cavalli
Abstract:	<p>Trimethylation at histone H3K27 is central to the polycomb repression system. Juxtaposed to H3K27 is a widely conserved phosphorylatable serine residue (H3S28) whose function is unclear. To assess the importance of H3S28, we generated a <i>Drosophila</i> H3 histone mutant with a Serine to Alanine mutation at position 28. H3S28A mutant cells lack H3S28ph on mitotic chromosomes but support normal mitosis. Strikingly, all methylation states of H3K27 drop in H3S28A cells, leading to Hox gene derepression and to homeotic transformations in adult tissues. These defects are not caused by active H3K27 demethylation nor the loss of H3S28ph. Biochemical assays show that H3S28A nucleosomes are a suboptimal substrate for PRC2, suggesting that the unphosphorylated state of Serine 28 is important to assist the function of Polycomb complexes. Collectively, our data indicate that the conserved H3S28 residue in metazoans have a role in supporting PRC2 catalysis</p>



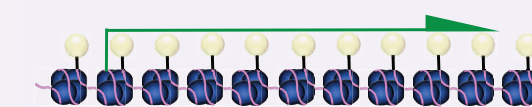
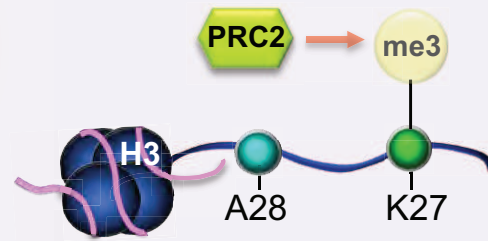
Drosophila histone mutant model

Wild type Histone H3
Robust deposition of H3K27me3



- Efficient Gene Repression
- Normal development

H3S28A mutation
Crippled catalysis of H3K27me3



- Derepression of PcG targets
- Homeotic transformation

**Histone H3 Serine 28 is essential for efficient Polycomb-mediated gene repression in
*Drosophila***

Philip Yuk Kwong Yung^a, Alexandra Stuetzer^b, Wolfgang Fischle^{b,1}, Anne-Marie
Martinez^{a,c,1}, and Giacomo Cavalli^{a,1}

^a Institute of Human Genetics, UPR1142 CNRS, 141 Rue de la Cardonille, 34396,
Montpellier Cedex 5, France.

^b Laboratory of Chromatin Biochemistry, Max Planck Institute for Biophysical Chemistry,
Am Fassberg 11, 37077 Göttingen, Germany.

^c Université de Montpellier, Place Eugène Bataillon, 34095 Montpellier Cedex 5, France

¹Correspondence should be addressed to Giacomo.Cavalli@igh.cnrs.fr, Anne-Marie.Martinez@igh.cnrs.fr or to wfischl@gwdg.de

Keywords: Polycomb, Histone, Chromatin, Epigenetics.

Short title: Essential role of H3S28 in Polycomb silencing

Summary

Trimethylation at histone H3K27 is central to the polycomb repression system. Juxtaposed to H3K27 is a widely conserved phosphorylatable serine residue (H3S28) whose function is unclear. To assess the importance of H3S28, we generated a *Drosophila* H3 histone mutant with a Serine to Alanine mutation at position 28. *H3S28A* mutant cells lack H3S28ph on mitotic chromosomes but support normal mitosis. Strikingly, all methylation states of H3K27 drop in *H3S28A* cells, leading to Hox gene derepression and to homeotic transformations in adult tissues. These defects are not caused by active H3K27 demethylation nor by the loss of H3S28ph. Biochemical assays show that H3S28A nucleosomes are a suboptimal substrate for PRC2, suggesting that the unphosphorylated state of Serine 28 is important to assist the function of Polycomb complexes. Collectively, our data indicate that the conserved H3S28 residue in metazoans have a role in supporting PRC2 catalysis.

Highlights

- *Drosophila H3S28A* mutation supports normal mitosis despite the lack of H3S28ph
- *H3S28A* mutant shows reduced H3K27 methylation and compromises Polycomb silencing
- *H3S28A* defects are not caused by active H3K27 demethylation nor by loss of H3S28ph
- H3S28A reduces the ability of PRC2 to methylate H3K27 on nucleosomal substrates

Introduction

Polycomb group (PcG) proteins are epigenetic regulators essential for repression of key developmental genes. Canonical targets of PcG proteins include the Hox genes, which specify the identities of body segments along the anterior to posterior axis. PcG mutants fail to maintain repressive chromatin states, leading to derepression of Hox genes and to homeotic transformations (Di Croce and Helin, 2013; Grossniklaus and Paro, 2014; Margueron and Reinberg, 2011; Schuettengruber et al., 2007; Simon and Kingston, 2013). *Drosophila* PcG proteins assemble into at least five different multiprotein complexes, namely Polycomb Repressive Complex 1 (PRC1) (Shao et al., 1999), PRC2 (Cao et al., 2002; Czermin et al., 2002; Kuzmichev et al., 2002; Muller et al., 2002), Pho-Repressive Complex (Pho-RC) (Klymenko et al., 2006), dRing Associated Factor (dRAF) (Lagarou et al., 2008) and Polycomb Repressive Deubiquitinase (PR-DUB) (Scheuermann et al., 2010). Enhancer of zeste, E(z), the catalytic subunit of PRC2 methylates the lysine 27 residue of histone H3 (H3K27me) on target chromatin regions. dRing is an active E3 ligase subunit in dRAF that monoubiquitinates nucleosomal H2A. In the canonical model, H3K27me₃-binding by the chromodomain of polycomb (Pc) helps to recruit PRC1 to target genes (Cao et al., 2002; Fischle et al., 2003; Kuzmichev et al., 2002; Min et al., 2003). Recent studies suggest an alternative recruitment hierarchy whereby H2Aub initiates PRC2 chromatin targeting and the establishment of H3K27me₃ domains (Blackledge et al., 2014; Cooper et al., 2014; Kalb et al., 2014).

The local chromatin environment modulates the repressive functionality of PcG complexes (Muller and Verrijzer, 2009; O'Meara and Simon, 2012). For example, both H3K27me₃ (Margueron et al., 2009) and H2Aub (Kalb et al., 2014) stimulate PRC2 activity, whereas active histone marks such as H3K4me₃ and H3K36me₃ (Schmitges et al., 2011) inhibit its function. Notably, the serine residue juxtaposed to H3K27, H3S28, is widely conserved

and present in every species that has a canonical PRC2-dependent silencing system (Figure S1A). In contrast, it is absent in species like fission yeast that do not possess PRC2. H3S28 is mainly phosphorylated during mitosis (Giet and Glover, 2001), but whether this mitotic phosphorylation is required for mitosis in metazoans is unknown. Interphase H3S28ph has also been detected in mammals, where it was shown to counteract mammalian PRC1 and PRC2 chromatin binding. This mark derepresses PcG target genes in response to stress and developmental signaling (Gehani et al., 2010; Lau and Cheung, 2011) and activates stress response genes via displacement of HDAC corepressor complexes (Sawicka et al., 2014). However, biochemical studies showed that H3K27me3S28ph is refractory to demethylation by UTX (Sengoku and Yokoyama, 2011) and JMJD3 (Kruidenier et al., 2012). Hence, on one hand H3S28ph might evict PcG proteins and on the other hand it might preserve H3K27me3. H3S28ph is established by the mitotic Aurora B kinase and, like H3S10ph, it is highly enriched during the course of mitosis (Giet and Glover, 2001). As such, H3S28ph might play a role in PcG repression and epigenetic inheritance. However, whether this is the only function of H3S28 remains unknown. In particular, the putative *in vivo* function of its non-phosphorylated state has not been investigated.

To assess the importance of the highly conserved H3S28 residue and to investigate the physiological relevance of mitotic H3S28ph in modulating PcG repression, we have established an *in vivo Drosophila* model where the endogenous source of histone H3 is replaced by a non-phosphorylatable serine 28 to alanine mutation. Surprisingly, this mutation did not significantly affect mitosis. However, methylation of H3K27 was severely impaired and Polycomb-mediated silencing of Hox genes was partially lost, resulting in homeotic transformations in the adults. The deregulation of PcG silencing associated with *H3S28A* mutation is independent of active demethylation and cannot be recapitulated upon the loss of Aurora B kinase. These observations are consistent with in

in vitro experiments showing that PRC2 activity is impaired upon H3 Serine to Alanine mutation at position 28 (*H3S28A*). Collectively, our data suggest that one main function of H3S28 is to support Polycomb-mediated silencing via PRC2-dependent methylation of H3K27.

Results

All H3K27 methylation states are reduced in the *H3S28A* mutant

In the *Drosophila* genome, canonical core and linker histones are encoded by the histone gene unit (HisGU), which is organized as a multicopy gene array residing at a single locus known as the histone gene cluster (*HisC*). Previous studies showed that embryos carrying homozygous *HisC* deletion (Δ *HisC*) die in late blastoderm, after exhaustion of maternally deposited histone reserves (Gunesdogan et al., 2010; McKay et al., 2015). A histone replacement genetic platform has been developed based on the fact that reintroduction of a minimum of 12 copies of wild-type transgenic HisGU is sufficient to rescue lethality of the Δ *HisC* mutant. Likewise, HisGU carrying different point mutations can be introduced in this system to study the biological functions of specific histone residues and modifications thereof (Gunesdogan et al., 2010). In a previous study a *H3K27R* mutant was analyzed (McKay et al., 2015; Pengelly et al., 2013). It was reported that the limited number of cell divisions during late embryogenesis was not sufficient to completely replace wild-type, chromatinized maternal histones, resulting in chromatin with a mixture of wild-type and mutant histones. To circumvent this limitation, mosaic analysis of histone mutants was developed with the use of FLP-FRT mediated recombination (Figure S1B). This way, homozygous Δ *HisC* clones are detected when they are supplemented with 12xHisGU of either WT or mutated histones in larval tissues (Hodl and Basler, 2012; Pengelly et al., 2013). We adopted the same system to generate a *H3S28A* mutant. In parallel, histone

replacement lines carrying *WT* and *H3K27R* histone mutants were established as controls. This system replaces all canonical histones, leaving the endogenous genes coding for the histone variant H3.3 (*His3.3A* and *His3.3B*) intact. To simplify the nomenclature, we refer to homozygous Δ *HisC* clones supplemented with different transgenic 12xHisGU as *WT*, *H3S28A* and *H3K27R* lines, unless otherwise stated.

Consistent with previous reports (Hodl and Basler, 2012; Pengelly et al., 2013), homozygous Δ *HisC* clones (lacking GFP) induced with a heat shock pulse of FLP died (data not shown). Reintroducing 12xHisGU in the form of WT-H3, H3S28A or H3K27R mutants displayed DAPI and H3 staining patterns similar to the neighboring GFP-positive tissues (Figure 1 and Figure S1C). Importantly, *H3S28A* clones specifically lost the mitotic H3S28ph signal, while they retained normal levels of H3S10ph (Figure 1B). Likewise and as previously reported (McKay et al., 2015; Pengelly et al., 2013), *H3K27R* clones almost completely lost the H3K27me3 mark, without affecting neighboring mitotic phosphorylation at H3S28 (Figure S1D). These results imply that the native pool of histone variant H3.3 neither supports mitotic H3S28ph nor H3K27me3. This may be linked to the transcription-coupled deposition pathway of H3.3, which restricts its distribution to active promoters, resulting in genomic distributions that might not be compatible with PRC2 catalysis. Importantly, mitotic H3S10ph, H3S28ph and H3K27me3 signals were not affected in WT clones (Figure 1A, 1C and S1D).

Since H3K27 and H3S28 are adjacent to each other, and as H3S28ph was shown to evict PcG (Gehani et al., 2010; Lau and Cheung, 2011) and to prevent H3K27me demethylation (Kruidenier et al., 2012; Sengoku and Yokoyama, 2011), we asked whether the loss of H3S28ph in *H3S28A* clones affects H3K27 methylation. Strikingly, H3K27me3 and H3K27me1 were strongly reduced in *H3S28A* clones (Figure 1D). Considerable reduction of H3K27me2 was also detected. This was in stark contrast to active chromatin marks,

where H3K27ac was only mildly decreased and H3K4me3 was unaffected in *H3S28A* clones. As a control, *WT* clones showed normal staining levels indistinguishable from neighboring tissues for all histone marks examined (Figure 1C). These findings show that H3S28 is specifically required for PRC2 function in vivo.

***H3S28A* and *H3K27R* mutants both cause derepression of Hox genes**

In various PRC2 mutants (Beuchle et al., 2001; Birve et al., 2001; Muller et al., 2002), as well as in the *H3K27R* histone mutant clones where H3K27me3 levels are compromised (McKay et al., 2015; Pengelly et al., 2013), canonical PcG targets such as Hox genes are derepressed. Hence, we analyzed Hox gene expression in the *H3S28A* mutant in comparison to the *H3K27R* mutant.

Endogenous expression of *Scr* is limited to a patch of cells located at the base of antennal discs (asterisks) and is absent within the antennal disc proper (Abzhanov et al., 2001). *Scr* was derepressed across the entire antennal disc in both *H3S28A* and *H3K27R* mutant clones (Figure 2A). In line with a previous report (Pattatucci and Kaufman, 1991), low levels of endogenous *Scr* expression were observed in the adepithelial cells of the 2nd and 3rd leg discs (Figure S2A, asterisks). We observed strong derepression of *Scr* in *H3S28A* and *H3K27R* mutant clones of these tissues (Figure S2A). Moreover, *Scr* derepression was occasionally detected in the notum region of wing discs in both histone mutant clones (Figure S2A), similar to what was previously reported in *Pc*^{3/+} heterozygous mutant background (Pattatucci and Kaufman, 1991).

We also detected strong derepression of *Ubx* in antennal and wing discs of both *H3S28A* and *H3K27R* mutant clones (Figure 2A and S2A). *Ubx* derepression was mainly restricted to the wing pouch region at a level comparable to its native expression in the haltere disc. For *Abd-B*, strong derepression was detected in *H3K27R* clones across the entire eye-

antennal and wing discs (Pengelly et al., 2013), whereas *H3S28A* clones showed no obvious derepression in the same tissues (Figure 2A and S2A), suggesting that the partial loss of H3K27me3 was not sufficient to induce Abd-B derepression in *H3S28A* clones. No changes in expression of Hox genes were detected in the imaginal discs of WT-H3 clones. In addition to the aforementioned Hox genes, we observed derepression of Antp in the antennal discs of *H3S28A* and *H3K27R* mutant clones (Figure 2B and S2A). Similar to the *Antp^{Ns}* mutant with ectopic expression of Antp in the antennal disc (Figure S2B), GAL4-driven overexpression of various Hox genes in the antennal disc are known to silence the antennal selector gene Hth and cause antenna-to-leg transformation (Yao et al., 1999). In agreement with this observation, the *H3S28A* and *H3K27R* clones also showed Hth silencing, which was most prominent in the *H3K27R* mutant (Figure 2B).

Since Hox gene derepression can induce homeotic transformations, we investigated the phenotypic consequence of the induction of *H3S28A* or *H3K27R* clones in adults. Consistent with the Hox derepression and Hth silencing phenotypes in larval tissues, adult flies developing from clonal *H3S28A* and *H3K27R* mutant backgrounds displayed antenna-to-leg transformation. Wild-type *Drosophila* adults showed distinct antenna segmentation into a1-a3 and arista, as annotated on *w¹¹¹⁸* in Figure 2C. Notably, the *H3K27R* mutant displayed an enlarged a3 antennal segment, from which massive outgrowth developed with leg-like features. This resembled the antennapedia phenotype of the *Antp^{Ns}* mutant. The *H3S28A* mutant showed milder transformations, with smaller a3 segment protrusions and thickening of arista resembling the aristapedia phenotype. In contrast, WT histone replacement flies showed normal antenna structures (Figure 2C).

In summary, the partial loss of H3K27me3 in the *H3S28A* mutant induces loss of Polycomb silencing, although the effects were milder than those of the *H3K27R* mutant, as

indicated by Abd-B staining which only shows derepression in *H3K27R* clones (Figure 2A and S2A).

Deregulation of PcG silencing in *H3S28A* mutant is independent of active demethylation and cannot be recapitulated by depletion of Aurora B kinase

We investigated the mechanistic basis for the loss of silencing induced by the *H3S28A* mutation. Since H3S28ph was shown to evict PcG protein binding to H3K27me₃ but also to prevent H3K27me₃ demethylation, one explanation for the observed deregulation in PcG silencing in *H3S28A* mutant could be active H3K27me demethylation upon the loss of H3S28ph. If this were correct, combining *dUtx* null background with the *H3S28A* mutation should alleviate the reduction of H3K27me levels and PcG silencing defects. By recombining *dUtxΔ* mutation (Copur and Muller, 2013) with $\Delta HisC$, we generated double homozygous mutants by recombination over a single FRT element. As shown in Figure S3A, the *dUtxΔ*, *H3S28A* mutant clone is depleted of dUtx. However, all H3K27 methylation states are not rescued under such condition (Figure 3A). We also tested the possibility that the *H3S28A* phenotype is a consequence of the absence of H3S28 phosphorylation. We therefore induced RNAi against the Aurora B kinase in the wing imaginal disc. This resulted in robust depletion of Aurora B (Figure S3B) and mitotic H3S10ph and H3S28ph (Figure S3C). Consistent with previous reports, loss of Aurora B caused aneuploidy and enlarged nuclei (Giet and Glover, 2001). If the decrease in H3K27me and the loss of Hox gene silencing observed in the *H3S28A* mutant was depending on the absence of H3S28 phosphorylation, one would expect to observe these phenotypes upon loss of Aurora B. In contrast, we did not observe reduction of H3K27me₃ levels, nor *Ubx* derepression in the knockdown region of wing discs (Figure 3B). Taken

together, these data suggest that demethylation by dUtx and the loss of H3S28 phosphorylation per se do not compromise Polycomb silencing in the *H3S28A* mutant.

H3S28A impairs H3K27-methylation of nucleosomes by PRC2

Together, the results described above suggested the possibility that the serine-to-alanine substitution per se might affect PRC2 activity. To directly test this hypothesis, we performed in vitro histone methyltransferase (HMT) assays using a reconstituted, 4-component core *Drosophila* PRC2 complex that includes Esc, Su(z)12, E(z) and Nurf55 (Muller et al., 2002; Schmitges et al., 2011). As shown by previous reports (Margueron et al., 2009; Schmitges et al., 2011), when assayed on WT nucleosomes supplied with a *trans*-acting histone peptide carrying H3K27me₃, PRC2 activity was robustly enhanced in a dose-dependent manner (Figure 4). Only basal HMT activities were detected when H3S28ph, unmodified or no histone peptides were added to the reaction mixtures. Interestingly, the stimulatory effect of H3K27me₃ was retained when combined with the H3S28A mutation (H3K27me₃S28A, Figure 4A). By contrast, the PRC2-stimulatory activity was abolished in context of the H3K27me₃S28ph “double mark” (Figure 4A). Available structural data shows that the stimulatory effect relies on the binding of H3K27me₃ to the beta-propeller structure of Esc with the side chain of H3S28 pointing away from the binding side (Margueron et al., 2009; O'Meara and Simon, 2012). Apparently, this interaction is not affected by the loss of the hydroxyl group in the serine-to-alanine substitution in H3K27me₃S28A peptides. However, the introduction of the more bulky and charged phosphate group on H3S28 prevents any stimulatory effect. We assume that this is due to hampered binding of the H3K27me₃S28ph peptide to Esc.

We then performed PRC2 HMT assays with H3S28A mutant nucleosomes. In this context, enzymatic activity was considerably reduced, with or without supplementation of

stimulatory H3K27me₃-containing peptides *in trans* (Figure 4B). Similar to WT nucleosomal substrates, the stimulatory effect of H3K27me₃ and H3K27me₃S28A peptides was comparable on H3S28A nucleosomes. Therefore, the H3S28A effect can be ascribed to inhibition of PRC2-dependent methylation of H3K27.

Discussion

In this report, we have established a *H3S28A* histone mutant in *Drosophila*. In theory, this mutation could have two different effects on the polycomb system. i) it could be that PcG proteins are not evicted from H3K27me₃ binding sites in the absence of H3S28ph and, thus, PcG target genes might become ectopically repressed or ii) the mutation at H3S28 or the absence of H3S28ph could compromise PcG functions, resulting in derepression of PcG target genes. We found no evidence for the first possibility, although it is formally possible that H3S28 is phosphorylated under certain developmental conditions or in response to particular stimuli to counteract Polycomb silencing. Instead, our data points to an inhibition of PRC2 activity by the *H3S28A* mutation. This inhibition is independent of active H3K27 demethylation by dUtx. Besides, RNAi against Aurora B kinase and hence depletion of H3S28ph, did not hamper polycomb silencing. On the other hand, H3S28A nucleosomes proved to be a suboptimal substrate for *in vitro* PRC2 HMT activity. Although a 3D structure of the human Ezh2 SET domain is available (Antonysamy et al., 2013), the exact contribution of the hydroxyl group of H3S28 for H3K27 methylation is difficult to deduce from the available data. vSET, the only other protein capable of H3K27 methylation in the absence of PRC2 subunits, does not require H3S28 for catalysis, while it does use H3A29 to define substrate specificity (Wei and Zhou, 2010). Clearly, more work will be required to determine the exact structural and biochemical role of H3S28 in PRC2 catalysis. Consistent with the *in vitro* HMT assays, *in vivo* the *H3S28A* mutant exhibits

defects in H3K27 methylation and shows similar, though milder, Hox derepression profiles and transformation phenotypes to those observed in *H3K27R* mutant flies.

Interestingly, the “KS” module is frequently found in Ezh2 substrates other than K27S28 of histone H3. These include K26S27 of human histone H1 variant H1b (H1.4), K38S39 of the nuclear orphan receptor ROR α and K180S181 of STAT3 (Kim et al., 2013; Kuzmichev et al., 2004; Lee et al., 2012; Pasini et al., 2004). Whether these serine residues act similarly to H3S28 to support methylation of the adjacent lysine residue remains unknown. Of note, some other Ezh2 substrates can be methylated despite the lack of a “KS” module. These include K26 of mouse histone H1 variant H1e, K49 of STAT3 and K116 of Jarid2 (Dasgupta et al., 2015; Kuzmichev et al., 2004; Sanulli et al., 2015), where the lysine residue is followed by an alanine, glutamate and phenylalanine respectively. Moreover, the link between peptide sequence and enzymology of Ezh2 was shown to differ in non-histone substrates (Lee et al., 2012). Hence the role of serine following the Ezh2 methylation target amino acid might not be extrapolated to all other Ezh2 substrates, and should be tested individually.

Previous reports revealed discrepancies in *Drosophila* PcG protein localization on mitotic chromosomes depending on staining protocols and tissue types (Buchenau et al., 1998; Fanti et al., 2008; Follmer et al., 2012; Fonseca et al., 2012). Nonetheless, live imaging of Pc-GFP, Ph-GFP and E(z)-GFP in early *Drosophila* embryos (Cheutin and Cavalli, 2012; Steffen et al., 2013) all suggested that the majority of these PcG components are dissociated from mitotic chromosomes. Since stress-induced H3S28ph evicts PcG complexes during interphase (Lau and Cheung, 2011; Schmitges et al., 2011), one might expect rebinding of PcG proteins on mitotic chromosomes depleted of H3S28ph. While we did observe loss of Ph from mitotic chromosomes in WT background, we did not observe significant Ph association in *H3S28A* mutant condition (Figure S4). The reduced levels of

H3K27me3 in the *H3S28A* mutant could contribute to this observation. Alternatively, other mechanisms might operate to dissociate the majority of PcG proteins during mitosis.

The establishment of the histone replacement system in *Drosophila* has proven to be an important tool to complement functional characterization of chromatin modifiers (Hodl and Basler, 2012; McKay et al., 2015; Pengelly et al., 2013). While depletion of H3K27 methylation, either by mutation of the histone mark writer *E(z)* or by mutation of the histone itself in the *H3K27R* mutant, leads to similar loss of Polycomb-dependent silencing (McKay et al., 2015; Pengelly et al., 2013), other histone mutations revealed different phenotypes than the loss of their corresponding histone mark writers. For example, *H3K4R* mutations in both H3.2 and H3.3, hence a complete loss of H3K4 methylation, did not hamper active transcription (Hodl and Basler, 2012). Also, the loss of H4K20 methylation upon *H4K20R* mutation unexpectedly supports development and does not phenocopy cell cycle and gene silencing defects reported upon the loss of the H4K20 methylase PR-Set7 (McKay et al., 2015). Here, by comparing the phenotype of Aurora B knockdown and *H3S28A* mutation in vivo, together with in vitro HMT assay, we specifically attribute the requirement of the unmodified H3S28 residue in supporting PRC2-deposition of H3K27 methylation.

While the published data suggest that H3S28 phosphorylation might be important for eviction of PcG components for derepression of PcG target genes upon stimulatory cues (Gehani et al., 2010; Lau and Cheung, 2011; Sawicka et al., 2014), our data reveals a so far unacknowledged function of the unphosphorylated state of H3S28. We show that serine 28 is required to enable proper methylation of H3K27 by PRC2 and thus to establish Polycomb-dependent gene silencing. Serine 28 of histone H3 is universally conserved in species that display canonical PRC2-dependent silencing mechanisms. Given the fact that we find no major mitotic defects upon its mutation, we propose that the major role of this

residue is to ensure optimal PRC2 function while facilitating the removal of Polycomb proteins in response to signals that induce phosphorylation.

Supplemental Information for this article is available online.

Experimental Procedures

Plasmids

Construction of integration plasmids $p\phi C31attB3xHisGU$ carrying either wild type H3, H3K27R or H3S28A mutation followed published procedures (Gunesdogan et al., 2010). Entry vectors $pENTR221-HisGU$, $pENTRL4R1-HisGU$, $pENTRR2L3-HisGU$ and their H3K27R mutant derivatives, together with the destination vector $pDEST3R4-\phi C31attB$ were obtained from Alf Herzig (Max-Planck-Institut für Infektionsbiologie, Berlin, Germany). Gene synthesis (Eurofins Scientific S.E.) of a DNA fragment carrying the codon exchange AGT→GCC introduced the H3S28A mutation. Subcloning of the H3S28A DNA fragment into entry vectors and subsequent recombineering followed the procedures published for generating the *H3K27R* mutant (Gunesdogan et al., 2010).

***Drosophila* Stocks**

Site-specific transgenesis and fly genetics were performed as previously described (Gunesdogan et al., 2010). The histone deficiency mutant ($\Delta HisC$) used in this study (*Df(2L)BSC104*) was obtained from Konrad Basler (Institute of Molecular Life Sciences, Zurich, Switzerland) in the form of *Df(2L) BSC104, FRT40A* recombinant (Hodl and

Basler, 2012). The *dUtxA* line was obtained from Jürg Müller (The Max Planck Institute of Biochemistry, Martinsried, Germany) in the form of *dUtxA*, *FRT40A* (Copur and Muller, 2013) recombinant.

Mosaic analysis and Immunostaining

Egg depositions were allowed over a 24 hr time window at 25°C. Larva developed for two days before they were heat shocked at 37°C for 1 hr. L3 larva emerged 3 days after heat shock, and they were selected for the lack of green balancer before dissection. Inverted larvae heads were fixed in 4% formaldehyde in PBS for 20 min at room temperature. After washing with PBS, the samples were permeabilized twice with 0.3% TritonX-100 in PBS for 30 min at room temperature. After blocking with 3% BSA 0.03% TritonX-100 in PBS for 1 hr, the samples were incubated with primary antibodies in 0.03% Triton X-100 in PBS overnight at 4°C. Samples were then incubated secondary antibodies conjugated to Alexa (Invitrogen) fluorophores before DAPI staining. Thorough washes were applied in between incubations. Imaginal discs were carefully removed and mounted with ProLong Gold (Invitrogen) antifade reagent. Micrographs were acquired on a Zeiss LSM 780 inverted confocal microscope. Raw micrographs were processed with ImageJ and assembled using Adobe Illustrator.

Scanning electron microscopy

Adult fly heads were fixed as described (Wolff, 2011) using the critical-point-dried method. They were then sputter-coated with a 10 nm thick gold film and examined under a scanning electron microscope (Hitachi S4000) using a lens detector with an acceleration voltage of 10kV at calibrated magnifications.

In vitro PRC2 histone methyltransferase assay

Nucleosomes and chromatin arrays were reconstituted by the salt gradient dialysis method as described (Luger et al., 1999), using recombinant *Xenopus laevis* core histones. Nucleosomes contained a 187bp long DNA fragment with the 601 DNA sequence at its center (Munari et al., 2012). The histone mutant H3S28A was generated by site-directed mutagenesis. All reconstitutions were analyzed by native gel electrophoresis.

H3 peptides corresponding to H3 amino acids 21-33 were synthesized according to standard procedures. A non-natural tyrosine was added at the C-terminus for quantification.

Histone methyltransferase (HMT) reactions were performed using 1 µg nucleosomes in a total volume of 15 µl for 1 h at 30°C. HMT reactions were carried out in presence of 0.8 µCi [methyl-³H]-S-Adenosyl-L-methionine (³H-SAM) and 325 ng PRC2 (75 nM) in HMT buffer (50 mM Tris-HCl (pH = 8.8), 5 mM MgCl₂, 4 mM DTT). Recombinant *Drosophila melanogaster* PRC2 complex, comprised of Su(z)12, E(z), Nurf55 and Esc, was a kind gift of Nicolas Thomä (Friedrich Miescher Institute, Basel, Switzerland) and was purified as described (Schmitges et al., 2011). PRC2 HMT assays in presence of H3₂₁₋₃₃ peptides *in trans* contained 5 or 40 µM of peptide. Reactions were stopped by addition of SDS sample buffer followed by separation by SDS-PAGE. Reactions were analyzed by fluorography.

More details on the experimental procedures can be found in the Supplemental Information.

Author contributions

P.Y.K.Y., A-M.M. and G.C. conceived and designed the *Drosophila* experiments. A.S. performed the in vitro PRC2 HMT assays with input from W.F.. P.Y.K.Y. performed all other experiments. All authors analyzed the data. P.Y.K.Y. and G.C. wrote the manuscript with help from A.S. and W.F..

Acknowledgements

We are grateful to Natalia Azpiazu, Konrad Basler, Walter Gehring, David Glover, Peter J. Harte, Alf Herzig, Martina Hödl, Ginés Morata, Jürg Müller, Nicolas Thomä and Feng Tie, for providing research reagents. Boyan Bonev, Thierry Cheutin, Satish Sati and Bernd Schuettengruber provided helpful comments on the manuscript. We thank Chantal Cazevieille for assistance with scanning electron microscopy and in the use of the Montpellier RIO imaging facility. Research in the laboratory of G.C. was supported by grants from the European Research Council (ERC-2008-AdG No 232947), the CNRS, the European Network of Excellence EpiGeneSys, the Agence Nationale de la Recherche, and the Fondation ARC pour la Recherche sur le Cancer. Funding of P.Y.K.Y. was supported by the Croucher Foundation and La Ligue contre le Cancer. Research in the laboratory of W.F. was supported by the Max Planck Society.

Conflict of interest

The authors declare that they have no conflict of interest.

References

- Abzhanov, A., Holtzman, S., and Kaufman, T.C. (2001). The *Drosophila* proboscis is specified by two Hox genes, proboscipedia and Sex combs reduced, via repression of leg and antennal appendage genes. *Development* *128*, 2803-2814.
- Antonyamy, S., Condon, B., Druzina, Z., Bonanno, J.B., Gheyi, T., Zhang, F., MacEwan, I., Zhang, A., Ashok, S., Rodgers, L., *et al.* (2013). Structural context of disease-associated mutations and putative mechanism of autoinhibition revealed by X-ray crystallographic analysis of the EZH2-SET domain. *PLoS One* *8*, e84147.
- Beuchle, D., Struhl, G., and Muller, J. (2001). Polycomb group proteins and heritable silencing of *Drosophila* Hox genes. *Development* *128*, 993-1004.
- Birve, A., Sengupta, A.K., Beuchle, D., Larsson, J., Kennison, J.A., Rasmuson-Lestander, A., and Muller, J. (2001). Su(z)12, a novel *Drosophila* Polycomb group gene that is conserved in vertebrates and plants. *Development* *128*, 3371-3379.
- Blackledge, N.P., Farcas, A.M., Kondo, T., King, H.W., McGouran, J.F., Hanssen, L.L., Ito, S., Cooper, S., Kondo, K., Koseki, Y., *et al.* (2014). Variant PRC1 complex-dependent H2A ubiquitylation drives PRC2 recruitment and polycomb domain formation. *Cell* *157*, 1445-1459.
- Buchenau, P., Hodgson, J., Strutt, H., and Arndt-Jovin, D.J. (1998). The distribution of polycomb-group proteins during cell division and development in *Drosophila* embryos: impact on models for silencing. *J Cell Biol* *141*, 469-481.
- Cao, R., Wang, L., Wang, H., Xia, L., Erdjument-Bromage, H., Tempst, P., Jones, R.S., and Zhang, Y. (2002). Role of histone H3 lysine 27 methylation in Polycomb-group silencing. *Science* *298*, 1039-1043.
- Cheutin, T., and Cavalli, G. (2012). Progressive polycomb assembly on H3K27me3 compartments generates polycomb bodies with developmentally regulated motion. *PLoS Genet* *8*, e1002465.
- Cooper, S., Dienstbier, M., Hassan, R., Schermelleh, L., Sharif, J., Blackledge, N.P., De Marco, V., Elderkin, S., Koseki, H., Klose, R., *et al.* (2014). Targeting polycomb to pericentric heterochromatin in embryonic stem cells reveals a role for H2AK119u1 in PRC2 recruitment. *Cell Rep* *7*, 1456-1470.
- Copur, O., and Muller, J. (2013). The histone H3-K27 demethylase Utx regulates HOX gene expression in *Drosophila* in a temporally restricted manner. *Development* *140*, 3478-3485.
- Czermin, B., Melfi, R., McCabe, D., Seitz, V., Imhof, A., and Pirrotta, V. (2002). *Drosophila* enhancer of Zeste/ESC complexes have a histone H3 methyltransferase activity that marks chromosomal Polycomb sites. *Cell* *111*, 185-196.
- Dasgupta, M., Dermawan, J.K., Willard, B., and Stark, G.R. (2015). STAT3-driven transcription depends upon the dimethylation of K49 by EZH2. *Proceedings of the National Academy of Sciences of the United States of America*.
- Di Croce, L., and Helin, K. (2013). Transcriptional regulation by Polycomb group proteins. *Nat Struct Mol Biol* *20*, 1147-1155.
- Fanti, L., Perrini, B., Piacentini, L., Berloco, M., Marchetti, E., Palumbo, G., and Pimpinelli, S. (2008). The trithorax group and Pc group proteins are differentially involved in heterochromatin formation in *Drosophila*. *Chromosoma* *117*, 25-39.
- Fischle, W., Wang, Y., Jacobs, S.A., Kim, Y., Allis, C.D., and Khorasanizadeh, S. (2003). Molecular basis for the discrimination of repressive methyl-lysine marks in histone H3 by Polycomb and HP1 chromodomains. *Genes Dev* *17*, 1870-1881.

Follmer, N.E., Wani, A.H., and Francis, N.J. (2012). A polycomb group protein is retained at specific sites on chromatin in mitosis. *PLoS Genet* 8, e1003135.

Fonseca, J.P., Steffen, P.A., Muller, S., Lu, J., Sawicka, A., Seiser, C., and Ringrose, L. (2012). In vivo Polycomb kinetics and mitotic chromatin binding distinguish stem cells from differentiated cells. *Genes & development* 26, 857-871.

Gehani, S.S., Agrawal-Singh, S., Dietrich, N., Christophersen, N.S., Helin, K., and Hansen, K. (2010). Polycomb group protein displacement and gene activation through MSK-dependent H3K27me3S28 phosphorylation. *Mol Cell* 39, 886-900.

Giet, R., and Glover, D.M. (2001). Drosophila aurora B kinase is required for histone H3 phosphorylation and condensin recruitment during chromosome condensation and to organize the central spindle during cytokinesis. *J Cell Biol* 152, 669-682.

Grossniklaus, U., and Paro, R. (2014). Transcriptional Silencing by Polycomb-Group Proteins. *Cold Spring Harb Perspect Biol* 6.

Gunesdogan, U., Jackle, H., and Herzig, A. (2010). A genetic system to assess in vivo the functions of histones and histone modifications in higher eukaryotes. *EMBO Rep* 11, 772-776.

Hodl, M., and Basler, K. (2012). Transcription in the absence of histone H3.2 and H3K4 methylation. *Curr Biol* 22, 2253-2257.

Kalb, R., Latwiel, S., Baymaz, H.I., Jansen, P.W., Muller, C.W., Vermeulen, M., and Muller, J. (2014). Histone H2A monoubiquitination promotes histone H3 methylation in Polycomb repression. *Nat Struct Mol Biol* 21, 569-571.

Kim, E., Kim, M., Woo, D.H., Shin, Y., Shin, J., Chang, N., Oh, Y.T., Kim, H., Rhee, J., Nakano, I., *et al.* (2013). Phosphorylation of EZH2 activates STAT3 signaling via STAT3 methylation and promotes tumorigenicity of glioblastoma stem-like cells. *Cancer Cell* 23, 839-852.

Klymenko, T., Papp, B., Fischle, W., Kocher, T., Schelder, M., Fritsch, C., Wild, B., Wilm, M., and Muller, J. (2006). A Polycomb group protein complex with sequence-specific DNA-binding and selective methyl-lysine-binding activities. *Genes & development* 20, 1110-1122.

Kruidenier, L., Chung, C.W., Cheng, Z., Liddle, J., Che, K., Joberty, G., Bantscheff, M., Bountra, C., Bridges, A., Diallo, H., *et al.* (2012). A selective jumonji H3K27 demethylase inhibitor modulates the proinflammatory macrophage response. *Nature* 488, 404-408.

Kuzmichev, A., Jenuwein, T., Tempst, P., and Reinberg, D. (2004). Different EZH2-containing complexes target methylation of histone H1 or nucleosomal histone H3. *Molecular cell* 14, 183-193.

Kuzmichev, A., Nishioka, K., Erdjument-Bromage, H., Tempst, P., and Reinberg, D. (2002). Histone methyltransferase activity associated with a human multiprotein complex containing the Enhancer of Zeste protein. *Genes & development* 16, 2893-2905.

Lagarou, A., Mohd-Sarip, A., Moshkin, Y.M., Chalkley, G.E., Bezstarosti, K., Demmers, J.A., and Verrijzer, C.P. (2008). dKDM2 couples histone H2A ubiquitylation to histone H3 demethylation during Polycomb group silencing. *Genes & development* 22, 2799-2810.

Lau, P.N., and Cheung, P. (2011). Histone code pathway involving H3 S28 phosphorylation and K27 acetylation activates transcription and antagonizes polycomb silencing. *Proceedings of the National Academy of Sciences of the United States of America* 108, 2801-2806.

Lee, J.M., Lee, J.S., Kim, H., Kim, K., Park, H., Kim, J.Y., Lee, S.H., Kim, I.S., Kim, J., Lee, M., *et al.* (2012). EZH2 generates a methyl degron that is recognized by the DCAF1/DDB1/CUL4 E3 ubiquitin ligase complex. *Molecular cell* 48, 572-586.

Luger, K., Rechsteiner, T.J., and Richmond, T.J. (1999). Expression and purification of recombinant histones and nucleosome reconstitution. *Methods Mol Biol* 119, 1-16.

Margueron, R., Justin, N., Ohno, K., Sharpe, M.L., Son, J., Drury, W.J., 3rd, Voigt, P., Martin, S.R., Taylor, W.R., De Marco, V., *et al.* (2009). Role of the polycomb protein EED in the propagation of repressive histone marks. *Nature* 461, 762-767.

Margueron, R., and Reinberg, D. (2011). The Polycomb complex PRC2 and its mark in life. *Nature* 469, 343-349.

McKay, D.J., Klusza, S., Penke, T.J., Meers, M.P., Curry, K.P., McDaniel, S.L., Malek, P.Y., Cooper, S.W., Tatomer, D.C., Lieb, J.D., *et al.* (2015). Interrogating the Function of Metazoan Histones using Engineered Gene Clusters. *Dev Cell* 32, 373-386.

Min, J., Zhang, Y., and Xu, R.M. (2003). Structural basis for specific binding of Polycomb chromodomain to histone H3 methylated at Lys 27. *Genes & development* 17, 1823-1828.

Muller, J., Hart, C.M., Francis, N.J., Vargas, M.L., Sengupta, A., Wild, B., Miller, E.L., O'Connor, M.B., Kingston, R.E., and Simon, J.A. (2002). Histone methyltransferase activity of a Drosophila Polycomb group repressor complex. *Cell* 111, 197-208.

Muller, J., and Verrijzer, P. (2009). Biochemical mechanisms of gene regulation by polycomb group protein complexes. *Curr Opin Genet Dev* 19, 150-158.

Munari, F., Soeroes, S., Zenn, H.M., Schomburg, A., Kost, N., Schroder, S., Klingberg, R., Rezaei-Ghaleh, N., Stutzer, A., Gelato, K.A., *et al.* (2012). Methylation of lysine 9 in histone H3 directs alternative modes of highly dynamic interaction of heterochromatin protein hHP1beta with the nucleosome. *J Biol Chem* 287, 33756-33765.

O'Meara, M.M., and Simon, J.A. (2012). Inner workings and regulatory inputs that control Polycomb repressive complex 2. *Chromosoma* 121, 221-234.

Pasini, D., Bracken, A.P., Jensen, M.R., Lazzarini Denchi, E., and Helin, K. (2004). Suz12 is essential for mouse development and for EZH2 histone methyltransferase activity. *The EMBO journal* 23, 4061-4071.

Pattatucci, A.M., and Kaufman, T.C. (1991). The homeotic gene *Sex combs reduced* of *Drosophila melanogaster* is differentially regulated in the embryonic and imaginal stages of development. *Genetics* 129, 443-461.

Pengelly, A.R., Copur, O., Jackle, H., Herzig, A., and Muller, J. (2013). A histone mutant reproduces the phenotype caused by loss of histone-modifying factor Polycomb. *Science* 339, 698-699.

Sanulli, S., Justin, N., Teissandier, A., Ancelin, K., Portoso, M., Caron, M., Michaud, A., Lombard, B., da Rocha, S.T., Offer, J., *et al.* (2015). Jarid2 Methylation via the PRC2 Complex Regulates H3K27me3 Deposition during Cell Differentiation. *Molecular cell* 57, 769-783.

Sawicka, A., Hartl, D., Goiser, M., Pusch, O., Stocsits, R.R., Tamir, I.M., Mechtler, K., and Seiser, C. (2014). H3S28 phosphorylation is a hallmark of the transcriptional response to cellular stress. *Genome Res* 24, 1808-1820.

Scheuermann, J.C., de Ayala Alonso, A.G., Oktaba, K., Ly-Hartig, N., McGinty, R.K., Fraterman, S., Wilm, M., Muir, T.W., and Muller, J. (2010). Histone H2A deubiquitinase activity of the Polycomb repressive complex PR-DUB. *Nature* 465, 243-247.

Schmitges, F.W., Prusty, A.B., Faty, M., Stutzer, A., Lingaraju, G.M., Aiwazian, J., Sack, R., Hess, D., Li, L., Zhou, S., *et al.* (2011). Histone methylation by PRC2 is inhibited by active chromatin marks. *Molecular cell* *42*, 330-341.

Schuettengruber, B., Chourrout, D., Vervoort, M., Leblanc, B., and Cavalli, G. (2007). Genome regulation by polycomb and trithorax proteins. *Cell* *128*, 735-745.

Sengoku, T., and Yokoyama, S. (2011). Structural basis for histone H3 Lys 27 demethylation by UTX/KDM6A. *Genes & development* *25*, 2266-2277.

Shao, Z., Raible, F., Mollaaghababa, R., Guyon, J.R., Wu, C.T., Bender, W., and Kingston, R.E. (1999). Stabilization of chromatin structure by PRC1, a Polycomb complex. *Cell* *98*, 37-46.

Simon, J.A., and Kingston, R.E. (2013). Occupying chromatin: Polycomb mechanisms for getting to genomic targets, stopping transcriptional traffic, and staying put. *Mol Cell* *49*, 808-824.

Steffen, P.A., Fonseca, J.P., Ganger, C., Dworschak, E., Kockmann, T., Beisel, C., and Ringrose, L. (2013). Quantitative in vivo analysis of chromatin binding of Polycomb and Trithorax group proteins reveals retention of ASH1 on mitotic chromatin. *Nucleic Acids Res* *41*, 5235-5250.

Wei, H., and Zhou, M.M. (2010). Dimerization of a viral SET protein endows its function. *Proceedings of the National Academy of Sciences of the United States of America* *107*, 18433-18438.

Wolff, T. (2011). Preparation of *Drosophila* eye specimens for scanning electron microscopy. *Cold Spring Harb Protoc* *2011*, 1383-1385.

Yao, L.C., Liaw, G.J., Pai, C.Y., and Sun, Y.H. (1999). A common mechanism for antenna-to-Leg transformation in *Drosophila*: suppression of homothorax transcription by four HOM-C genes. *Dev Biol* *211*, 268-276.

Figure Legends

Figure 1. *H3S28A* mutant specifically depletes mitotic H3S28ph and compromises all H3K27 methylation states.

Eye-antenna (A) and (B) or wing (C) and (D) imaginal discs of the indicated histone replacement genotype. Immunostaining with the indicated antibodies is shown; DNA was stained with DAPI. Clones of interest were marked by the lack of GFP signal and are indicated by dashed lines. (A) and (B) Comparison of H3S10ph (green) and H3S28ph (red) levels in mitotic cells from GFP-negative (histone replacement) clones with GFP-positive normal tissue. (C) and (D) Arrowheads highlight *H3S28A* clones with considerable drop in H3K27 methylation levels. Insets represent the magnified region indicated by dashed lines. For clarity of composite micrographs, GFP is pseudocolored to blue in (A) and (B). In order to capture mitotic cells at different focal planes, a Z-projection is applied in (A) and (B). Scale bars in (A) and (B) correspond to 5 μm , while those in (C) and (D) correspond to 100 μm . See also Figure S1.

Figure 2. Deregulation of Hox and antenna selector genes in *H3K27R* and *H3S28A* mutants and their associated transformation phenotypes.

(A and B) Antennal discs of *WT*, *H3S28A* and *H3K27R* clones were immunostained with anti-GFP and the indicated antibodies. DNA was stained with DAPI. Mutant clones are marked by the absence of GFP signal. Scale bars in antennal discs represent 100 μm . (A) Expression of Scr, Ubx and Abd-B in the antennal discs. Endogenous expression of Scr is marked by asterisks. (B) Expression of Antp and Hth in the antennal discs. Clones with derepressed Antp and silenced endogenous Hth expressions are marked by yellow arrowheads, those with silenced Hth but without Antp derepression are marked by magenta

arrowheads. (C) Electron micrographs of adult *Drosophila* heads derived from w^{1118} , *Antp^{Ns}* and the indicated mosaic histone replacement lines. Normal segmented antenna structures are annotated as a1, a2, a3 and ar (arista). *Antp^{Ns}* was shown as a positive control for antenna-to-leg transformation. Scale bars correspond to 100 μm . See also Figure S2 and S4.

Figure 3. *dUtxA*, *H3S28A* double mutant does not rescue H3K27 methylation levels and loss of Aurora B kinase does not perturb polycomb-silencing

(A) Wing discs carrying clones with either *H3S28A* alone, or in combination with *dUtxA* were immunostained with the indicated antibodies. (B) Wing imaginal discs of L3 larvae with *en-GAL4* directed RNAi against Aurora B at the posterior compartment (knocked down cells are in the region marked by GFP and dotted lines) were immunostained with the indicated antibodies. DNA was stained with DAPI. Scale bars correspond to 100 μm . See also Figure S3.

Figure 4. H3S28A impairs H3K27-methylation of nucleosomes by PRC2.

(A) In vitro HMT assay using reconstituted *Drosophila* PRC2 complex, WT nucleosomes and $^3\text{H-SAM}$ as substrates. Reactions were supplied *in trans* with the indicated histone peptides at concentrations of 5 and 40 μM . (B) In vitro PRC2 HMT assay as in (A) but using nucleosomal substrates assembled with either WT-H3 or H3S28A mutant protein. Reactions were separated by SDS-PAGE and analyzed by fluorography. Fluorographs with different exposures are shown. Coomassie staining of the histones serves as loading control.

Fig. 1

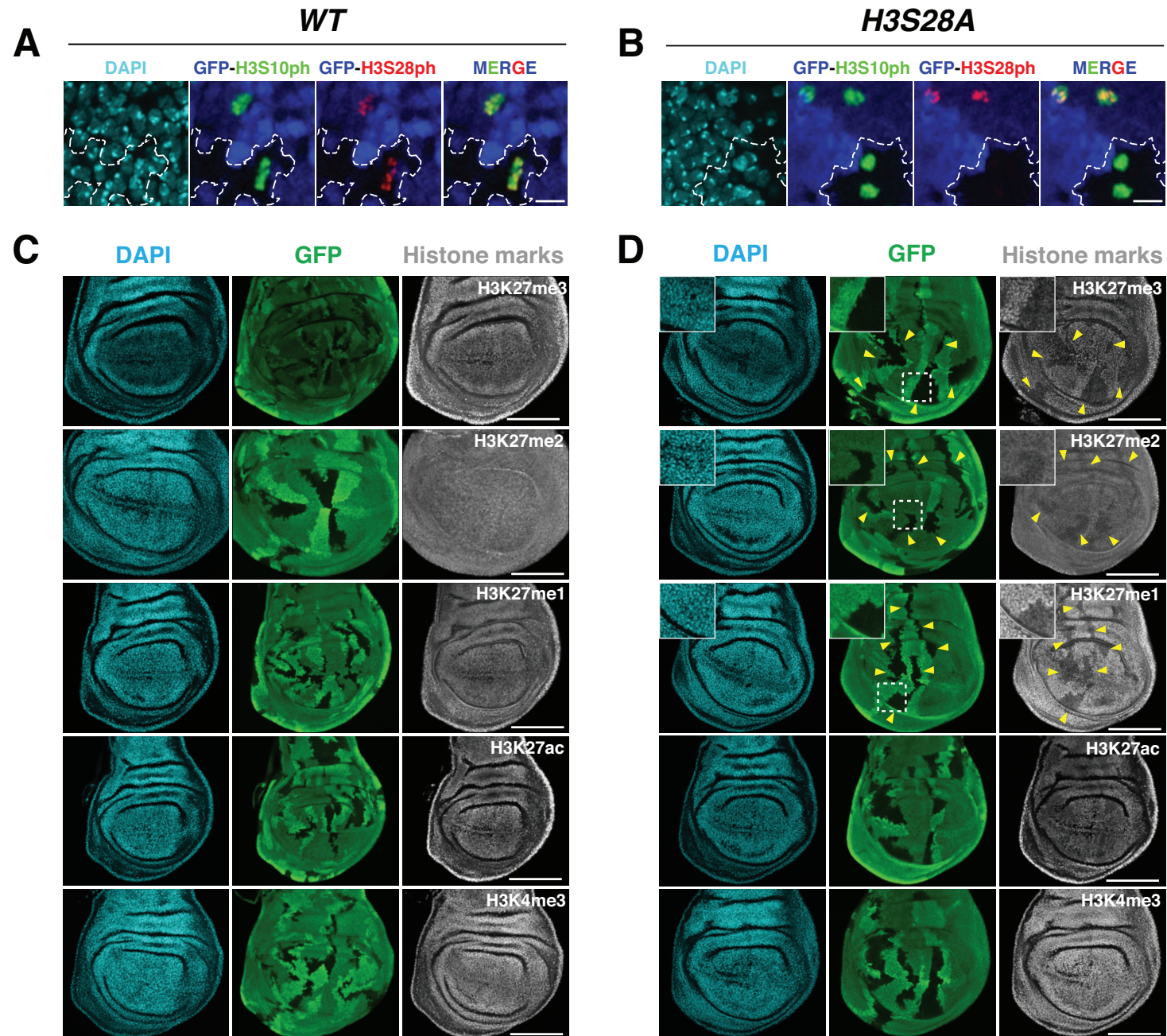


Fig. 2

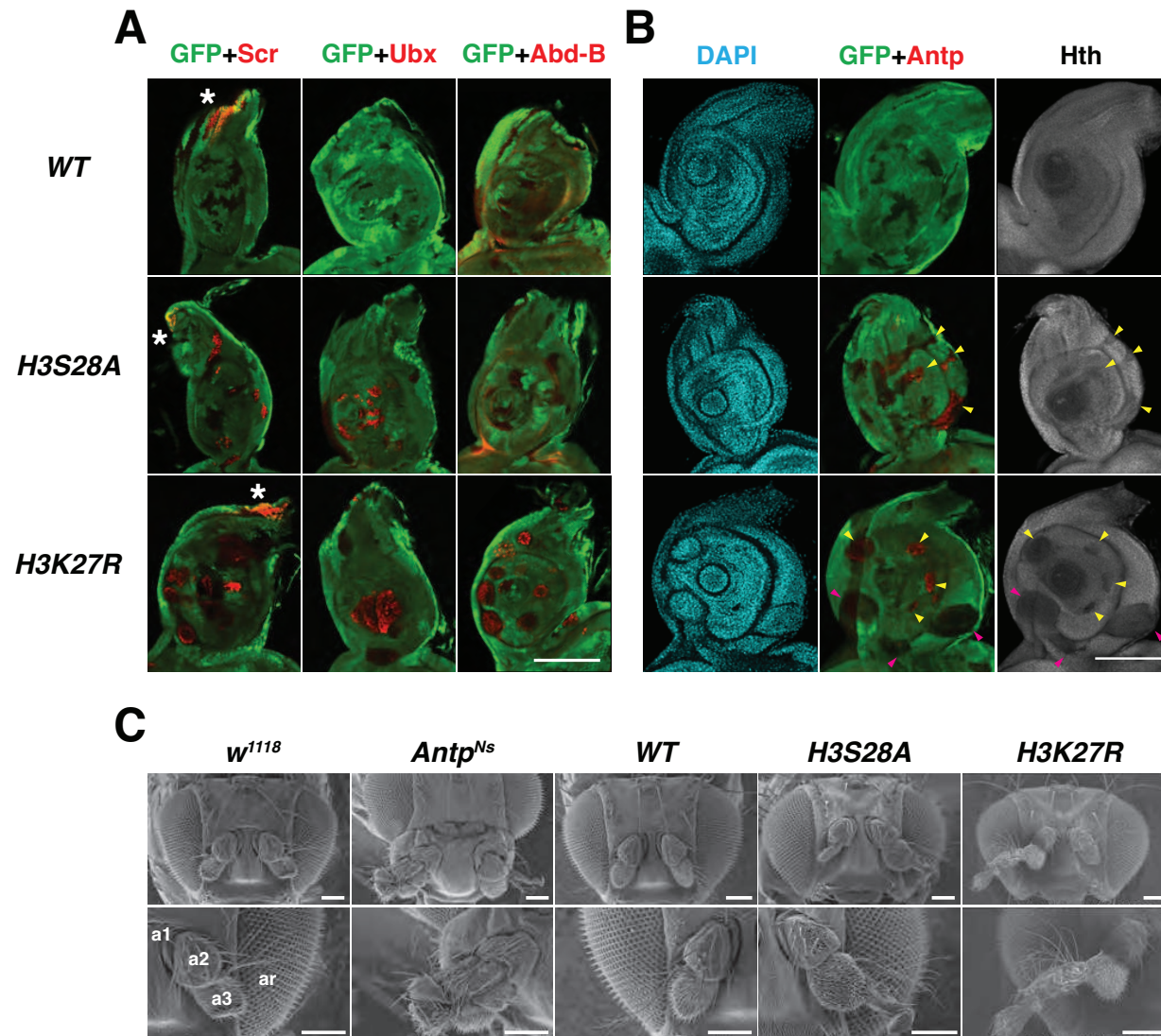


Fig. 3

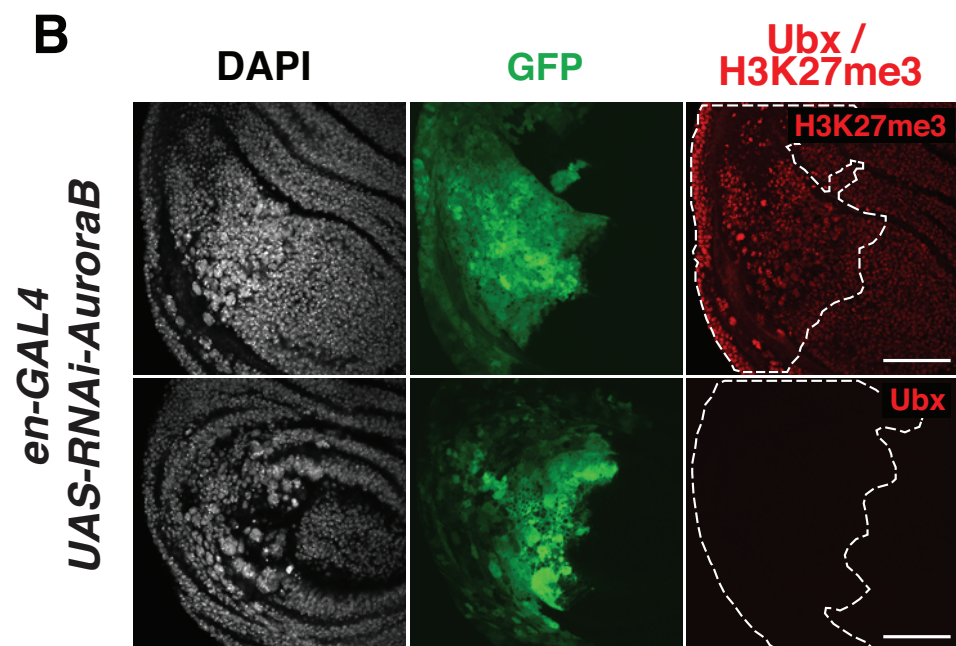
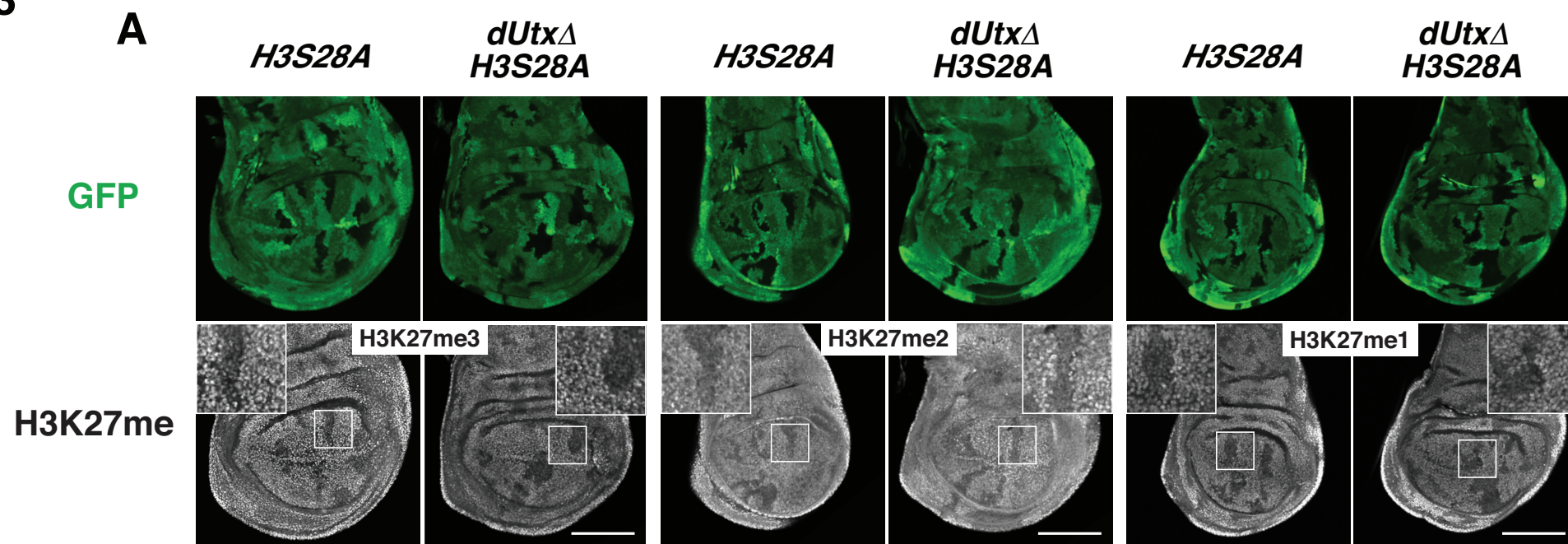
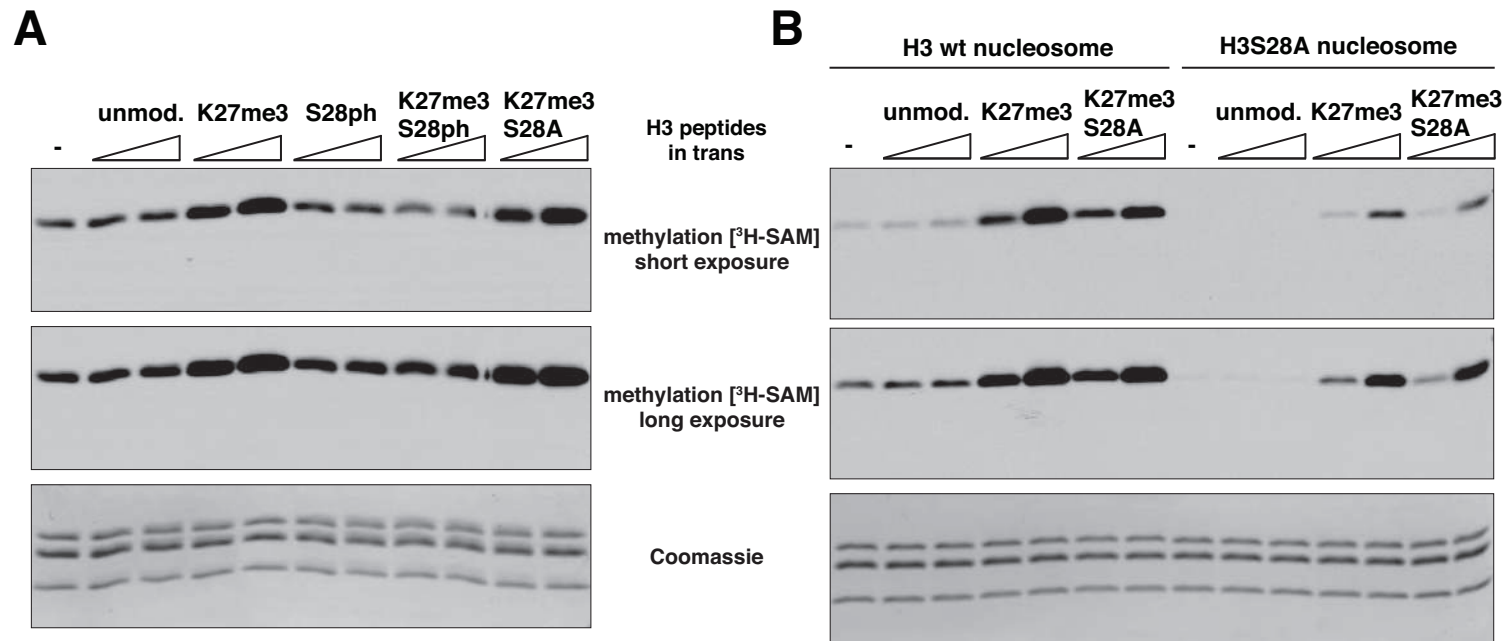


Fig. 4



Supplemental Information

Supplemental Figures S1-S4

- **Figure S1, Related to Figure 1. Schematic overview of the system for assaying the function of H3S28 and validation on histone replacement clones in larval imaginal discs.**
- **Figure S2, related to Figure 2. Hox gene derepression profiles in histone mutants (*H3S28A* and *H3K27R*) clones and *Antp^{Ns}*.**
- **Figure S3, related to Figure 3. Validation of clone induction of *dUtxΔ*, *H3S28A* double mutant and of in vivo RNAi against Aurora B kinase.**
- **Figure S4, related to Figure 2. Nuclear staining patterns of Ph remain unchanged in *H3S28A* mutant.**

Supplemental Figure Legends S1-S4

Supplemental Experimental Procedures

Supplemental References

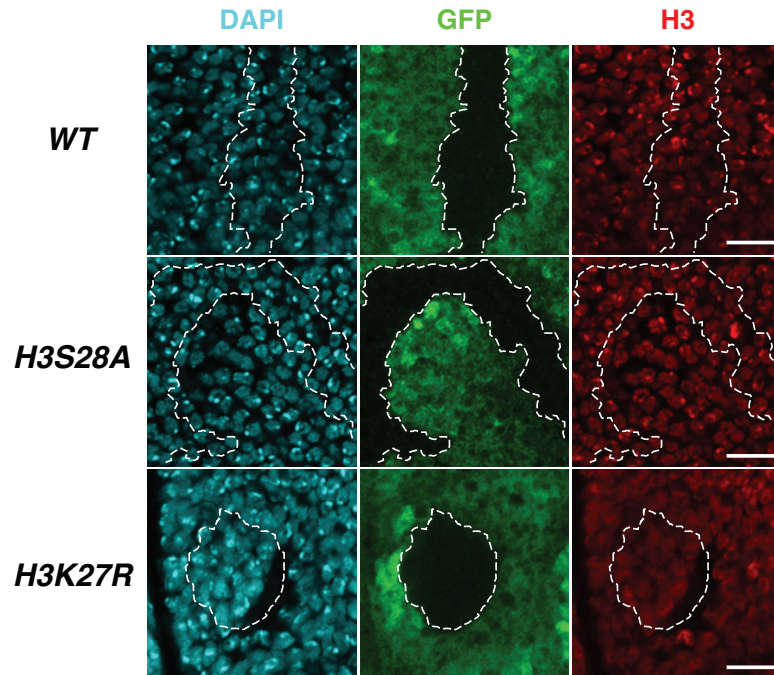
Supplemental Figures

Figure S1

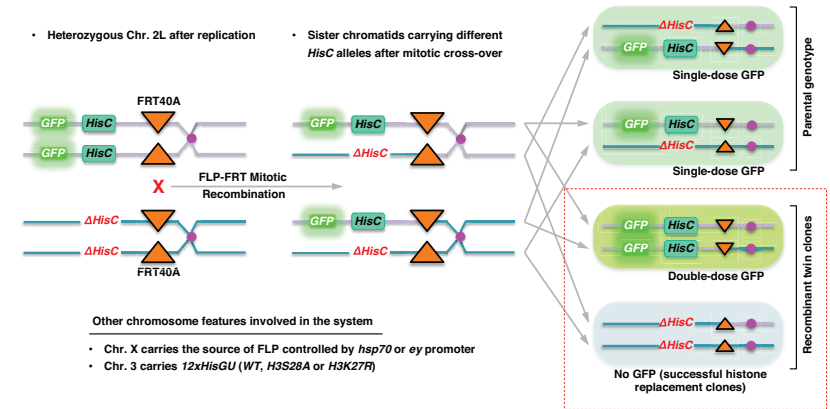
A

<i>S. pombe</i>	ARTKQTARKSTGGKAPRKQLASKAARK	SAPATGGVKKPHRYRPGTVALRE
<i>T. thermophila</i>	ARTKQTARKSTGAKAPRKQLASKAARK	SAPATGGIKKPHRFPGTVALRE
<i>N. crassa</i>	ARTKQTARKSTGGKAPRKQLASKAARK	SAPSTGGVKKPHRYRPGTVALRE
<i>D. melanogaster</i>	ARTKQTARKSTGGKAPRKQLATKAARK	SAPATGGVKKPHRYRPGTVALRE
<i>X. laevis</i>	ARTKQTARKSTGGKAPRKQLATKAARK	SAPATGGVKKPHRYRPGTVALRE
<i>D. rerio</i>	ARTKQTARKSTGGKAPRKQLATKAARK	SAPATGGVKKPHRYRPGTVALRE
<i>M. musculus</i>	ARTKQTARKSTGGKAPRKQLATKAARK	SAPATGGVKKPHRYRPGTVALRE
<i>H. sapiens</i>	ARTKQTARKSTGGKAPRKQLATKAARK	SAPATGGVKKPHRYRPGTVALRE
<i>A. thaliana</i>	ARTKQTARKSTGGKAPRKQLATKAARK	SAPATGGVKKPHRFPGTVALRE

C



B



D

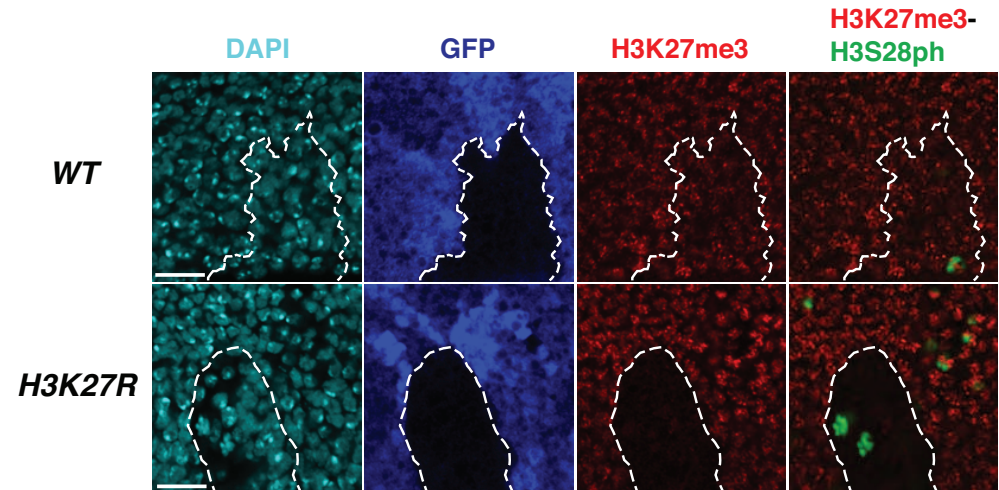


Figure S2

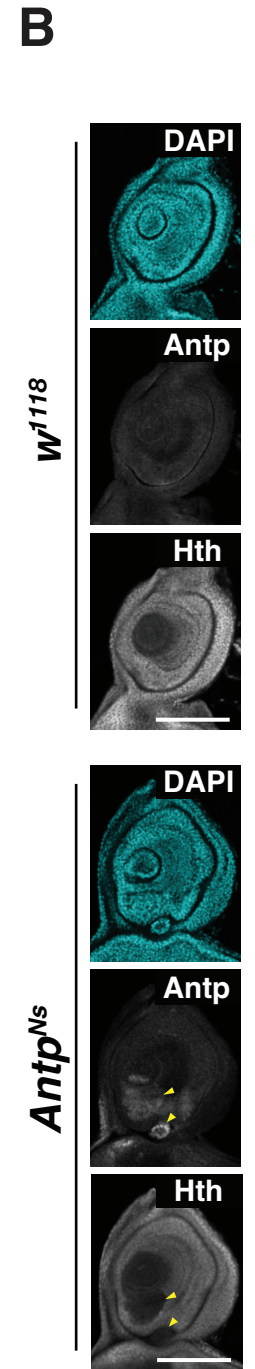
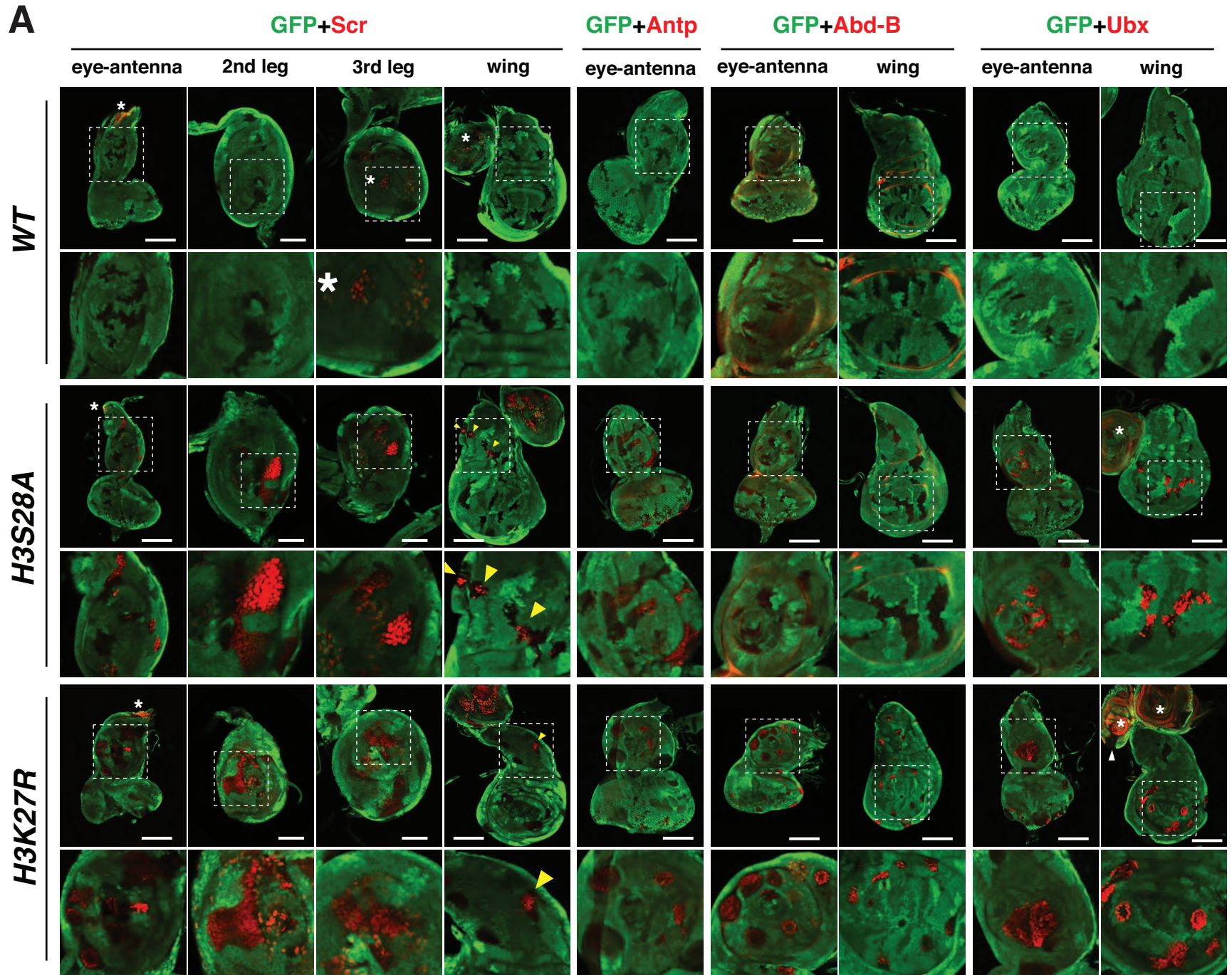


Figure S3

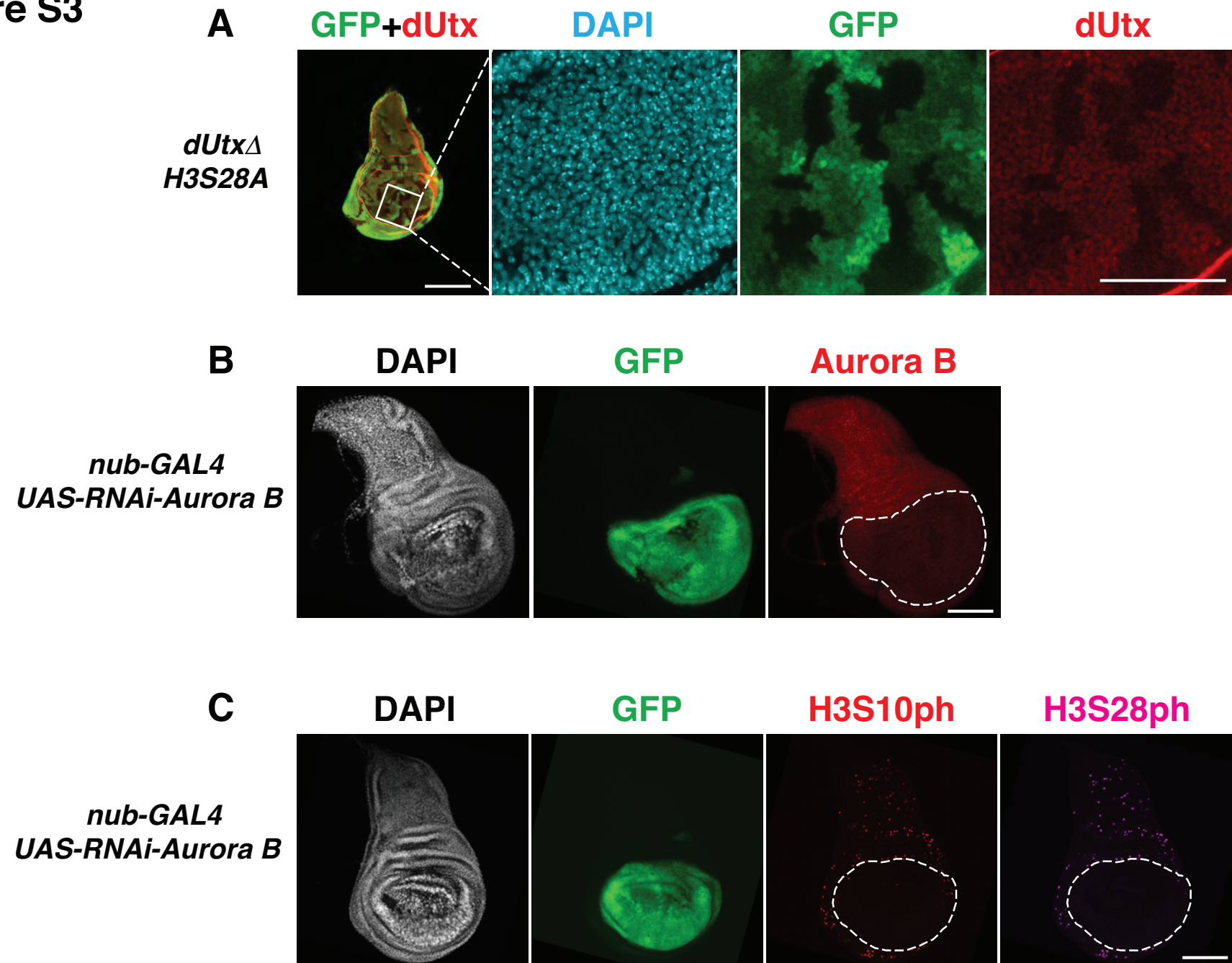
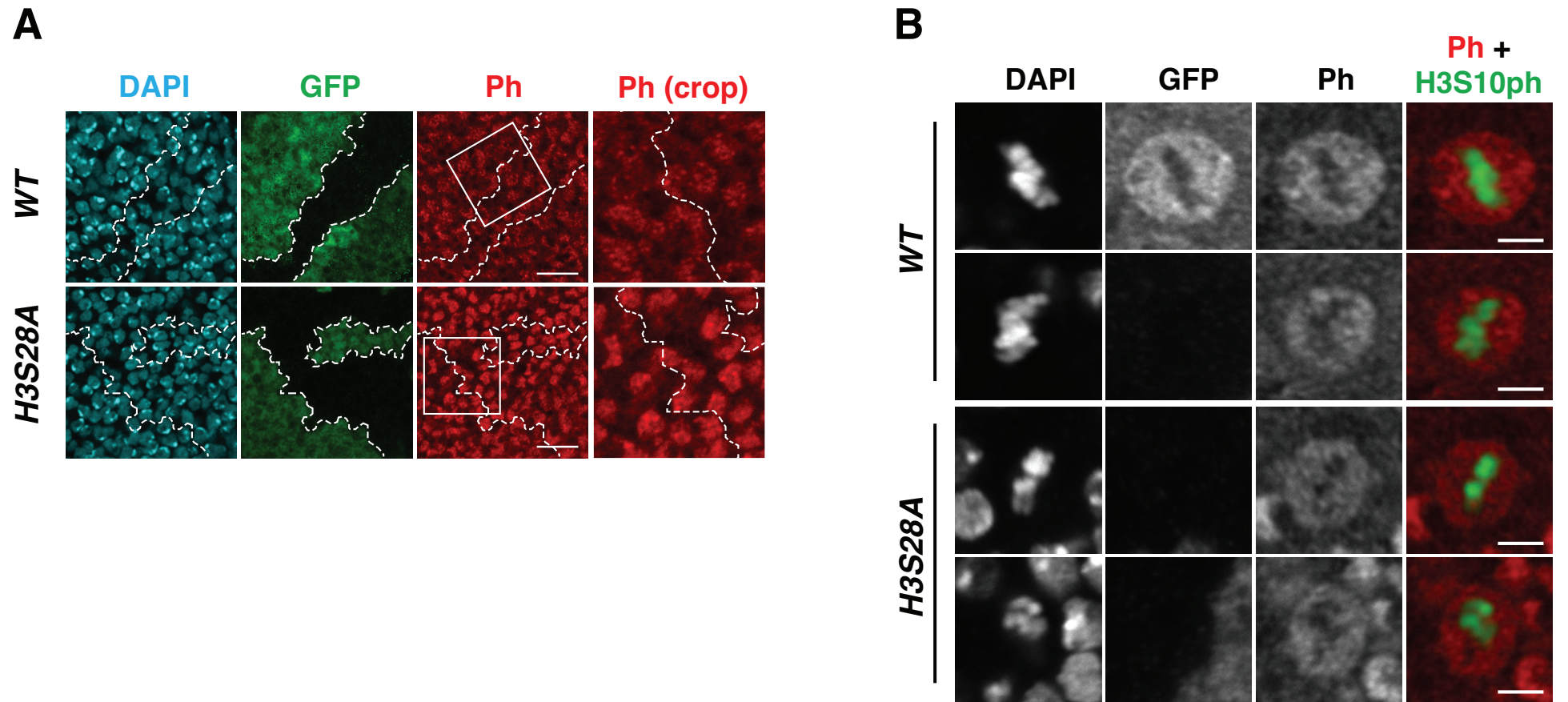


Figure S4



Supplemental Figure Legends

Figure S1, Related to Figure 1. Schematic overview of the system for assaying the function of H3S28 and validation on histone replacement clones in larval imaginal discs.

(A) The serine residue at position 28 of the histone H3 protein is conserved. Alignment of the N-terminal 1-50 amino acids of H3 from various eukaryotes. H3K27, the methylation target site of PRC2, is highlighted in red; the conserved H3S28 residue is highlighted in yellow and the variant alanine is highlighted in green. (B) Principle of mosaic analysis of *Drosophila* histone mutants. Inductions of mosaic histone mutant clones begin with parental cells that are heterozygous for the histone locus. Mitotic crossover occurs at FRT40A with the supply of FLP. And upon appropriate segregation of sister chromatids (bottom box in the right part of the figure), homozygous *HisC* alleles either in WT or deleted forms can be generated. Because of their co-emergence, they are also referred to as twin clones. Homozygous $\Delta HisC$ clones are marked by the lack of GFP, while twin WT *HisC* clones show twice the GFP expression compared to the surrounding heterozygous cells. Since chromosome 3 is integrated with 12xHisGU, the endogenous source of H3 can be replaced by different H3 alleles in the $\Delta HisC$ clones. (C) and (D) Wing imaginal discs of homozygous $\Delta HisC$ clones supplemented with 12xHisGU transgenes carrying either H3 *WT*, *H3S28A* or *H3K27R* alleles. Immunostaining with the indicated antibodies is shown; DNA was stained with DAPI. Clones of interest are marked by the lack of GFP signal and are indicated by dashed lines. (C) Comparison of H3 staining in WT (GFP positive) tissue with clones containing *WT*, *H3S28A* or *H3K27R* histone replacement. Note that all histone replacement clones displayed normal H3 staining (red) level similar to the surrounding GFP positive (green) cells. (D) Comparison of H3K27me3 (red) levels in GFP-negative (histone replacement) clones with GFP-positive normal tissue. Note that *H3K27R* mutant cells (bottom row) were depleted of H3K27me3 despite having normal mitotic H3S28ph signal (green). *WT* clones supported robust H3K27me3 levels indistinguishable from the surrounding GFP positive cells. For clarity of composite micrographs, GFP is pseudocolored to blue in (D). Scale bars correspond to 10 μm .

Figure S2, related to Figure 2. Hox gene derepression profiles in histone mutants (*H3S28A* and *H3K27R*) clones and *Antp*^{Ns}.

(A) Micrographs showing full-scale imaginal discs described in Figure 2 and main text. For each imaginal disc, a selected region (dashed line) is magnified and displayed below the corresponding micrograph. Asterisks mark zones of endogenous expression of Scr and Ubx. Yellow arrowheads highlight weak Scr derepression occasionally detected in the notum region of wing discs in both *H3S28A* and *H3K27R* mutant clones. The white arrowhead indicates ectopic silencing of endogenous Ubx expression in the haltere disc carrying *H3K27R* clones. Scale bars of wing and eye-antenna discs represent 100 μm and those of leg discs represent 50 μm . (B) Antennal discs of *w*¹¹⁸ (top panel) and *Antp*^{Ns} (bottom panel) were immunostained with the indicated antibodies. DNA was stained with DAPI. Arrowheads indicate ectopic expression of Antp and silencing of the antennal selector gene Hth. Scale bar corresponds to 100 μm .

Figure S3, related to Figure 3. Validation of clone induction of *dUtxA*, *H3S28A* double mutant and of in vivo RNAi against Aurora B kinase.

(A) Wing imaginal discs with clones homozygous of the combined *dUtxA*, *H3S28A* mutants were immunostained with the indicated antibodies. DNA was stained by DAPI. Clones were marked by the absence of GFP, which correspond to a drastic reduction of dUtx signal. (B) and (C) *Drosophila* wing imaginal discs of L3 larva with *nub-GAL4* directed RNAi against Aurora B at the wing pouch compartment marked by GFP and dotted lines. Wing discs were immunostained with the indicated antibodies and DNA was stained with DAPI. Scale bar of full-disc micrograph represents 100 μm and those of magnified regions in (A) represents 40 μm .

Figure S4, related to Figure 2. Nuclear staining patterns of Ph remain unchanged in *H3S28A* mutant.

(A) Immunostaining of wing imaginal discs for Ph. *WT* (top row) and *H3S28A* (bottom row) clones are identified by the lack of GFP signal and are marked by dashed lines. Samples were stained with DAPI and the indicated antibodies. Regions at the clone borders were further cropped and magnified. (B) Selections of mitotic cells from *WT* and *H3S28A* clones in wing imaginal discs were compiled to show the distribution of Ph during mitosis in the corresponding backgrounds. Only GFP-positive internal controls of *WT* clones are shown. Scale bars in (A) and (B) represent 10 μm and 2.5 μm , respectively.

Supplemental Experimental Procedures

***Drosophila* Stocks**

The following fly lines were used in this study

y, w; P{Ubi-GFP.D}33, P{Ubi-GFP.D}38, FRT40A (Bloomington #BL5189)

y, w, hsp70-flp; Df(2L) BSC104, FRT40A/CyO, twist-Gal4, UAS-GFP; MKRS/TM6B (Hodl and Basler, 2012)

y, w; dUtxΔ, FRT40A/CyO, twist-Gal4, UAS-GFP (Copur and Muller, 2013)

y, w, hsp70-flp122; P{Ubi-GFP.D}33, P{Ubi-GFP.D}38, FRT40A; 6xHisGU

y, w, hsp70-flp122; P{Ubi-GFP.D}33, P{Ubi-GFP.D}38, FRT40A; 6xHisGU^{H3S28A}

y, w, hsp70-flp122; P{Ubi-GFP.D}33, P{Ubi-GFP.D}38, FRT40A; 6xHisGU^{H3K27R}

w; Df(2L) BSC104, FRT40A /CyO, Kr-Gal4, UAS-GFP; 6xHisGU

w; Df(2L) BSC104, FRT40A /CyO, Kr-Gal4, UAS-GFP; 6xHisGU^{H3S28A}

w; Df(2L) BSC104, FRT40A /CyO, Kr-Gal4, UAS-GFP; 6xHisGU^{H3K27R}

w; dUtxΔ, Df(2L) BSC104, FRT40A /CyO, Kr-Gal4, UAS-GFP; 6xHisGU

w; dUtxΔ, Df(2L) BSC104, FRT40A /CyO, Kr-Gal4, UAS-GFP; 6xHisGU^{H3S28A}

y, w, ey-FLP1; P{Ubi-GFP.D}33, P{Ubi-GFP.D}38, FRT40A; 6xHisGU

y, w, ey-FLP1; P{Ubi-GFP.D}33, P{Ubi-GFP.D}38, FRT40A; 6xHisGU^{H3S28A}

y, w ey-FLP1; P{Ubi-GFP.D}33, P{Ubi-GFP.D}38, FRT40A; 6xHisGU^{H3K27R}

Antp^{Ns}/TM3, Ser (Kindly provided by Walter Gehring lab.)

w¹¹¹⁸

Mosaic analysis and Immunostaining

Primary antibodies used for immunostaining in this study:

Hox antibodies were purchased from the Developmental Studies Hybridoma Bank (DSHB). Mouse anti-Scr (DSHB 6H4.1, 1:20), mouse anti-Antp (DSHB 8C11, 1:20), mouse anti-Ubx (DSHB FP3.38, 1:20), mouse anti-Abd-B (DSHB 1A2E9, 1:10), mouse anti-En (DSHB 4D9, 1:20), mouse anti-H3 (ActiveMotif 39763, 1:500), mouse anti-H3S10ph (Millipore 05-806, 1:1000), rat anti-H3S28ph (Millipore MABE76, 1:1000), rabbit anti-H3K27me3 (Millipore 07-449, 1:500), rabbit anti-H3K27me2 (Upstate 07-452, 1:500), rabbit anti-H3K27me1 (Millipore 07-448, 1: 250), rabbit anti-H3K27ac (Abcam Ab4729, 1:500), rabbit anti-H34me3 (Millipore 04-745, 1:500), rabbit anti-Pc ((Grimaud et al., 2006), 1:500), rabbit anti-Ph ((Grimaud et al., 2006), 1:500), guinea pig anti-Hth (a gift from Ginés Morata, 1:200), rabbit anti- Aurora B (a gift from David Glover, 1: 200), rabbit anti-dUtx (a gift from Feng Tie and Peter J. Harte, 1: 200) chicken anti-GFP (Invitrogen A10262, 1:500).

Supplemental References

Copur, O., and Muller, J. (2013). The histone H3-K27 demethylase Utx regulates HOX gene expression in *Drosophila* in a temporally restricted manner. *Development* 140, 3478-3485.

Grimaud, C., Bantignies, F., Pal-Bhadra, M., Ghana, P., Bhadra, U., and Cavalli, G. (2006). RNAi components are required for nuclear clustering of Polycomb group response elements. *Cell* 124, 957-971.

Hodl, M., and Basler, K. (2012). Transcription in the absence of histone H3.2 and H3K4 methylation. *Curr Biol* 22, 2253-2257.

Supplemental Information Inventory

Supplemental Figures S1-S4

- **Figure S1, Related to Figure 1. Schematic overview of the system for assaying the function of H3S28 and validation on histone replacement clones in larval imaginal discs.**
- **Figure S2, related to Figure 2. Hox gene derepression profiles in histone mutants (*H3S28A* and *H3K27R*) clones and *Antp*^{Ns}.**
- **Figure S3, related to Figure 3. Validation of clone induction of *dUtxA*, *H3S28A* double mutant and of in vivo RNAi against Aurora B kinase.**
- **Figure S4, related to Figure 2. Nuclear staining patterns of Ph remain unchanged in *H3S28A* mutant.**

Supplemental Figure Legends S1-S4

Supplemental Experimental Procedures

- **List of fly lines used in this study.**
- **List of primary antibodies used in this study.**